# The Role of Substance P

# In

# Experimental Intracerebral Haemorrhage

Timothy J. Kleinig, M.B.B.S. (Hons.), B.A., F.R.A.C.P.

Discipline of Pathology,
School of Medical Sciences,
University of Adelaide

May 2010

A thesis submitted in partial fulfilment of the requirements for the degree of Doctor of Philosophy

# 1. Spontaneous intracerebral haemorrhage: topic review and a putative pathophysiological role for substance P

## 1.1 Definition

Intracerebral haemorrhage (ICH), or bleeding within the substance of the brain, is the second most common cause of stroke, defined by the World Health Organisation as 'rapidly developing signs of focal (or global) disturbance of cerebral function lasting more than 24 hours (unless interrupted by surgery or death) with no apparent cause other than of vascular origin.'[1] Other causes of stroke include ischaemia (or a lack of blood flow to the brain), spontaneous subarachnoid haemorrhage (bleeding between the pial and arachnoid meningeal layers surrounding the brain) and spontaneous subdural haemorrhage (bleeding between the arachnoid and dural meninges).

ICH may also occur following traumatic brain injury, but in this setting is accompanied by mechanical disruption of brain tissue and the cerebral vasculature, with subsequent axonal injury as well as ischaemia. This thesis will focus on intracerebral haemorrhages which are also strokes, that is, symptomatic intracerebral bleeding not precipitated by trauma.

## 1.2 Epidemiology

Approximately one out of every six people will suffer a stroke at some stage in their lives.[2] Worldwide, stroke is ranked the second-largest cause of death after ischaemic heart disease. It accounts for approximately 10% of deaths in both high- and low-middle-income countries.[3] It also ranks second in high-income nations as a cause of disease burden (or disability adjusted life-years),[4] and ranks fifth in developing countries, where infant and child mortality from a variety of causes is common.[3] Stroke-associated disease burden in developing countries has increased significantly in recent years and is expected to match high-income country rates in time.[3]

Specifically in Australia, stroke ranks second after ischaemic heart disease as a cause of death, for years lost due to premature death and for disease burden.[5] It is estimated that more than 30,000 strokes occur every year in Australia, or one every 15 minutes.[6]

ICH is the second most common form of stroke, less common than cerebral ischaemia, but more common than spontaneous subarachnoid or subdural haemorrhage. The incidence of ICH varies greatly between populations. It accounts for around 10-15% of all strokes in Western countries, but up to 30% in Asian countries. The annualised adjusted incidence rate

of ICH is around 10-30 per 100,000 people per year.[7-9] Therefore, around 1 in 40 people worldwide will suffer an ICH at some stage in their life.[2]

Difference in ICH incidence rates between populations may be due to population differences in blood-pressure and cholesterol levels– ICH is strongly linked to hypertension, but inversely linked to total cholesterol.[10] The risk factor profile of coexistent hypertension and low total serum cholesterol is most common in Asia. Certain ethnic groups also have higher ICH incidence rates, such as African-Americans,[11] again, perhaps due to genetic differences in blood pressure. In the Unites States of America hospitalisation rates for ICH appear to be rising,[12] possibly due to population ageing and/or increasing use of antiplatelet medications and anticoagulants.[13]

ICH was the cause of approximately 15% of strokes in a recent Australian incidence study; around 5000 spontaneous ICHs occur every year in Australia, or one every 100 minutes.[6] Although the Australian incidence of ICH has declined in the latter part of the twentieth century,[14] probably through better treatment of major cardiovascular risk factors and declining smoking rates,[15] the ageing of the population will lead to rising crude incidence rates unless further gains are made.[14]

Intracerebral haemorrhage leads to greater mortality and morbidity than ischaemic stroke. Around 30-50% of patients die within the first month after an intracerebral haemorrhage; half of these deaths occur in the first two days.[9, 16-19] Only a small proportion of survivors regain functional independence.[20] ICH is more costly than ischaemic stroke.[21] In Australia it is estimated that each ICH incurs about $100,000 in lifetime costs, and that ICHs occurring in any given year cost society an estimated A$ 500million in lifetime costs (1997 figures adjusted for inflation).[21]

## 1.3 Aetiology and prognostic factors

In broad terms intracerebral haemorrhage (ICH) is caused by rupture of abnormal cerebral blood vessels, coagulopathic states, or a combination of the two. ICH occurs in characteristic cerebral locations (Figure 1). The most common site is the deep grey matter of the brain (basal ganglia and thalamus (Figure 1a)). Slightly less frequent are ICHs located in the cortex and subcortex (so-called ‘lobar’ haemorrhages (Figure 1b)). The pons and cerebellum are the next most common locations.[11]

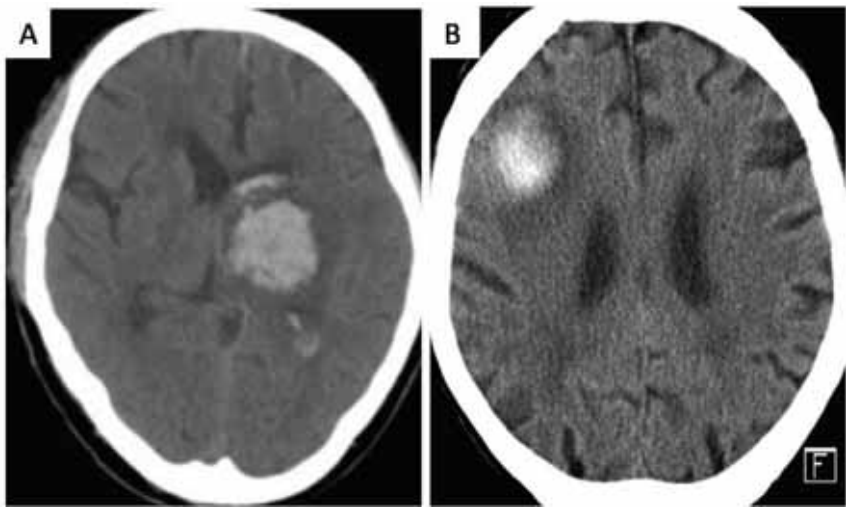


**Figure 1. (A) Typical location hypertensive ICH (thalamic) with mild surrounding oedema, midline shift and intraventricular extension. (B) Typical location ICH secondary to amyloid angiopathy, with mild surrounding oedema. In both cases there is periventricular hypodensity, suggestive of a diffuse vasculopathy.**

The commonest cause of ICH is chronic hypertensive angiopathy, which causes defects in arterial walls at bifurcation points, predisposing to rupture.[22-24] Rarely, the haemodynamic stresses of acute hypertension, as may occur in pre-eclamptic spectrum disorders[25] and sympathomimetic ingestion,[26] may cause an accelerated vasculopathy and subsequent ICH.

The second commonest cause is amyloid ('congophilic') angiopathy (Figure 1b), in which breakdown fragments of amyloid precursor protein are deposited in the vessel walls, increasing vascular fragility.[27] Other rarer causes include rupture of congenital or acquired vascular anomalies, cerebral vasculitis, cerebral venous thrombosis, and bleeding into neoplasms.[9] Coagulopathic states, which may be congenital (e.g. haemophilia), acquired (e.g. acute leukaemia) or, most commonly, iatrogenic (anticoagulation or antiplatelet therapy) lower the threshold for ICH – the underlying pathology in these so-called secondary haemorrhages mirrors that underlying most common primary ICHs (i.e. hypertensive or congophilic angiopathy[28]). If severe enough, however, a coagulopathy can cause spontaneous intracranial bleeding.

Various aetiologies are associated with specific ICH locations. Deep grey matter and brainstem haemorrhages are typically hypertensive in aetiology, whereas amyloid angiopathy and arteriovenous malformations typically cause lobar bleeds.[29, 30] Isolated intraventricular haemorrhage is frequently due to an arteriovenous malformation.[30]

Although the aetiology of ICH is heterogeneous, the relative preponderance of hypertensive vasculopathy and amyloid angiopathy cases allows overarching risk factors to be delineated. Unsurprisingly, given that hypertensive vasculopathy is the most common cause of ICH,

untreated hypertension is the most potent risk factor.[31-34] Age is a significant contributor, with a rough doubling of incidence rates with each decade of life.[31] Other factors which have been linked to increased ICH risk include cigarette smoking,[35, 36] heavy alcohol intake,[37, 38] diabetes mellitus,[31] and high serum fibrinogen levels.[39] High levels of serum cholesterol appear protective.[31]

Warfarin and antiplatelet therapy significantly increase the risk of ICH, especially if these therapies are combined.[26] High-dose statin therapy has also been shown recently to increase ICH risk in patients with prior stroke.[40]

The presence of multiple previous micro- or macrohaemorrhages on specialised MRI scans denotes a high risk of ICH recurrence.[41] This appears especially the case in amyloid angiopathy, which overall has a high recurrence rate (although whether this is the case independent of the presence of other microbleeds on MRI is unclear).[41] Following lobar haemorrhage, the presence of multiple microbleeds on MRI suggests a recurrence risk of around 20% per annum, as opposed to a risk of between 1-5% for ICH as a whole.[42-45]

Genetic polymorphisms affecting inflammation, haemostasis and vascular function have been linked to increased ICH risk.[46-50] The most pertinent of these are the E2 and E4 polymorphisms of the apolipoprotein E gene, both of which predispose to amyloid angiopathy[51] (interestingly, whereas E4 also prediposes to Alzheimer's disease (also related to β-amyloid deposition), the E2 polymorphism is protective).

Regarding monogenic disorders, familial forms of amyloid angiopathy caused by mutations in the cystatin C[52] and amyloid precursor protein genes[53] have been described. A mutation which impairs collagen type IV production (a vital component of the cerebrovascular basement membrane) leads to increased risk of silent and symptomatic intracerebral haemorrhage.[54] Vascular malformation-associated ICH may also be familial.[55]

Mortality and outcome in intracerebral haemorrhage is most strongly correlated with haemorrhage volume.[56] Haemorrhage volumes greater than 150mL are incompatible with life, as intracerebral pressure rises acutely and cerebral perfusion pressure drops to zero.[57] However even with lesser volumes (between 30 and 150mL) mortality and morbidity rates are high.[56] Other independent predictors of outcome include age, the presence of intraventricular extension, initial Glasgow Coma Scale and infratentorial location.[58] The prognosis of ICH can be reliably assessed at admission if these variables are incorporated into a weighted scale.[58, 59]

## 1.4 Histological and imaging appearances and their changes over time

The histopathological appearance and evolution of experimental ICH has been systematically studied in animals, in particular in the rat. As experimental ICH only approximates human spontaneous ICH, caution needs to be taken in applying these studies to humans. Systematic studies of hyperacute human ICH are not available. However, the limited available hyperacute autopsy studies are generally concordant with animal data.[60]

In the rat, following both collagenase ICH (where dissolution of the basement menebrane causes haemorrhage) and autologous ICH (where blood is directly injected), a central dense haematoma containing islands of intact brain cells is initially seen, well demarcated from surrounding tissue. Tongues of blood dissect along white matter tracts and blood vessels.[61, 62] After 24 hours two zones may be distinguished; a dense central zone where haemorrhage encases islands of necrotic tissue, and a peripheral zone, with varying degrees of neuronal injury and an increasing inflammatory reaction.[62] Peri-lesional oedema develops over hours, peaking between 1 and 5 days.[62, 63] Neutrophilic infiltration occurs during the first and second days, followed by recruitment of activated lymphocytes.[64, 65] Microglia are recruited and activated early and remain in an activated state around the lesion for several weeks. Red cell lysis occurs from 24 hours onwards and haemosiderin-laden macrophages appear in increasing numbers. A vascularised gliotic ring is formed around the periphery, which becomes increasingly well organised and contracts centripetally.[61, 62, 64-67]

Computerised tomography (CT) and autopsy studies suggest that human ICH evolves in a similar fashion.[68, 69] The pathological appearance of ICH in humans is similar, regardless of the cause.[60] The only reported pathological difference between hypertensive and amyloid angiopathy is a greater frequency elsewhere in the brain of deep grey matter microhaemorrhages in the former and cortical/cerebellar microhaemorrhages in the latter, reflecting the location predilection of the underlying vasculopathy.[41]

Oedema is evident on hyperacute CT imaging as the blood separates into clot and serum compartments. This process is disrupted in the setting of coagulopathy and in these patients gravity-dependent blood-fluid levels are often noted.[70] Over the next 24 hours oedema progresses significantly, although to a lesser degree in coagulopathic patients.[71] In contrast to animal models, oedema following human ICH seems to progress for up to 2 weeks.[72, 73] A vascularised gliotic ring can be visualised on imaging studies as peripheral post-contrast enhancement, which gradually contracts.[66] ICHs clearly visible on acute CT imaging not infrequently leave no residual detectable lesion on follow-up scans.[74, 75] The resultant degree of surrounding atrophy therefore becomes a better marker of chronic injury than the cyst volume demonstrated radiologically or histologically (Figure 2).[76]

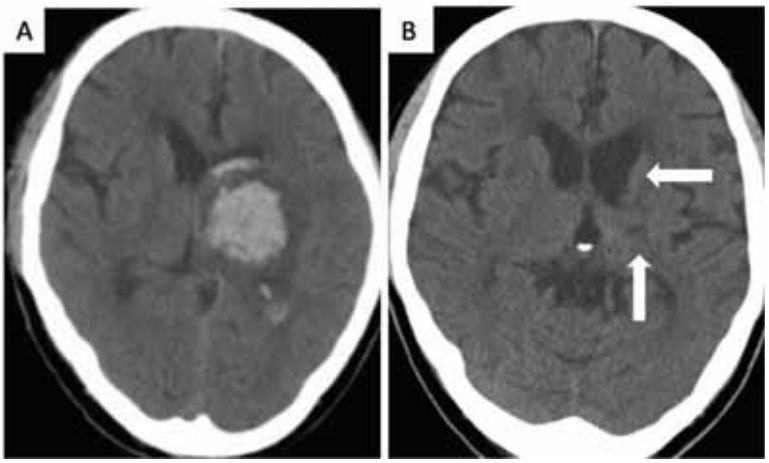


**Figure 2. (A) Significant thalamic ICH. (B) 6 months later only a tiny residual slit is seen on CT (vertical arrow). However significant atrophy is demonstrated by ventricular enlargement (horizontal arrow). The patient was moderately disabled.**

Magnetic resonance imaging (MRI) can provide complementary information to CT scanning. The interpretation of acute haemorrhage in MRI is complicated by the dynamic responses of haemoglobin to various imaging parameters, as opposed to CT scanning which shows a hyperdensity, regardless of haematoma age.[77] However, when the correct parameters are selected and the viewer is experienced, MRI is as sensitive as CT for the detection of acute ICH and much more sensitive for the detection of chronic ICH.[78]

## 1.5 Secondary injury in intracerebral haemorrhage

The mechanisms of injury in acute intracerebral haemorrhage remain a subject of intense investigation, as it is becoming increasingly clear that brain injury progresses over time and is therefore potentially ameliorable.[57]

Prompted by research into the evolution of ischaemic stroke,[79] it was initially thought that intracerebral haemorrhage may also acutely cause an 'ischaemic penumbra', a hypoperfused area of brain which may survive if blood flow is restored.[80] Reduced blood flow was demonstrated surrounding the haematoma in experimental models[80, 81] and similar reductions in local blood flow was also detected in humans.[82] However, positron emission tomography (PET), CT perfusion and MRI studies have all demonstrated that decreased blood flow does not reach critical levels. PET has also failed to demonstrate an increased oxygen extraction fraction, the most sensitive radiological indicator of an ischaemic penumbra.[83-86]

These studies raise the possibility that imaging studies have merely not been performed early enough, and that reversible ischaemia may occur hyperacutely. However, in experimental ICH, levels of adenosine triphosphate (a histological marker of inadequate perfusion) do not

fall[87] and ischaemic lactate pyruvate ratios are not found.[88] Therefore, decreased perihaematomal blood flow is due to decreased metabolic demand, not a cause of perihaematomal injury. This decreased metabolic demand has its genetic correlate in the overwhelming downregulation of neuronal signalling genes post-ICH in both humans and rats.[89, 90] The evidence does not, therefore, suggest that ischaemia plays a significant role in the pathophysiology of ICH.

However, it has become increasingly clear that intracerebral haemorrhage is in other ways a dynamic process. Clinically, deficits in ICH progress or remain static for much longer than in ischaemic stroke,[91] suggesting that delayed secondary injury occurs. Opportunities therefore exist to limit the sequelae of ICH.

### 1.5.1 Secondary pathological events in ICH

Several secondary post-ICH pathophysiological processes have been identified in recent years. It has been demonstrated that further bleeding occurs after the initial symptom onset in a significant proportion of patients.[92-97] Intracerebral blood products directly cause injury beyond that caused by their mass effect, and secondary responses of the brain and the immune system to these blood products, and to injured or dying tissue can be additively deleterious.[57, 98] Resultant oedema and the development of hydrocephalus can lead to secondary vascular compromise or herniation.[57] These secondary events (Figure 3) will be addressed in the subsequent sections.

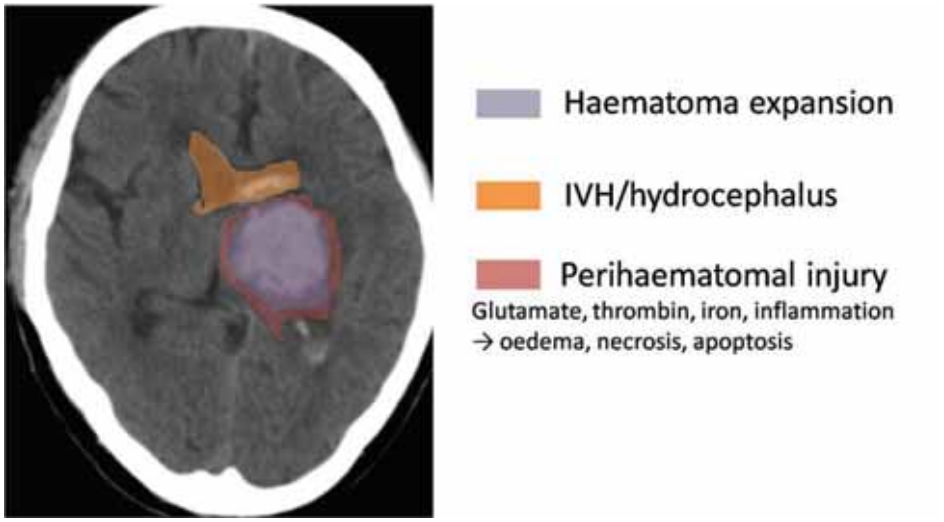


**Figure 3. Main secondary injury mechanisms following damage caused by initial ICH mass lesion.**

#### *1.5.1.1 Secondary pathological events: Haematoma expansion*

ICH growth is limited by activation of the coagulation system and tamponade, although the relative contribution of each component has not been elucidated. The previously held view, that ICH volume peaks essentially at onset, has been disproven. Haematoma expansion is common and correlates with clinical deterioration.[92-97] The earlier the initial CT scan is performed, the more commonly further bleeding is detected, suggesting that haematoma expansion may occur even in the majority of ICH patients.[99] There is a close correlation between haematoma size and short-term mortality[100] and haematoma expansion is an independent predictor of mortality.[99]

Risk factors for haematoma expansion include contrast extravasation on CT,[101-103] conventional angiography or contrast-enhanced MRI,[104] anticoagulant[105] and antiplatelet therapy,[106] high leukocyte counts, high fibrinogen levels, low platelet counts, high cellular fibronectin and interleukin-6 levels, elevated serum glucose and creatinine and large baseline haematoma volume.[107] The mechanism of haematoma expansion is unclear, although it is likely that haemostasis failure, secondary vascular injury and hypertension all play roles.

#### *1.5.1.2 Secondary pathological events: Intraventricular extension and hydrocephalus*

Intraventricular haemorrhage (IVH) extension is an independent marker of poor prognosis in ICH,[58, 108, 109] and is linked to early neurological decline.[110] The pathophysiological link between intraventricular bleeding and poor outcome is incompletely elucidated. If hydrocephalus develops secondary to IVH, the probability of poor outcome is increased further.[111] It is unclear whether hydrocephalus in ICH is merely a passive marker of increased haemorrhage volume, or whether it significantly decreases cerebral perfusion.[112, 113] Perhaps the former is more likely, as surgical therapies for reducing ICP in this setting have been unimpressive.[114] This suggests injury is caused by the mass effect of ventricular blood, inflammation,[115] and/or direct toxicity of thrombin and red-cell breakdown products.[116]

In animal models, intraventricular blood is slow to resorb, and produces, as in human IVH, severe neurological deficits, ependymal/subependymal gliosis, hydrocephalus and progressive ventricular enlargement.[116] Intraventricular thrombolytic therapy, which activates plasminogen to cleave fibrin, has been reported in rats, pigs and dogs to accelerate clot resorption, reduce or reverse ventricular dilatation and improve neurologic outcome.[116-119] However, higher doses of thrombolytics can increase periventricular oedema and leucocyte infiltration.[118] Whether a safe 'middle ground' can be found in humans is being currently explored.[120]

### *1.5.1.3 Secondary pathological events: Cerebral oedema*

Post ICH oedema is common and can produce secondary mass effect, brainstem distortion, raised intracranial pressure and neurological worsening (Figure 4).[91, 121-123] One study found that oedema-induced neurological deterioration occurred in nearly 20% of patients,[91] however lesser proportions have been found in other studies.[123-125] Early oedema (especially within the first three hours) actually predicts better recovery.[124, 126]

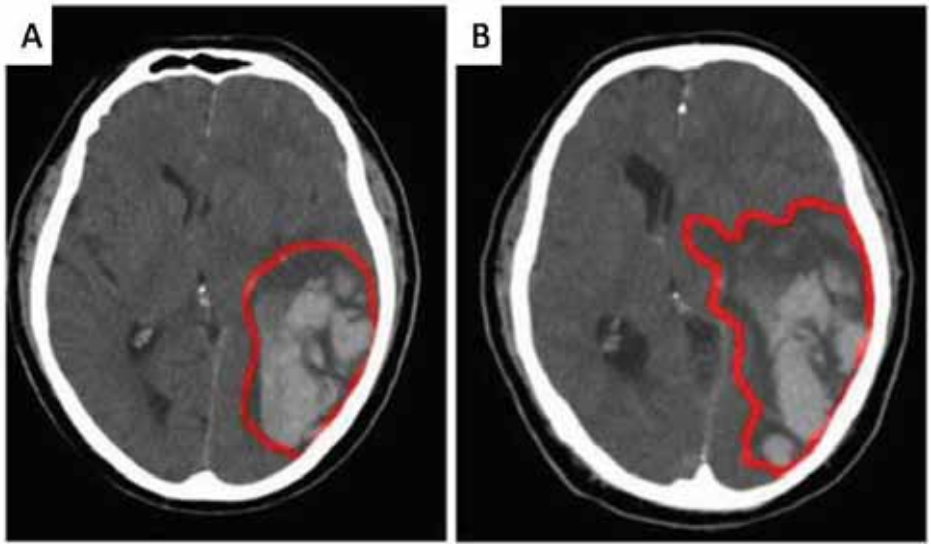


**Figure 4. Progressive oedema leading to coma following ICH. (A) There is a moderately large 'lobar' ICH (subsequently proven due to amyloid angiopathy). (B) Within twelve hours progressive oedema has led to brain stem compression and secondary hydrocephalus (due to third ventricular compression). The patient required a decompressive craniotomy, but made a good recovery.**

Oedema post-intracerebral haemorrhage is demonstrable on CT imaging as a hypodense rim surrounding a hyperdense area. There is no evidence to suggest that oedema progresses differently according to underlying vascular pathology. It is visible on initial hyperacute scans, almost doubles within the first 24 hours[71] and continues to increase for approximately two weeks,[73, 125] by which time the clinical state has started to improve.[72] One study suggested that oedema which progresses in the first 2-3 days is associated with clinical deterioration, whereas later oedema is not.[125] Most neurological deterioration occurs in the first few days,[56] when oedema progresses quickly and the haematoma has not yet been absorbed. Not all studies have demonstrated this correlation, however,[123] and longer term intensive clinical-radiological studies are required. In experimental ICH neurological deficits increase in parallel with early (day 1-3) but not subsequent oedema.[127] Summarising the literature as a whole, hyperacute oedema is probably beneficial, oedema in the next 2-3 days is probably detrimental, and the clinical effect of subsequent oedema is uncertain.

Three pathophysiological stages of oedema in ICH have been identified.[57] The first involves clot retraction, that is, the separation of the intracerebral blood into serum and clot. This occurs rapidly, and does not involve a true gain of volume above that of the haematoma. It is unlikely, therefore, to be clinically important and may be the cause of the 'hyperacute' oedema which correlates with better outcome[128] (theoretically this hyperacute oedema may inversely correlate with haematocrit, and therefore haemoglobin content, and therefore subsequent haemoglobin-mediated secondary injury (see below)). The second phase occurs over hours to days and is related to thrombin production.[129] The third occurs over days to weeks[123] and is associated with lysis of red blood cells.[73, 129] Whether haematomal mass effect can in itself cause oedema is unclear; infusion of microspheres plus thrombin caused no increase in oedema above that caused by thrombin alone.[130] However, in a separate experiment, both temporary and permanent inflation of a microballoon did increase brain water content.[131]

### *Cerebral oedema: concepts, definitions and the blood-brain barrier*

Cerebral oedema has traditionally been divided into two categories: cytotoxic, and vasogenic. Cytotoxic oedema involves ion shifts from extra- to intracellular compartments with secondary water influx and cell swelling. Vasogenic oedema is due to leakiness of the blood-brain barrier (BBB) and denotes a hydrostatically- driven isotonic extracellular influx of fluid, ions and proteins.[132] As commonly understood, only vasogenic oedema causes a net gain of cerebral fluid. It causes no cellular swelling, as ionic homeostasis is maintained. However, this dichotomous understanding does not account for the severe hemispheric swelling often seen in large ischaemic stroke in the setting of an intact BBB. [133] A revised classification, adding the category 'ionic oedema', has therefore been proposed.[133] Ionic oedema refers to the transendothelial flux of water occurring secondary to sodium influx, which compensates for the extracellular sodium depletion caused by cytotoxic oedema. It is dependent on continued (or recovered) blood flow.[133] The relative contributions of ionic and vasogenic oedema in ICH have not been elucidated, but both probably occur.[63]

The BBB refers to the tight functional and physical separation of cerebral intra- and extra-vascular compartments. This unique separation is necessary, as stable neuronal function requires much tighter homeostatic control of the surrounding microenvironment than cellular function elsewhere in the body.[134] The BBB tightly regulates influx and efflux of ions, energy substrates, water and inflammatory cells. The main components of the BBB are the capillary and post-capillary venular endothelium, pericytes, the basement membrane and astrocytic endfeet (Figure 5).[134] Cerebral endothelium has fewer pinocytic vesicles than extracerebral endothelium and fewer fenestrations, consistent with lower rates of both active and passive substance influx.[135] Adhesion between endothelial cells is tighter than

elsewhere in the body, due to cell membrane tight junctions, adherent junctions and junctional adhesion molecules.[135] The brain endothelium has a much greater number of mitochondria than elsewhere, suggesting high metabolic demands, and possesses a number of enzymes for metabolism of blood-borne neuroactive substances.

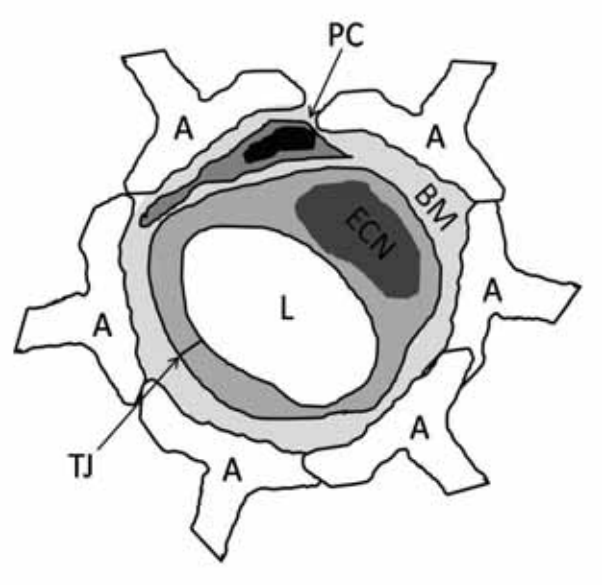


**Figure 5. Main constituents of the blood-brain barrier. A=astrocyte, PC=pericyte, BM=basement membrane, ECN=endothelial cell nucleus, TJ=tight junction, L=lumen**

The BBB is highly regulated by proximate glia and neurons; it is estimated that all neurons are located within 10 microns of a capillary.[136] The tight correlation of neuronal and glial activity with vessel and barrier function has formed the concept of 'the neurovascular unit',[137] in which interrelationships and crosstalk between co-located cerebral cells are emphasised.

BBB dysfunction can be either selective or non-selective. In selective BBB dysfunction a normal physiological process becomes dysregulated with deleterious consequences (such as water influx in ionic oedema or inflammatory cell infiltrate in autoimmune diseases.) In non-selective BBB dysfunction (i.e. vasogenic oedema) intercellular endothelial junctions and the basal lamina are physically disrupted. Subsequent influx of intravascular components is determined by blood pressure and fenestration size (Starling's law).[133] Conceptually, the most severe form of BBB dysfunction is intracerebral haemorrhage.

Although most water flux in the body occurs passively across membranes, rapid water flux in kidney, lung and brain is regulated by aquaporins. These small membrane proteins only allow water to pass under certain conditions (e.g. binding of anti-diuretic hormone in the kidney distal collecting duct). Aquaporins exclude the passage of ions and charged solutes, thus

maintaining electrical homeostatasis. Some aquaporins also allow the passage of uncharged solutes, such as $CO_2$, urea and lactate.

Aquaporin-4 is the predominant brain aquaporin and is expressed predominantly in astrocytic end-feet at fluid-astrocyte interfaces (CSF and vascular).[138] Aquaporin-1 is the predominant aquaporin found in the choroid plexus and is pivotal in CSF formation.[139] Aquaporin-4 can play a protective or detrimental role, depending on the form of brain injury. In the setting of ionic oedema, where the BBB is intact (water intoxication and ischaemic stroke), aquaporin-4 allows water into the brain, and is hence detrimental.[140] However, in vasogenic oedema, where the BBB in damaged and fluid enters alongside, rather than through astrocytes (abscess formation,[141] cortical freeze lesion, tumour implantation and parenchymal fluid infusion[142]), aquaporin-4 is needed to facilitate fluid efflux from brain into CSF and vessels, and hence is protective.

Thus, the role of aquaporin-4 in ICH may be detrimental or beneficial, depending on whether ionic or vasogenic oedema predominates. Certainly, upregulation of aquaporin-4 is a consistent finding in animal studies[143] (although, interestingly, in the sole human genomic ICH study, aquaporin-9, not -4, was the form found to be upregulated[89]). However the pivotal knock-out or inhibitor study has not been performed, and thus the relative importance of ionic and vasogenic oedema in the various phases of post-ICH swelling remains to be determined.

#### *1.5.1.4 Secondary pathological events: Delayed cellular death*

Neuronal, glial and endothelial cell death can occur long after the original insult in ICH. In experimental ICH, regardless of the model employed, degenerating neurons can be detected as late as four weeks after ICH is induced.[144] Delayed cell death can be precipitated by the initial physical injury to cells and their supplying blood vessels, by the toxic effects of blood products and by the effects of red cell lysis. Delayed cell death can be increased by the subsequent inflammatory response (for instance by the respiratory burst of neutrophils or the matrix disruption caused by matrix metalloproteinases (MMPs)), as well as by the deleterious effects of hydrocephalus or oedema.

It has long been recognised that cell death can take various forms. Kerr and colleagues,[145] identified a form of cell death they termed ‘apoptosis’, from the Greek ‘to fall away’, referring to a planned as opposed to inadvertent form of cell death, analogous to the ‘falling away’ of autumnal foliage. Cells dying in this fashion demonstrate cellular shrinking, condensation and margination of nuclear chromatin, with subsequent ‘budding’ of the plasma membrane. Cells subsequently degenerate into apoptotic bodies, containing cell

organelles and/or nuclear material surrounded by an intact plasma membrane, which are then phagocytosed.

Schweichel and Merker[146] classified cell death into three main forms: apoptotic cell death (type I), autophagic degeneration (type II), marked by autophagic cytoplasmic vacuolisation, and cytoplasmic cell death (type III), marked by disintegration and deletion of organelles. Autophagy can be viewed as a protective response, where a deprived cell cannibalises itself, pending restoration of energy substrates; however, if energy supplies are not restored, the cell dies (autophagic cell death).[147] Complex crosstalk occurs between these three main cell-death pathways.[147] Perhaps most simply, cell death can be viewed as existing along an 'aponecrotic' spectrum,[148] where one end denotes a controlled, regulated process, with little subsequent inflammation, and the other an uncontrolled, passive process, with cellular lysis and a resultant inflammatory response.

The cellular machinery underlying apoptosis was outlined through studies in *Caenorhabditis elegans*;[149, 150] homologous pro- and anti-apoptotic proteins, cysteine aspartic acid-proteases ('caspases') were subsequently demonstrated in higher organisms.[151-153] Non-caspase mediated forms of apoptotic cell death also occur in higher organisms.[154]

Consistent with the known complexity of interactions between cell death pathways, there is no 'gold standard' method of detecting apoptosis;[148, 155-157] morphological characteristics, DNA laddering, terminal deoxynucleotidyl transferase biotin-dUTP nick end labelling (TUNEL) staining, caspase positivity and cell death prevention with caspase inhibition are methods commonly employed, but each has its limitations.[147]

Why do cells die of apoptosis? Genetic complement deficiencies, which disrupt the normal clearance of apoptotic cells, lead to auto-immunity.[158] Teleologically it is therefore proposed that cells with sufficient energy stores to commit suicide but insufficient stores to survive apoptose in order to limit secondary inflammation and subsequent damage to normal cells.[157] This has led to the concern that preventing apoptosis in brain injury may simply force cells down the default necrosis pathway, actually increasing damage. However, the general experimental neuroprotective efficacy of apoptosis inhibitors suggests that the dominant form of apoptosis in brain injury is *aberrant* apoptosis[159] – that is, unnecessary cell suicide. Interventions seeking to limit delayed cell death can target two broad mechanisms: those 'upstream' mechanisms which are inducing necrosis or apoptotic machinery, or the 'downstream' apoptotic (and perhaps necrotic)[160] mechanisms subsequently activated.

In ICH, neurons and glia (which degenerate for up to 4 weeks following ICH)[144] may have characteristics which suggest they are at either the 'necrotic' or 'apoptotic' end of the

spectrum. Granted that there is no gold-standard marker for apoptosis, various apoptotic markers have all been detected in ICH (TUNEL staining,[161, 162] caspase-3 immunoreactivity[161] and cytochrome c release[163]). Matsushita *et al* demonstrated colocalisation of astrocytic and neuronal apoptotic morphological change with TUNEL staining and furthermore reduced these changes with a broad-spectrum caspase inhibitor.[164] Evidence of necrotic and apoptotic cell death has been demonstrated in the peri-haematomal region of human ICH. Apoptosis may even be the predominant form of cell death in ICH.[165]

### 1.5.2 Mediators of perihaematomal secondary injury

#### *1.5.2.1 Secondary injury mediators: glutamate and non-specific damage sensors*

Some damage following ICH clearly occurs extremely rapidly and irreversibly. The mass effect of the haematoma mechanically disrupts blood vessels, neurons and glia, causing cellular death directly.[57] ICH has therefore been modelled by inflation of a microballoon into the rat basal ganglia.[131] Temporary or permanent inflation caused similar levels of histologic damage.

However, this rapid, irreversible injury to cells and blood vessels could potentially initiate secondary injury pathways which may damage surviving surrounding cells. Similarly to ischaemic stroke, injured neurons and glia may release increased levels of the dominant excitatory neurotransmitter, glutamate, which can prove toxic to adjacent cells.[166, 167] There is increasing evidence for a pathophysiological role of excessive glutamate in ICH: peri-haematomal glutamate is strongly elevated in the first day after ICH in both humans and animals [88, 166, 168, 169] and experimental glutamate inhibition is neuroprotective in animal models.[170] In humans serum glutamate level is an independent predictor of poor outcome and eventual cavity size.[172] It has been hypothesised that pathological amounts of glutamate may also infuse directly into the brain at ICH onset.[172] Cortical spreading depression, a glutamate-mediated trigger of secondary injury in ischaemic stroke,[173] has been demonstrated in experimental ICH.[174]

Additionally, recent work in the ischaemic stroke field (reviewed by Kleinig and Vink [175] suggests that dead or dying tissue can itself stimulate deleterious inflammatory responses (see below). Proteins released from dead or dying cells and disrupted matrix, such as high mobility group box-1 protein (HMGB-1), heparan sulfate and heat-shock proteins ligate extracellular receptors such as Toll-Like-Receptors (TLRs), CD36 and receptor for advanced glycosylation end-products (RAGE) which are linked to intracellular pro-inflammatory cascades. Intracellularly, the IL-1β inflammasome[176] can also be upreglated by non-specific cerebral injury markers, such as uric acid and potassium. Whether or not all these factors are

also involved in secondary injury post-ICH remains to be confirmed, however they are highly unlikely to be specific to cerebral ischaemia. Caspase-1 (interleukin-1 converting enzyme), a crucial part of the IL-1β inflammasome, has recently been shown to be strongly upregulated following both rat[90] and human ICH.[89]

#### *1.5.2.2 Secondary injury mediators: thrombin*

Thrombin, the mediator of the second stage of oedema, is a serine protease produced from prothrombin as part of the final common pathway of the clotting cascade. It produces fibrin from fibrinogen, which then polymerises to form a blood clot. However thrombin has multiple other non-clotting effects, mediated predominantly through the proteinase (or protease) activated receptors (PARs)-1, -3 and -4. Thrombin cleaves these receptors within N-terminal extracellular domains exposing tethered ligand domains that bind to a separate extracellular loop, initiating transmembrane signalling.[177] PAR-1 mediates most of the known pro-inflammatory effects of thrombin.[178] PAR-2 is predominantly activated by trypsin and tryptase. Many other endogenous and exogenous PAR agonists have been identified (reviewed recently by Luo *et al* [179]).

PARs are found throughout the body, but are also expressed widely throughout the rat brain and in the dorsal root ganglia.[180, 181] They are present and/or are induced in pathological conditions on cerebrovascular endothelium,[182] neurons, astrocytes, microglia, and oligoendrocytes.[179] PAR-1 is also expressed in the human brain, most intensely in astrocytes,[183] but also in neurons, pericytes and probably endothelial cells.[184] Thrombin can enter the brain under pathological conditions which cause breakdown of the BBB, but can also be produced intracerebrally. Thrombin can be detected in normal brains by immunohistochemical methods in neurons and some astrocytes.[185] It can also be produced by neuronal, astrocytic, microglial, oligodendroglial[185] and cerebrovascular endothelial[186] cultures.

It has been demonstrated that thrombin infusion into the brain can cause oedema, inflammation, neuronal death, gliosis and functional deficits.[187] Depending on the dose administered, a volume of striatum adjacent to the injection site can become frankly necrotic.[188] A pathogenic role for thrombin has been suggested in ICH, ischaemic stroke,[189-191] Parkinson's disease,[192, 193] Alzheimer's disease,[185] and traumatic brain injury.[194] Thrombin and/or PAR-1 inhibition, either pharmacologic or genetic, has proven neuroprotective in these conditions. Pre-insult exposure to lesser amounts of thrombin can, however, be neuroprotective.[195-197] This phenomenon has been termed 'thrombin preconditioning'[197] and has parallels in the neuroprotective efficacy of sublethal cerebral ischaemia, hypoxia,

hyperoxia and hyperthermia, which induces tolerance to a subsequent otherwise harmful insult.[198]

Significant amounts of thrombin are produced by an intracerebral haemorrhage.[129] If equivalent amounts of thrombin normally found within an appropriately-sized blood clot are infused directly into the brain, BBB disruption,[199] oedema, inflammation[187] and cellular death,[161] ensues. Cerebral blood flow or vasoreactivity are unaffected.[199] Intracerebral infusion of plasma causes oedema only if the infused prothrombin is also converted to thrombin.[200] Thrombin produces these effects in a fibrinogen-independent manner; in experimental 'artificial' ICH where various blood components were removed, thrombin, with or without fibrinogen, produced a similar degree of oedema to whole blood infusion. Fibrinogen alone produced no oedema.[130] Thus, non-clotting thrombin-activated mechanisms play a crucial role in post-ICH oedema. These are most likely predominantly mediated by PAR receptors,[201, 202] although other pathways may participate. Inhibition of complement is an effective neuroprotective strategy post-ICH;[203] thrombin can directly generate active complement fragments (e.g. C5a[204]) and complement inhibition limits thrombin-induced brain injury. [205]Plasmin, which activates PAR-2 receptors, may act to potentiate thrombin's toxicity.[206] Although it is only toxic when injected at high doses directly into the brain,[188] at physiological levels it can enhance thrombin-mediated injury.[206]

Experimental ICH where thrombin is depleted, inactivated or blocked produces minimal oedema in the first few days after the injury (Figure 6).[127, 130, 199, 200, 207-209]

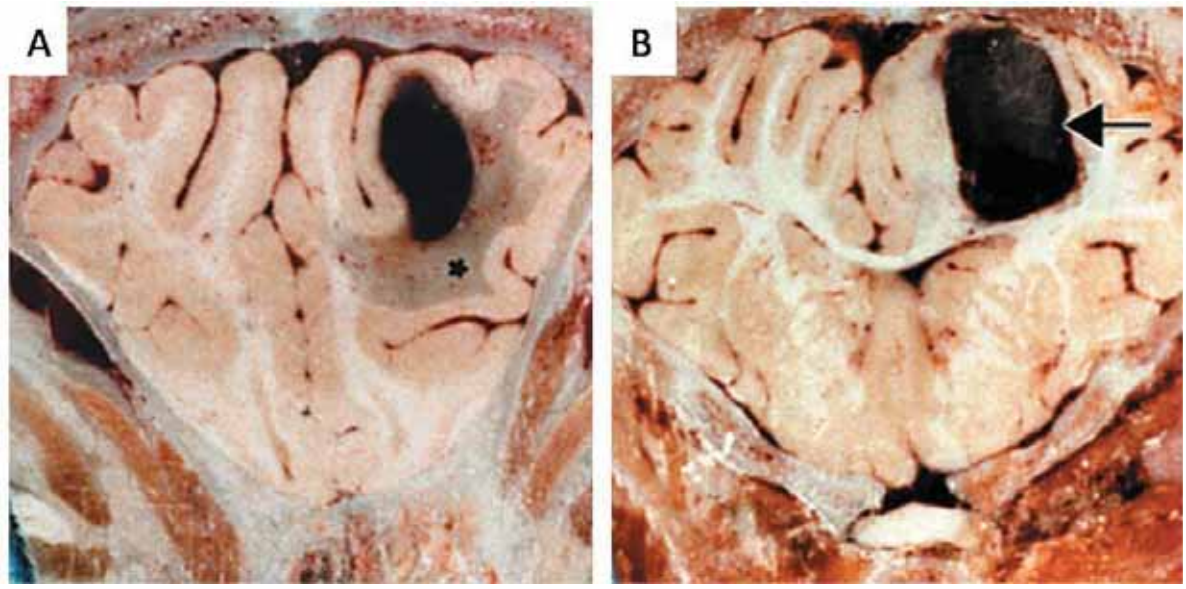


**Figure 6. Blocking thrombin reduces oedema following ICH. (A) 24h following injection of unheparinised blood in the pig there is significant perihaematomal oedema. (B) However, heparinisation of injected blood markedly reduces oedema.[208]**

A role for thrombin in human ICH-associated oedema is suggested by the marked difference in oedema formation between spontaneous ICH and ICH occurring after treatment with heparin and fibrinolytic agents (thrombin is inhibited by heparin).[70, 128] Pre-ICH warfarin use, which blocks production of various clotting factors including thrombin, is likewise associated with decreased oedema volumes.[126] Statins (e.g. atorvastatin) are linked to decreased oedema[210] and possibly improved outcome[211, 212] following ICH. Although statins have many mechanisms of action, decreased PAR-1 expression may be responsible.[213]

Thrombin can not only promote oedema and inflammation in ICH, it can also directly cause neuronal apoptosis,[214, 215] possibly by causing aberrant re-entry of neurons into cell cycle.[216] Neuronal death can be induced by thrombin through both PAR-dependent and –independent mechanisms,[217] one of the latter being conversion of pro-MMP-9 (see below) to its active form.[202, 217] Thrombin may also play a role in enhancing glutamate-induced 'excitotoxicity'. Thrombin both enhances astrocytic glutamate release[218] and potentiates glutamatergic activity.[219]

Incidentally, thrombin may also play a role in the microvascular injury which is the underlying cause of ICH. A direct thrombin inhibitor, dabigatran, prevents clot formation in humans more effectively than warfarin (which inhibits multiple clotting factors, including thrombin).[220] Yet despite this enhanced anticoagulant effect, high-dose dabigatran dramatically reduces the incidence of ICH (relative risk=0.26),[220] suggesting that thrombin may be vasculopathic.

#### *1.5.2.3 Secondary injury mediators: red cell lysis*

Red cell lysis occurs progressively over the first few days following ICH.[67, 221] Energy failure and complement activation are two known causative factors.[222] Secondary injury from erythrocytes occurs only following haemolysis; experimental infusion of whole red cells produces little initial oedema, but significant oedema and BBB breakdown is seen after several days.[207] However, infusion of lysed erythrocytes causes the rapid accumulation of oedema and inflammatory cells.[223] Thus lysis of red blood cells appears to produce the delayed third phase of oedema in ICH.[73] Differences in the rate of erythrocyte lysis may account for differences in the tempo of oedema formation in rats and humans; red cells haemolyse by day three in rats[207] and oedema decreases after this time. Haemolysis is delayed in humans,[73] and this perhaps explains the slow and continued progression of oedema over the first two weeks post-ICH.[73, 123, 125]

Haemoglobin is the main component of red blood cells, accounting for around 98% of dry weight. After red cells lyse haemoglobin is broken down into globin and haem. Globin

appears relatively inert and is recycled into its amino acid constituents. Haem oxygenase (using NADPH (nicotinamide adenine dinucleotide phosphate) as the reducing agent) catabolises haem to biliverdin, iron and carbon monoxide.[224] Haem oxygenase (HO) exists in two isoforms, HO-1, mostly expressed in microglia/macrophages, and HO-2, constitutively expressed in neurons and forming the bulk of HO activity in the brain.[225] Biliverdin is metabolised to bilirubin by biliverdin reductase,[226] whereas iron is phagocytosed by macrophages and subsequently bound to iron binding proteins such as ferritin. Following haemorrhage the iron-binding capacity of ferritin is overwhelmed, leading to formation of haemosiderin, a poorly characterised inert compound which contains up to 25% inert iron.[224] Iron is not easily exported in this form, and intracerebral haemosiderin can persist for years, forming the basis for detection of chronic haemorrhages by heavily $T_2$-weighted MRI sequences ('microbleeds').[227]

Infusion of haemoglobin, lysed red blood cells, bilirubin and ferrous (but not ferric) iron all rapidly produce oedema and inflammation.[207, 228, 229] Haemoglobin injections are epileptogenic and cause focal gliosis and cavity formation.[230] Serum ferritin levels, an indirect measure of tissue iron stores, are positively correlated with post-ICH peri-haematomal oedema in humans.[231] Leakage of intravascular iron in the form of holo-transferrin at the time of ICH may also potentiate brain oedema.[232] Deferoxamine, an iron-chelator, reduces ICH-induced injury,[233] but inhibition of HO has produced discordant results. Non-specific haem oxygenase inhibitors seem to improve outcome,[234, 235] as does HO-1 knock-out.[236] However, inhibition of HO-2 has variously been reported as both detrimental and beneficial.[236, 237]

Thrombin may synergistically increase iron-induced injury: a combined injection of iron and thrombin in singularly non-oedematogenic doses causes oedema and brain injury,[232] perhaps due to thrombin-induced enhancement of neuronal iron uptake.[197] Haemoglobin also enhances excitotoxicity; non-toxic levels of haemoglobin increase cell death induced by glutamate in cell culture.[238]

The mechanism by which RBC breakdown products produce oedema is obscure, but probably multifactorial: enhancement of aquaporin expression,[143] ionic oedema (though causing cytotoxicity) and vasogenic oedema (through direct BBB toxicity and enhancement of downstream inflammation) may all contribute.

It might be expected, given the toxicity of iron in the CNS, that early surgical removal of blood would improve outcome. This remains to be proven[239] however experimental approaches to directly remove blood less invasively are an object of intensive research (see below).[240]

### *1.5.2.4 Secondary injury mediators: downstream inflammatory pathways*

Thrombin- and red cell lysis-mediated secondary injury can occur directly (see above) but also via, and modulated by, the inflammatory response. Post-ICH inflammation is also probably triggered by non-specific damage sensors (see above) as well as pro-inflammatory PAR-mediated pathways,[179] and is mediated by a complex interplay of inflammatory cells, chemokines and cytokines (Figure 7). Modulating the inflammatory response appears to be broadly beneficial in experimental ICH. The post-ICH inflammatory response is best characterised in animal models, although findings are broadly corroborated by the limited human studies performed to date.[68, 69, 89, 241]

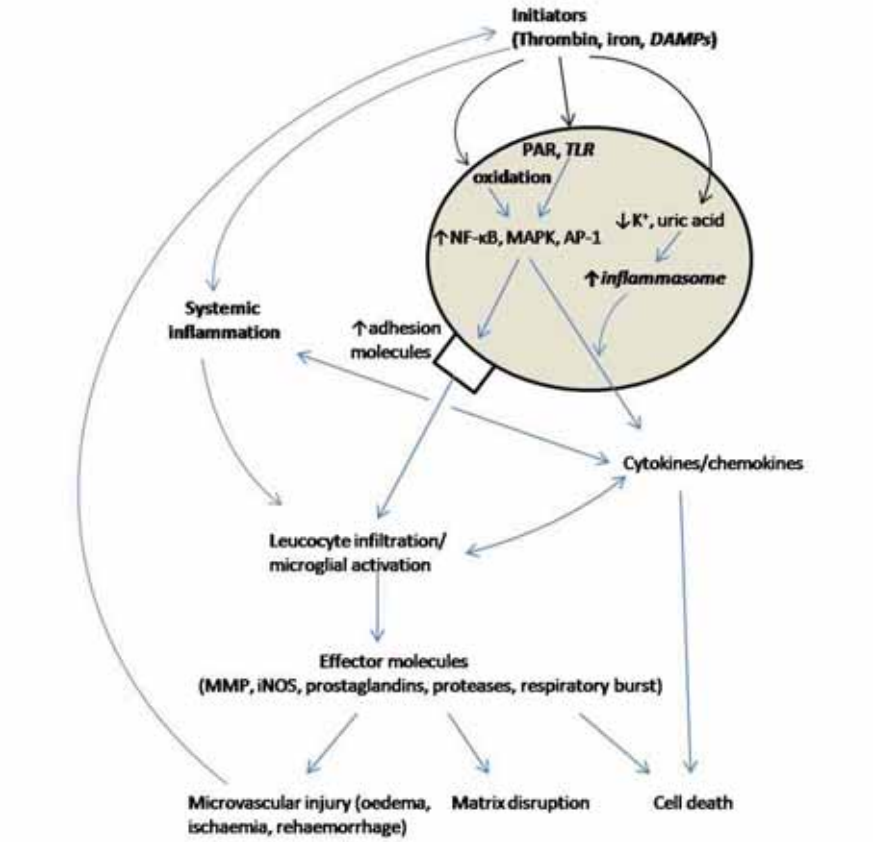


**Figure 7. Probable and proven causes and consequences of post-ICH inflammation. Data are extracted from studies in ICH and/or ischaemic stroke (italics). DAMP=damage associated molecular patterns, PAR=protease activated receptor, TLR=Toll-like receptor, NFκB=nuclear factor kappa-B, MAPK=mitogen-associated protein kinase, AP-1=activator protein-1, MMP=matrix metalloproteinases, iNOS=inducible nitric oxide synthase. Adapted from Kleinig and Vink (2009).[175]**

As in ischaemic stroke,[242] inflammation after intracerebral haemorrhage can be either adaptive or maladaptive. Inflammation is necessary to remove iron and dead tissue, but may be over-exuberant and hence a source of secondary oedema and tissue injury.[98] The

beneficial effects of global leucocyte depletion in experimental ICH suggests that post-ICH inflammation is predominantly maladaptive.[243]

ICH-induced inflammation has both cellular and molecular components. The cellular components include resident microglia, cerebral mast cells and infiltrating neutrophils, lymphocytes and macrophages. The molecular components include various cytokines (e.g. interleukins), chemokines, complement, growth factors and proteases.[98, 244, 245]

Resident microglia play a vital short- and long-term role in coordinating the cerebral inflammatory response, and are the first cells to be activated in ICH.[98] In the rat autologous blood model, activated microglia appear as early as the first 1-4 hours and persist for several weeks.[64, 144, 162] Microglia are involved in phagocytosis of dead tissue, but also secrete pro- and anti-inflammatory cytokines and growth factors. Neurological outcome after experimental ICH was significantly improved by both pre- and post-haemorrhage administration of macrophage/microglia inhibitory factor (tuftsin fragment 1 to 3, Thr-Lys-Pro).[246] The beneficial effects of HO-1 knock-out may be mediated by a 'knock-down' of deleterious microglial activity.[247]

Neutrophils begin to marginate in the blood vessels surrounding human ICH within several hours, infiltrate shortly thereafter and are cleared by 3-5 days.[68, 69] Similar time-profiles of neutrophil infiltration are seen in experimental ICH.[64, 65] Cerebrospinal fluid neutrophils are elevated in human ICH[248] and high peripheral neutrophil counts are associated with an increased risk of neurological decline.[110] Mice lacking CD18, essential for firm neutrophil-endothelial adherence before diapedesis, have less oedema and lower mortality rates following ICH.[249] Total body irradiaton in rats (which depletes platelets, lymphocytes and neutrophils) has also proved neuroprotective.[243]

Lymphocytes start to infiltrate the peri-haematomal region subsequent to neutrophils and persist around the lesion for several weeks.[64, 144] Calcineurin inhibition, which reduces T-lymphocyte proliferation and the subsequent immune amplification, has been shown to be weakly neuroprotective.[250]

Cerebral mast cells are resident inflammatory cells located perivascularly and capable of releasing a wide range of pro-inflammatory factors.[251] Both inhibition of mast cell degranulation and mast cell knock-out improve outcome and reduce swelling in experimental ICH.[252] These approaches also decreased haematoma volume in an autologous blood ICH model, suggesting that secondary inflammatory factors may precipitate further bleeding distal to the initial haemorrhage source.

Various pro-inflammatory intracellular transcription pathways are elevated in experimental and human ICH, including the nuclear factor kappa-B (NFκB) pathway, interleukin-1 related genes, leucocyte (especially neutrophil) chemokines, the complement pathway and matrix metalloproteinases.[89, 90]

The NFκB pathway controls expression of multiple pro-inflammatory genes, including interleukins-1 and -6 and tumour necrosis factor alpha (TNF-α).[172, 244, 253] It also upregulates expression of adhesion molecules by cerebrovascular endothelium. The NFκB pathway is upregulated early after both experimental and human ICH[89] and subsequently co-localises with apoptotic neurons.[162] In ischaemic stroke this pathway is activated by toll-like receptor (TLR) ligation;[254] whether or not this pathway is significant in ICH remains to be demonstrated, however TLR-1 has been shown to be upregulated following human ICH.[89] Thrombin is also probably a cause of early post-ICH NFκB upregulation,[255] although, again, this has not been definitively shown. Suppression of NFκB by an agonist of peroxisome proliferator-activated receptor-gamma (PPAR-γ) improves behavioural outcome and reduced neutrophil infiltration and neuronal death in experimental ICH.[256]

Cytokines, secreted factors which regulate inflammation, can be produced by most intracerebral cells (in particular activated microglia) as well as infiltrating inflammatory cells.[242] Interleukin-1β is a strongly pro-inflammatory cytokine; both interleukin-1β and interleukin converting enzyme are strongly upregulated after experimental[90] and human[89] ICH. Interleukin-1β blockade reduces oedema, inflammation and injury in experimental ICH as well as after intracerebral thrombin injection.[257] TNF-α is similarly upregulated following ICH and thrombin injection and antagonism in these settings is neuroprotective.[258, 259] The neuroprotective efficacy of both cyclo-oxygenase[260] and complement inhibition[203, 222, 261] has also been demonstrated.

Matrix metalloproteinases (MMPs) are a family of zinc-dependent endopeptidases, capable of degrading the extracellular matrix and non-matrix proteins.[262] They are essential for normal brain modelling and repair, but may play a deleterious short-term role in both ischaemic and haemorrhagic stroke.[263] They can be released by neurons, glia, endothelial cells and infiltrating inflammatory cells.[264] MMP-related genes are upregulated in experimental ICH[90, 265, 266] MMP-9 levels are also elevated systemically in humans following ICH[267] as well as peri-haematomally.[241]In human ischaemic stroke [241, 268] and possibly animal models,[269] infiltrating neutrophils appears to be the primary source of deleterious MMP-9.

However, it remains unclear whether MMPs play a detrimental, beneficial or mixed role; studies of MMP broad-spectrum inhibitors[265, 269] and MMP-9 knockout mice [201, 270] have demonstrated, alternately, both detriment and benefit. MMP-3 knockout is reportedly

beneficial,[202] however, concerns remain that MMP-3 is needed to prevent neuronal apoptosis.[269] Thrombin appears to potentiate the deleterious effect of both MMP-3 and -9.[201, 217] A possible synthesis of these disparate studies is that, overall, MMPs play a detrimental role acutely, but are required longer-term for tissue repair and regeneration.[263]

It has recently been demonstrated that the systemic inflammatory response to intracerebral haemorrhage influences the subsequent intracerebral inflammatory response, and hence outcome; when neural stem cells (NSCs) were injected intravenously and intracerebrally post-collagenase ICH (cICH), only intravenous injections proved beneficial.[271] These beneficial effects were evident within the first few days post-ICH, at which time-point NSCs were mainly residing in the spleen. Pre-ICH splenectomy without NCS injection was moderately beneficial (although not to the same extent); any benefits of NSC injection were completely abrogated in this latter group. Thus the neuroprotective effect of NSC injection appeared mediated by modulation of the splenic inflammatory response. Similarly, in experimental ischaemic stroke, early benefits of haematopoietic stem cell transplantation in experimental ischaemic stroke were associated with a blunting of the splenic immune response, preceding any infiltration of stem cells into the brain.[272]

#### *1.5.2.5 Secondary injury mediators: oxidative stress*

Excessive glutamate, iron and inflammation can all induce 'oxidative stress', in which high levels of extra- or intracellular reactive oxygen species (ROS) injure membranes, proteins and DNA. The brain, by virtue of its high oxygen consumption, high lipid concentrations and relatively low levels of ROS neutralizing compounds, is particular susceptible to this form of injury. The term 'reactive oxygen species' encompasses superoxide ($O_2^{\cdot-}$), hydrogen peroxide ($H_2O_2$), the hydroxyl ion ($^{\cdot}OH$), nitric oxide (NO) and peroxynitrite ($ONOO^-$). ROS are continually produced by the cell during normal activity and under normal conditions are uneventfully deactivated.[273] In experimental ICH clear evidence of ROS-induced injury has been detected, suggesting that these protective mechanisms are overwhelmed.[274-276]

Protein carbonyl formation, a marker of oxidative stress, is increased rapidly after ICH by both plasma and lysed whole blood infusions.[274-276] However, these results have not been replicated in the only relevant study of human ICH to date.[277] Oxidative stress-induced DNA injury can be detected after striatal injection of both autologous blood and iron.[278] Various anti-oxidants are upregulated after experimental ICH.[90]

The generic free-radical trapping agent NXY-059 shows some efficacy in experimental ICH,[250] as does edaravone, a similar agent.[279] Knock-out of the superoxide-producing NADPH oxidase gene significantly reduces oedema, haemorrhage volume, disability and mortality in a mouse

collagenase stroke model.[280] Deferoxamine therapy reduces oxidative stress-induced DNA injury post-ICH in rats,[233] as does haem oxygenase-1 and possibly -2 knockout in mice.[237, 247]

#### *1.5.2.6 Secondary injury mediators: Hyperthermia*

There is very strong evidence from animal and human studies that increased temperature exacerbates brain injury, and that hypothermia ameliorates it. Hyperthermia increases and hypothermia decreases post-injury metabolic demands, oxidative stress, excitotoxicity, inflammation and apoptosis.[281] This has led to successful clinical use of hypothermia following cardiac surgery,[282] neonatal hypoxia[283] and cardiac arrest.[284, 285] Hyperthermia is consistently associated with poorer outcome following human ICH.[286] A consistent reduction in oedema has been seen with therapeutic hypothermia in experimental ICH,[287-290] however a reduction in lesion volume or disability has not always been demonstrated.[289, 290] A large clinical trial of moderate temperature lowering in both ischaemic stroke and ICH suggested a possible benefit in patients with baseline hyperthermia.[291]

## 1.6 Approaches to limit secondary injury after ICH

### 1.6.1 Medical approaches

Arresting haematoma expansion has been the focus of trials targeting the clotting cascade[292] and hypertension.[107] Activated factor seven potently initiates coagulation at sites of injury, and is widely used for this purpose in patients with haemophilia. It can also reduce bleeding in patients with normal coagulation.[293] In a phase two trial in patients with acute ICH, activated factor seven decreased haematoma expansion, morbidity and mortality.[292] Unfortunately the subsequent phase III trial showed no significant clinical benefit, despite a similar reduction in haematoma expansion.[294] Differing patient baseline characteristics in the two trials may explain the marked disparity of outcomes; a sub-group of younger patients treated earlier may benefit, and a further trial is envisaged.[295]

A phase II trial of intensive blood pressure lowering suggests that anti-hypertensive therapy can, likewise, reduce haematoma expansion,[296] although its effects on long-term outcome remain to be determined in a larger study.

Progressive oedema or hydrocephalus can lead to herniation of the brain, either contralaterally, inferiorly or both. These compartmental shifts can either disrupt crucial cerebral pathways directly or compress blood supply at the circle of Willis or upper brainstem and can be fatal. Although there is little evidence that simple oedema-reducing measures

(e.g. mannitol) improve cerebral perfusion in ICH patients generally,[297] there is some suggestion that a comprehensive approach to maintaining cerebral perfusion pressure in the setting of raised intracranial pressure can improve outcome.[298] Additionally, a single-centre study has reported that timely aggressive management of oedema (hypertonic saline and hyperventilation) at the point of transtentorial herniation can improve long-term outcome.[299]

The deleterious consequences of thrombin-mediated secondary injury have not yet been addressed in large scale human studies, although a small non-randomised trial of a direct thrombin inhibitor commenced 24 hours post-ICH was suggestive of benefit.[300] Pre-ICH statin therapy (which may downregulate PAR-1)[213] is associated with decreased mortality and perihaematomal oedema in some[210, 212] but not all studies[211] and a pilot randomised controlled trial is ongoing. Anti-oxidant therapy with NXY-059 caused a non-significant reduction in haematoma expansion and oedema, but no reduction in mortality or morbidity.[301]

### 1.6.2 Surgical approaches

Surgical approaches in ICH have generally had the goal of removing the haematoma, through either open or microscopic approaches. The potential benefits include reducing mass effect and reducing secondary iron- and thrombin-mediated injury. The main risks are precipitation of rebleeding and direct trauma to already-compromised perihaematomal tissue. In recent years less invasive surgical approaches have been combined with the use of intrahaematomal or intraventricular thrombolytics to help clear the haematoma. Other surgical procedures used include hemicraniectomy (reducing the mass effect without disturbing the brain parenchyma[302]) and ventriculostomy for hydrocephalus.[303] Presently no therapeutic approach is of proven benefit.

It is clear, anecdotally, that some patients benefit (Figure 4), but it is unclear whether these patients can reliably be prospectively identified. In the largest trial to address the issue, no benefit was seen with surgery.[239] However, the trial was based on the principle of clinical equipoise (that is, only patients in whom the benefit of surgery was deemed uncertain by the responsible surgeon were included). There was also considerable crossover from the non-surgical to the surgical arm. Meta-analysis of surgical trials suggests benefit in patients with superficial, but not deep ICH. A randomised controlled trial in this group is ongoing.[303] The benefit of haematoma evacuation in cerebellar ICH where the bleed is greater than 3cm in diameter is generally accepted on the basis of several case series.[304] Hemicraniectomy to relieve mass effect may possibly be of benefit in supratentorial ICH (either alone or in combination with clot evacuation.)[305, 306]

Minimally invasive surgery is widely used in some parts of the world as a treatment for ICH.[307] One randomised trial of clot aspiration alone suggested that mortality may be reduced at the expense of greater morbidity.[308] Subgroup analysis in this study suggested significantly improved morbidity in patients with subcortical and/or smaller haematomas. A further trial restricted to putaminal haemorrhage suggested benefits in both morbidity and mortality.[309]

Combination of thrombolytic therapy with endoscopic aspiration may both speed clot removal and allow a greater percentage to be removed. The largest human trial to date of aspiration combined with thrombolytics however was negative.[310] Although early oedema was reduced in one animal study with a combined approach,[311] later oedema and inflammation may be enhanced,[312, 313] raising the possibility that the neurological toxicity of thrombolytics[314] may outweigh the potential benefit of clot removal.

Intraventricular haemorrhage is clearly linked to poor outcome, probably both as a result of blood's toxic effects and as a result of secondary hydrocephalus. Patients with IVH and hydrocephalus are commonly treated with external ventricular drainage, with or without thrombolysis and subsequent conversion to lumbar drainage.[7] Although definitive evidence for the clinical efficacy of these approaches is lacking, a small randomised trial suggested a radiologic improvement following intraventricular thrombolysis.[315] A larger randomised trial is ongoing.[115] Concerns regarding the neurologic toxicity of thrombolytics would also apply to intraventricular administration, as rat studies of IVH have demonstrated periventricular oedema and inflammation following intraventricular tissue plasminogen activator (tPA).[118] Endoscopic clot evacuation is an alternative promising,[316] but unproven approach.

## 1.7 SP as a potential mediator of secondary injury in ICH

### 1.7.1 Background, structure and receptors

Substance P (SP) was first identified as a vasoactive substance with gastrointestinal prokinetic activities by von Euler and Gaddum in 1931.[317] Pernow subsequently demonstrated that SP is widely distributed throughout the body, particularly in the myenteric plexi, dorsal part of the spinal cord, dorsal root ganglia (including the trigeminal ganglion), autonomic nerves, substantia nigra and hypothalamaus.[318]

The structure of SP was determined by Leeman and colleagues in 1971.[319] It is an undecapeptide synthesised from the TAC-1 gene (Figure 8), also known as pre-protachykinin A gene (PPTA), which can also be processed by alternative RNA splicing to produce neurokinin A .[320] A closely related peptide, neurokinin B, is synthesised from the TAC-3 (or PPTB) gene (or from TAC-2 in rodents). Additional related peptides, the endokinins[321] and

haemokinins[322] have recently been discovered. Together they comprise the tachykinin family, so-called because of their rapid-onset action, as opposed to the slower-acting bradykinins.

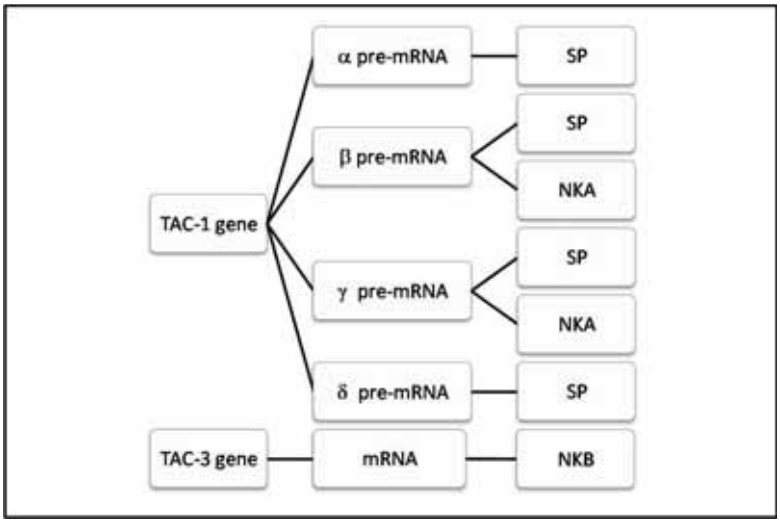


**Figure 8. Transcription and translation of human tachykinins. Substance P can be synthesised from all TAC-1 mRNA isoforms, whereas synthesis of NK-A is restricted to TAC-1 beta- gamma- isoforms; NK-B is synthesised from the TAC-3 gene.** [323-325]

SP largely acts through the neurokinin 1 (NK1) receptor, as do haemo-[322] and endokinins.[321] Neurokinin A acts primarily through the NK2 receptor and neurokinin B through the NK3 receptor, although a degree of cross-reactivity exists.[326, 327] An additional NK4 receptor, homologous to NK3 and activated by neurokinin B has also been described.[328]

SP expression is most prominent in brain and nerves. However, as essentially all tissue are innervated, SP can be found throughout the body.[327] Although mRNA for other neurokinin receptors is detectable in many cells and regions,[329] the relative preponderance of the NK1 receptor in the human adult brain [329] makes SP the dominant tachykinin of interest in the pathophysiology of ICH.

The NK1 receptor is a G-protein coupled receptor, activation of which can lead to at least four apparently independent second messenger systems: phospholipase C-mediated Ca2+ mobilisation (from both intra- and extracellular sources); phospholipase A2-mediated arachidonic acid mobilisation; adenylated cyclase-mediated cAMP accumulation;[330] and arrestin 2-mediated MAPK activation.[331] A truncated form of the NK1 receptor has also been described.[332] It is widely expressed in both the brain and periphery, and its associated second messenger systems most likely differ from the full-length isoforms.[333]

Stimulation of the NK1 receptor by substance P leads to rapid tachyphylaxis. This is predominantly mediated by receptor internalisation, which is followed by slow recycling of

the receptor to the cell surface over several hours.[334] Ligand-activated G protein-receptor uncoupling can also limit receptor signalling.[335] Genetic knockout of beta-arrestin, which mediates both receptor uncoupling and endocytosis, exacerbates vasogenic oedema in some tissues.[335] The truncated form of the NK1 receptor is less prone to desensitisation.[336]

### 1.7.2 Peripheral actions

Around 75% of SP produced by cells of the dorsal root ganglion is released antidromically (that is, into peripheral tissues). The remaining 25% is released in the spinal cord.[327] SP is present in the sensory nerve fibres which innervate vessels, both peripherally and centrally.[337] SP-containing afferent neurons also innervate bowel, heart, bladder and airway smooth muscle.[338] SP is also released from autonomic neurons and from the intrinsic neurons of the gastrointestinal tract.[338] SP produce diverse effects, evoking smooth muscle contraction or relaxation, protein extravasation, inflammatory cell infiltrates and glandular secretion, though to different degrees in different tissues and species.[338] Platelets and other blood components also possess NK1 receptors,[339] although whether blood components respond predominantly to SP or haemokinin is not yet known. A potentially pathophysiological role for SP has been proposed in numerous inflammatory conditions, including anaphylaxis,[340] inflammatory arthropathies,[341] inflammatory bowel disease,[342] asthma and chronic obstructive airways disease[343] and inflammatory skin conditions.[344]

SP is co-localised[345, 346] in sensory ganglia and coreleased[347] with calcitonin gene related peptide (CGRP) and NKA. All three peptides have vasodilatory actions.[348, 349] Only SP and NKA induce vascular permeability,[349, 350] although CGRP potentiates SP-mediated oedema.[350] SP-induced vascular permeability is induced by opening post-capillary venular endothelial gaps,[351, 352] although the precise intracellular pathways leading to gap formation are yet to be elucidated.[353]

Studies on SP releasing factors have mostly been conducted in the skin due to relative ease of access (Figure 9).Heat, capsaicin, acidosis,[354, 355] thrombin,[178] trypsin, tryptase[356] and possibly bradykinin[357] can all directly release antidromic neuronal SP. Compounds incapable of directly releasing SP, but capable of lowering the threshold for release by the above factors include adenosine triphosphate (ATP), prostaglandins, tumour necrosis factor-α (TNF-α ), interleukin1, interleukin-6 and possibly serotonin and nitric oxide.[358]

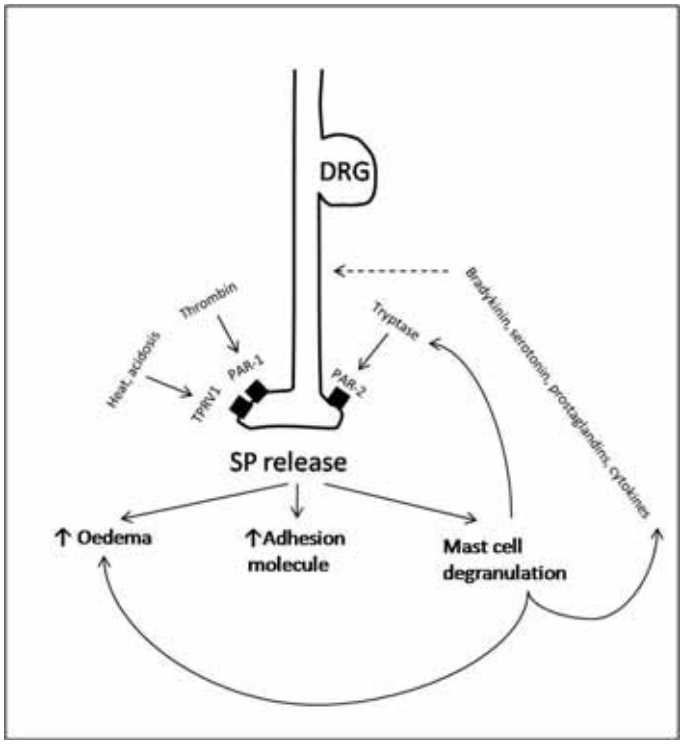


**Figure 9. Summary of the main peripheral inflammatory actions and triggers of SP release. Solid lines indicate direct actions, dashed lines indirect. DRG=dorsal root ganglion, TRPV=transient potential receptor vanilloid, PAR=protease activated receptor.**

Heat and acidosis cause substance P release via the capsaicin receptor. Capsaicin, the active ingredient of chilli peppers, has long been known to induce SP release and in higher doses is a neurotoxin specific to SP-containing neurons.[359] Repeated exposure of subtoxic doses leads to desensitisation. As capsaicin can deplete the majority of SP-containing dorsal root ganglion cells, most must co-express the capsaicin receptor.[345]

The capsaicin receptor, transient potential receptor vanilloid 1 (TPRV1) is a calcium-preferring non-selective cation channel.[355] Noxious heat (>48 degrees C) gates the TRPV1 channel; capsaicin and acidosis can lower the threshold for activation such that room temperature is sufficient.[354] Various intrinsic and extrinsic compounds such as anandamide,[360] TNF-$\alpha$,[361] endothelin,[362] arachidonic acid metabolites, alcohol and nicotine[363] can also modulate TRPV1 sensitivity. It is unclear whether bradykinin causes SP release directly[357] or through lowering the TPRV1 activation threshold.[364]

Peripherally administered thrombin can directly induce SP release and oedema, with cleavage of dorsal root ganglia proteinase-activated receptor 1 (PAR-1) being a necessary intermediary step.[178] PAR-1 can also be activated by tPA and plasmin.[189]

A complex feedback loop exists between neurogenic SP release and mast cells. SP can cause mast cell degranulation directly[365] or lower the threshold for degranulation by other means.[366] As well as causing degranulation, SP can, via an NK1R-dependent mechanism, stimulate mast cell secretion of numerous cytokines and chemokines, including monocyte chemoattractant protein-1, RANTES (regulated on activation, normal T-cell expressed and secreted) and TNF-α.[367]

To complete the feedback loop, mast cell tryptase can directly cause SP release and oedema by cleaving the PAR-2 receptor present on sensory axons.[356] Other mast-cell degranulation products (bradykinin, histamine and serotonin) can both directly cause oedema and potentiate further SP release.[358, 368, 369] In inflammatory skin conditions sensory neurons containing SP are in direct contact with mast cells,[370] arguing for the pathophysiological relevance of these experimental observations.

The effects of SP on inflammatory cells apart from mast cells are complex and incompletely elucidated. Although SP potentiates the adhesion of neutrophils to endothelial cell layers in culture,[371, 372] whether[373] or not[374, 375] subcutaneous microinjection of SP causes neutrophilic infiltration *in vivo* is controversial. However, SP plays a clear role in enhancing neutrophil accumulation induced by other substances, including TNF-α,[376] immune complexes[377] and IL-1β.[378] It has been reported that TNF-α can *only* cause neutrophil accumulation in the presence of SP,[376] which , without SP, can only cause intravascular accumulation of neutrophils, perhaps due to a failure of tight leucocyte adhesion. SP has been shown to upregulate both LFA-1[372] (leucocyte function antigen-1) and ICAM-1 (intercellular adhesion molecule-1)[379] in neutrophils and endothelial cells, respectively. These interact to mediate firm neutrophil-endothelium adhesion. Conversely and somewhat paradoxically, NK1 antagonism increases the neutrophilic infiltration induced by subcutaneous thrombin injection.[178]

SP causes chemotaxis of both lymphocytes and monocytes.[380, 381] It promotes TNF-α release[382, 383] and upregulates cyclo-oxygenase-2 (COX-2).[384] SP also stimulates macrophage[385] and neutrophil[386, 387] reactive oxygen species production – including the neutrophil respiratory burst.[388] In macrophages, SP stimulates the production of macrophage inflammatory protein-2 and monocyte chemoattractant protein-1 via NF-κB dependent pathways,[389] and downregulates anti-inflammatory transforming growth factor-β (TGF- β) pathways.[390]

Haemokinin also acts through the NK1 receptor[322] and is widely expressed in leucocytes.[391] However, SP can also be detected in macrophages,[392] lymphocytes,[393] neutrophils and mast

cells.[394] The relative importance of these two tachykinins in leucocyte biology and how they might interact is not known.

### 1.7.3 Central nervous system SP

Neuronal central nervous system (CNS) SP is found predominantly in the striatum, substantia innominata, deep cortical layers, hypothalamus, colliculi, periaqueductal grey and limbic system.[395] Substance P of trigeminal nuclear origin can also be found surrounding pial arteries.[396] SP can also be imported or exported across the BBB through interaction with the NK1 receptor.[397, 398] In addition to neurons, SP can be synthesised by brain endothelial cells,[399] microglia,[400] blood-derived monocytes transformed to a microglia phenotype[401] and perivascular astrocytes.[402-404]

CNS SP has two broad functions, excitatory neurotransmission and promotion of inflammation.

With regards to excitatory neurotransmission, SP plays a role in memory,[405] mood regulation,[406] motor function,[407] sensory neurotransmission,[408-410] and nausea.[411] A pathophysiological role for 'excitatory' SP has been proposed in chemotherapy-induced nausea and vomiting,[411] chronic pain states,[409, 411, 412] depression and anxiety,[413, 414] post-stroke depression,[413] migraine,[415] and epilepsy.[416]

SP may also be neurotoxic under certain conditions.[417] This effect is mediated by the NK1 receptor and takes the form a non-apoptotic programmed cell death – that is, it is dependent on transcription and translation but not leading to apoptotic morphologic features or DNA fragmentation.[417] This effect was evident *in vitro* at physiological relevant (i.e. nanomolar) concentrations, however it is not yet clear whether substance P can cause neuronal death *in vivo*. Indirect evidence supportive of a neurotoxic role for SP comes from studies of methamphetamine-related striatal injury; administration of an NK1R antagonist significantly reduces striatal neuronal apoptosis.[418] This is somewhat contradicted by other studies showing a neuroprotective role for SP against amyloid-induced cerebellar granule cells neurotoxicity.[419]

Despite intensive research into 'excitatory' CNS substance P, however, only one therapy has entered clinical use as a result: aprepitant, an oral NK1 antagonist proven to be effective in reducing chemotherapy-induced nausea and vomiting.[411] Human studies in depression and anxiety are, however, ongoing.[414]

SP derived from astrocytes, microglia and cerebrovascular endothelium is presumed to be pro-inflammatory.[420] This postulate is supported by the demonstrated pro-inflammatory role of substance P in experimental models of multiple sclerosis,[421] trypanosomiasis,[422] cerebral toxocariasis,[423] Parkinson's disease,[424] HIV encephalitis,[425] subarachnoid haemorrhage,[426] ischaemic stroke[427] and traumatic brain injury.[428]

It remains to be demonstrated whether SP of trigeminal ganglion origin can cause true 'neurogenic inflammation' (that is, oedema caused by antidromal release of sensory ganglion neuropeptides). Pial vessels in numerous mammalian species are densely innervated by SP-containing nerve fibres.[396] Depletion of perivascular SP by capsaicin treatment diminishes oedema following traumatic brain injury.[429] However, when trigeminal nerves are electrically stimulated, oedema is observed only in extracranial trigeminally-innervated structures and dura, not the brain.[430] Injecting SP systemically, likewise, produces peripheral, but not intracerebral vasogenic oedema.[430] It is not known whether stereotactic injection of intracerebral SP causes oedema and inflammation. Therefore trigeminovascular SP release appears insufficient to cause cerebral vasogenic oedema, although it remains possible that it may enhance oedema initiated by other means.

Whether or not SP causes 'neurogenic inflammation' (strictly defined) there are numerous studies which point to a neuroinflammatory role[420] in both acute and chronic CNS inflammatory states.

Regarding, firstly, chronic inflammatory states: circulating HIV envelope proteins can induce BBB breakdown by increasing perivascular SP.[431] SP/NK1r interactions have been shown necessary for the initiation and/or progression of CNS inflammation caused by certain bacterial CNS pathogens.[432] The initiation and maintenance of experimental allergic encephalomyelitis, a multiple sclerosis model, is NK1 receptor dependent.[421, 433] Astrocytes bordering human multiple sclerosis plaques also express SP.[434]

Regarding more acute CNS injuries: application of capsaicin to the surface of the brain increases BBB permeability by causing release of an NK1 receptor agonist (probably SP).[435] In experimental ischaemic stroke, TRPV1 blockade reduces oedema, probably through reducing SP release.[435] Post-ischaemic stroke, perivascular astrocytes express SP and this expression is temporally related to the presence of oedema.[404, 436] SP is released following traumatic brain injury and NK1 antagonism in this setting significantly reduces BBB dysfunction, oedema and functional deficits.[428, 429] SP immunostaining is also increased acutely following spinal cord injury.[437] In endothelial cultures, TNF-$\alpha$ and interferon-$\gamma$ mediated endothelial permeability and adhesion molecule expression are SP-dependent.[399]

The *in vivo* triggers of CNS SP release have not been elucidated in detail, but probably include TRPV1 and PAR agonists. As previously mentioned, PAR receptors are widespread throughout the brain, often highly expressed in similar regions to SP-expressing cells.[179, 182-184] A link between CNS PAR activation and SP release is therefore likely, but has not been assessed. PAR agonists which may play an important role include thrombin, plasmin, brain trypsin IV, mast cell tryptase, trypsin-like protease P22 and oligodendroglial kallikrein 6.[362]

Similarly TRPV1 receptor expression is greatest in SP-producing regions.[438] As mentioned above, TRPV1 activation causes oedema probably by inducing SP release.[435] Cerebral endogenous ligands for TRPV1 (anandamide[439] and N-arachidonoyl-dopamine (NADA))[440] have been described and presumably also cause SP release. Anandamide injected intracerebroventricularly[441] produces cerebral oedema by a TRPV1-depedent mechanism. Pro-inflammatory cytokines can cause increased endothelial SP production, but whether directly or by intermediary factors is unclear.[399] Factors known to potentiate SP release in the periphery (e.g. ATP, bradykinin, and arachidonic acid metabolites) may also do so centrally but have not been studied.

Most cells with putative roles in CNS inflammation express NK1 receptors (microglia,[442] astrocytes,[443, 444] endothelial cells[445] and infiltrating immune cells).[400, 446] SP has been shown to stimulate release of microglial prostanoids,[447] and neutrophil[387] and microglial[448] reactive oxygen species, possibly by upregulating NF-kappaB.[442] SP enhances interleukin 1β release in astrocytes;[449] interleukin 1β can subsequently increase NK1 expression in astrocytes, suggesting a possible positive feedback loop.[444, 450] SP is necessary for cerebral endothelial adhesion molecule expression,[421] and probably causes BBB dysfunction and plasma extravasation via NK-1 receptor-mediated endothelial gap formation,[399] similarly to in the periphery.[353] However, analogous to studies of SP and neutrophil accumulation, there remains debate as to whether SP can cause microglia and astrocytes directly to secrete pro-inflammatory cytokines, or whether it can merely enhance production induced by other means (e.g. bacterial pathogens[432] or lipopolysaccharide[451]).

SP is largely metabolised in the brain by neutral endopeptidase (NEP) and angiotensin converting enzyme (ACE).[452, 453] ACE polymorphisms with lower enzymatic activity lead to higher levels of brain SP.[454] Research in our laboratory has demonstrated that acute ACE inhibition worsens traumatic brain injury and ischaemic stroke, further strengthening the case for the pathogenicity of substance P.

### 1.7.4 A putative role for substance P in intracerebral haemorrhage

The role of substance P in ICH has not been studied in any form. However, evidence from multiple angles suggests that SP may play an important role in mediating post-ICH inflammation and oedema.

Firstly, in broad terms, SP plays a key role in mediating inflammation and BBB dysfunction in other conditions: inflammation and BBB breakdown are significant events in ICH[57] and on these terms alone a link is possible. More specifically, there is a great deal of overlap in secondary injury mechanisms between subarachnoid haemorrhage, ischaemic stroke, traumatic brain injury and ICH.[57, 455-457] Many experimental therapies (for instance MMP inhibition, anti-inflammatory, anti-apoptotic therapies, anti-oxidant and anti-excitotoxic therapies) have been successfully used in all four forms of brain injury. SP plays a demonstrable role in the first three conditions[426] and there is therefore a reasonable *a priori* possibility that SP is also deleterious in ICH.

Additionally, the PAR agonists thrombin and tryptase, which both have demonstrable roles in the pathophysiology of intracerebral haemorrhage,[57, 252] directly cause peripheral substance P release.[178, 356] Coupled with experiments demonstrating the positive effects of both thrombin inhibition and NK1R antagonism following subarachnoid haemorrhage[426, 458] ischaemic stroke[189, 459] and traumatic brain injury,[460, 461] a causal link between PAR agonists (especially thrombin) and SP in acute brain injury seems likely.

Substance P also enhances the pro-inflammatory effects of haem oxygenase-1,[462] complement,[377] interleukin 1-$\beta$[378] and TNF-$\alpha$.[399] Inhibition of all four has proven neuroprotective in experimental ICH.[222, 247, 257-259, 261] Lastly, CNS SP can cause NF-κB upregulation,[442] reactive oxygen species production,[387, 448] pro-inflammatory cytokine secretion, [400, 447, 449] blood-brain barrier dysfunction[399, 463] and endothelial cell-adhesion molecule expression,[399] all of which are implicated in the pathophysiology of ICH-induced secondary injury.[57, 98, 172]

Arguing against an important role for SP in ICH was the failure to detect TAC1 upregulation at 24 hours post-ICH by micro-array techniques.[89, 90] However, unpublished work by our laboratory suggests that TAC1-derived mRNA is upregulated hyperacutely, but then downregulated at 24 hours following traumatic brain injury, a setting in which NK1R antagonism is clearly beneficial. A possible explanation for these findings in traumatic brain injury is that ligation of NK1R by newly synthesised SP may limit further synthesis to prevent uncontrolled inflammation. A similar mechanism for limiting inflammation may apply in ICH. A potential concern is that tachykinins acting through the NK1 receptor have been shown to

play a role in inducing platelet aggregation,[339] and that inhibiting substance P may increase bleeding, even if it decreases secondary injury pathways.

## 1.8 Animal models of intracerebral haemorrhage

In order to test the hypothesis that substance P may play a pathophysiologically relevant role in ICH, the correct model must be selected. While research in human subjects would be ideal, interventional studies without prior experimental work in animals is unjustifiable and prohibitively expensive. There are no imaging techniques that can resolve the research question in humans, and direct application of a substance P antagonist to a human population would not be feasible without animal data.

A wide variety of animals and stroke models have been used to model stroke in general and ICH in particular. The various advantages and disadvantages of various species and models have been extensively reviewed.[240, 464-468]

Large animal models, such as primate, cat, dog, sheep and pig, offer closer approximation to human subjects (that is gyrencephalic anatomy, more white matter and presumably fewer differences in molecular cascades) at the expense of less homogenous lesion volumes, greater logistical hurdles and public unacceptability.

Small animal models – mice, rats, hamster, gerbil and rabbit – produce more homogenous lesions and pose fewer logistical and ethical difficulties than large animal models. Mice models in particular allow the impact of various genetic modifications to be assessed.

Two main animal models of experimental ICH are used: injection of autologous blood and injection of bacterial collagenase. Avulsion of intracerebral blood vessels is also described,[144] but produces a mixed ischaemic/haemorrhagic lesion, as does delayed post-ischaemic thrombolysis.[469] Cerebral amyloid angiopathy has been modelled in mice and produces spontaneous intracerebral haemorrhage most closely mimicking human ICH.[470] However acute haemorrhages obviously cannot be predicted or responded to swiftly enough to test pathophysiological hypotheses or acute intervention strategies.

Autologous blood injection is the longest-standing method.[61, 471] It has been applied to rodents, pigs, cats, dogs, primates and rabbits.[468] Lobar or deep ICH can be produced by injection or at infusion at arterial pressure. This method replicates the histopathological changes in human ICH moderately well, although it does not involve vessel rupture and hence therapies which may influence haematoma volume cannot be assessed. Long-term functional deficits are generally mild, making studies of long-term functional recovery

difficult.[127, 472] Additional problems include blood tracking along the needle path and intraventricular extension, both of which can be lessened by a 'double injection' technique,[473] in which a small volume of blood is injected initially to seal the needle track, followed later by the rest of the volume. The formation of thrombin – crucial in ICH pathogenesis – may not be as physiological in this model. In the brief period between drawing and injecting blood, significant blood clotting occurs in the injecting set (if blood is withdrawn into the glass portion of the syringe, thrombin may also adsorb to the syringe wall[474]). To overcome this, some researchers add a small amount of heparin.[475] Either way, the activity of thrombin may be diminished.

The collagenase method has been applied to rats,[62] mice[476] and pigs.[174] Collagenases are secreted by inflammatory and some tumour cells, and dissolve collagen, a component of the basal lamina of the BBB. Infusion of collagenase produces a dose-related reproducible ICH.[62] Unlike the direct injection method it allows assessment of interventions targeted at reducing haematoma volumes. However it causes diffuse leakage of blood and BBB disruption[477] rather than a single punctate bleeding site as probably occurs in human ICH.[24] It may produce more inflammation than the autologous injection model or human ICH[144, 468] and the resultant haematoma produces a greater degree of functional and histological injury, adjusted for haematoma volume, than does the direct injection method.[472] Blood-brain barrier disruption is greater and progresses over a longer time-frame.[472]

Behavioural testing is vital for establishing the efficacy of any therapeutic intervention. Of all the species listed above, the best characterised and validated behavioural tests in ICH have been developed for rats.[127, 468, 478]

## 1.9 Hypotheses

Following intracerebral haemorrhage various secondary processes are initiated, including reactive oxygen species formation, oedema and inflammation, the initial phase of which appears to be largely thrombin-mediated. These secondary injury processes may, at least in part, be substance-P dependent. This thesis therefore investigates this broad postulate by testing the following hypotheses:

1. That peri-haematomal SP is increased acutely following both collagenase and autologous blood ICH in male Sprague-Dawley rats, in a time-frame and distribution consistent with a possible pathophysiological role.

2. That NK1 antagonism decreases functional deficits, neuronal injury, oedema, blood-brain barrier disruption and neutrophil infiltration after collagenase ICH.

3. That, following intracerebral thrombin injections, SP is increased around the thrombin injection site, and that NK1R antagonism decreases injury post-thrombin injection.

4. That intracerebral injection of SP, in pathophysiologically relevant quantities, produces inflammation and oedema, and that this effect can be blocked by an NK1R antagonist.

For the purposes of testing these hypotheses rats were deemed the most suitable species for two main reasons: first, that the high-throughput needed to test these hypotheses in the relevant timeframe could not have been achieved with other species, and, second, that behavioural outcomes are best assessed in rats. For the testing of hypothesis 2, collagenase ICH was deemed most suitable, as thrombin is assumed to be more fully active in collagenase than autologous ICH. Additionally any possible detrimental effects of NK1R antagonism on haematoma expansion can be determined in this model (given the possible pro-coagulant effect of SP[339]).

# 2 Materials and methods

## 2.1 Animal Care

### 2.1.1 Animal ethics

All experimental work was in accordance with the guidelines established by the National Health and Medical Research Council, and was approved by the ethics committees of the University of Adelaide (approval numbers M-008-2008 and M-079-2008) and the Institute of Medical and Veterinary Science (approval numbers 163/07 and 158/08).

### 2.1.2 General

All experimental work was performed on male Sprague-Dawley rats, weighing between 300 and 340gm. These were obtained from the Gilles Plains Animal Resource Centre (Gilles Plains, South Australia) or from the Animal Resource Centre (Canning Vale, Western Australia). All animals were obtained at least 4 days prior to experiments. Animals were housed a minimum of two to a cage, at 24$^{o}$C in a conventional rodent room, on a 12-hour light-dark cycle, and fed and watered *ad libitum*. Animal numbers used in each experiment are detailed in the relevant chapters.

## 2.2 Experimental procedures

### 2.2.1 Anaesthesia

#### *Isoflurane and ventilation*

Isoflurane (VCA) was obtained from Independent Veterinary Supplies (Melrose Park, South Australia) and stored in a drug safe away from light and at a constant temperature. General anaesthesia was induced by placing animals in a transparent chamber and delivering 5% isoflurane in a 30:70 mix of oxygen and nitrogen via a calibrated vaporiser at a flow rate of 1.4L/min. Following induction, animals were either intubated (autologous blood injection group) or placed on a nose cone (all other animals). The decision to intubate autologous animals was based on two factors. First, as these animals were, by necessity, already arterially cannulated, blood gases could be easily obtained and ventilation optimised. Additionally, as surgery duration was considerably longer than in other experimental groups (75 versus 25 minutes), any uncorrected respiratory perturbations could have prejudiced the results. Conversely, intubation, arterial cannulation and ventilator titration would have more than doubled the length of surgery in other experimental groups, and this was felt more likely to lead to experimental error than a brief period of possibly suboptimal respiration.

Animals from the autologous blood group were intubated using a rat laryngoscope and with 14G plastic intravenous cannula, which was sutured under local anaesthesia to the cheek. Animals were connected via silicone tubing to a Harvard rodent ventilator (Harvard Instruments) and ventilated with 2% isoflurane in a 30:70 oxygen nitrogen mix, at between 60 and 80 breaths per minute with a tidal volume of 2.5ml and 3cm $H_2O$ of positive end expiratory pressure. Minute volume and oxygen was adjusted to maintain the pH between 7.4-7.5, $pO_2$ between 100-150mmHg and $pCO_2$ between 35-45mmHg.

Anaesthesia in all other animals was maintained at 2% via a nose cone with a 30:70 oxygen nitrogen mix at 1.4L/min. Post-surgery, aICH animals were extubated once making an adequate respiratory effort. Once breathing adequately, all animals were placed by themselves in a recovery box on a heatpad until moving spontaneously.

Animals requiring decapitation without perfuse fixation (ELISA, PCR, Evan's blue and brain water assessment groups) were deeply anaesthetised in an induction box with 5% isoflurane in a 30:70 oxygen nitrogen mix for approximately 5 minutes before decapitation.

#### *Local anaesthesia*

Bupivacaine 0.5% (AstraZeneca) was obtained from IVS and stored at room temperature in a drug safe. All animals received approximately 0.3mL bupivacaine via a 23g needle (while under general anaesthesia) prior to any skin incision, and again immediately prior to wound closure.

#### *Pentobarbital*

Pentobarbital (300mg/mL; Rhone Merieux) was obtained from IVS and stored at room temperature in a drug safe. Animals requiring perfuse fixation were administered 0.5-1mL of 30mg/mL pentobarbital intraperitoneally via a 25 gauge needle, with dose titration until all responses to pain were abolished.

### 2.2.2 Stereotactic injection of substance P

Substance P was titrated into aliquots on ice under oxygen free-conditions and using oxygen-free water to minimise the chance of any oxidisation (which can substantially reduce biologic activity).[479] After anaesthesia induction as described, the animal was placed in a stereotactic frame (Kopf Instruments) on a heat pad. A rectal thermometer was inserted and temperature maintained between 36.5-37.5$^{o}$C with the heat pad and a heat lamp, if necessary. The scalp was shaved, swabbed with alcohol and bupivacaine instilled. A midline scalp incision was made and the skull exposed. A burrhole was drilled with a hand drill 0.7mm anterior and 3.0mm lateral to Bregma.[480] Using a syringe driver (Harvard Instruments) and a 25 µL syringe

(Hamilton Company) varying amounts of substance P (Sigma S6883) were infused in 10µL oxygen-free normal saline over 5 minutes via polyethylene tubing attached to a 30G dental needle, which was inserted via the burrhole 6.0mm ventral to Bregma. The needle was left in place for five minutes, then withdrawn slowly. The hole was sealed with bone wax and the scalp wound closed with wound clips (Becton Dickinson, 9mm Autoclip) after irrigation with bupivacaine.

### 2.2.3 Autologous blood infusion intracerebral haemorrhage

Animals in the autologous blood were anaesthetised as described. They were then placed supine on a heat pad. A rectal thermometer was inserted and temperature maintained between 36.5-37.5$^{o}$C. The right femoral region was shaved, sterilised with alcohol and bupivacaine instilled. An incision from groin to knee was made and, using blunt dissection, the femoral artery isolated. An 8cm length of polyethylene tubing, bevelled at the front and connected to a truncated 23G needle (Becton Dickinson), was inserted into the artery and advanced 4cm. The tubing was tied in place and flushed with normal saline. Blood was drawn for analysis and respiratory parameters adjusted as necessary.

The animal was then turned prone and placed into a stereotactic head frame (Kopf instruments). The scalp was shaved, swabbed with alcohol and bupivacaine instilled. A midline scalp incision was made and the skull exposed. A burrhole was drilled with a hand drill 0.7mm anterior and 3.0mm lateral to Bregma.[480] 100 µL autologous blood was drawn from the femoral line directly into a 26 gauge syringe (Hamilton Company). This was then attached to the stereotactic frame and lowered 5.5mm ventral to Bregma. 10 µL blood was instilled over 1 minute and the needle advanced into the centre of the basal ganglia, a further 0.5mm ventral (to prevent blood back-tracking along the needle tract[473]). After a 2 minute pause, the rest of the blood was instilled by hand over 9 minutes (pilot experiments had shown that this gave a smoother injection than an infusion pump, which infused erratically due to pressure build-up from intraluminal blood clot.) The needle was then left in place for 5 minutes. During this time the arterial line was withdrawn and the femoral artery tied off. After further bupivacaine the femoral wound was closed with wound clips. The intracerebral injecting needle was slowly withdrawn and the burr hole closed with bone wax. Bupivacaine was instilled and the wound closed with wound clips. Anaesthesia was ceased and once adequate respiratory effort was present, the animal extubated. Vehicle controls underwent an identical procedure, save that normal saline alone (100µL) was injected

### 2.2.4 Collagenase infusion intracerebral haemorrhage

In the pilot phase various doses of collagenase were trialled. 0.1U caused a small ICH and 0.4 U a fatal ICH. As has been previously reported,[472] 0.2U caused a large ICH with persistent neurological deficits and minimal mortality, suitable for study.

After anaesthesia induction as described, the animal was placed in a Kopf stereotactic frame on a heat pad. A rectal thermometer was inserted and temperature maintained between 36.5-37.5$^{o}$C. The scalp was shaved, swabbed with alcohol and bupivacaine instilled. A midline scalp incision was made and the skull exposed. A burrhole was drilled with a hand drill 0.7mm anterior and 3.0mm lateral to Bregma.[480] Using a syringe driver (Harvard Instruments), 0.2U collagenase in 2 µL was infused over 4 minutes via polyethylene tubing attached to a 30G dental needle, which was inserted via the burrhole 6.0mm anterior to Bregma. The needle was left in place for five minutes, then withdrawn slowly. The hole was sealed with bone wax and the scalp wound closed with wound clips after irrigation with bupivacaine. Vehicle controls underwent an identical procedure, save that normal saline alone (2 µL) was injected.

### 2.2.5 Stereotactic thrombin injection

This was performed in an identical fashion to collagenase and substance P injections, save that 5U of rat thrombin (Sigma T5772), in 5mcL oxygen-free normal saline was injected over 5 minutes. Care was taken to ensure that all thrombin remained within the plastic tubing, rather than entering the syringe itself, as thrombin is known to adhere to glass.[474]

### 2.2.6 Splenectomy

A group of rats was splenectomised 2 weeks prior to collagenase ICH (cICH) to examine the interaction between NK1R antagonism and the post-ICH peripheral inflammatory response.

Animals were anaesthetised as above and placed on a nose cone. A rectal thermometer was inserted and temperature maintained between 36.5-37.5$^{o}$C. The abdomen was shaved, swabbed with alcohol and bupivacaine instilled. A 2cm incision was made, parallel and just lateral to the midline. The peritoneum was retracted and the spleen externalised. The vascular bundles were tied off and/or cauterised and the spleen removed. The muscle layer was closed with absorbable sutures and the skin closed with wound clips.

### 2.2.7 Post-surgery recovery

All animals were placed by themselves in a recovery box on a heatpad until moving spontaneously. They were then returned to their homecage, which was placed half-on and half-off a heatpad for a minimum of 24 hours or until animals were grooming, feeding and ambulating at normal levels (whichever was longest).

### 2.2.8 Perfuse fixation

At pre-determined post-surgery timepoints, animals for histological assessment were perfuse-fixed with 10% neutral buffered formalin (NBF) for optimal assessment of paraffin-embedded specimens.

Animals were given 5000U in 1mL of porcine heparin via a 25G needle intraperitoneally 10 minutes prior to perfusion. Anaesthesia was induced with pentobarbital as described and titrated until pain responses were completely abolished. The upper peritoneal cavity was exposed, the diaphragm incised, and the thorax opened bilaterally and retracted. The left ventricular apex was grasped with a towel clip and a blunt 19G needle inserted through the left ventricle into the aorta. The right atrium was incised and 10% NBF driven under pressure (180mmHg) until fluid from the right atrium was clear. Animals were decapitated 1 hour later (to minimise artefactual damage to blood vessels). The brains were extracted and placed in NBF for processing a minimum of 24 hours later.

## 2.3 Drug treatments

Animals were randomly assigned to intravenous N-acetyl-L-tryptophan and L-733,070 treatment groups (detailed in appropriate chapters) with the surgeon blinded to treatment assignment. Animals were briefly anaesthetised during the injection. Anaesthesia was induced as described, and animals placed supine on a heat pad, with their tails in warm water. Tails were cleaned, a tourniquet applied and the treatment slowly injected into the tail vein via a 30 gauge needle.

### 2.3.1 N-acetyl-L-tryptophan

N-acetyl-L-tryptophan (NAT, Sigma A-6376) is a selective antagonist of rat NK1 receptors.[461] It is non-blood brain barrier penetrant under normal circumstances. It is stored at 4$^{o}$C. It was prepared by dissolving 2.5mg/mL in basic normal saline, which was then pH adjusted to 7.4. The solution was stored at 4$^{o}$C until injection (less than 3 hours). A dose of 2.5mg/kg was administered 2 hours after injury (this dose has been previously shown in our laboratory to be optimal in both traumatic brain injury [461] and experimental stroke.[481])

### 2.3.2 L-733,060

L-733,060 (Tocris, 1145) is a specific blood-brain barrier penetrant antagonist of the rat NK1 receptor. It was stored at room temperature and dissolved at a concentration of 1mg/mL in pH adjusted normal saline. The solution was stored at 4$^{o}$C until injection (never longer than 3 hours) and administered at a dose of 1mg/kg. This dose was 5-fold greater than the dose required to abolish plasma extravasation in the dura following electrical stimulation.[482]

## 2.4 Neurological assessment

Functional deficits were assessed at various time-points following both collagenase intracerebral haemorrhage (see individual chapters for details). All tests were performed at a consistent time in the morning, in the same room, on the same equipment, by the same investigator and in the same order, to minimise confounding factors. The assessor was blinded to treatment assignment. These tests were assessed in a pilot fashion in chapter three, with occasionally minor modifications of the original protocol, to ensure both reproducibility and sensitivity to injury.

### 2.4.1 Rotarod

The rotarod has been extensively used in our laboratory[483] and elsewhere as a test of integrated sensori-motor function following rodent brain injury of various kinds, including ICH.[484] It tests motor strength, speed and coordination and consists of a motorised rotating assembly of eighteen 1 mm metal rods on which the animals are required to walk for a period of 2 minutes (Figure 10). After a 10 second acclimatisation period, the rotational speed of the apparatus is increased by 3 rpm every 10 seconds until maximal speed is reached (30 rpm). The test is complete if the animal reaches the maximum time allowable (120 seconds) or if the animal is unable to continue (i.e. the animal falls off or rotates twice without walking).

| Time | Rotarod speed |
|---|---|
| 0-10 seconds | 0rpm |
| 10-20 seconds | 3 rpm |
| 20-30seconds | 6 rpm |
| 30-40 seconds | 9 rpm |
| 40-50 seconds | 12 rpm |
| 50-60 seconds | 15 rpm |
| 60-70 seconds | 18 rpm |
| 70-80 seconds | 21 rpm |
| 80-90 seconds | 24 rpm |
| 90-100 seconds | 27 rpm |
| 100-120 seconds | 30 rpm |

**Figure 10. Rotarod. The rat is placed on the rotarod, which accelerates every 10 seconds as shown to a maximum speed of 30rpm and duration of 120 seconds. The test is complete when the animal either rotates twice in a row, falls off, or completes the two minutes.**

Animals are pre-trained on the rotarod device for 5 days prior to surgery. Baseline uninjured performance is determined at the end of the 5 day training period, and compared with post-injury performance.

### 2.4.2 Sticky label test

Focal injury to the basal ganglia commonly causes sensory neglect (a preference of attention to the uninjured side). If the injury extends into the lateral thalamus or internal capsule, it may also cause a sensory deficit. For these reasons, following basal ganglia injury, animals will take longer to respond to a novel stimulus on the contralateral forepaw, and longer to remove that stimulus.

The sticky label test is a reliable and sensitive measure of this injury[485] and has been successfully used in rats following intracerebral haemorrhage.[478] Various forms of the test exist. In the form reported in this thesis, the animal is restrained and a 1x1cm piece of adhesive sticky tape applied diagonally across either forepaw (right or left in random order (Figure 11)). The animal is then placed on top of an open metal tray, with gentle pressure applied simultaneously to both forepaws, and released. Both the time to touch and time to remove the tape are recorded. The test is aborted at 180 seconds if the rat has not removed the stimulus by this time. The test is repeated 3 further times (i.e. 2x each forepaw). The average latencies to touch and to remove are averaged and the latency difference between left and right recorded.

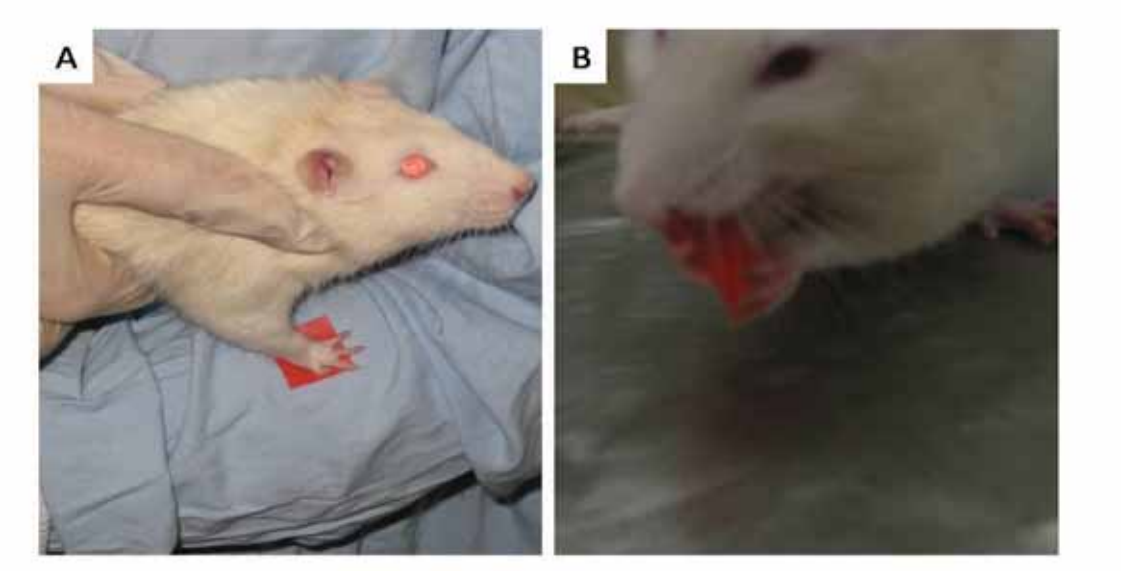


**Figure 11.Sticky label test. (A) A square sticky label is applied diagonally across the forepaw. (B) The animal is released on a metal table. Healthy animals contact and remove the label within 10 seconds.**

### 2.4.3 Tapered ledged beam test

Injury to the rat basal ganglia, causes a motor deficit, as well as sensory deficits and neglect. Researchers had, in the past, assessed this with a balance beam, measuring the number of paw slips contralateral to injury. However, not only was this potentially distressing to rats, rats quickly adjusted to the motor deficit. However, by adding a side ledge, not only are rats less likely to fall, a chronic injury can be demonstrated, as rats use the ledge as a 'crutch'.[486]

The ledged beam is tapered as shown (Figure 12), with a 'stinky dark box' at the far end filled with food and interesting objects to provide an incentive for the rats to move to the other side. The beam is placed in front of a mirror to allow both sides of the beam to be viewed simultaneously. Trials are videotaped and each rat is assessed three times.

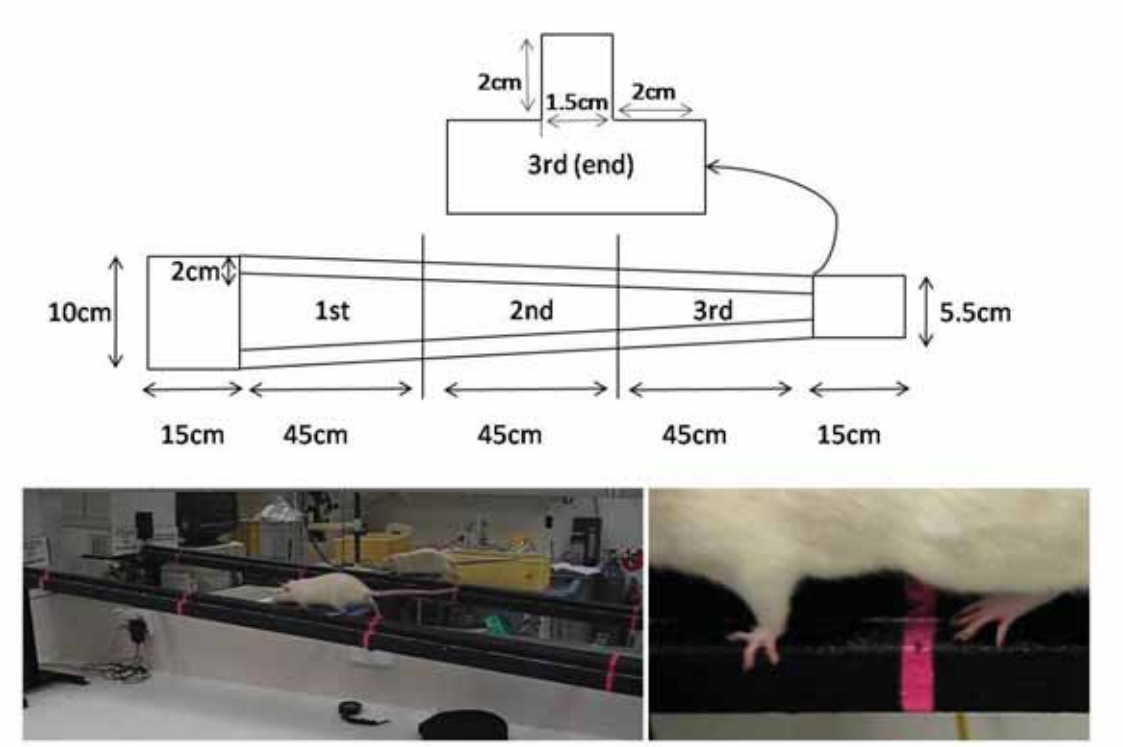


**Figure 12. Tapered ledged beam. Schematic diagram (not to scale). Animals are placed in the loading bay and encouraged along the beam to the 'stinky box' at the end. A 2cm ledge traverses the length of the beam on each side to provide a 'crutch'. Faults in loading and offloading sections (15cm long) are not counted. A forepaw 'full' and hindpaw 'half' foot fault are demonstrated.**

Rats are placed in the 'staging area', and encouraged with a gentle push across the beam. Animals are pre-trained 5 times per day for 5 days and videotaped on the final day, to establish any baseline asymmetry. Rats are then tested 3 times on each day of post-injury functional assessment. Trials are videotaped and scoring is performed later 'off-line' to allow slow-motion replay. Animals unable to traverse the beam were scored as 100% foot faults. Full foot-faults were scored if the whole paw and heel were placed on or over the ledge, and

half-faults if any part of the paw touched the ledge. The time to traverse the beam was also recorded. Twenty seconds was the maximum time allowable.

Scoring of asymmetry is performed as follows.[486] The total number of steps along the tapered portion of the beam is counted, and then divided by six. Then, for each of the three sections, the number of full- and half-faults is counted for both contralateral and ipsilateral fore- and hindlimbs, yielding six 'footfault' scores. Each of these is divided by the number obtained above to give the percentage faults per step. For each section, the percentage ipsilateral footfaults per step is then subtracted from percent contralateral faults per step to give a percent asymmetry for the three sections. Higher percentages denote a greater relative degree of faulting with the contralesional limb.

Post-injury, deficits are seen most consistently in accurate negotiation of the third (most narrow) stage. Total footfaults and time to traverse the beam are less sensitive to injury.[485]

### 2.4.4 Vibrissae-elicited stimulation test

As well as causing sensory neglect, focal injury to the basal ganglia can interfere with reflex sensorimotor processing. Normal rats reflexively respond to vibrissae stimulation and, if vibrissae are touched while the animal is suspended, will invariably, rapidly and accurately reach out with the forepaw towards the source of stimulus.[485, 487]

In the vibrissae-elicited stimulation test (VEST), animals are restrained and the forepaw contralateral to injury is allowed to dangle freely. The vibrissae are brushed against the corner of a table (Figure 13). Animals with a basal ganglia injury will fail to reach out, or miss the target. As animals recover, the percentage of correct placements improves.

**Figure 13. Vibrissae elicited stimulation test. The relaxed animal's hindlimbs and torso are restrained, and its vibrissae are brushed against the corner of a table. The uninjured rat quickly, invariably and accurately places its ipsilateral forelimb on the corner; animals with striatal injuries fail to do so.**

Animals are acclimatised to handling for five days prior to testing to minimise struggling during the test, and then tested at various timepoints following injury. The test is repeated a total of twenty times, with a minimum of 4 rest periods in between. If the animal struggles, it is briefly rested and the test recommenced. A trial is only included if the rat does not struggle. Each trial is scored as successful or unsuccessful and the total testing period scored as a mark out of twenty.

### 2.4.5 Elevated drag test

As well as causing neglect and interfering with rapid sensorimotor processing, basal ganglia injury can cause unilateral bradykinesia or akinesia (slow or absent movements). In the pilot behavioural phase of this PhD, it was noted that there was a marked difference in forelimb use between injured and uninjured animals, when dragged backwards by the tail with the hindlimbs elevated (Figure 14). Normal animals, when dragged backwards by the tail with hindlimbs elevated, will perform rapid, alternating stepping movements in an attempt to either impede backward movement, or to rotate around towards the examiner. With basal ganglia injury, these reflex movements of the contralateral forepaw are slowed or absent.

**Figure 14. Elevated drag test. Rats are pulled backwards by the tail with the hindlimbs elevated. The normal response is to use both forelimbs alternately, in an attempt to either retard backwards movement or to turn the body around. The speed of the drag is adjusted to prevent the body turning.**

The elevated drag test is a variation on the 'stepping test' which is often used for assessment of forelimb akinesia in experimental Parkinson's disease.[488] This is of relevance in intracerebral haemorrhage as the target of dopamine released from the substantia nigra is the striatum – which is lesioned in experimental ICH. In the elevated drag test the animal is gently lifted by the tail and dragged backwards over a distance of 1.35m, at a speed which

induces adjustment steps in the paw ipsilateral to injury (the unaffected side), but which prevents the animal from turning towards the direction of movement. Normally no asymmetry is seen, although some variation does exist.

No acclimatisation to the test is required: animals are assessed pre-injury to assess for any baseline asymmetry, and then assessed at various timepoints post-injury. Six trials are conducted, with rests in between. The trials are videotaped, and the total ICH-induced asymmetry determined using the following formula:

$$\% \text{ asymmetry} = \frac{(\text{steps (R)} - \text{steps (L)})}{(\text{total steps})} \times 100 - \text{baseline \% asymmetry}$$

### 2.4.6 Other pilot behavioural tests

The five tests outlined above were determined to be most sensitive at detecting neurological injury following cICH, as determined by behavioural testing of the day 7 cICH group outlined in chapter 3. Two additional behavioural tests were performed in this pilot study: the elevated body swing test [489] and the modified[490] limb placing test.[491] The former involves lifting the rat from a flat surface and observing which way the body swings, over 20 trials. It has been previously reported that this is a sensitive measure of striatal injury. The latter scores a series of 6 limb placing tasks in response to various postural and environmental stressors.

These tests were found to be insensitive in detecting the level of injury induced by cICH at 7 days (see chapter 3). Therefore they were not used in assessing the effect of interventional therapy, as the likelihood of false negative conclusions was high.

## 2.5 Histological analysis

### 2.5.1 Brain sectioning

Following either perfuse fixation or fresh decapitation (for Evans blue, wet weight/dry weight, PCR and ELISA studies) brains were placed in a Kopf rodent brain blocker (Kopf, PA002). The frontal pole and olfactory bulbs were excised and discarded.

For histological assessment, the brain was sectioned into 5 consecutive 2mm slices (Figure 15). The needle tract lay at the border of the second and third slices, which also contained the bulk of the striatum, the intracerebral haemorrhage and its perihaematomal zone. For wet weight/ dry weight assessment and ELISA/PCR experiments, a four millimetre slice was taken, with the injection point at the centre (corresponding to slices 2 and 3 on the figure shown); this slice was divided into left and right. For PCR and ELISA experiments this slice was

bisected; the dorsal half was used for PCR studies and the ventral half for ELISA. For determination of brain water content (wet-weight/dry weight) the cerebellum was also excised and used as a control.

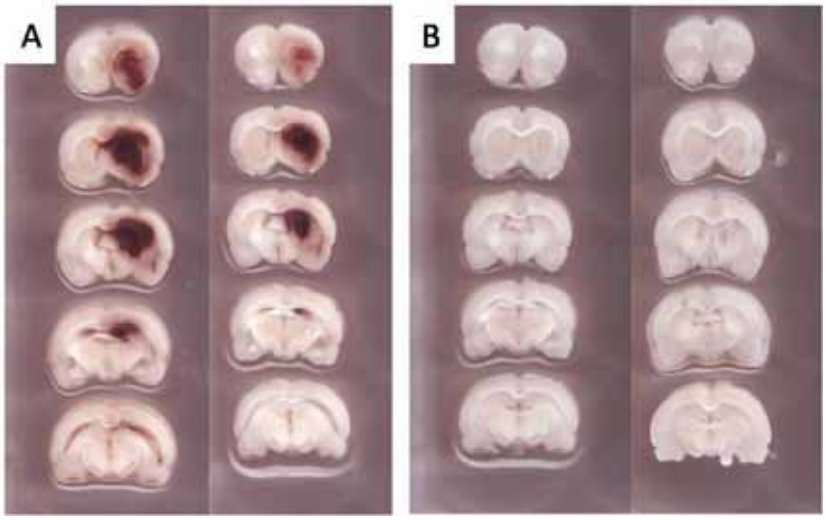


**Figure 15. Brain sectioning. Representative sections of rat brain 24 hours following 0.2U collagenase (A) or vehicle (B). Sections 2 and 3 from the top contain the striatum and the bulk of the haematoma.**

Prior to further processing, sections obtained for histological assessment and determination of Evans blue extravasation were then scanned at high resolution (600 dpi) on a flatbed scanner (Canon, LIDE 100).

### 2.5.2 Haemorrhage quantification

From scanned sections as described above, the haematoma extent in each section was selected automatically by Adobe Photoshop (Adobe Systems Inc., v6.0.1) using the 'magic wand' function - 'anti-aliased' and 'contiguous' with the default tolerance of '32'. This automatically outlines a smooth contiguous region (i.e. the haematoma), determined to be sufficiently similar to a user-defined point (in this case the haematoma centre) and dissimilar to surrounding areas (the striatum) by virtue of its imaging statistics, lessening the probability of error and bias (default settings were sufficient).

The anterior and posterior haematoma area in $mm^2$ for each slice was obtained by dividing the total number of haematoma pixels by the scanned resolution (558 per $mm^2$). The volume of haematoma (µL) in each slice was reached by multiplying the average haematoma area (front and back) by the slice thickness (20mm).

### 2.5.3 Brain processing for histological assessment

After sectioning, perfuse-fixed brains were placed in cassettes in NBF for a further 24 hours. They were then processed the following night, spending 20 minutes in each ethanol bath of

increasing concentration (50%, 70%, 80%, 95%, 100%, 100%), followed by 2 xylene baths (90 minutes each) and then paraffin baths of increasing duration (30, 60, 60 and 90 minutes). Sections were embedded the following morning in paraffin wax, sectioned (5 µm) with a microtome (Microm, HM330) and floated onto glass slides (Menzel-Glaser, Super-frost plus). Slides were then dried in hot air and stored for further processing in a humidified oven at 37$^{o}$C.

### 2.5.4 Haematoxylin and eosin (H&E) staining

Sections were dewaxed by heating, then passed through 2 changes each of xylene and ethanol (2 minutes each). Slides were then placed in haematoxylin (4 minutes), acid alcohol (5 dips) and lithium carbonate (1 minute), washing before and after each step. They were then placed in eosin (2 minutes), ethanol (2x 2 minutes), histolene (2x 2 minutes) and mounted in DePeX (BDH, UN1993). They were assessed with light microscopy (Olympus, BX45) or scanned at high resolution (Nanozoomer, Hamamatsu) and viewed with the associated proprietary viewing software (NDP view v1.1.27, Hamamatsu.)

### 2.5.5 Immunohistochemistry

Sections were immunostained with the 3,3’ diaminobenzidine (DAB) method for substance P and its NK1 receptor, myeloperoxidase ((MPOX) a neutrophil marker), ED-1 (a marker of activated microglia), IBA1 (a pan-microglia marker), albumin (a marker of blood-brain barrier dysfunction) and glial fibrillary acidic protein ((GFAP) an astrocyte marker).

Sections were taken to water as described above. Endogenous peroxidase activity was blocked by incubation with 0.5% hydrogen peroxide in methanol for 30 minutes. Sections were washed in phosphate-buffered saline ((PBS) 2x 3 minutes) and retrieved by heating at close to boiling point for 10 minutes (SP in EDTA, others in citrate (except albumin, which requires no retrieval)).

Once cooled, specimens were washed in PBS (2x 3minutes) and blocked with 3% normal horse serum in PBS for 30 minutes. The primary antibody was applied overnight ((goat anti-SP 1:2000, Santa Cruz sc-9758), (rabbit anti-NK1R 1:1500, Advanced targeting systems AB-N04), (mouse anti-ED-1 1:400, AbD Serotec MCA341R), (rabbit anti-GFAP 1:40000, Dako Z0334), (rabbit anti-MPOX 1:60000, Dako A0398), (rabbit anti-IBA1 1:50000, Abcam ab 5076) and (goat anti-albumin 1:20000, Cappel 0113–0341)). The following morning, after 2x PBS washes, the appropriate anti-species IgG biotinylated antibody was applied (1:250, 30 minutes). Sections were again washed (2x 3 minutes PBS) and then incubated with streptavidin peroxidase conjugate (1:1000, 60 minutes). After a further 2x 3 minute PBS washes, the immunocomplex was visualised by the precipitation of DAB (Sigma, D-5637) in

the presence of hydrogen peroxide. Sections were then washed, lightly counterstained with haematoxylin, dehydrated and mounted in DePeX from histolene. Sections were assessed with light microscopy or scanned at high resolution and viewed with viewing software.

### 2.5.6 Immunofluorescence double labelling

In order to determine the cellular localisation of substance P and its NK1 receptor, double labelling was performed with both GFAP and IBA1/ED-1. In preliminary investigation it was determined that both substance P and NK1 receptor immunofluorescence was most effective with a three-stage process (that is primary antibody, then biotinylated secondary antibody, then streptavidin-conjugated fluorophore). All other immunofluorescence was performed in a two-stage process (primary antibody, then fluorophore-conjugated secondary.)

Slides were prepared identically to immunohistochemistry slides until the addition of the primary antibody, with the exception that all antibody retrieval was performed with EDTA. At this stage, while anti-substance P and anti-NK1 receptor antibodies were applied as previously, slides were co-incubated with a higher dilution of the second antibody (GFAP 1:6000, ED-1 1:60, IBA1 1:7500, and for NK1R , mouse anti-GFAP (1:200, Dako M0761)). After overnight incubation and two PBS washes, an anti-goat or –rabbit biotinylated secondary antibody was applied (1:250) along with the appropriate anti-mouse or anti-rabbit conjugated fluorophore (1:250 AlexaFluor 594, Molecular Probes). After 30 minutes, specimens were washed and the tertiary streptavidin conjugated fluorophore (1:500 Alexa Fluor 488, molecular probes) was applied for 1 hour. After 2 further washes, slides were mounted (ProlongGold anti-fade reagent, Molecular Probes), sealed with nail polish and viewed with a fluorescence microscope (Olympus, BX6).

### 2.5.7 Fluoro-Jade staining

Sections were dewaxed by heating, then passing through 2 changes each of xylene and ethanol (2 minutes each). Slides were then placed for 2 minutes in 70% alcohol, and subsequently washed twice for two minutes in $dH_20$. Potassium permanganate (0.06%) was applied (from 240mg in 400mL $dH_20$) for 10 minutes. Slides were briefly dipped in $dH_20$, then placed for two minutes in a new container of $dH_20$. Slides were then incubated in the dark for twenty minutes with fluoro-Jade C (FJC) staining solution, which was prepared by adding 1mL of 0.01% FJC stock (1mg in 10mL $dH_20$) to 99mL of 0.1% glacial acetic acid solution (396µL in 396 mL $dH_20$). All further steps were also performed in the dark: first, 3x1 minute $dH_20$ washes, then drying at 45$^{o}$C for 30 minutes, then placing in histolene and mounting in DePeX. Sections were scanned at high resolution and viewed with the associated proprietary viewing software.

## 2.6 Oedema measurement

Brain water content was assessed with the wet weight- dry weight method.[492] Animals were deeply anaesthetised with 5% isoflurane and decapitated. Brains were quickly removed, and a 4mm slice of brain sectioned, 2mm either side of the injection site. This was bisected into right and left hemispheres, and placed in pre-weighed air-tight glass vials, which were then again weighed to obtain 'wet weight'. The cerebellum was also removed and weighed. Specimens were then placed in an oven and dried at 100$^{o}$C for 24 hours with the lids off. Lids were then replaced and jars allowed to cool for five minutes. Specimens were then weighed ('dry weight'). Percentage brain water was calculated according to the following formula:

$$\text{Percentage brain water} = \frac{\text{(Wet weight – dry weight)}}{\text{Wet weight}} \times 100$$

## 2.7 Assessment of blood-brain barrier permeability

Animals were assessed for permeability of brain vasculature with Evans Blue (Sigma, E-2129), a blue dye which binds tightly to albumin.[493] Albumin cannot cross the blood-brain barrier (BBB) except under pathological conditions. Hence quantification of Evans Blue (EB) within the brain can quantify BBB disruption.

Evans blue could not reliably be injected into the tail vein. Hence, animals were briefly reanaesthetised (approximately 20 minutes), the right femoral vein exposed and cannulated, and 4% EB in NS (1.5mL/kg) injected (this concentration is routinely used in the literature and successfully used in our laboratory.) The vessel was tied off and the wound closed with wound clips after instillation of bupivacaine.

Various injection and decapitation time-points were assessed to determine the optimal exposure period (Figure 16). Following cICH, there was gross leakage of EB from 5-8 hours, suggestive of ongoing bleeding, and minimal leakage from 8-12 hours. It was finally determined that injection of EB 12 hours post-haemorrhage, and detection at 23 hours was optimal. Optimal injection/detection timepoints following substance P and thrombin injection were 0-5 and 4-8 hours (data not shown).

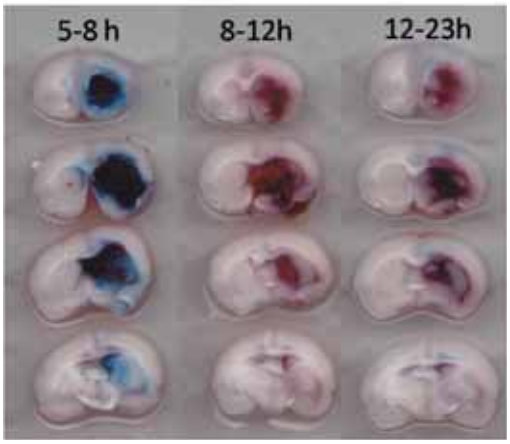


**Figure 16. Evans blue extravasation at various timepoints. There is gross leakage at the early timepoint, probably from ongoing bleeding. Little EB is present from 8-12 hours. Faint haematomal (purple tinge to haematoma) and peri-haematomal leakage can be detected at the later timepoint.**

Animals were deeply anaesthetised with isoflurane, and the aorta cannulated as for perfuse fixation. To minimise any bleeding caused by exposure to heparin, but to allow adequate blood flushing, 5000U heparin in 1mL was instilled directly into the aorta and allowed to circulate for twenty seconds. The right atrium was then incised and animals were perfused with 0.9% normal saline until the perfusate from the right atrium was clear. Animals were then decapitated, the brain removed and placed in a Kopf rodent blocker, and cut into 2mm sections. Sections were scanned on a flatbed scanner (Canon, LIDE 100).

The 2x2mm slices incorporating the haemorrhage site centrally were taken, divided into left and right, and placed in a pre-weighed cryotubes. A cerebellar section was also taken. The specimens were immediately weighed, then frozen at -80$^{o}$C.

At a later time, specimens were thawed and homogenised in 1mL of distilled water. 1mL of the potent solvent dimethylformamide ((DMFA) Sigma, D-4551) was added to dissolve the EB out of tissues, and tubes vortexed. Samples were placed in an oven at 60$^{o}$C overnight. The following morning they were vortexed twice for 10 minutes at 13,200 rpm. 1mL of supernatant was added to 1mL distilled water. The absorbance was measured at 620nm using a Nanophotometer (Implen, Australia) and using a 3:1 ratio of $dH_2O$:DMFA as a blank. The amount of extravasated EB was obtained from a previously obtained standard curve of EB in water/dimethylformamide, and expressed as ng/mg brain tissue.

## 2.8 ELISA for substance P

Brain tissue extracted for ELISA consisted of the ventral half of the striatum (a 4mm thick slice centred on the injection site) and the overlying cortical and subcortical structures.

### *Protein extraction and estimation*

Immediately following decapitation, the tissue was weighed, snap frozen and stored at -80$^{o}$C. At a later time-point, tissue was thawed and placed in a glass homogeniser and a 10:1 ratio of homogenisation buffer was added. The homogenate was vortexed on ice every 5 minutes for 20 minutes, then centrifuged at 8500 rpm for 15 minutes. The pellet was discarded and the supernatant refrozen.

A 50µL aliquot was used to estimate protein concentration against a standard curve derived from serial dilutions of bovine serum albumin (BSA (Sigma A2153)). 5µL of supernatant or BSA was added to recommended amounts of Biorad protein assay reagents (500-0113, -0114 and -0115). Three wells were performed for each specimen and readings averaged. Absorbance was read at 620nm.

### *ELISA*

Specimens were diluted in TRIS buffered saline (TBS) to derive protein concentrations of 400ng per 100µL. 100µL of sample in triplicate was then added to a 96-well plate (Nunc, F96 Maxisorp). Blank wells (a minimum of 6) were included as controls. Specimens were allowed to coat the wells overnight at 4$^{o}$C. The samples were then tipped out and wells blocked with 0.5% gelatine for 1 hour. After 3 TBS rinses 100µL SP antibody (Chemicon, 1:1000, AB1566) was added and incubated at 37$^{o}$C for one hour. Three further rinses were performed and 100µL anti- rabbit horse radish peroxidase added (Molecular and Life Sciences Biobar, 1:500), incubating as above. Specimens were drained and rinsed 4 times in TBS. The liquid substrate system 3,3,5,5-tetramethylbenzidine (TMB) was added (100µL/well) for 150 seconds. The reaction was stopped with 50µL 0.5M $H_2SO_4$. Absorbance was read at 450nm.

## 2.9 Real-time RT-PCR for SP and NK1 receptor mRNA

### *RNA Extraction*

Total RNA was extracted from the left and right dorsal striatum with overlying cortex using the RNeasy Lipid Tissue kit (Qiagen) according to the manufacturer's instructions. Fifty mg tissue was used in each RNA extraction, which included an on-column DNase treatment step (Qiagen). RNA was quantified by UV spectrometry using the Nanophotometer (Implen) to measure absorbance at 230, 260 and 280 nm. RNA integrity was evaluated using the Agilent Bioanalyzer RNA 6000 Nano Chip (Series II) kit.

### *Reverse Transcription*

Complementary DNA was synthesised using the SuperScript III Reverse Transcription kit (Invitrogen). Two µg total RNA was added to 250 ng random hexamers (Geneworks), 1 mM of each dNTP (deoxynucleoside triphosphate (Invitrogen) and nuclease-free water to 13 µL.

Reactions were heated to 65°C for 5 minutes then immediately placed on ice for 1 minute. To each tube, 4.75 µL 5x First Strand Buffer, 1 µL RNase OUT (Invitrogen), 0.02 M dithiothreitol and 200 units SuperScript III reverse transcriptase were added. Reactions containing nuclease-free water in place of enzyme served as negative controls. Reactions were incubated at 25°C for 5 minutes, 55°C for 60 minutes and 70°C for 15 minutes. cDNA was diluted to 10 ng/µL with nuclease-free water and stored at -80°C.

### *Real-time PCR*

Primer sequences are shown in table 1.

Table 1: Details of primer sequences used in real-time RT-PCR amplification.

| Symbol | Accession No. | Name | Primer Sequences[1] (5′ → 3′) | Size[2] (bp) | $T_{A3}$ | Reference[4] |
|---|---|---|---|---|---|---|
| SP | NM_012666 | Substance P | tggtcagatctctcacaaaagg<br>tgcattgcgcttctttcata | 99 | 60 | Novel |
| NK1R | NM_012667 | Neurokinin1 receptor | tacttcctgcctctactggt<br>gttgatgtagggcaggagga | 210 | 62 | Yamaza[494] |
| GAPDH | NM_017008 | Glyceraldehyde-3-phosphate dehydrogenase | tgcaccaccacctgcttagc<br>ggcatggactgtggtcatgag | 87 | 57 | Li[495] |
| β2MG | NM_012512 | β-2-microglobulin | acatcctggctcacactgaa<br>atgtctcggtcccaggtg | 109 | 60 | Novel |
| POL2R | XM_001079162 | RNA Polymerase II | tttgaggaaacggtggatgt<br>tggcccagcataatattctca | 92 | 56 | Novel |
| HPRT | NM_012583.2 | Hypoxanthine guanine phosphoribosyltransferase | ttgttggatatgcccttgact<br>ccgctgtcttttaggctttg | 105 | 60 | van Wijngaarden[496] |
| GUSB | NM_017015 | β-glucuronidase | tccttccatgtatcccaagg<br>tggtaggggtggtgtacagg | 104 | 60 | Novel |
| TBP | NM_001004198 | TATA Box Binding Protein | cagccttccaccttatgctc<br>tgctgctgtctttgttgctc | 165 | 60 | Pohjanvirta[497] |
| SDHA | AB072907 | Succinate dehydrogenase complex, subunit A | agacgtttgacaggggaatg<br>tcatcaatccgcaccttgta | 160 | 60 | Pohjanvirta[497] |

**1** Forward primer sequence on upper line, reverse sequence on lower line.
**2** Amplicon lengths in base pairs.
**3** TA indicates optimum annealing temperature (ºC).
**4** Novel indicates that primers were designed by our laboratory using Primer3Plus software.

Real-time RT-PCR was carried out using 10µL 2x Invitrogen Platinum SYBR Green SuperMix-UDG, 300nM forward and reverse primers (400nM for POL2R and GAPDH), 1µL cDNA and nuclease-free water in a total volume of 20µL. One hundred mM $MgCl_2$ (Invitrogen) was added to POL2R reactions. A set of standards was included in each run, comprising five-fold

serial dilutions made from aliquots of pooled cDNA, derived from an RNA pool of all samples. Serial dilutions contained the following amounts of cDNA: 50ng, 10ng, 2ng and 0.4ng. The standard series encompassed the unknown cDNA concentrations.

Amplification was carried out in a Rotor-Gene 3000 (Corbett Research) with an initial UDG incubation of 50$^{o}$C for 2 minutes, initial denaturation of 95$^{o}$C for 2 minutes, followed by 40 cycles of: 95$^{o}$C for 15 sec denaturation, primer-specific annealing temperature for 15 sec,[498] and 72$^{o}$C for 15 sec extension. Fluorescence data were collected during the extension step of each cycle. Specificity of amplicons was verified by melting curve analysis after 40 cycles (72$^{o}$C to 95$^{o}$C) and 2 % agarose gel electrophoresis stained with ethidium bromide and visualised under UV light. All cDNA samples were run in triplicate. Negative controls containing water instead of cDNA present in all runs. No-reverse transcriptase controls were included for each gene to test for genomic DNA amplification.

### *Data Analysis*

Standard curves made from serial dilutions of pooled cDNA were used to calculate PCR efficiency. The cycle threshold (Ct) of an individual sample reflects the cycle at which a detectable number of PCR products have accumulated above background fluorescence.[499] Ct values were calculated from the standard curve, entered into the qBasePlus software[500] and used to generate an input file for geNorm v3.5.[501]

geNorm determined the most stable reference genes out of the panel of candidate genes using expression stability analysis by pairwise correlations. An expression stability measure, *M*, was assigned to each gene, which was used to rank candidate reference genes in order of stability. The most stable reference genes were determined in the following groups: all cICH and saline vehicle samples; 5 hour cICH and saline vehicle samples; 24 cICH and all saline vehicle samples; RBG only from all cICH and saline vehicle samples; LBG only from all cICH and saline vehicle samples. The most stable genes across timepoints were β2MG, GUSB, POL2R and GAPDH. Normalised mRNA levels of SP and NK1R were calculated using qBasePlus once the most stable reference genes had been determined.

## 2.10 Quantitation of immunohistochemical staining

Quantitation of protein is arguably best assessed by ELISA – however, such quantitation only allows large areas to be assessed. For instance, the perihaematomal zone is difficult to isolate in fresh tissue. Additionally, for each timepoint assessed by ELISA, an additional group of animals (at least five) needs to be sacrificed. Immunohistochemical staining for protein allows visualisation of distinct regions and cell subpopulations. However, assessment of up- or downregulation of a particular protein is open to bias and, at best, only partially quantitative.

Ruifrok and Johnston[502] described a mathematical method for separation and quantification of histochemical staining by deconvolution of the colour information in RGB images. The method they describe can reliably separate the blue of haematoxylin staining from the brown of diaminobenzidine.

As part of this thesis we developed a method for the semiquantitation of deconvolved Diaminobenzidine staining. With this method objective semi-quantitation of protein levels in brain regions and subregions can be performed, and combined with histological assessment of protein distribution and concentration, without the need for extra animal groups as would be necessary for ELISAs.

Slides previously stained by the DAB method were scanned at high resolution (Nanozoomer, Hamamatsu) and viewed with the associated proprietary viewing software (NDP view v1.1.27, Hamamatsu.) Either whole hemispheres or smaller areas were virtually dissected using this software. Jpeg images were exported into ImageJ (v1.40g NIH, Bethesda, USA). Haematoxylin and DAB stains were separated using an NIH ImageJ macro,[503] following background subtraction with color correction (the 'rolling ball' method).

Once the DAB stain is separated, the relative brownness of each pixel in the image can be obtained from a histogram (each pixel has a colour intensity weighting from 0-255). The total number of pixels in any given section multiplied by 255 expresses the maximum theoretical 'brownness'. If the actual brownness values (0-255) for all pixels are added together, and then divided by this theoretical number, the result is a measure of actual versus maximum possible 'brownness', expressed as a fraction of 1 ('DABwt%'). Pixels with mimimal (0 or 1) 'brownness' were discarded as these represented empty blood vessels, ventricles or areas outside the brain. As the basic principle of immunohistochemistry is that staining intensity varies with the amount of protein present, a semi-quantitative measure of protein content can thus be reached.

One of the potential criticisms of semi-quantitative analysis using colour deconvolution of DAB-stained slides is that DAB does not follow the Beer-Lambert law, as it scatters, rather than absorbs light, and has different spectral characteristics at light and dark staining intensities[504] (the Beer-Lambert law describes a linear relationship between the concentration of a compound and its optical density). To determine whether this potential limitation invalidated the method described (at commonly used DAB staining intensities), we stained control sections of human brainstem for substance P using serial dilutions of primary antibody (a minimum of 2 per dilution) to act as a surrogate measure of antigen dilutions

(Figure 17a). We also studied the relationship between DABwt% and time of DAB incubation (Figure 17b).

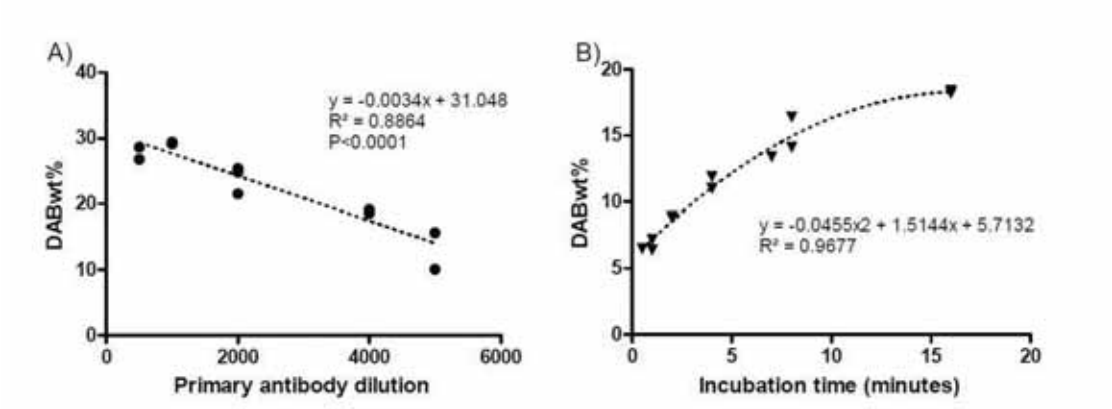


**Figure 17. (A) DABwt% assessed in human brainstem with variable dilutions of primary antibody to substance P (primary antibody dilutions serve as a surrogate of protein content). There was a highly significant correlation which did not differ from linearity (Runs test) across the DABwt% commonly used for visual (subjective) analysis. Similar results were demonstrated with other antibodies in common use (not shown). (B) DABwt% assessed in human brainstem with variable DAB incubation periods. There was a highly significant correlation (non-linear due to the saturability of the reaction with DAB).**

Using the method described, there appeared to be an inversely linear relationship between antigen concentration and DABwt% (Figure 17a) - and therefore linear correlation with antigen concentration. The method also clearly distinguishes and quantifies the increasing DAB intensity observed with increasing incubation times (Figure 17b).

A more experimentally relevant example is shown in Figure 18 and Figure 19, where the progressive increase in albumin immunoreactivity (IR) 5 and 24 hours following thrombin injection is semi-quantified.

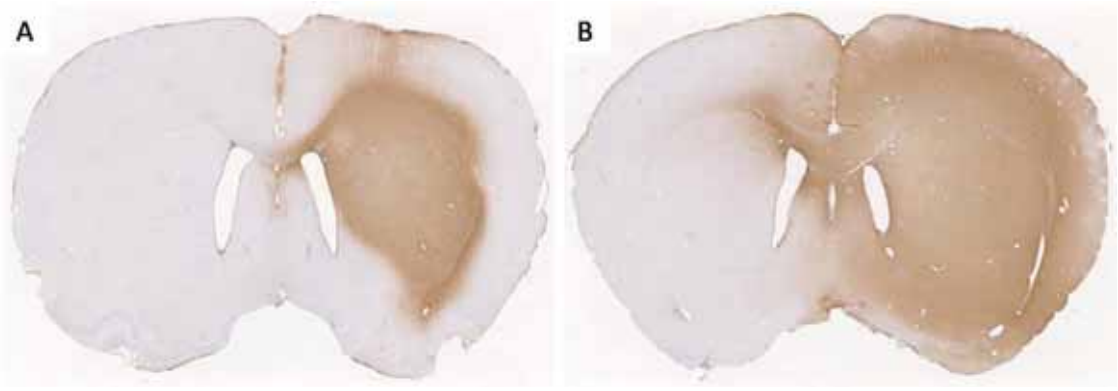


**Figure 18. Intrastriatal thrombin causes a progressive increase in albumin-IR. (A) Coronal section through rat striatum, albumin immunohistochemistry 5 hours post-striatal injection of 1U rat thrombin. There is considerable immunoreactivity in the striatum, extending to the cortex along the needle path. (B) At 24 hours there is a subjective increase bilaterally compared with (A).**

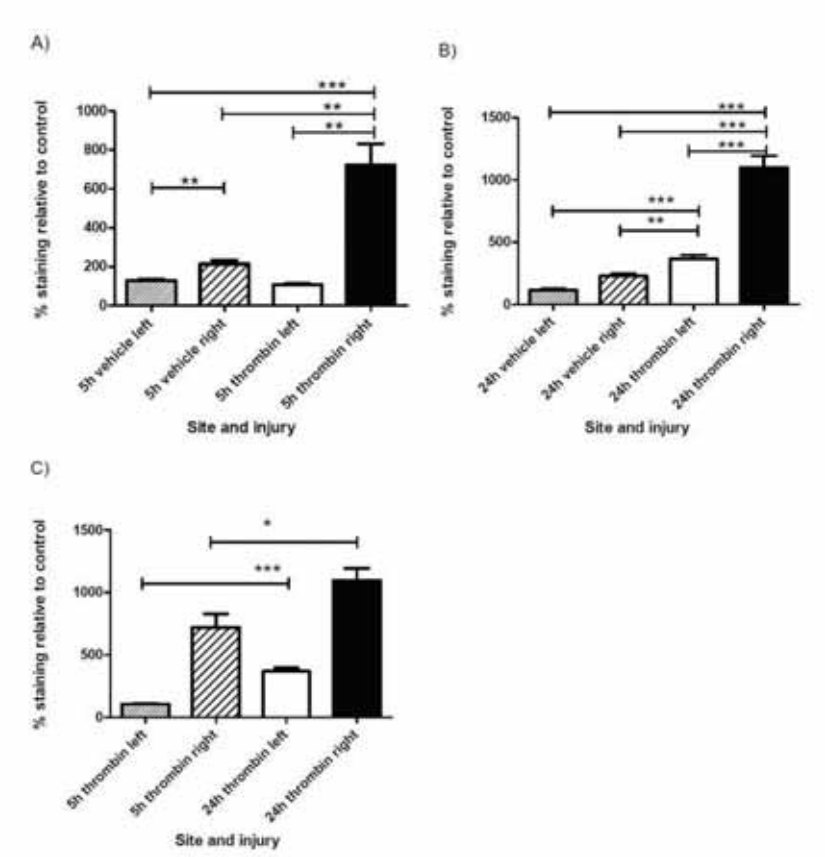


**Figure 19. Semi-quantitation by colour deconvolution: albumin immunoreactivity post-thrombin injection. Analysis of sections obtained 5 (A) and 24 (B) hours following 1U of intrastriatal rat thrombin (and vehicle controls) confirms the subjective impression of greater immunostaining intensity compared with vehicle controls, and also that there is greater IR at 24 hours than at 5 hours, both ipsi- and contralaterally (C). *, **, ***= p<0.05, 0.01 and 0.001 respectively.**

One potential difficulty in the process described above is that if technical issues cause variable 'background' staining intensity (Figure 20a-c), semi-quantitation may not pick up a true difference, or falsely conclude that a difference exists (Figure 21). This potential source of error can be mitigated if an internal control area can be identified - a region in which staining is present, but unaltered by injury (Figure 20d). For substance P immunostaining, the interhemispheric leptomeninges meet this criteria, both following cICH and thrombin injections. If the value obtained for each micro-dissected section is expressed as a percentage of internal control staining, valid conclusions can still be obtained regarding relative protein expression levels (Figure 21), even when processing and staining differences are quite extreme.

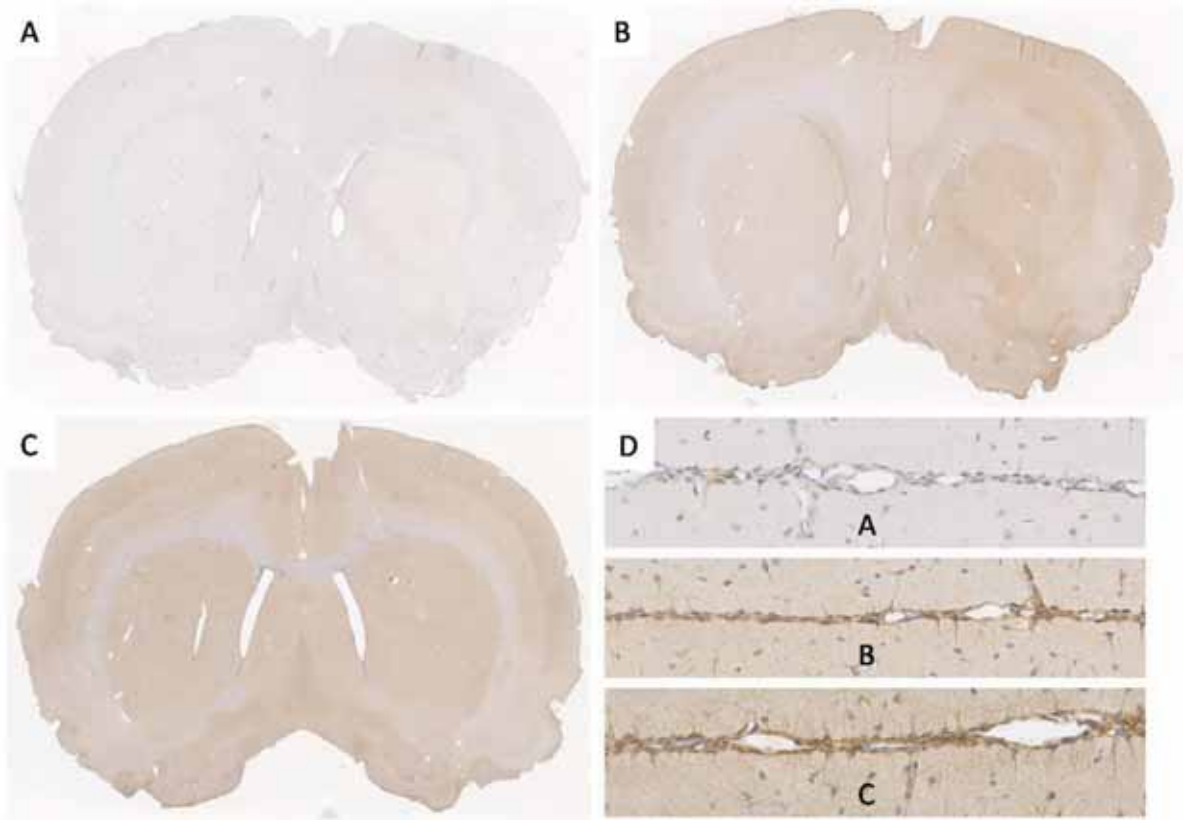


**Figure 20. Variations in processing technique alter levels of SP-IR. (A) Coronal section through rat striatum, SP immunohistochemistry 24 hours post-striatal injection of 1U rat thrombin, section dewaxed on hot air blower for 5 minutes. There is very faint SP-IR, seemingly more right than left. (B) Adjacent section to (A), dewaxed for 1 minute. There is a marked increase in SP-IR adjacent to the injection site. (C) Similarly located and stained section 24 hours post-vehicle control, dewaxed for 1 minute. (D) There is variability in interhemispheric leptomeningeal staining intensity (this staining is not affected by injury).**

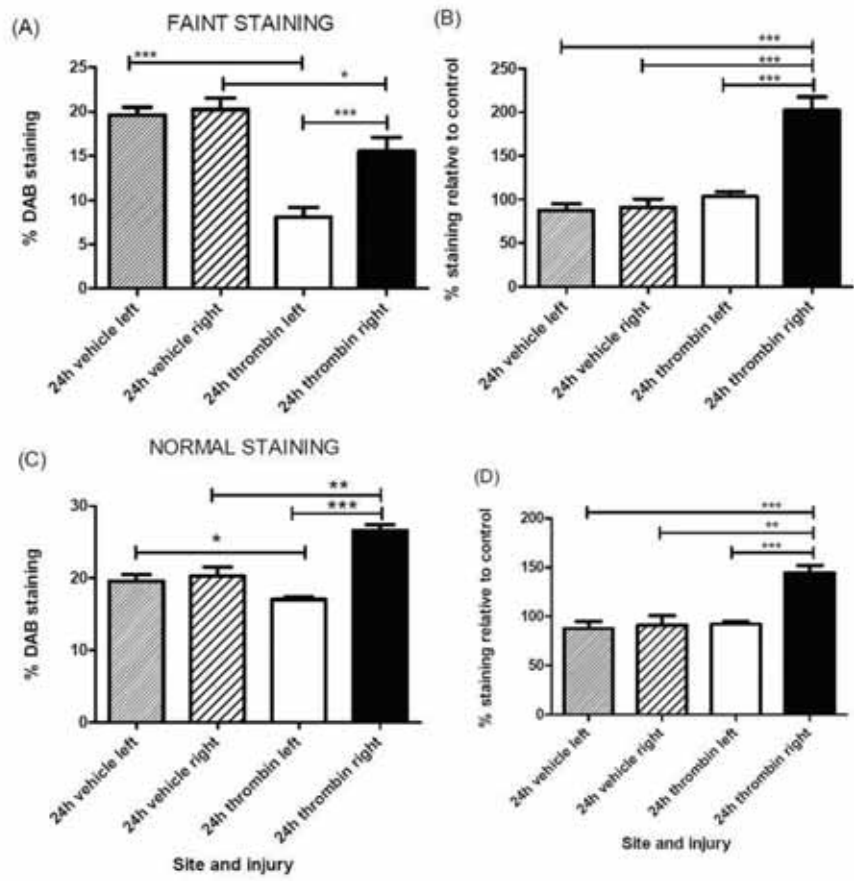


**Figure 21. Selection of a control area can adjust for both extreme and subtle staining variability. (A,B) and (C,D) correspond to images (A) and (B) above, respectively. (A) when unadjusted for a control area, semi-quantitation (of images (A) and (C) above) could suggest that thrombin injection causes SP-IR to decrease bilaterally (L>R). Adjusting for a control area prevents this error. (C) Even subtle variations in technique can lead to mistaken conclusions. Unadjusted semi-quantitation (of images (B) and (C) above) might suggest that intrastriatal thrombin causes SP-IR to increase ipsilaterally, but decrease contralaterally. However following use of a control area (D) only the ipsilateral increase is apparent. *, **, ***= p<0.05, 0.01 and 0.001 respectively.**

## 2.11 Automated cell counting

To assess inflammatory cell infiltrate, neutrophils (myeloperoxidase) and activated microglia (ED-1) were counted on a single section for each rat for the entire ipsilateral hemisphere, through the centre of injury. Images were exported at 10x resolution from NDPview into ImageJ (v1.40g NIH, Bethesda, USA). Haematoxylin and Diaminobenzidine stains were separated using color deconvolution as above. The deconvolved image was thresholded to remove background staining and 'watershed' function selected to separate touching cells. 'Analyze particles' was then selected, specifying particle size (25-250 pixels) to ensure that

only whole cells were counted. Manual counting was also performed on five sections to ensure the validity of this approach.

Degenerating neurons were also quantified in the peri-haematomal zone 24 hours following NAT or vehicle control, after fluoro-Jade C staining. This was performed by exporting an image (20x resolution) containing the haematoma and peri-haematomal zone into ImageJ and adjusting the windowing to remove background autofluorescence (Figure 22a). This was converted to a 32 bit grey-scale image (Figure 22b), then a binary image (Figure 22c). Cells were counted with 'analyse particles', selecting 'fill holes' and specifying a circularity of 0.4-1.0 and pixel size 100-300, to eliminate particulate and linear staining (Figure 22d).

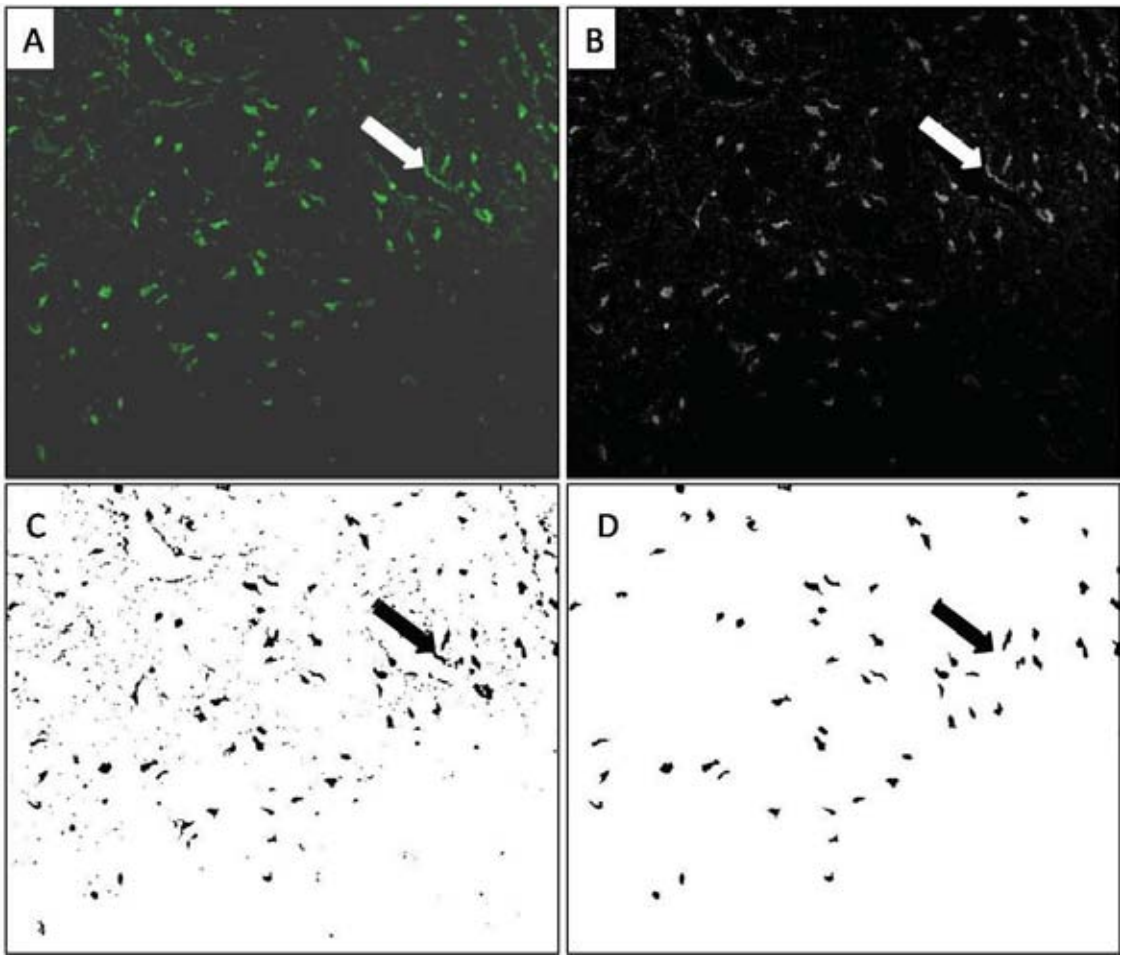


**Figure 22. Automated cell counting of Fluoro-Jade C-positive neurons. Images were exported at 20x resolution from NDPView to ImageJ, where they were windowed to minimise background auto-fluorescence (A). Images were converted to a 32-bit grey-scale image (B), then a binary image (C). 'Analyse particles' was selected, specifying size (100-300 pixels) and shape (circularity 0.4-1.0) to exclude particulate staining and vascular staining (arrow).**

## 2.12 Power calculations

For the functional outcome experiments, we expected a 20 percent standard deviation (SD) within each group. To detect a 33 percent change in functional outcome between the treatment groups, the power calculation showed that an n=10/group would detect a significant difference at the 0.05 level with the power of 0.95.

For the neuropathology/immunohistochemistry and oedema experiments, we expected to see a 10 percent SD within the groups. To detect a 25 percent difference between the treatment groups, the power calculation showed that an n=5/group would detect a significant difference at the 0.05 level with a power 0.95.

For the BBB experiments, we expected to see a 10 percent SD within the groups. To detect a 40 percent difference between the treatment groups, the power calculation shows that and an n=7/group would detect a significant difference at the 0.05 level with a power 0.95.

## 2.13 Statistical analysis

Categorical data was analysed by Fisher's exact test. Parametric variables were assessed by 2-tailed unpaired student's t-test or analysis of variance (ANOVA - one- or two-way, and/or repeated measures, as appropriate), followed by Bonferroni tests for multiple comparisons. Non-parametric variables were assessed by either Kruskal-Wallis or Friedman's ANOVA (as appropriate) followed by individual Dunn's multiple comparisons test. A P value of $<0.05$ was deemed significant. All graphical data is expressed as +/- standard error of the mean (SEM) and all tabulated data as +/- standard deviation.

# 3 Characterisation of substance P immunostaining and expression following collagenase and autologous blood experimental ICH

## 3.1 Introduction

Intracerebral haemorrhage is a common and devastating illness, affecting around 1 in 40 adults during their lifetime.[2] Mortality rates approach 50%[7] and survivors rarely regain functional independence.[20] In Australia, ICHs occurring in any given year cost society around A$ 500 million in lifetime costs.[21]

Following ICH, intracerebral blood products can initiate secondary responses such as oedema formation, excitotoxicity, apoptotic machinery, blood-brain barrier (BBB) dysfunction and oxygen free-radical release, which may worsen brain injury beyond that caused by the initial mass lesion.[57] Minimising secondary brain injury after ICH is a research priority.[240]

Increased levels of cerebral substance P have been noted experimentally in a variety of pathological brain states, including transient middle cerebral artery occlusion,[505] traumatic brain injury (TBI),[461] experimental allergic encephalomyelitis[433] and trypanosomiasis.[422] These varied cerebral injuries all lead to a significant inflammatory response and BBB dysfunction, a feature they share with intracerebral haemorrhage. Inflammation and brain injury can be reduced in all these settings by inhibition of the neurokinin-1 receptor (NK1R), the main receptor for substance P.

Thrombin appears to be the precipitant of early stage (5-48 hours) post-ICH cerebral oedema and inflammation,[57] and, in the periphery, causes oedema via neuronal SP release.[178] A deleterious role for thrombin has been demonstrated or suggested following subarachnoid haemorrhage,[458] cerebral ischaemia[189] and TBI.[460] In all these conditions NK1R inhibition has also proven protective.[426, 459, 461] It is therefore possible that thrombin causes post-ICH oedema at least partially through SP, and that inhibiting the main SP receptor may reduce oedema and inflammation without precipitating rebleeding, the main concern limiting use of thrombin antagonists post-ICH.

Experiments in this chapter were designed to answer the following questions: 1) is substance P increased in the peri-haematomal zone following experimental ICH; 2) if so, what is the location of increased SP immunostaining and its time-course; 3) is there also upregulation of the main substance P receptor (NK1R), and; 4) is the pattern of SP and NK1R change consistent with a role in thrombin-mediated post-ICH oedema and inflammation.

Disruption of the BBB commences in both experimental and human intracerebral haemorrhage within several hours of injury[63, 84] and precedes the development of oedema, which peaks between 24 and 48 hours.[62, 63] Previous experiments have shown that NK1R antagonism significantly inhibits acute blood-brain barrier breakdown and oedema in both transient focal ischaemia and traumatic brain injury.[461, 481] Therefore substance P immunostaining was studied at relevant acute post-ICH timepoints, commencing 5 hours post-injury, using visual qualitative analysis, semi-quantitative methods, immunofluorescence double labelling and ELISA. This was related to expression of RNA for SP and the NK1R, as well as inflammatory cell activity and gliosis. Both collagenase and autologous ICH methods were employed.

## 3.2 Experimental design

Ninety five male Sprague-Dawley rats (300-340gm) were used for the experiment, as described in chapter 2.

Eighty animals were examined for histological and immunohistochemical changes following collagenase ICH ((cICH) n=20), autologous ICH ((aICH) n=20) or appropriate volume saline injections (n=2x20) at each time point (5, 24, and 48 hours and 7 days, n=5 per group). As there were no detectable changes observed in the contralateral hemisphere following ICH or vehicle injection at any time-point, additional sham animals were not deemed necessary. The 5 animals in the cICH group at 7 days were also followed for pilot behavioural studies to determine the most appropriate tests for the assessment of therapeutic interventions (chapter 4). A new batch of collagenase was used for this 7 day group; neurological deficits in this group were noticeably less post-operatively, and haematoma volumes were presumably much smaller (day 7 lesion size was much smaller than in the vehicle treated cICH 7 day group in chapter 4, which were administered collagenase from a subsequent batch). However, as a milder injury was induced, this group was eminently suitable for pilot behavioural experiments to determine which tests were most sensitive to degrees of injury.

Additionally, 15 rats were studied for ELISA and real-time RT-PCR (5 hours and 24 hours post-ICH, plus 24 hours post-saline injection, n=5 per group), as described in chapter 2.

### 3.2.1 Haematoma quantification

Unstained freshly fixed 2mm thick specimens were scanned at high resolution as described. The haematoma was automatically outlined using the ‘magic wand’ function of Adobe Photoshop (Adobe Systems Inc., v6.0.1). Haematoma volumes were assessed by summing for each slice the product of average area (front and back of each slice) and slide thickness.

### 3.2.2 Histology and immunohistochemistry

At the pre-specified timepoints animals were perfuse-fixed with formalin. Brains were extracted, sectioned, scanned and processed as described. Immunohistochemical staining through the needle injection site (the haematoma centre) was performed for albumin, ED-1, IBA-1, NK1R, GFAP, MPOX and SP, and H&E and FJC staining undertaken, as described. Slides were scanned at high resolution and viewed with appropriate viewing software.

Double-labelling was performed for substance P, NK1R, ED-1, IBA-1, MPOX and GFAP as described. Slides were viewed and photographed.

### 3.2.3 Semi-quantitation of SP immunostaining

As outlined above, colour deconvolution provides a method of by which immunostaining can be objectively semi-quantified, removing observer bias. Both striatal and cortical substance P staining was assessed as shown and expressed as a percentage of interhemispheric leptomeningeal staining(Figure 23). Areas, rather than whole hemispheres, were selected to ensure that it was parenchymal SP which was assessed, rather than haematomal SP.

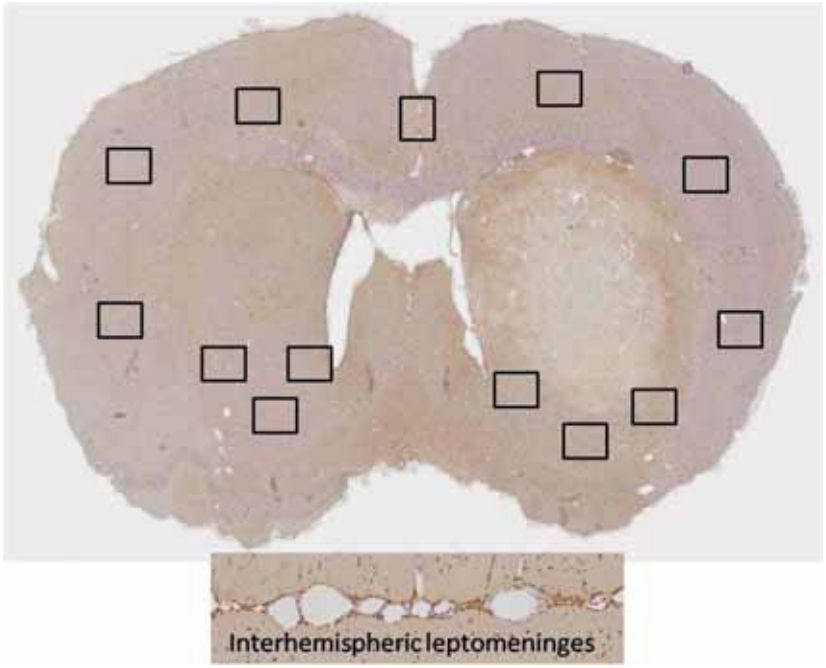


**Figure 23. Microdissection of areas for SP image analysis. For each section, three areas each from striatum and deep cortical layers, bilaterally, were exported at 10x resolution as shown. Following deconvolution, total DAB staining was obtained and averaged for left and right cortex and striatum, and expressed as a percentage of interhemispheric leptomeningeal staining (shown beneath), which was unaffected by injury.**

### 3.2.4 Cell counting

Inflammatory cell infiltrate (neutrophils and activated microglia) was assessed to compare the inflammatory response between autologous and cICH models, as described in chapter 2. Total cell counts for an entire section through the haematoma centre were obtained.

### 3.2.5 ELISA

At 5 and 24 hours following cICH, animals were decapitated and a 4mm thick brain slice was obtained, containing the striatum and the bulk of the haematoma. The ventral half was processed for ELISA as described. Animals at 24 hours post-vehicle injection served as controls. As there were no differences seen in this vehicle group between left and right SP immunostaining or ELISA levels, further animal control groups or shams were deemed unnecessary.

### 3.2.6 RT-PCR

The dorsal half of the 4mm thick perihaematomal brain slice described above was processed for real-time RT-PCR as described. Animals at 24 hours post-vehicle injection served as controls. Again as no differences were observed in the 24 hour vehicle group, further animal control groups or shams were deemed unnecessary.

### 3.2.7 Pilot behavioural studies

All animals in all groups were assessed for circling behaviour on recovery at five hours and daily thereafter. As only collagenase animals demonstrated consistent circling behaviour as a response to injury (see below) it was determined that behavioural outcomes would be best assessed in this group.

As outlined in chapter 2, various behavioural tests have been reported as sensitive measures of striatal injury. To assess which of these would be most suitable for determining the neuroprotective efficacy of any intervention, seven of these were selected for use in the 7 day cICH group: the tapered ledged beam, vibrissae-elicited stimulation test, elevated drag test, sticky label test, rotarod, elevated body swing test and the modified limb placing test. Animals were pre-trained as required and assessed days 0, 1, 2, 3, 5 and 7 post-injury.

### 3.2.8 Statistical analysis

Continuous variables were assessed by unpaired, two-tailed Student's t-tests. Histological changes over time (for instance SP immunostaining) were assessed by one-way ANOVA with Bonferroni post-tests. Behavioural tests were analysed using a repeated measures one-way ANOVA and Bonferroni post-tests for parametric data, and Friedman test with Dunn's post-tests for non-parametric data. Categorical data was assessed using Fisher's exact test.

## 3.3 Results

### 3.3.1 Baseline and surgical parameters

Apart from differences in anaesthesia duration resulting from the simplicity of the cICH technique, there were no differences observed in baseline or operative parameters between surgical groups, with body temperature and gases maintained essentially at the midpoint of the intended range (Table 2).

Table 2. Experimental parameters

| Group | Weight | Duration | T start | T finish | pH | $pO_2$ | $pCO_2$ |
|---|---|---|---|---|---|---|---|
| **Auto ICH** | 319±9 | 77±3 | 37.0±0.4 | 37.1±0.4 | 7.46±0.01 | 136±5 | 39±1 |
| **Auto (V)** | 314±13 | 78±5 | 37.0±0.3 | 37.0±0.4 | 7.45±0.01 | 126±4 | 39±1 |
| **Coll ICH** | 317±10 | 26±3 | 36.7±0.3 | 37.1±0.3 | ---- | ---- | ---- |
| **Coll (V)** | 321±21 | 29±3 | 36.9±0.4 | 37.1±0.3 | ---- | ---- | ---- |

**Experimental parameters (means +/-SD) for autologous ('auto') ICH, collagenase ('coll') ICH and applicable vehicle controls ('V'). There were no significant differences between groups, save for anaesthesia duration between autologous and autologous ICH ($p<0.001$). Blood gases were not measured in the latter group. Units: weight=grams, duration=minutes of anaesthesia, temperature ('T')=$^{o}$C, partial pressures=mmHg.**

### 3.3.2 Haematoma volumes

Acute haematoma volumes were around 30% smaller in the autologous ICH group at earlier timepoints (Figure 24). There was no measurable increase in haematoma volume in the collagenase group beyond 5 hours, suggesting that little ongoing bleeding occurred after this time-point.

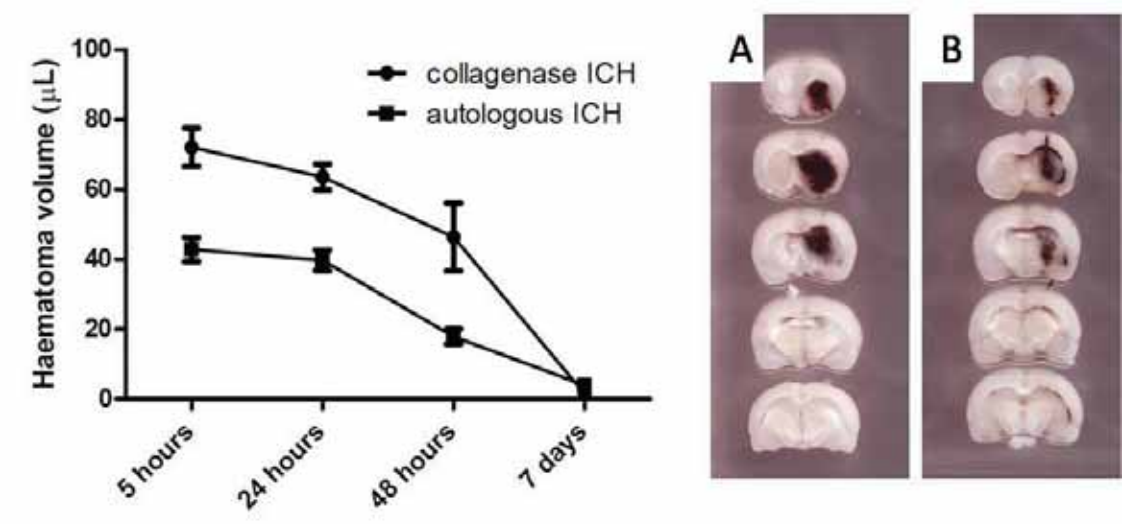


**Figure 24. Haematoma volumes following autologous and collagenase ICH. Volumes were around 30% smaller in the autologous group at 5, 24 and 48 hours (P<0.01). In the collagenase model (A) the haematoma was more spherical, and in the autologous model (B) a tendency was observed for dissection along the injection site, white matter tracts and into ventricles.**

Consistent with previous studies, haematoma absorption had already commenced at 48 hours and was largely complete by 7 days, in contrast with human ICH, which takes much longer to resorb.[472] The shape of the haematoma also differed between groups (Figure 24a and b), again in keeping with previously known differences.[472]

### 3.3.3 Collagenase ICH Histology

#### *H&E staining*

At five hours intact red cells could be seen around blood vessels dissecting through the striatum and forming, in the central injection site, an almost solid mass of clot with islands of intact tissue contained within (Figure 25a). By 24 hours red cells had started to lyse and a rim of oedematous tissue surrounded the haematoma, containing necrotic and apoptotic neurons and glia (Figure 25b, c). Appearances were largely similar at 48 hours, and by 7 days the haematoma had largely resorbed, leaving a macrophage-filled cavity with compensatory ventricular dilatation (Figure 25d). There was minimal injury seen at any time-point in vehicle controls, and no abnormalities seen in the contralateral hemisphere at any timepoint in controls or cICH brains.

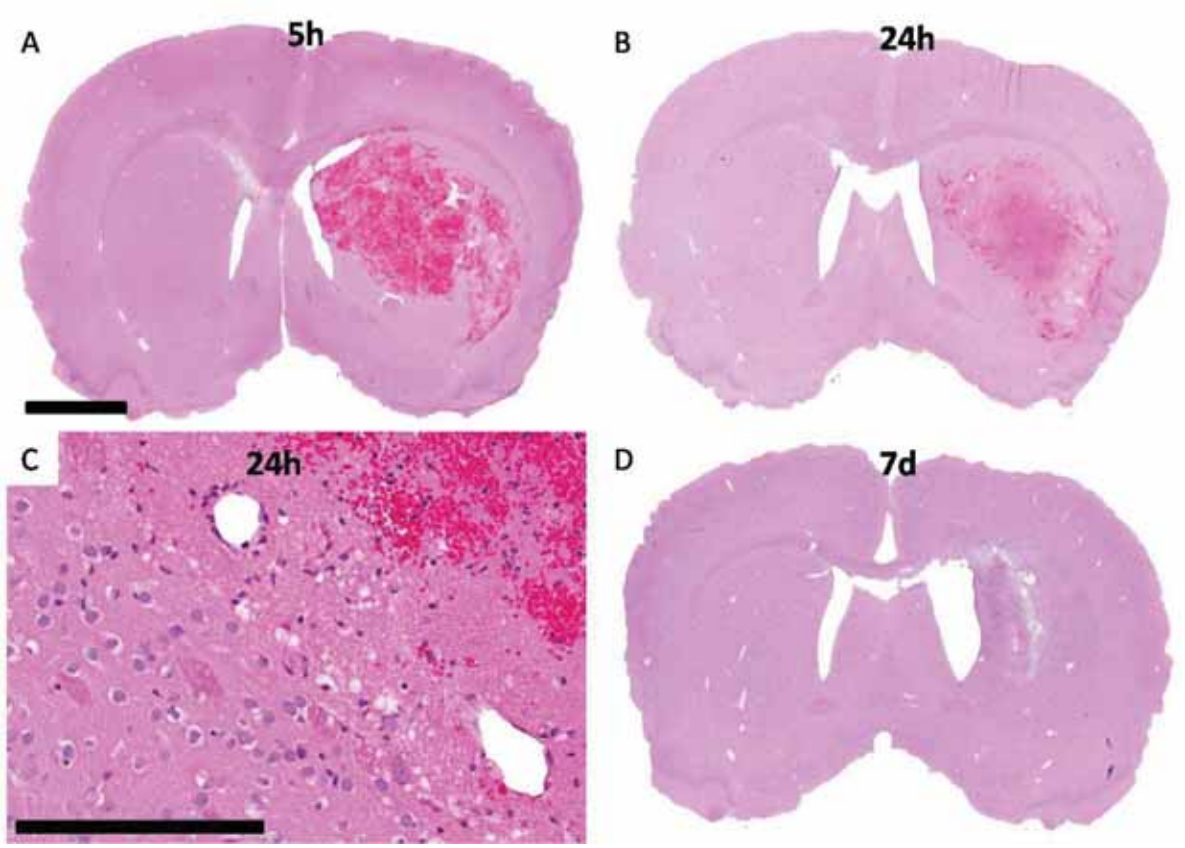


**Figure 25. H&E staining of collagenase ICH. Coronal sections through the haematoma centre at 5 hours (A), 24 hours (B,C) and 7 days (D). There is progressive haemolysis, then resorption of the haematoma. At 24 hours three distinct zones can be seen (C): a central zone of confluent haematoma surrounding island of necrotic tissue, a rim of degenerating and apoptotic neurons and glia, and an area of predominantly peri-cellular oedema. Scale bar=200μm or 2mm for whole sections.**

### *SP staining*

At five hours a diffuse increase in granular SP-IR could be seen surrounding the haematoma (Figure 26a). At this time-point there was no particular cell population exhibiting increased SP-IR (Figure 26b, c), and, contrary to previous studies in TBI and tMCAO,[436, 461] there was no definite early post-injury increase in perivascular staining.

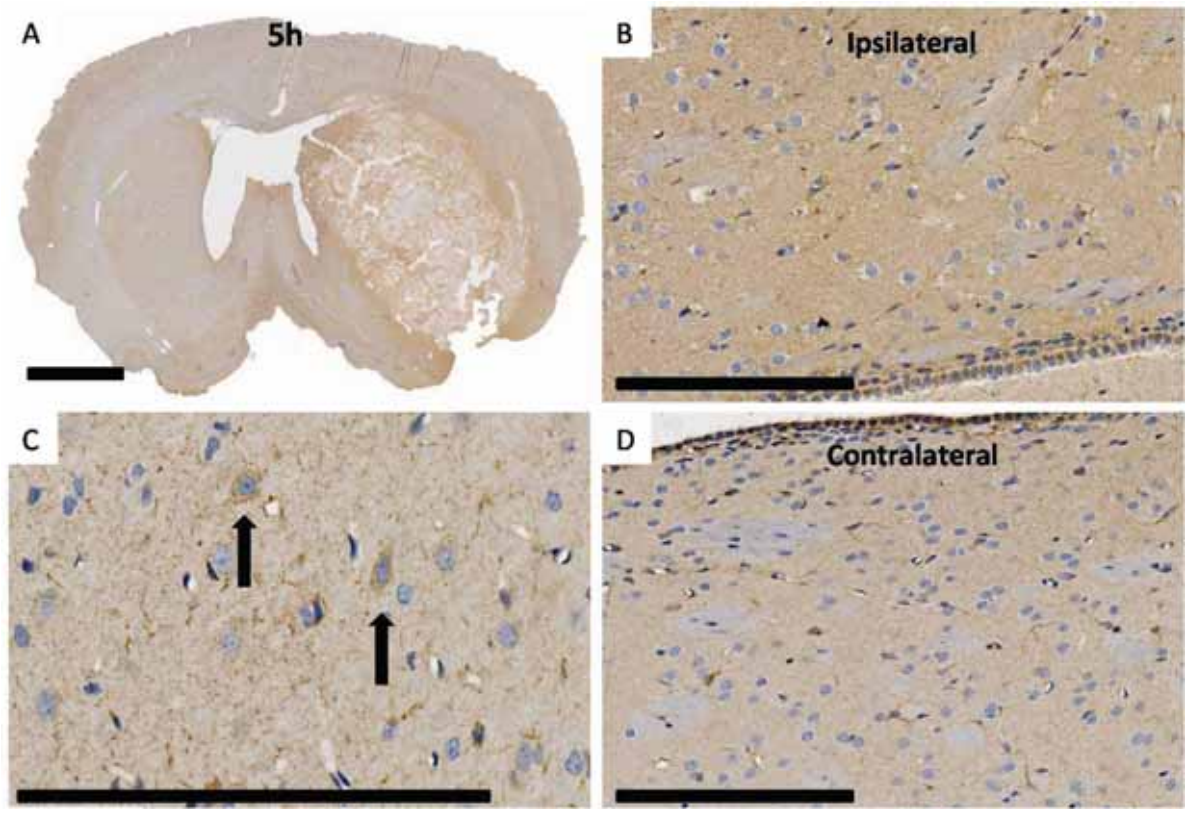


**Figure 26. SP immunostaining 5 hours after collagenase ICH. A perihaematomal rim of increased SP immunoreactivity is present (A). This appears diffuse and granular (B compared contralaterally (D)) rather than within particular cell populations. Neuronal SP (C) did not differ between hemispheres. Scale bar=200µm.**

At 24 hours the background SP granular staining had diminished (Figure 27a), however a clear increase in SP-IR was seen in what were later proven to be astrocytes. This astrocytic increase in SP-IR increased further by 48 hours (Figure 27c). By 7 days, the intensity of astrocytic SP-IR has returned to baseline; however, increased SP-IR was noted in macrophages (Figure 27d).

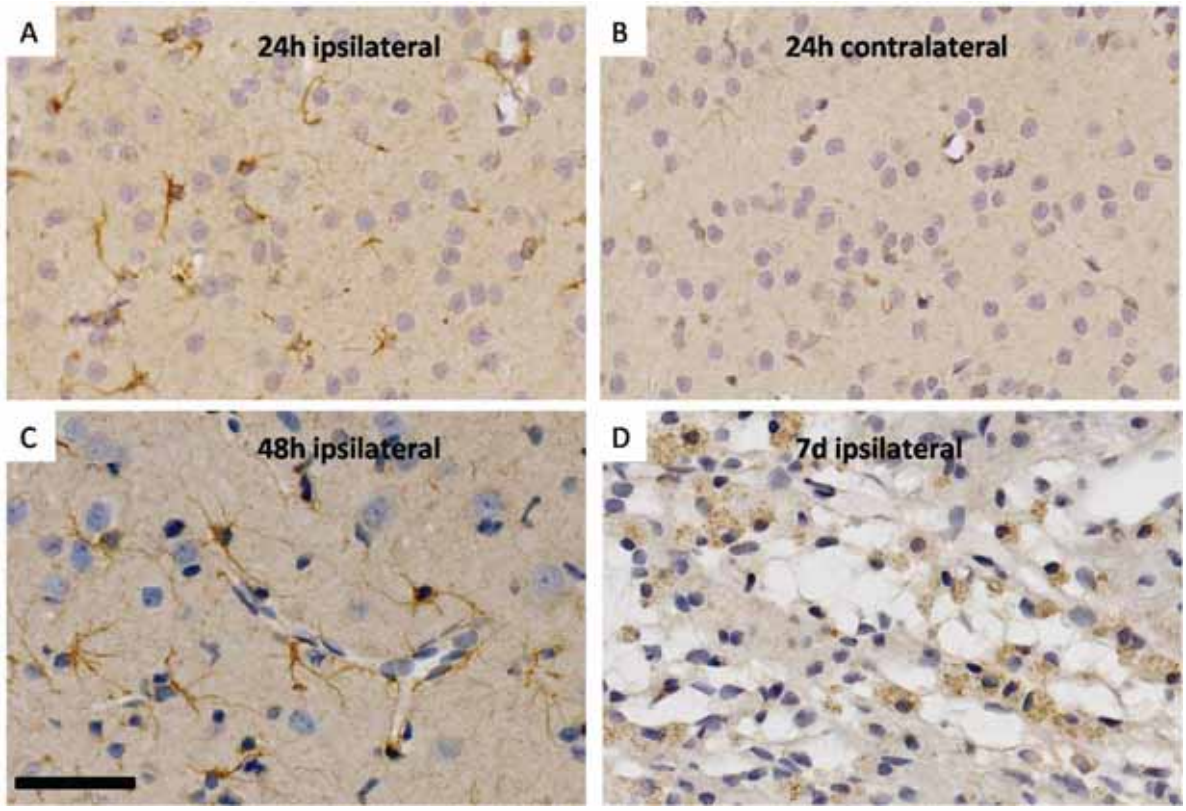


**Figure 27. SP immunostaining, collagenase ICH at later timepoints. (A,B) At 24 hours there is significantly greater perihaematomal SP immunoreactivity (A) compared with the contralateral side (B) and saline controls (not shown). Compared with at 5 hours, there is less granular background staining, but greater astrocytic staining. At 48 hours (C) the increased astrocytic SP can be seen along the whole astrocyte, enwrapping vessels. (D) By 7 days there is no longer increased astrocytic staining, however macrophages exhibit SP immunoreactivity. Scale bar=50µm.**

To objectively confirm the impression of increased substance P immunoreactivity, images were analysed following deconvolution at each timepoint (Figure 28). There was greater degree of SP-IR at all time-points, comparing both left and right, as well as comparing cICH rats and vehicle controls. At 7 days there was no longer increased cortical staining, as the increased SP immunoreactivity localised to striatal macrophages only (the ICH cavity did not extend to the cortex). The biphasic peak evident in both cortical and striatal immunoreactivity correlated with granular and astrocytic staining peaks observed at 5 and 48 hours respectively (Figure 28b and Figure 28c).

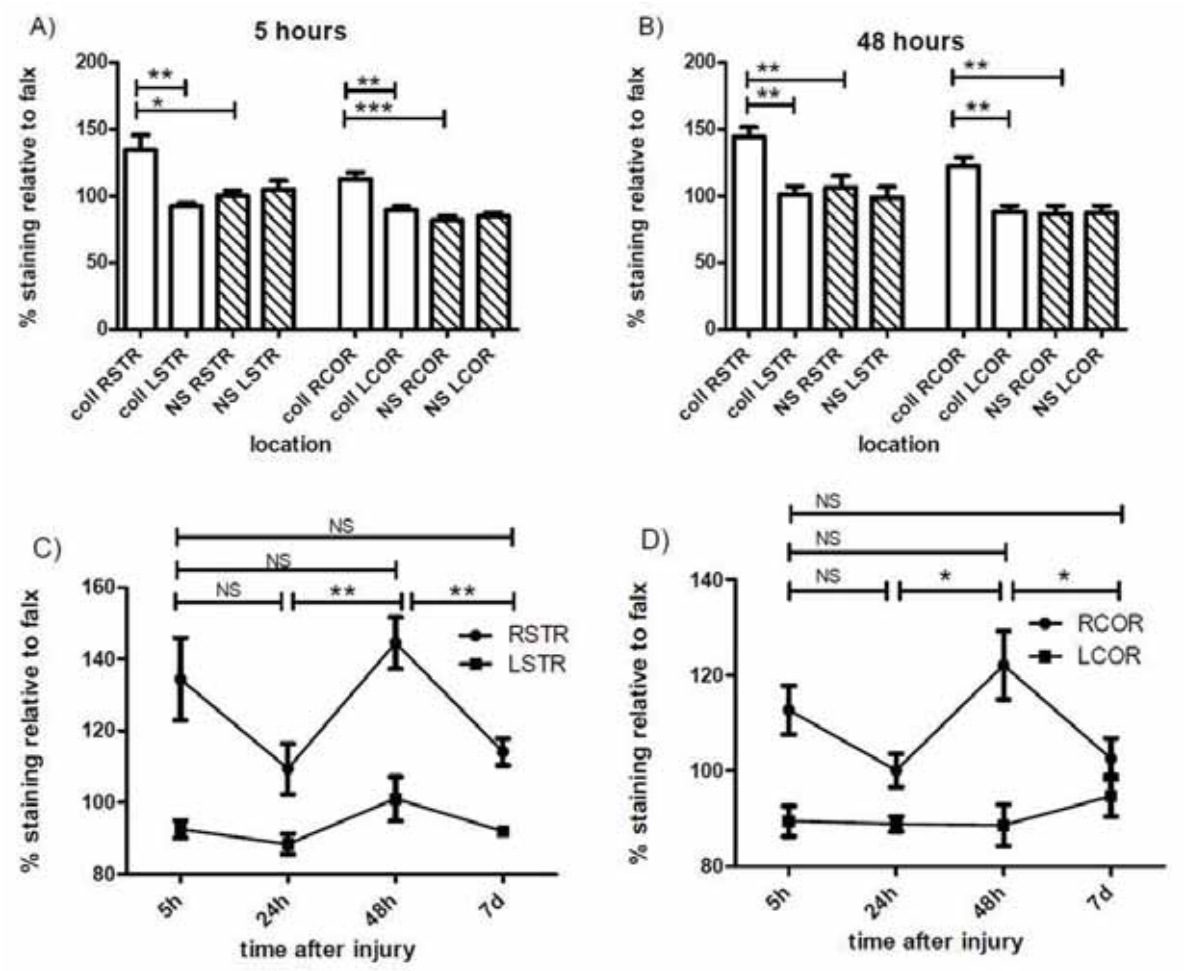


**Figure 28. SP immunostaining following collagenase ICH, semi-quantitated. There is increased SP immunostaining at all timepoints, especially at 5 (A) and 48 (B) hours post collagenase ICH. Both striatal (C) and cortical (D) SP exhibit this biphasic peak, correlating to the increases in diffuse granular and astrocytic staining demonstrated above. RCOR=right cortex, LCOR=left cortex, RSTR=right striatum, LSTR=left striatum. ***=p<0.001, **=p<0.01, *=P<0.05, NS=not significant.**

### *NK1R response*

In uninjured hemispheres and vehicle controls, NK1R-IR was found predominantly around neurons and neuronal processes, but also (more faintly) around vessels and glia (shown later to be astrocytes). The striatum contained the bulk of neurons possessing the NK1R. After injury there was little change at 5 hours, save that many of the striatal NK1Rs were destroyed or disrupted by the haematoma. At 24 and 48 hours a progressive increase in glial NK1R immunoreactivity was seen (Figure 29), with little change in neuronal NK1R levels. By 7 days appearances were similar to baseline. As the bulk of NK1R staining was neuronal, not glial, and given that neuronal staining did not appear to alter over time, semi-quantitative deconvolution analysis was not performed for this group.

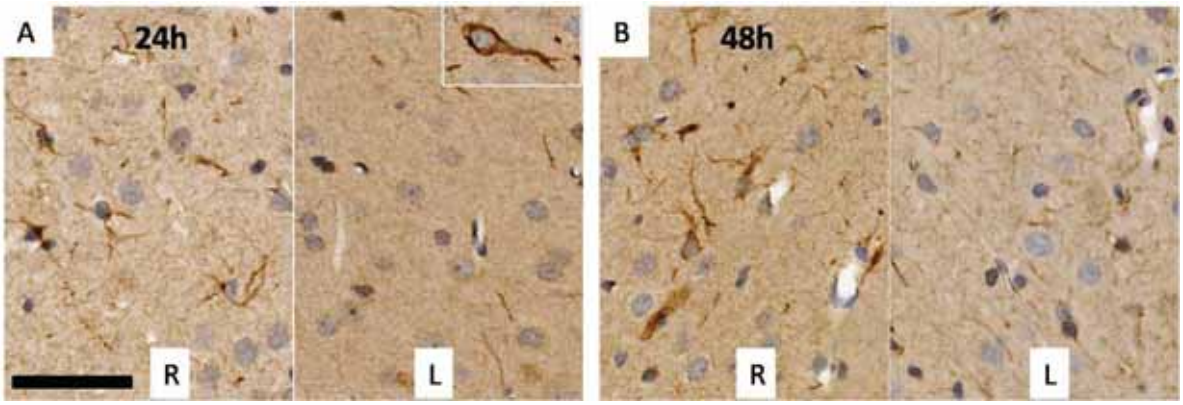


**Figure 29. NK1R immunostaining following collagenase ICH. While neuronal (insert) NK1R reactivity did not seem to be altered by the ICH, a progressive increase was seen in astrocytes at 24 (A) and 48h (B). By 7 days this had returned to baseline (not shown). Scale bar=50µm.**

### *Neuronal degeneration (Fluoro-Jade C)*

Degenerating neurons were evident on FJC staining in sparse numbers at 5 hours, however there was also significant fluorescence of red blood cells, which made identification problematic (not shown). By 24 hours numerous FJC-positive neurons were evident both within the haematoma and the surrounding peri-haematomal zone, which persisted, diminishing slightly at 48 hours especially for intra-haematomal neurons, which were presumably, first to die (Figure 30).

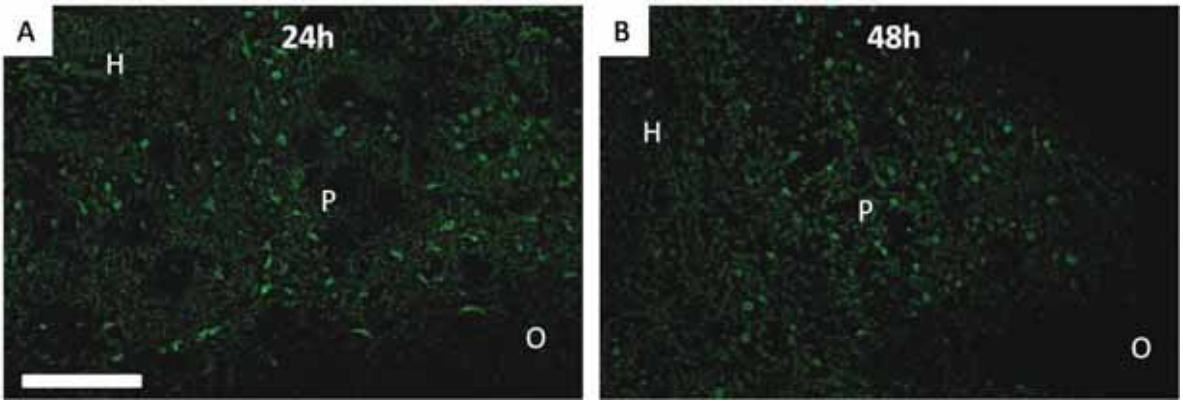


**Figure 30. Fluoro-Jade C staining following collagenase ICH. FJC positive neuronal staining peaked at 24h (A) and diminished slightly at 48h (B). Little or no neuronal staining was evident at 5 hours or 7 days (not shown). H=haematoma, P=penumbral zone, O=oedematous zone. Scale bar=100µm**

### *Inflammatory response: neutrophils (myeloperoxidase) and monocyte/ microglia (ED-1, IBA1)*

At five hours following cICH (Figure 31a) infiltrating neutrophils could be seen adhering to the microvasculature and/or infiltrating into perivascular spaces. At 24 hours this process was dramatically advanced (Figure 31b) and a dense perihaematomal rim of neutrophils was evident. At 48 hours (Figure 31c, d), many neutrophil apoptotic bodies were evident, however neutrophils were continuing to infiltrate. By 7 days, however, no neutrophils were found (not shown).

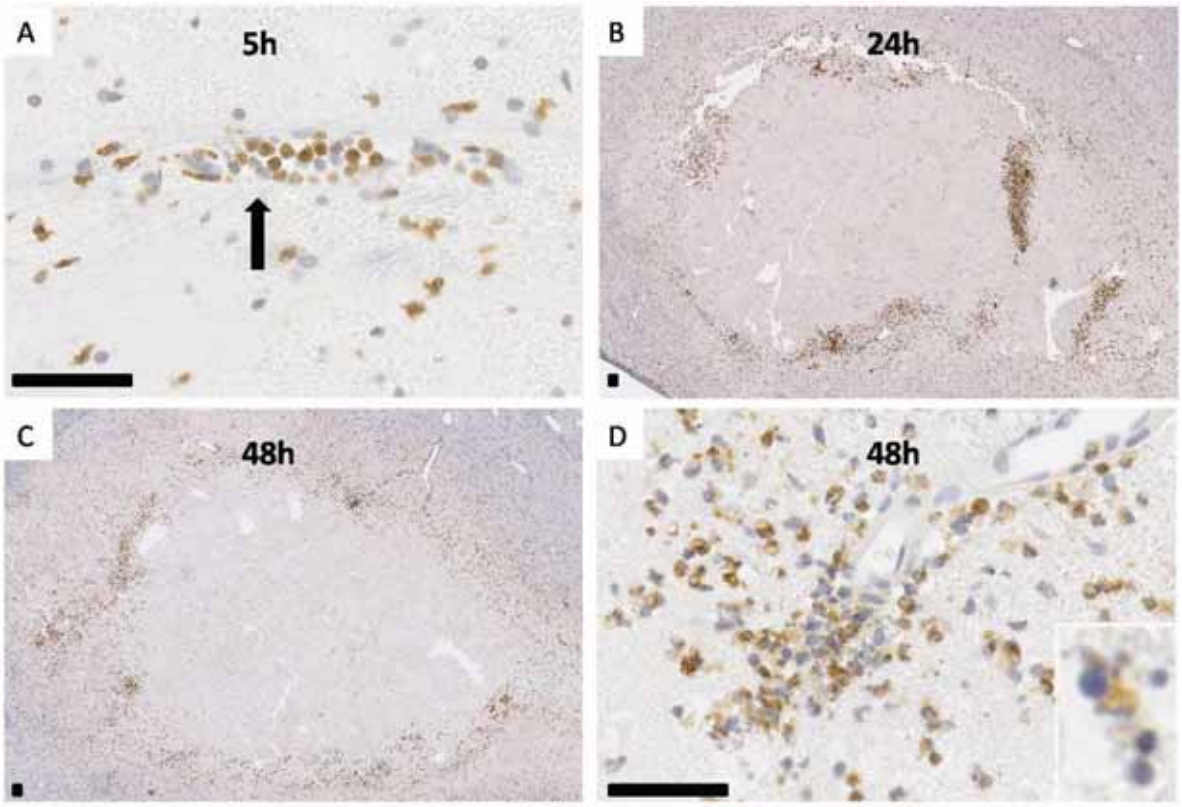


**Figure 31. Myeloperoxidase immunostaining post-collagenase ICH. (A) At five hours neutrophils can be seen adhering to perihaematomal vessels and diapodesing (arrow). (B) By 24 hours there is a dense perihaematomal rim of neutrophils, which persists at 48 hours (C). At 48 hours, although neutrophils are continuing to infiltrate ((D) see vessel superiorly) some neutrophils have degranulated and apoptosed, leaving leucocytoclastic nuclear debris (insert). Scale bar=50µm.**

Similarly to neutrophils, at 5 hours monocytes could be seen amassing in perihaematomal vessels and transmigrating (Figure 32). No parenchymal microglial response was noted at this time-point. As opposed to the neutrophil response, which peaks at 24-48 hours and then

rapidly diminishes, progressive activation/infiltration of microglia was seen at all timepoints (Figure 32a-d), not only involving the dense rim of surrounding microglia/macrophages, but also more broadly in the entire hemisphere ipsilateral to injury, and even, to some extent, extending across the corpus callosum contralaterally. IBA1 staining, which does not stain infiltrating monocytes, showed little change in the first 24 hours, but increasing numbers and ramification of endogenous microglia thereafter (not shown).

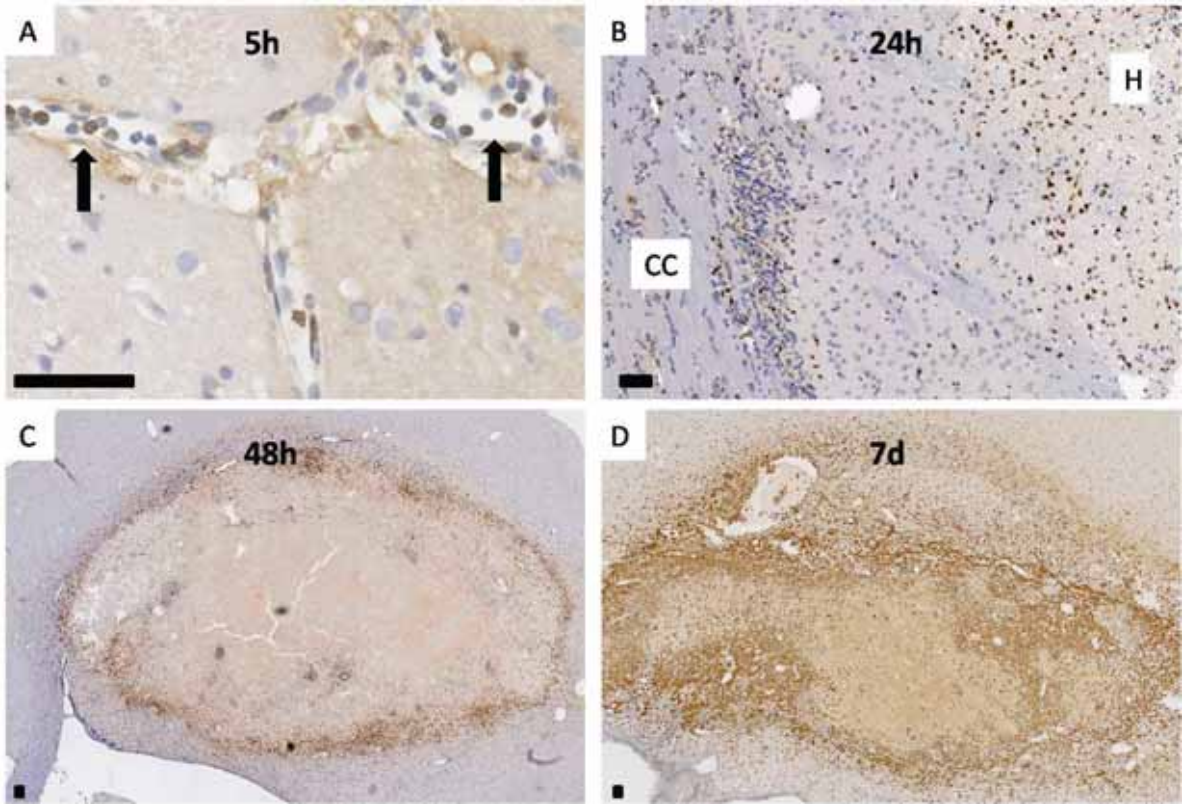


**Figure 32. Macrophage/activated microglia response following collagenase ICH. (A) At 5 hours infiltrating monocytes can be seen in and adjacent to perihaematomal vessels (arrows). (B) At 24 hours a peripheral rim of (presumably) infiltrating monocytes surrounds the haematoma (H), and adjacent microglia in the corpus callosum (CC) are beginning to activate. The response intensifies progressively at 48 hours (C) and 7 days (D). Scale bar=50µm.**

### *Astrocytic response (GFAP)*

There was little astrocytic reaction in the first 5 hours following ICH; remnant GFAP staining of disrupted astrocytes was evident within the haematoma. There was a progressive increase in GFAP immunoreactivity in the perihaematomal zone from 24 hours onwards (Figure 33a), extending centripetally as the haematoma was resorbed. The progressive increase in GFAP staining paralleled SP immunoreactivity at 24 and 48 hours, but whereas astrocytic SP had returned to baseline by 7 days, GFAP immunoreactivity continued to progress (Figure 33c, d).

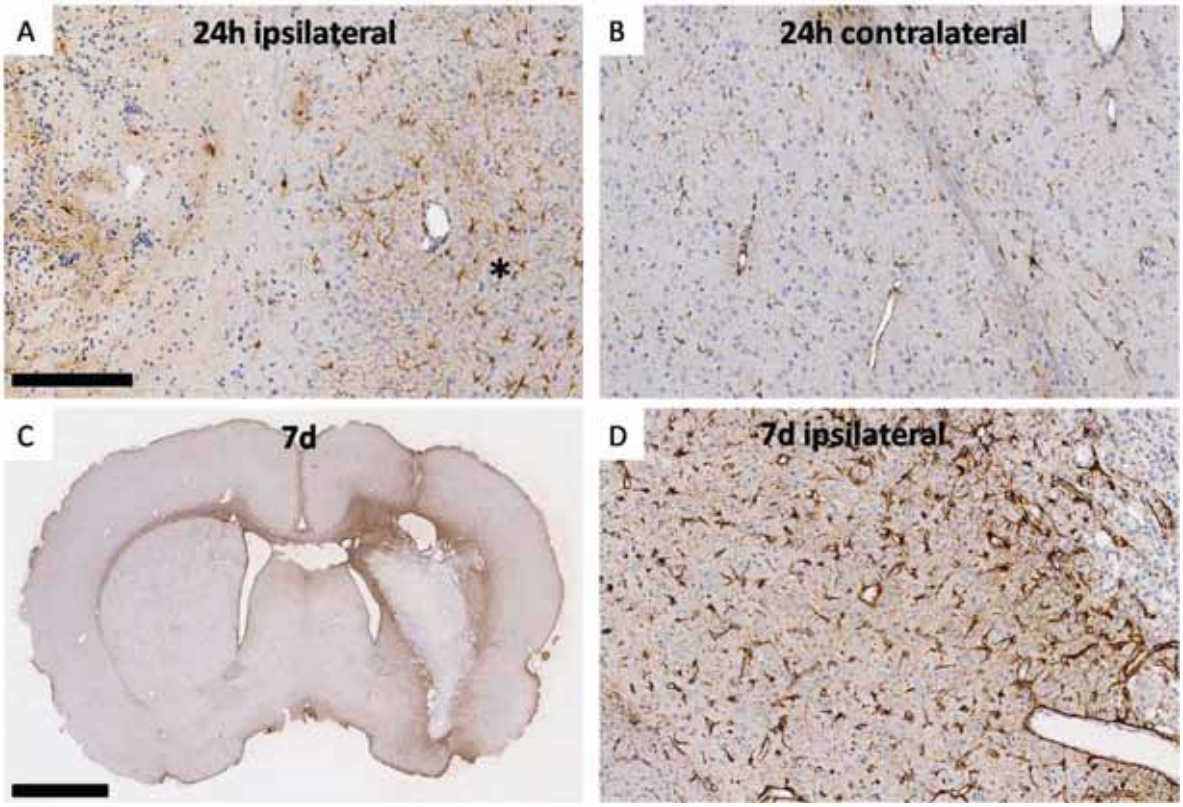


**Figure 33. Astrocytic (GFAP) response following collagenase ICH. (A) At 24 hours an increase in perihaematomal GFAP (asterix, A) is seen compared contralaterally (B). By 7 days (C,D) a dense gliotic ring of plump astrocytes is evident. Scale bar=200µm or 2mm for whole brain.**

### *Albumin immunohistochemistry*

In order to help plan and interpret Evans Blue testing for BBB disruption, albumin immunostaining was performed. As the haemorrhage itself contains albumin, disruption of the BBB cannot reliably be determined in this fashion, as it is impossible to determine whether the albumin has originated from the ICH, or as a secondary response.

At 5 hours there was already significant passage of albumin across the corpus callosum into the opposite hemisphere (Figure 34a), which progressed to a peak at 24 hours (Figure 34b). There was less contralateral albumin-IR at 48 hours, and almost none at 7 days post-ICH (Figure 34c), even though peri-haematomally significant amounts were detectable, suggestive of ongoing BBB disruption at these timepoints. Peak albumin-IR in vehicle controls occurred at 24 hours also (Figure 34d), although even at its peak it was dramatically less than in the interventional group.

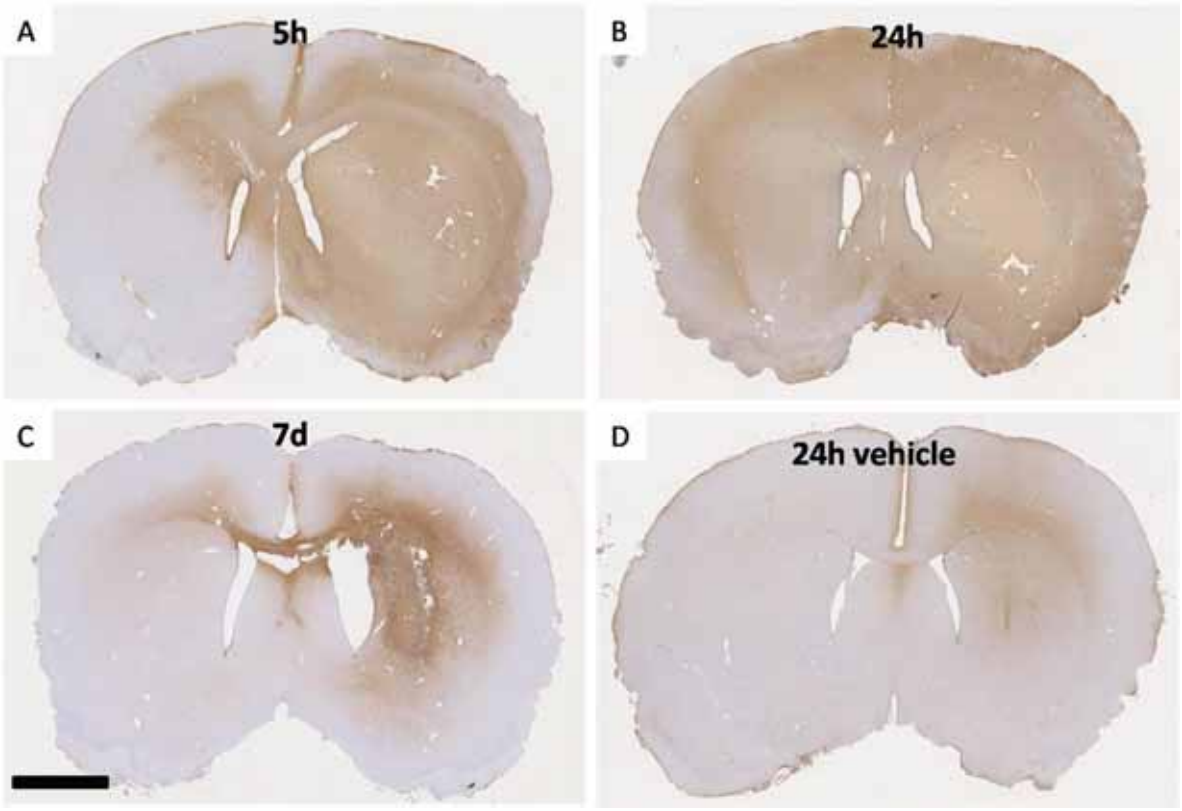


**Figure 34. Albumin immunohistochemistry post-collagenase ICH and vehicle. (A) At five hours there is considerable spread of albumin across the corpus callosum which peaked at 24 hours. (C) There is persistent albumin IR at 7d when contralateral staining has diminished, consistent with ongoing disruption of the BBB. (D) There was minimal BBB disruption with saline injection which peaked at 24 hours. Scale bar=2mm.**

### *Immunofluorescence double labelling*

In order to confirm that the increase in substance P immunostaining was in astrocytes, double labelling for SP with myeloperoxidase, ED-1, IBA-1 and GFAP was performed. This was performed at all timepoints for both vehicles and ICH animals.

As light microscopy suggested, the increased SP immunoreactivity seen at the 24 and 48 hour timepoints localised to astrocytes (Figure 35a-c). SP did not co-localise with neutrophils (not shown), infiltrating monocytes, or monocytes/activated microglia (Figure 35d-f), excepting faint co-localisation with occasional infiltrating monocytes at 24 hours (not shown). At 7 days the SP immunoreactivity seen within macrophages appeared to be part of phagocytosed material (Figure 35g-i).

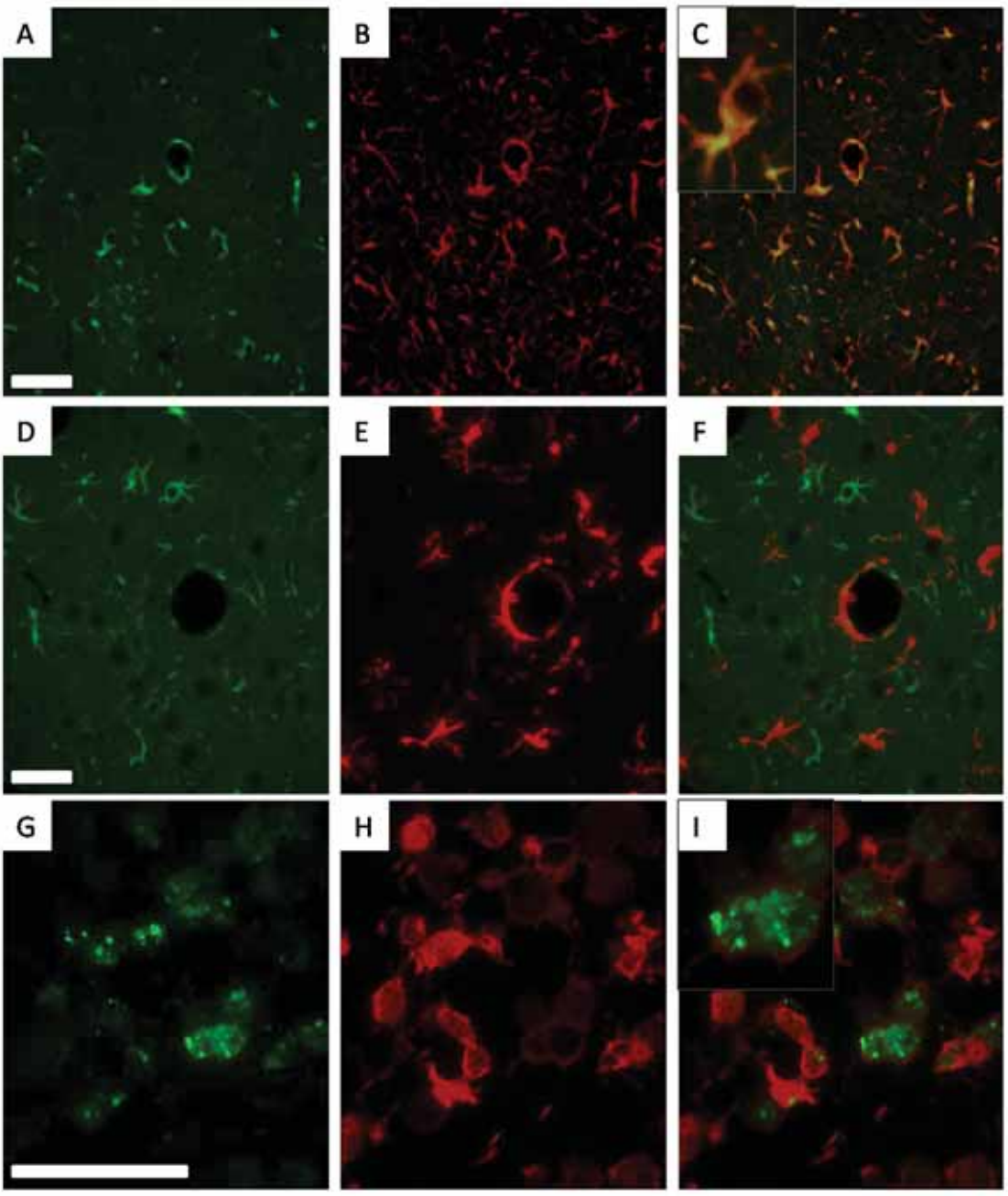


**Figure 35. Double labelling post-collagenase ICH localises increased SP immunostaining to astrocytes. Fluorescent immunohistochemistry double labelling for SP (left column) and either GFAP (B) or IBA1 (E, H), 24 hours (A-F) and 7 days (G-I) after ICH (right column represents merged images (yellow)). The marked increase in glial SP immunoreactivity seen with light microscopy is localised to astrocytes (A-C), not microglia (D-F). At 7 days SP is present within macrophages (G-I) although it appears to be located within phagocytosed intracellular material (insert). Scale bar=50μm.**

Double labelling for the NK1R was performed with ED-1, MPOX and m-GFAP. Again, as expected, all the increased NK1R staining localised to astrocytes (Figure 36a-f), although at the 48 hour timepoint some activated microglia expressed the NK1R (Figure 36g-i). Weak

NK1R expression was also noted at 5 hours in occasional monocytes (not shown). No NK1Rs were seen on neutrophils (not shown). Some faint NK1R staining was also noted on the luminal side of perivascular astrocytes (Figure 36c), suggesting that cerebrovascular endothelium may express the NK1R, but at lower levels than adjacent astrocytes.

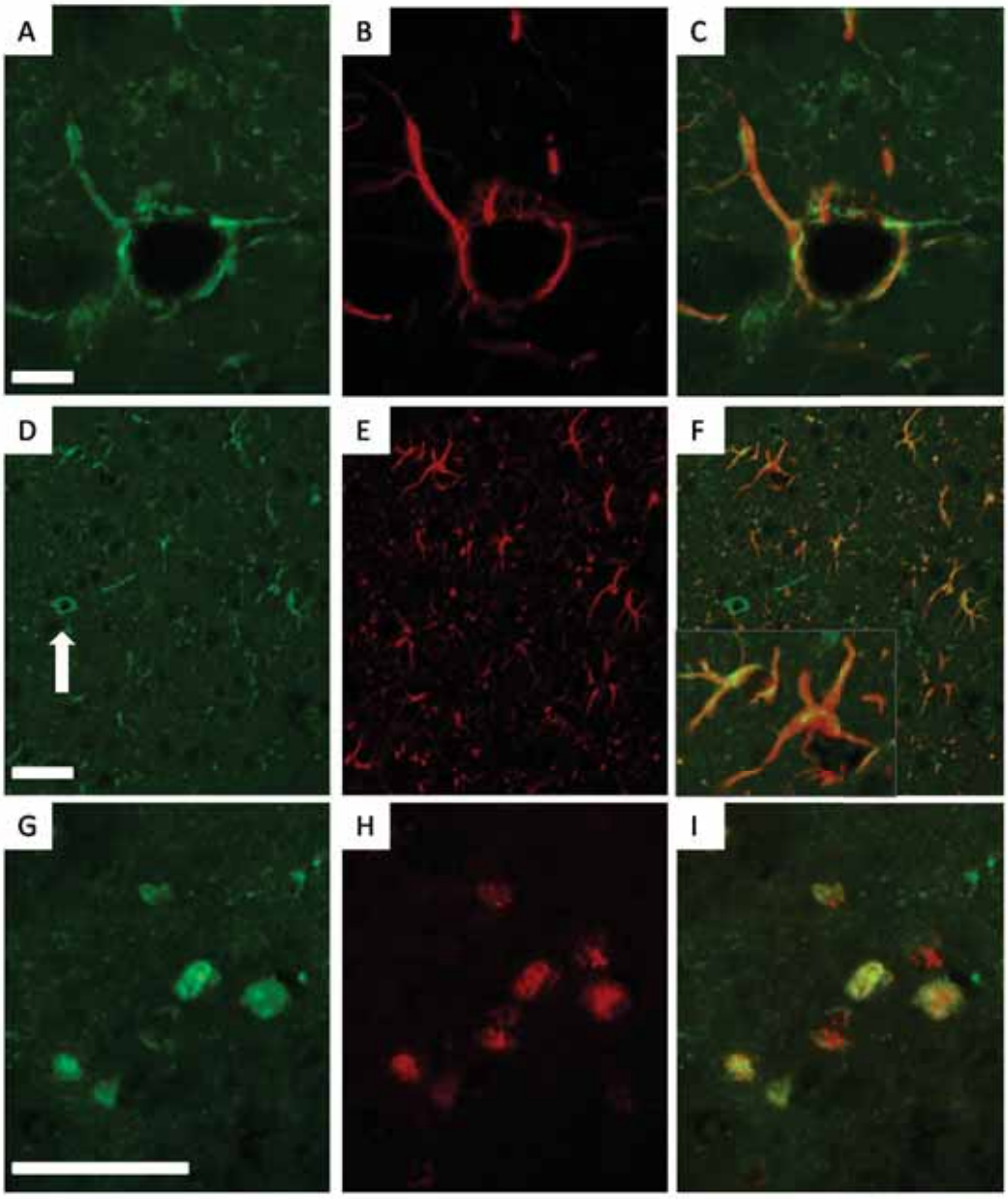


**Figure 36. Double labelling post-collagenase ICH localises increased NK1R immunostaining to astrocytes. Fluorescent immunohistochemistry double labelling for the NK1R (left column) and either mGFAP (B, E) or ED-1 (H), 5 hours (A-C), and 48 hours (D-I) after ICH (right column represents merged images (yellow)). At 5 hours perivascular NK1R localises to astrocytes in both vehicles and treated animals (A-C). Increased astrocytic and vascular (insert) staining is evident at 48 hours ((D-F) neuronal NK1R marked with arrow). At 48 hours evanescent double labelling of activated microglia was observed (G-I). Scale bar=50μm.**

### 3.3.4 Autologous ICH Histology

#### *HE staining*

Compared with cICH at five hours, a greater degree of dissection occurred along white matter tracts and into ventricles (Figure 37a). Earlier haemolysis was evident and also separate areas of fibrin thrombus were seen (not shown). Similar to collagenase ICH, at 24 hours a rim of oedematous tissue surrounding the haematoma was present (Figure 37b), containing in its inmost perimeter degenerating and apoptotic neurons and glia. . There was little change at 48 hours, and by 7 days the haematoma had, again, largely resorbed (Figure 37d), leaving a macrophage-filled cavity.

Significant haemoglobin crystallisation was noted at early timepoints, especially at 24 hours (Figure 37c). This occurred to a far greater extent than was seen following cICH (see Kleinig *et al*[506] for details). As detailed in the referenced publication, the presence of haemoglobin crystals evoked a potent neutrophilic and microglial reaction.

There was a greater injury with autologous ICH vehicle controls compared with cICH controls (Figure 37e, f), in keeping with the larger bore needle used (26G vs 30G) and greater volume of vehicle (100 vs 2µL). There were no abnormalities seen in the contralateral hemisphere at any timepoint in controls or aICH animals.

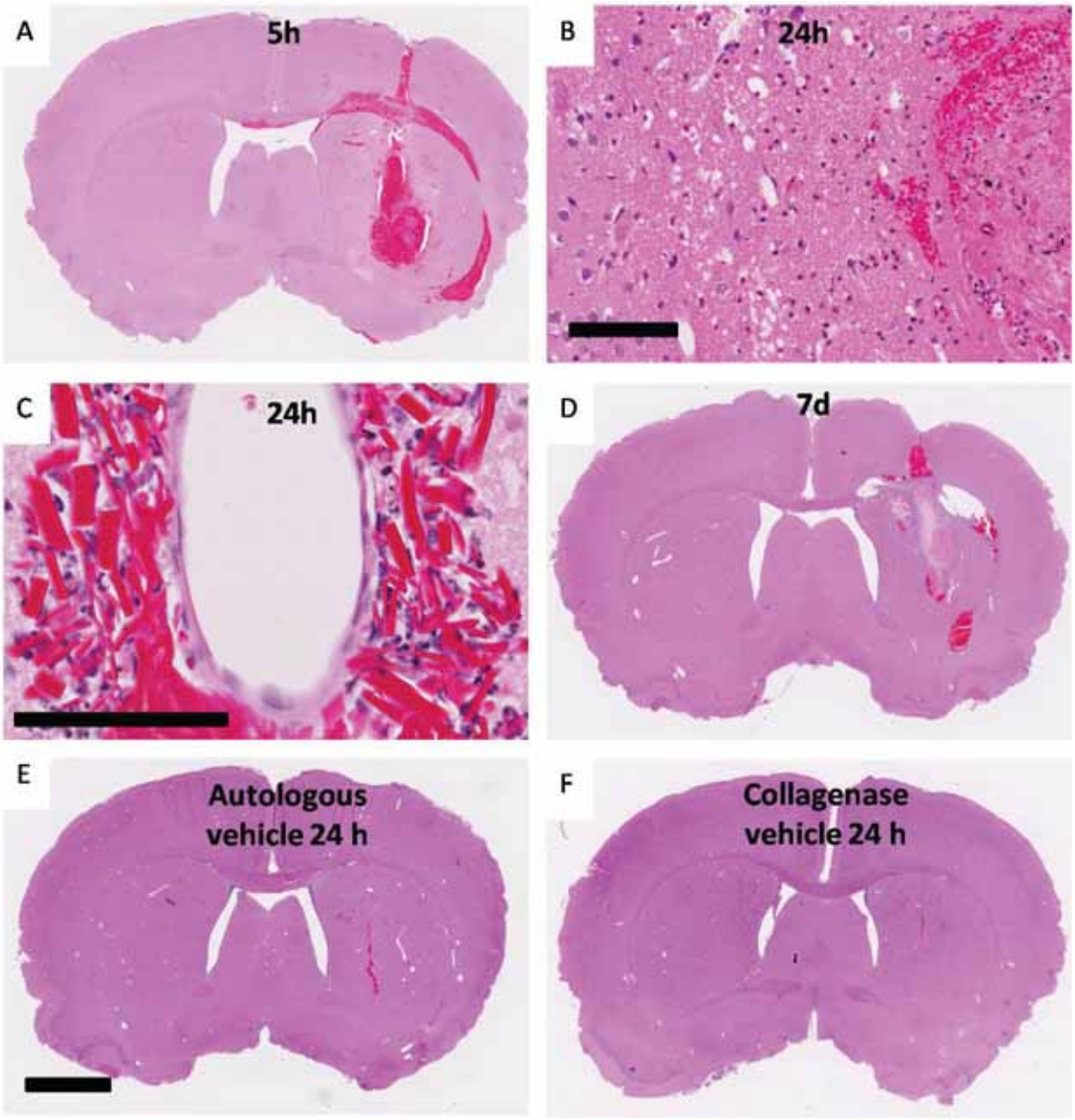


**Figure 37. H&E staining following autologous ICH. (A) At five hours areas the haematoma can be seen dissecting along the corpus callosum and into the ventricle. (B) At 24 hours distinct haematomal (right), perihaematomal necrotic/apoptotic (middle) and oedematous zones are evident. As in collagenase ICH, most erythrocytes have lysed. (C) There was also considerable haemoglobin crystallisation at this timepoint. (D) At 7 days a smaller glial-lined cyst is seen than following collagenase ICH. Both non-absorbed erythrocytes and residual fibrin are still evident. Vehicle injection caused a greater injury in autologous (E) than collagenase (F) controls. Scale bar=50µm or 2mm for whole sections.**

### *SP staining*

There were similar changes to cICH seen with SP immunostaining at all time-points following aICH, save that the intensity of the early granular and astrocytic changes was less marked (Figure 38).

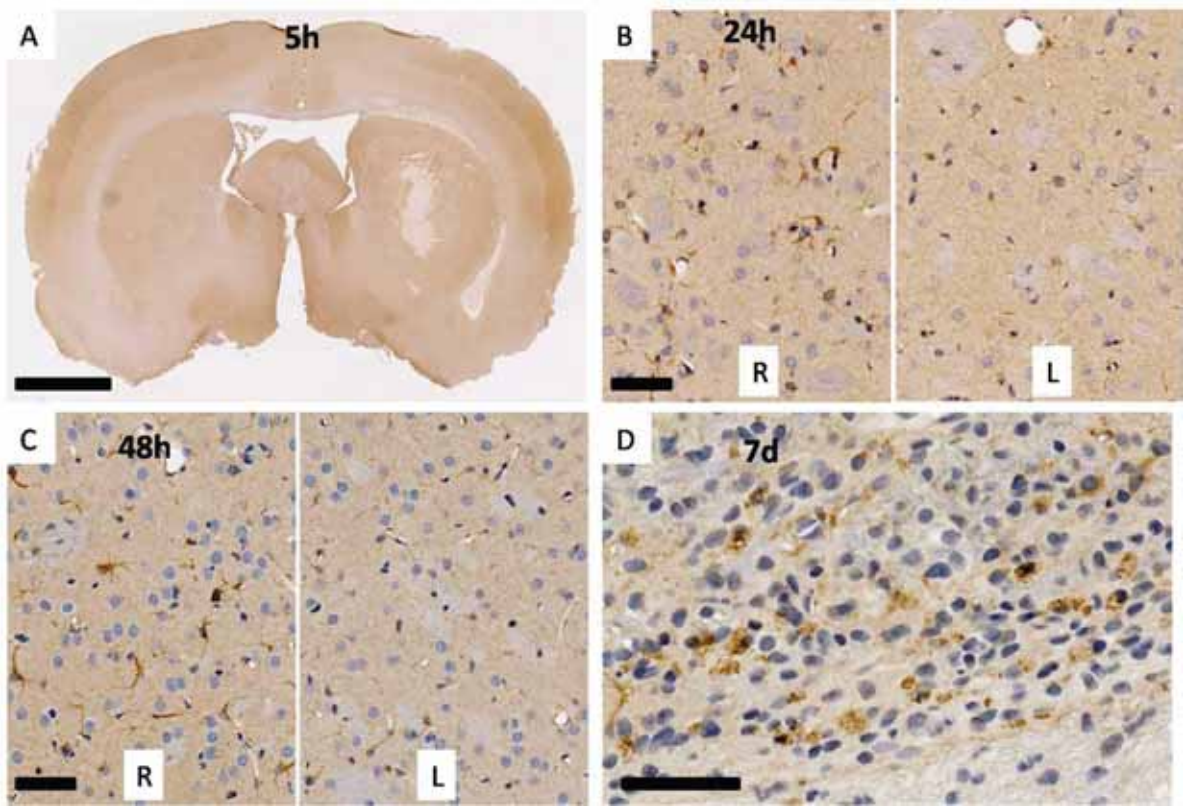


**Figure 38. SP immunostaining following autologous ICH. There was little peri-haematomal increased SP at 5 hours. (B) Similarly to post-collagenase ICH, there is increased astrocytic staining at 24 hours, which increased further at 48 hours (C) and was found within macrophages at 7 days (D). Scale bar=2mm (A) or 50µm (B-D).**

Again, to confirm subjective interpretation of SP immunostaining, images were semi-quantitated by colour deconvolution (Figure 39). Changes essentially mirrored those found in cICH, with perihaematomal cortical and striatal SP elevations, especially at 48 hours (Figure 39a), however the degree of change was much smaller and of, at best, borderline statistical significance (Figure 39c, d). Elevations of striatal SP ipsilateral to injection were also found at 24 hours in the vehicle group (Figure 39a).

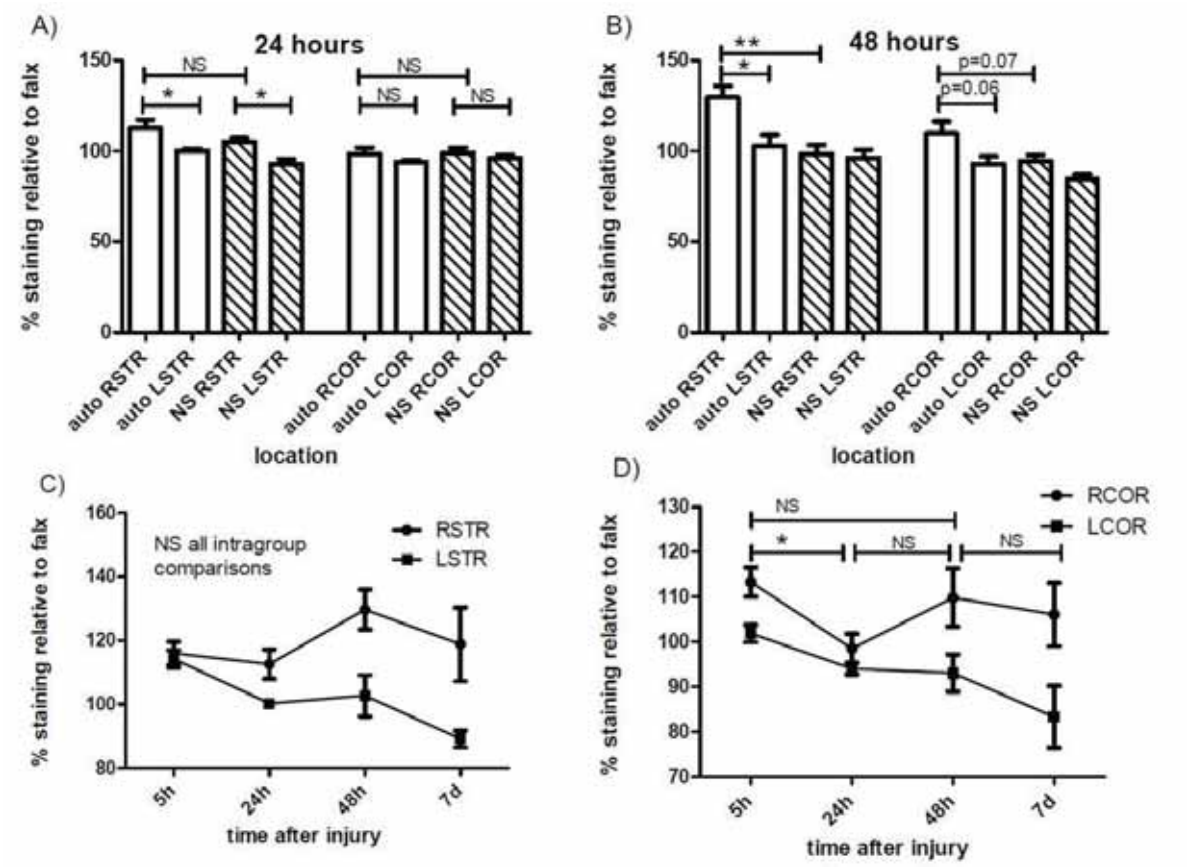


**Figure 39. SP immunostaining following autologous ICH, semi-quantitated. (A) An increase in striatal SP was noted at 24 hours following both blood and vehicle injection. (B) Peak ipsilateral/contralateral differences in SP immunostaining occurred at 48 hours. (C, D) Changes over time were overall similar to, but less marked than changes following collagenase ICH. RCOR=right cortex, LCOR=left cortex, RSTR=right striatum, LSTR=left striatum. **=p<0.01, *=P<0.05, NS=not significant.**

### *NK1R staining*

There was an increase in NK1R astrocytic staining noted at the 24 and 48 hours timepoints, in a similar pattern to cICH, but to a lesser extent (Figure 40a). Analogous to the SP response to large volume vehicle injection at 24 hours, astrocytes ipsilateral to vehicle injection also exhibited increased NK1R upregulation at this timepoint (Figure 40b), although the area of upregulated astrocytes was less extensive than in the autologous group. There was a similar increase in NK1R-IR seen in aICH animals, but not vehicle controls (not shown).

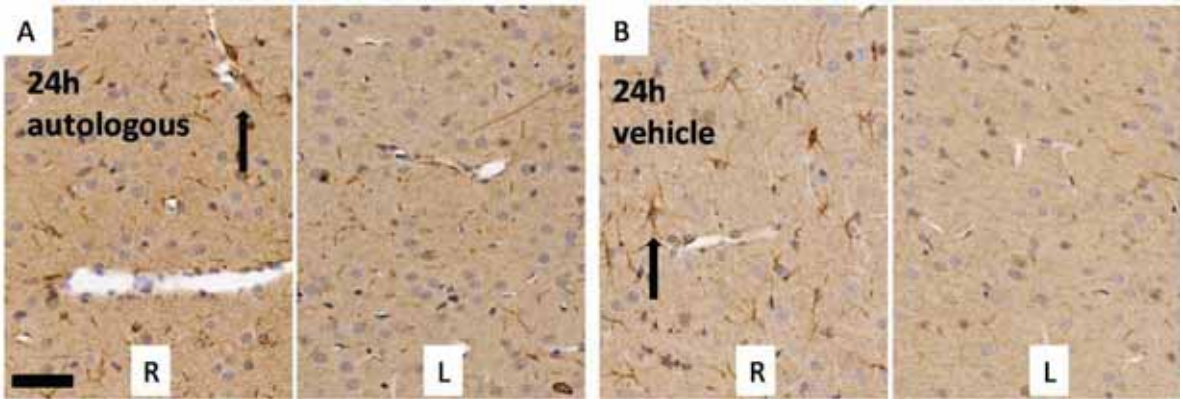


**Figure 40. NK1R immunostaining 24 hours after autologous ICH. (A) There is increased astrocytic NK1R-IR compared contralaterally (arrow), although this increase was also evident in vehicle controls (B, arrow). Scale bar=50µm.**

### *Fluoro-Jade C staining*

Appearances were similar to cICH, with peak staining at 24 hours (Figure 41a). However, more degenerating neurons were apparent at 5 hours, and fewer at 48 hours, suggesting that the process of neuronal degeneration is, in this model, accelerated. Additionally, as might be expected, vehicle injection caused a greater injury in this model (Figure 41b).

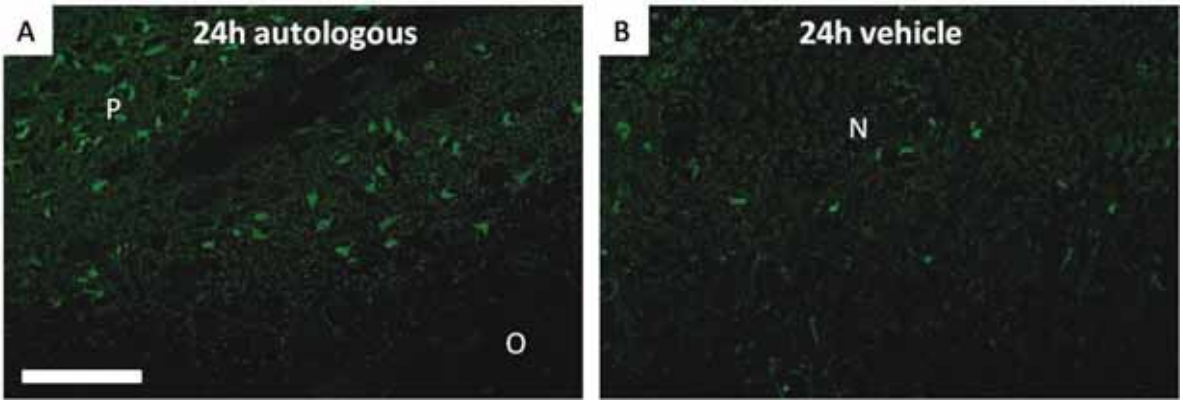


**Figure 41. FJC staining 24 hours following autologous ICH (A) and vehicle (B). Similarly to following collagenase ICH there are numerous FJC positive neurons within the penumbral zone (P). As opposed to the collagenase vehicle group, FJC positive neurons were easily identifiable following autologous vehicle (B). N=needle tract, O=oedematous zone. Scale bar=100µm.**

### *Inflammatory response: neutrophils (myeloperoxidase) and monocyte/ microglia (ED-1, IBA1)*

As in the collagenase model, neutrophils were seen at five hours accumulating in vessels or having just transmigrated into the brain (Figure 42a). Great variation was seen in the

neutrophil response at 24 and 48 hours in this model (Figure 42b, c). This appeared proportional to the degree of haemoglobin crystal formation, which was considerably more prominent in the aICH model.[506] Following aICH without crystal formation, a concentric ring of neutrophils around the haematoma was evident (Figure 42c, right), as following cICH. However when crystals were present, neutrophils were clustered in peri-crystalline microabscesses (Figure 42b, c left) – a finding which was not present in the collagenase model.[506] Again, almost no neutrophils were visible at 7 days (not shown). Injection of vehicle evoked a much stronger neutrophilic infiltrate than in collagenase control animals (Figure 42d).

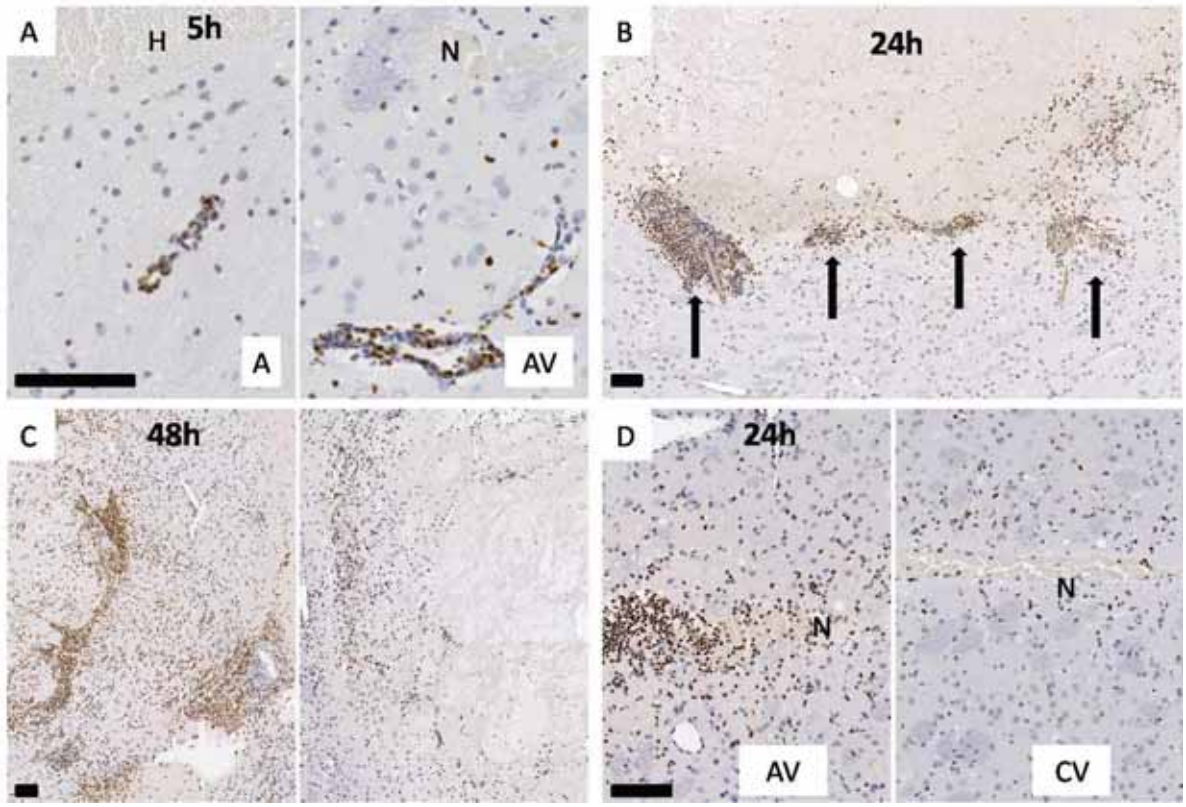


**Figure 42. Myeloperoxidase immunohistochemistry post-autologous ICH. (A) At five hours early chemotaxis of neutrophils is evident following both autologous ICH (A) and vehicle (AV). (B) At 24 hours intense neutrophil infiltrate is seen preferentially around crystal clusters (arrows). (C) At 48 hours a wide variation can be seen in the intensity of neutrophil infiltrate, depending on whether the haematoma contained many (left) or few (right) crystal clusters. (D) Vehicle controls for the autologous group (AV) had a greater neutrophilic infiltrate than collagenase vehicles (CV) at 24 hours. H=haematoma, N=needle tract. Scale bar=100µm.**

Early microglial responses essentially mirrored neutrophil responses – appearing at 5 hours and infiltrating asymmetrically around crystal clusters at 24 hours (Figure 43a). Thereafter, whereas neutrophil infiltration reached a plateau and then diminished, activated microglia were seen in greater numbers and in a more homogenous pattern at 48 hours and 7 days

(Figure 43a). When quantified, leucocyte responses (both neutrophils and activated microglia) were similar in time-course and extent, taking into account differing haematoma volumes in the two models (Figure 43b, c). The activated microglia and neutrophil response to vehicle injection was greater in autologous than collagenase controls (not shown).

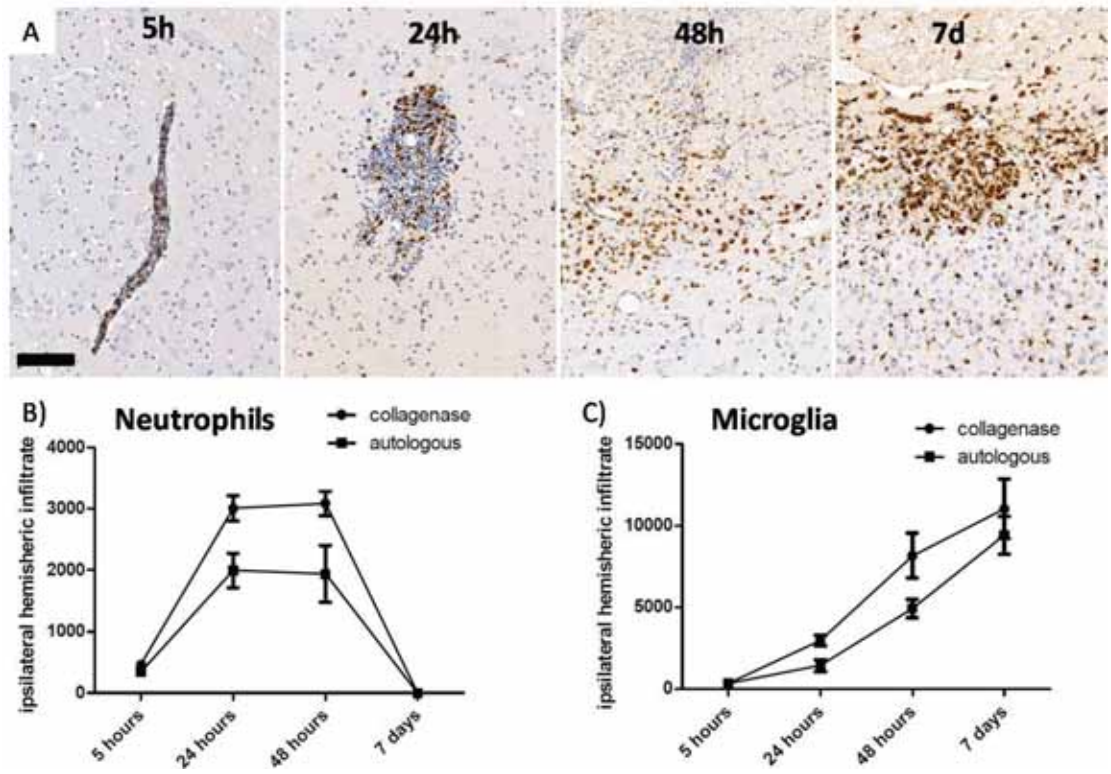


**Figure 43. Monocyte/microglial responses following autologous ICH and leucocyte quantification (both models). (A) Progressive infiltration of monocytes/microglia (from left) 5h, 24h, 48h and 7d following ICH. At 24 hours an exaggerated pericrystalline response is noted, but thereafter the infiltrate is more diffuse and homogenous. (B), (C) The degree and progression of hemispheric neutrophilic (B) and microglial/macrophage (C) infiltration is similar in both models, if adjusted for haematoma volume. Scale bar=100µm.**

### *Astrocytic response (GFAP)*

GFAP responses to aICH were not visible at five hours, but then progressed at each subsequent timepoint, as per following cICH (Figure 44). Once again, there was a significant difference in the degree of reaction to vehicle injection between the two models .

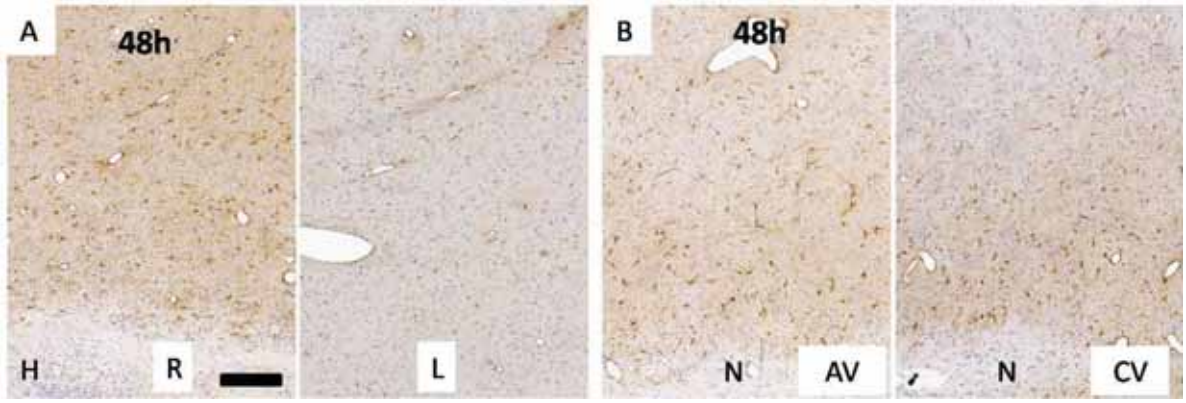


**Figure 44. Astrocytic response (GFAP) 48h following autologous ICH. (A) Autologous ICH led to a progressive increase in GFAP immunostaining at all timepoints. (B) The GFAP response following autologous vehicle (AV), while less than following autologous ICH, was considerably greater than following collagenase vehicle (CV). H=haematoma, N=needle tract. Scale bar=100µm.**

### *Albumin immunohistochemistry*

Differing from cICH, a biphasic peak in albumin immunostaining was seen at 5 and 48 hours (Figure 45a, c), suggestive of initial influx of albumin with the ICH, followed by a delayed peak BBB disruption. A peak was also seen with autologous vehicle injection at this timepoint (Figure 45e), the intensity of which was considerably greater than following collagenase vehicle injection (Figure 45f).

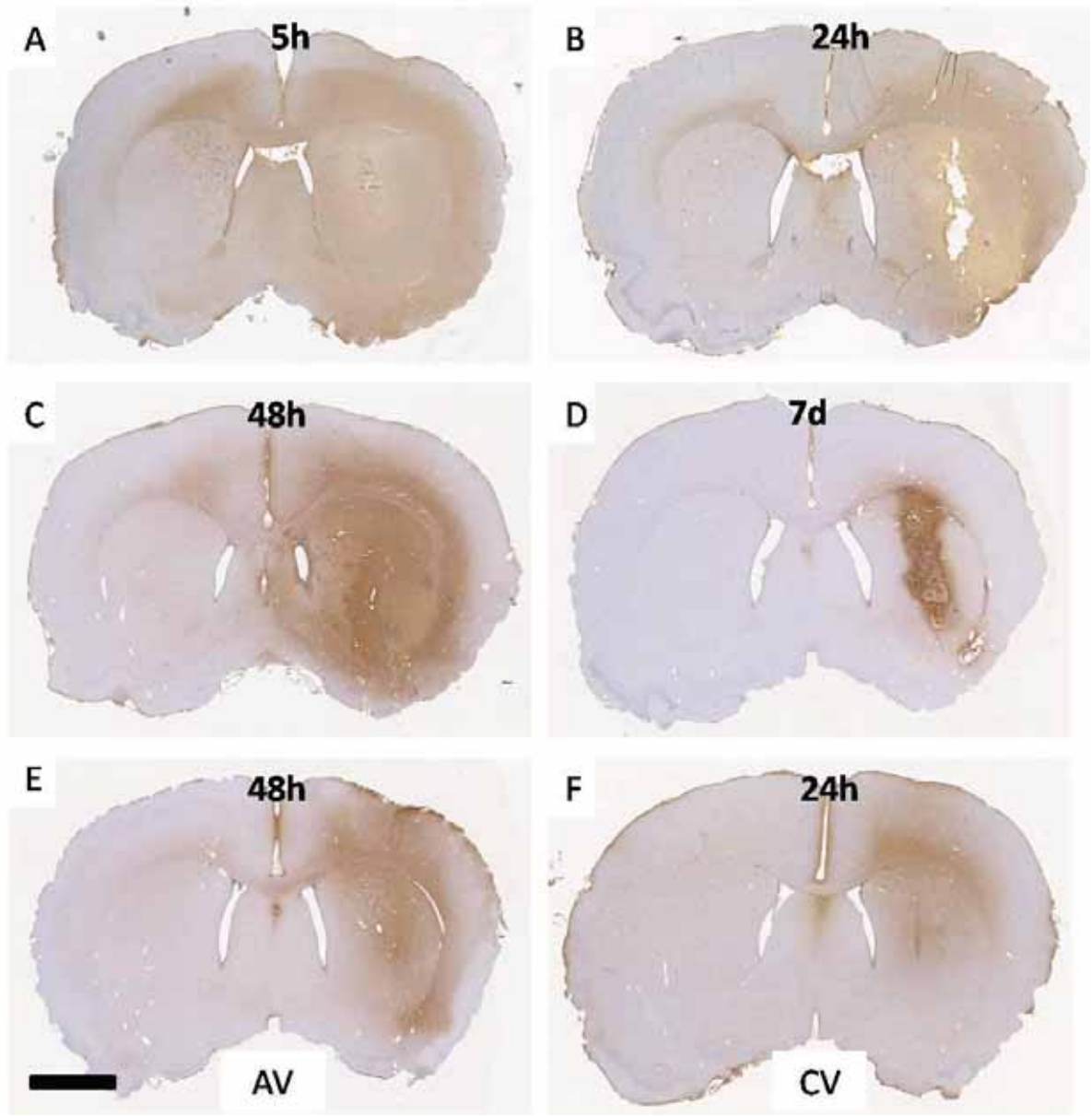


**Figure 45. Albumin immunostaining following autologous ICH and vehicle controls. (A) Albumin-IR is present bilaterally at 5 hours. (B) It diminishes somewhat at 24 hours, but has a second peak at 48 hours (C). (D) At 7 days persistent albumin-IR is present around the haematoma, consistent with ongoing BBB permeability. (E, F) Significantly more albumin immunoreactivity is seen in autologous (AV) vs collagenase (CV) vehicle controls at their relative staining peaks (48 and 24 hours respectively). Scale bar=2mm.**

### *3.3.5 Collagenase ICH SP ELISA*

In order to confirm the subjective impression of an early increase in SP immunoreactivity, and also to validate the method of semi-quantitation by colour deconvolution, ELISA was performed at the most relevant timepoints following cICH (Figure 46). Findings mirrored those determined subjectively and semi-quantitatively; namely, that ipsilateral to the ICH

there was a significant increase in SP, most marked at 5 hours. As ELISA appeared concordant with deconvolution findings at the first two time points, no further timepoints were assessed with this method. This investigation also confirmed the validity of the semi-quantitative method, and confirmed that a further sham surgery group was unnecessary.

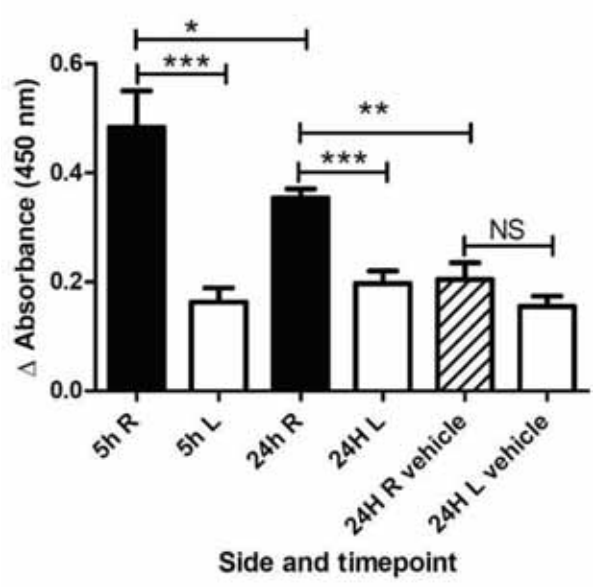


**Figure 46. SP ELISA 5 and 24h post-collagenase ICH and vehicle controls. There was a marked increase in SP concentrations ipsilateral (R) to the ICH at 5 hours, less marked at 24 hours. There were no differences between ipsi- and contralateral vehicle controls, or between this group and the intervention group contralateral to ICH. ***=p<0.001, **=p<0.01, *=p<0.05, NS=not significant.**

### *3.3.6 Collagenase ICH SP and NK1R ELISA*

Various sources could be responsible for the SP peak seen early following ICH - blood, perivascular trigeminal fibres, striatal neurons or astrocytes. Therefore, real-time RT-PCR was performed at 5 and 24 hours to determine which of these were more or less likely (Figure 47). RNA quality was excellent with an average RNA integrity number of 9.0 ± 0.3 (1 represents totally degraded RNA and 10 represents intact RNA.)

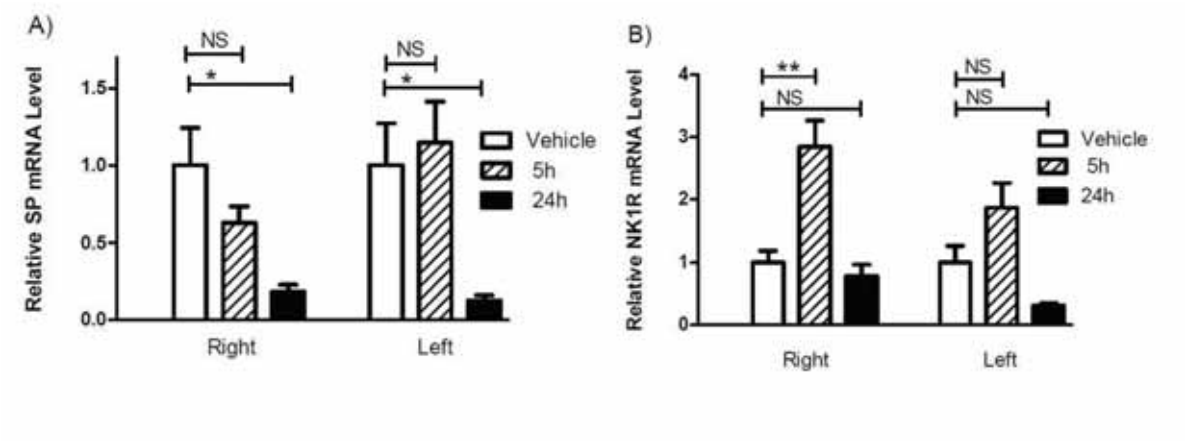


**Figure 47. SP and NK1R mRNA following collagenase ICH. (A) Following collagenase ICH a progressive decrease in mRNA levels is seen bilaterally. (B) A nearly threefold peak in NK1R mRNA is seen at five hours ipsilaterally, returning to baseline levels at 24 hours. Vehicle had no effect on mRNA levels. **=p<0.01, *=p<0.05, NS=not significant.**

Injection of vehicle had no effect on either SP or NK1R mRNA . There was no increase in SP mRNA at 5 hours, and, somewhat surprisingly, a decrease in SP mRNA seen bilaterally at 24 hours (Figure 47a). Conversely, elevated levels of NK1R mRNA were detected at 5hours, but not later (Figure 47b), preceding and therefore consistent with the elevated levels of NK1R astrocytic staining detected with immunohistochemistry at 24 and 48 hours.

### *3.3.7 Pilot behavioural studies*

In preliminary behavioural testing it was immediately apparent that aICH animals had a highly variable behavioural deficit following injury, as only 7/15, as opposed to 14/15 cICH animals demonstrated circling behaviour at 5 hours post-injury (p=0.014; Fishers' exact test.) This behavioural variability, along with the histological variability outlined above, led to the decision that further behavioural studies would only be performed following cICH.

As mentioned in the methods, the 7-day group had a milder injury due to a new batch of collagenase. This particular group was therefore eminently suitable for determining which of the published behavioural tests would be most suitable for distinguishing small- moderate improvements in functional outcome. Seven different behavioural tests were performed (Figure 48). In order, the most sensitive were the rotarod (p<0.0001), the tapered ledged beam (p=0.0018), the vibrissae elicited stimulation test (p=0.002), the elevated drag test (p=0.0023) and the sticky label test (p=0.046). The limb placing composite (p=0.1) and the elevated body swing test (p=0.2005) did not differ significantly from baseline and it was therefore decided that these tests were unsuitable for further use.

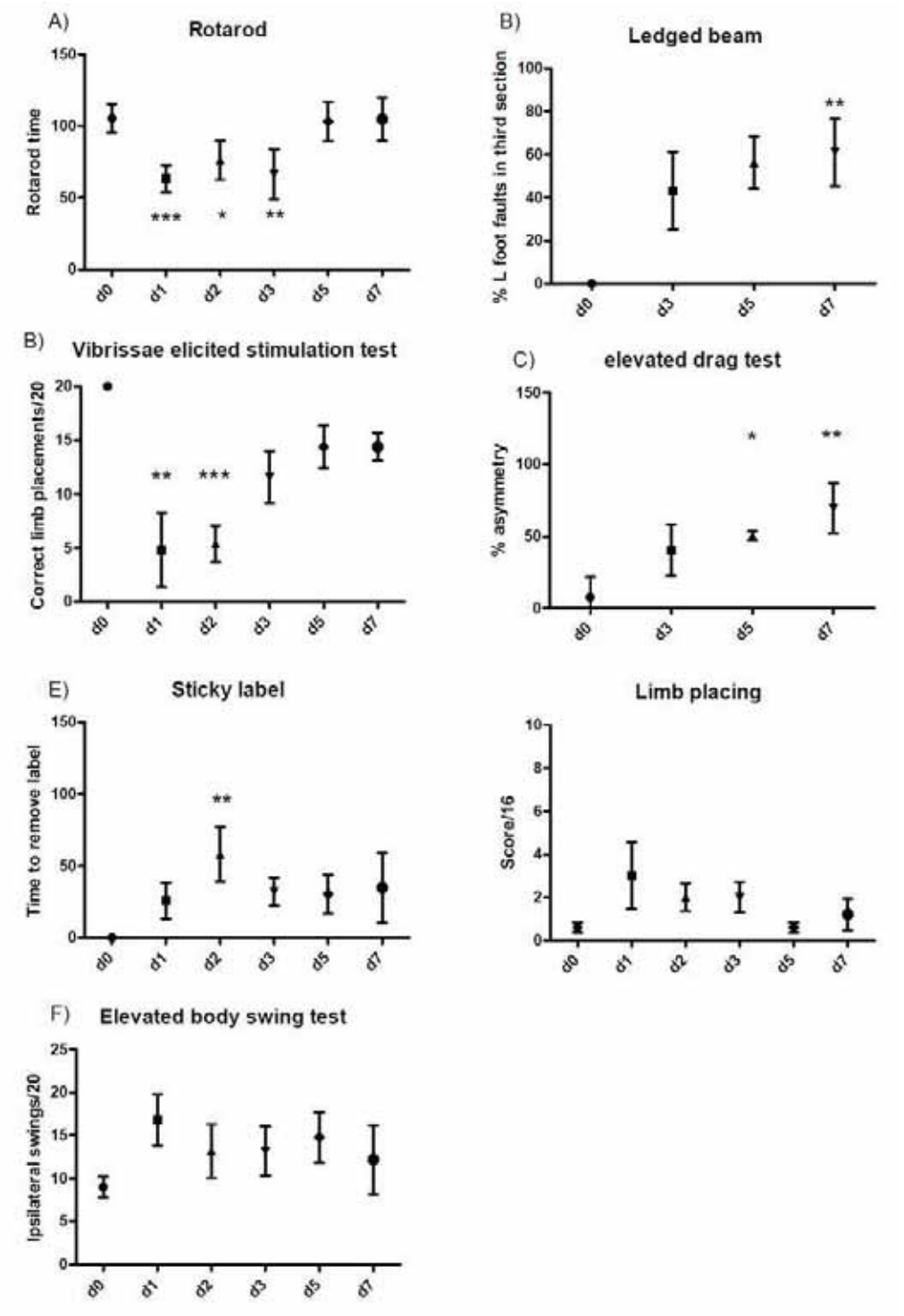


**Figure 48. Pilot behavioural tests post-collagenase ICH, ranked in order of sensitivity. The final two tests (F,G) were not significant by the Friedman test. d0 etc. =days post-ICH, ***=p<0.001, **=p<0.01, *=p<0.05 by Bonferroni post-tests.**

## 3.4 Discussion

The above experiments demonstrated that perihaematomal substance P was elevated acutely following both collagenase and autologous intracerebral haemorrhage. This occurred early enough to feasibly cause or exacerbate 'second stage' (presumed thrombin-mediated) oedema. It also preceded significant neutrophil and monocyte/microglial responses, consistent with a possible facilitatory role, and preceded perihaematomal neuronal cell death. Furthermore, increased levels of substance P were preferentially found in astrocytes, which are critically involved in blood-brain barrier function,[134] oedema[507] and inflammation.[508, 509] This cell population also demonstrated elevated levels of the NK1 receptor, suggestive of autocrine stimulation. Consistent with previous work,[461] perivascular NK1R and SP was detected in astrocytes even in uninjured tissue (although at lower levels), supporting the hypothesis that SP and its NK1R play a role in both normal and pathological BBB function.

The time-course and pattern of elevated SP was consistent with that found following traumatic brain injury (TBI) and transient middle cerebral artery occlusion (tMCAO).[461, 481] In both conditions elevated diffuse parenchymal and perivascular staining was found at 5-7 hours, diffuse astrocytic staining at 24-72 hours and macrophage staining at 7 days. In these two differing forms of brain injury, both NK1R inhibition and capsaicin ablation of sensory nerves have proved neuroprotective.[461, 481, 510] In the current study, vehicle injection also increased astrocytic SP (though not to levels seen following ICH), suggesting that the astrocytic SP response may be a non-specific deleterious reaction to brain injury, analogous to several other pathophysiological processes found deleterious in TBI, tMCAO and ICH (for instance IL-1β and glutamate release).[57, 456, 457]

These results were also concordant with other studies which have demonstrated the deleterious role of SP and the NK1R in more chronic experimental neuroinflammatory processes, such as experimental allergic encephalomyelitis,[433] a mouse model of multiple sclerosis, and encephalitis induced by varied CNS pathogens - administration of an NK1R antagonist or NK1R gene knock-out dramatically decreases pro-inflammatory cytokines and astrogliosis following infection with *Neisseria Meningitidis and Borrelia Burgdorferi* [432] and similar results have been following cerebral toxocariasis,[423] trypanosomiasis[422] and HIV encephalitis.[425] As acute post-injury inflammation is, broadly speaking, deleterious following ICH,[98] ischaemic stroke,[242] and traumatic brain injury,[457] the results presented in this chapter provide further support for the hypothesis that elevated levels of SP following ICH (and other forms of acute CNS injury) may exacerbate secondary damage via the post-ICH inflammatory response.

Although we confirmed the presence of NK1Rs in astrocytes following ICH,[511] we could not reproduce previous reports that microglia and neutrophils express the NK1R.[442, 446] Expression of NK1Rs was not detected at all in neutrophils, and only in a subgroup of infiltrating monocytes and activated microglia at 5 and 48 hours, respectively. It may be that the particular antibody we used was insufficiently sensitive to detect the low levels of NK1R expressed by these cell types. Of note, these previous reports assessed the NK1R either indirectly (using agonists, antagonists and SP knock-out mice),[374, 378, 384] or by Western Blot and RT-PCR.[432] No reports in the literature can be found in which NK1Rs were detected on these cells with immunohistochemical methods, whereas astrocytic NK1Rs have been detected immunohistochemically.[511] While the current study does not exclude a role for NK1Rs in neutrophils and microglia following ICH, the relative intensity of astrocytic staining may suggest that astrocytic responses are predominant.

Somewhat surprisingly, although elevated levels of NK1R mRNA were found at 5 hours, no elevation in TAC1 mRNA was evident at the timepoints studied, despite clear elevations in SP protein by two modalities, and localisation of increased SP to astrocytes. This raises the possibility that the source of early (5 hours) SP elevation may be exogenous: from haematoma, from plasma through the disrupted BBB, or from trigeminal neurons. Consistent with his possibility, following TBI, plasma levels of SP are elevated acutely (30 minutes) – providing evidence of a possible exogenous source.[461] Another possibility is that an early peak in mRNA was missed – studies in our laboratory following TBI demonstrated elevated levels of TAC1 mRNA at 3, but not 24 hours. Complex changes in TAC1 mRNA have been also noted following experimental ischaemic stroke; in situ hybridisation revealed increases in striatal but not cortical mRNA at 6 hours and an increase in cortical but decrease in striatal mRNA at 48 hours.[445] As our study pooled cortex and striatum, similar changes may have been missed as relative increases and decreases may have negated each other.

Additionally, SP plays dual roles in the striatum – as a neurotransmitter[327] and mediator of inflammation.[420] Cortical and striatal neurotransmitter mRNA are generally depressed following ICH,[89, 90] and inflammatory genes upregulated. It may be that while neurotransmitter mRNA is diminished, neuroinflammatory SP mRNA is increased. SP in each role may be translated, released and degraded at different speeds, accounting for discordant mRNA and protein results.

This series of experiments encountered several difficulties with the aICH model, some of which have been reported previously,[472] although some of which were novel. First, although it has been previously reported that 0.2U of collagenase and 100µL autologous blood were equivalent,[472] we found that haematoma volumes in the autologous group were around 30% smaller. Second, it was found that autologous animals had a generally milder and more

variable behavioural deficits (circling behaviour).[472] This was, histologically, reflected in the variability of haematoma shape, intraventricular extension and inflammatory response. Third, the autologous model appeared at least partly confounded by the presence of haemoglobin crystallisation (see Kleinig *et al*[506]) – which appeared at least in part responsible for the gross variability in inflammatory response. And, last, aICH at times induced changes which were not dramatically different from infusion of comparable amounts of vehicle, and considerably less than seen in cICH - most crucially for SP, GFAP and albumin immunostaining. Why this might be the case is unclear. However, one possibility is that exogenous blood clotting may limit the intracerebral effects of thrombin generation. If this is the case, it would be difficult to test one of our primary hypotheses in this model – that is, that thrombin causes oedema and inflammation post-ICH via substance P. For all these reasons it was determined that the collagenase model would be more appropriate for testing the anti-inflammatory, anti-oedema and behavioural effects of any anti-SP intervention.

## 3.5 Conclusion

In summary, elevated levels of substance P were seen acutely following ICH in a distribution and time-course consistent with a possible pathophysiological role. These effects were most marked in the collagenase model. We experienced several difficulties with the autologous model, most crucially wide variability in histological and behavioural changes post-ICH, which made this model less suitable than cICH for testing the next hypothesis: that inhibition of the NK1R following ICH would ameliorate oedema, BBB dysfunction, inflammation, brain lesion volume and functional deficits.

# 4 Inhibition of substance P via NK1 receptor antagonists: histological, behavioural, oedema and blood-brain-barrier experiments.

## 4.1 Introduction

The experiments detailed in the previous chapter were consistent with the hypothesis that SP may play a pathophysiological role post-ICH; SP was elevated acutely perihaematomally, and elevated levels of SP preceded the development of significant oedema, blood-brain barrier dysfunction, neuronal death and inflammatory cell infiltration/activation.

Such experiments can be suggestive only; elevated substance P could be an association, rather than a cause of the above-mentioned secondary injury mechanisms. However, previous experiments in varied CNS inflammatory states have suggested that SP is indeed pathogenic, as inhibiting elevated SP in these circumstances has proven beneficial, whether through the use of NK1 receptor antagonists[422, 432, 459, 461] or by employing knock-out mice models.[432]

Therefore there is a reasonable possibility that inhibiting SP post-ICH may prove neuroprotective. Caution is warranted in the evaluation of any putative neuroprotective therapy, as treatments reportedly beneficial in animal models have almost without exception failed when trialled in humans. There are many potential explanations for this failure, including species differences, injury model limitations, the heterogeneous nature of human, as opposed to laboratory brain injury and the comparative genetic heterogeneity of human disease populations.[512] However, one of the most significant reasons is the failure of many animal experiments to adhere to good research practices.[513] Taking the failed anti-oxidant neuroprotectant NXY-059 as an example,[514] animal studies which did not adhere to recommended practices reported a far greater benefit of therapy than higher quality studies [515] – findings which are repeated when assessing the neuroprotective literature as a whole.[516]

To limit the chance of a spurious finding, the methods described in this chapter adhered to the principles outlined in the Stroke Academic Industry Roundtable (STAIR) guidelines[517] for appropriate study of preclinical stroke therapies, including:
1) Initial interventional studies in small animals models,
2) Power calculations to determine sample sizes,
3) Randomisaton of animals to treatment groups,

4) Dosing in a route and timeframe relevant to human studies,
5) Blinding of surgeon to treatment group,
6) Control of temperature intra- and post-operatively,
7) Blinding of outcome assessment, and,
8) Both short and long-term histological and behavioural assessment.

Dose response calculations are also recommended in the STAIR guidelines, but have been reported previously in rats for both NK1R antagonists used in this chapter.[461, 482]

## 4.2 Experimental design

Sixty nine male Sprague-Dawley rats (300-340gm) were used for the experiment, as described in chapter 2, utilising the collagenase ICH (cICH) model for reasons outlined in chapter 3.

Thirty animals were sacrificed for histological and immunohistochemical analysis, after treatment with NAT (3x5 per group) or vehicle control (3x5 per group), at 24 hours, 7 days and 28 days post-ICH. The 28 day group was also followed for behavioural studies for the full 28 day period. An additional 10 animals were used in confirmatory behavioural and 28 day histology experiments following treatment with the blood-brain penetrant NK1R antagonist L733,060 or vehicle control (2x5 animals).

15 animals were used for brain oedema experiments (wet weight- dry weight): 5 animals each for NAT, L733,060 and vehicle control. Evans Blue studies were conducted only using NAT or vehicle control (7 animals in each arm).

Treatments were administered by injection into the tail vein, after being briefly reanaesthetised, as described in chapter 2. Animals were randomised to receive either NAT (1ml/kg of 2.5mg/ml NAT in normal saline), L733,060 (1ml/kg of 1mg/ml normal saline) or vehicle (1mL/kg). Animals were treated 2 hours post-ICH induction, to maximise the clinical applicability of any findings (it is not feasible to administer acute stroke therapies in humans earlier than this timepoint).

### 4.2.1 Haematoma quantification

To determine whether NK1R antagonist therapy had any effect on haematoma volume, unstained freshly fixed 2mm thick coronal brain slices from the 24 hour histology group were scanned at high resolution as described. The haematoma was automatically outlined using the ‘magic wand’ function of Adobe Photoshop. Haematoma volumes were calculated by

summing, for each slice, the product of average haematoma area (front and back of each slice) and slide thickness.

### 4.2.2 Brain lesion volume assessment

To investigate whether NK1R antagonists had any effect on post-ICH lesion volumes, freshly perfused 2mm coronal brain slices were scanned as described, following rat sacrifice at 28 days. Total, striatal and cortical volumes were assessed manually for the 2 slices (4mm in total) spanning the area of post-ICH injury. To control for inter-individual variability of brain size they were compared with the same rat's opposite hemisphere. Total, cortical and striatal lesion volumes were thus derived by subtracting ipsilateral from contralateral volumes.

### 4.2.3 Histology and immunohistochemistry

At the pre-specified timepoints animals were perfuse-fixed with formalin, and their brains were extracted, sectioned, scanned and processed as described. H&E and FJC staining was performed on sections through the needle injection site (the haematoma centre), as well as immunohistochemical staining for ED-1, GFAP, MPOX and SP, as described. Slides were scanned at high resolution and viewed with appropriate viewing software.

### 4.2.4 Semi-quantitation of SP immunostaining

Semi-quantitation of peri-haematomal SP was assessed 24 hours following injection of NAT or vehicle using the method outlined above. As in the previous chapter, peri-haematomal regions were analysed, rather than whole hemispheres, to ensure that it was parenchymal SP which was assessed, rather than haematomal SP.

### 4.2.5 Cell counting and evaluation of subventricular zone cellular proliferation

Inflammatory cell infiltrate (neutrophils and activated microglia) was assessed to compare the inflammatory response following treatment with either NAT or vehicle at 24 hours post-ICH, as described in chapter 2. Fluoro-Jade C cell counting was also performed at this timepoint to quantify neuronal degeneration following treatment. The area of cellular proliferation in and emanating from the subventricular zone (SVZ) suggestive of neural and glial precursor proliferation was quantified by outlining cell clusters ('nests') in NDPview in one section for each animal through the haematoma centre (which included the SVZ).

### 4.2.6 Brain oedema

The effect of treatment with both NK1R antagonists of brain water content following ICH was assessed by the wet weight dry weight method, as described in chapter 2. Animals were treated with either vehicle or drug, 2 hours post-injury, and sacrificed at 24 hours.

### 4.2.7 Blood-brain barrier permeability

The effect of NAT on BBB dysfunction was assessed by the Evans Blue method, as described in chapter 2. Animals were treated with either vehicle or NAT, 2 hours post-injury. Evans blue was injected at 12 hours post-injury and animals were sacrificed at 23 hours.

### 4.2.8 Behavioural studies

As demonstrated in chapter 3, the most sensitive behavioural studies were (in order) the rotarod, the tapered ledged beam, the vibrissae elicited stimulation test, the elevated drag test and the sticky label test. These tests were performed in animals following both NAT and L733,060 treatments, or vehicle controls.

Animals were acclimatised to all tests for 5 days pre-injury, trained specifically for the rotarod and ledged beam, and baseline pre-injury levels assessed for all tests except the sticky label. Animals were assessed, in random order, on days 1, 2, 3, 5, 7, 14, 21 and 28 post-injury, by the same assessor, in the same room, at the same time of day (morning), to minimise variability. The assessor was blinded to treatment allocation.

### 4.2.9 Statistical analysis

Continuous variables were assessed by unpaired Student's t-tests. Histological changes over time (for instance SP immunostaining) were assessed by one-way ANOVA with Bonferroni post-tests for selected inter-group comparisons. Brain water content and Evans blue quantification were also analysed by one-way ANOVA, with selected Bonferroni post-tests. Behavioural tests were analysed using a repeated measures two-way ANOVA and Bonferroni post-tests for parametric data, and Kruskal-Wallis one-way ANOVA with selected Dunn's post-tests for non-parametric data.

## 4.3 Results

### 4.3.1 Operative and physiological parameters

There were no significant baseline or operative differences between groups, and temperatures measured 24 hours after ICH (oedema and BBB groups only) were not altered by administration of an NK1R antagonist (Table 3).

Table 3. Experimental parameters: NK1RA vs vehicle.

| Group | Weight | Duration | T start | T finish | T 24 hours |
|---|---|---|---|---|---|
| **NK1RA** | 321±10 | 24±2 | 36.9±0.4 | 37.2±0.3 | 37.3±0.3 |
| **Vehicle** | 318±15 | 25±2 | 37.0±0.4 | 37.2±0.3 | 37.4±0.5 |

**There were no significant differences between groups. Results expressed as means ±SD.**
**Units: weight=grams, duration=minutes, temperature ('T')=°C, partial pressures=mmHg.**

### 4.3.2 Haematoma volumes

Injection of NAT or vehicle had no effect on haematoma volumes at 24 hours (Figure 49).

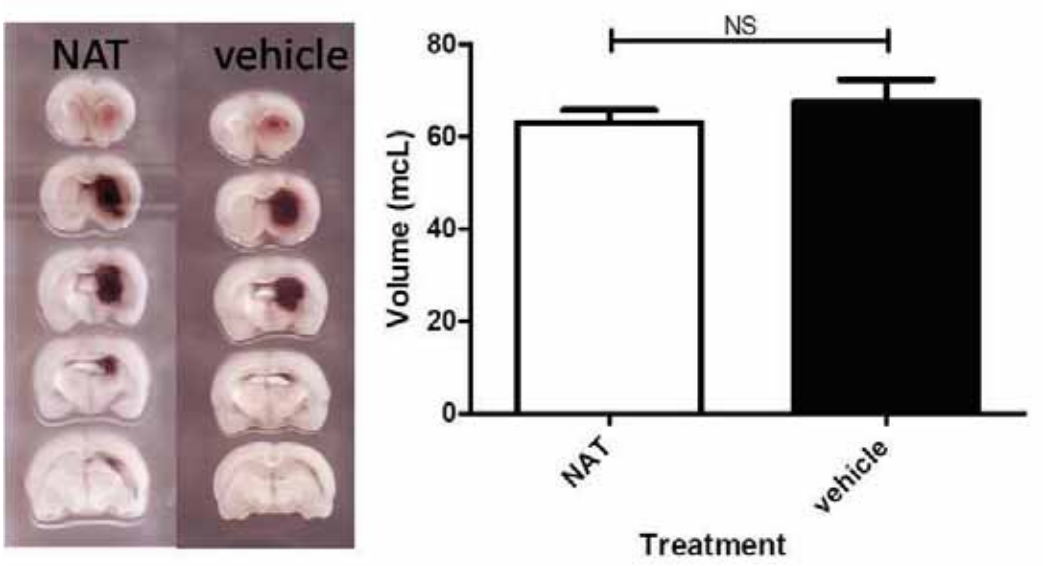


**Figure 49. The effect of NK1R antagonism on 24 hour haematoma volumes post-collagenase ICH. There were no significant differences between vehicle and NAT groups. NS=not significant.**

### 4.3.3 Lesion volumes 28 days after collagenase ICH

There was no consistent benefit from NK1R antagonists with regards to lesion volume at 28 days after ICH (Figure 50). There was a possible protective effect of NAT on cortical volume loss (P=0.041) but no effect was seen on striatal or total hemispheric volume loss, and the effect was neither replicated in animals treated with the structurally different NK1RA L 733,060, nor significant when the results of the two different NK1R antagonists were pooled. Thus it is possible that random variation may explain the finding.

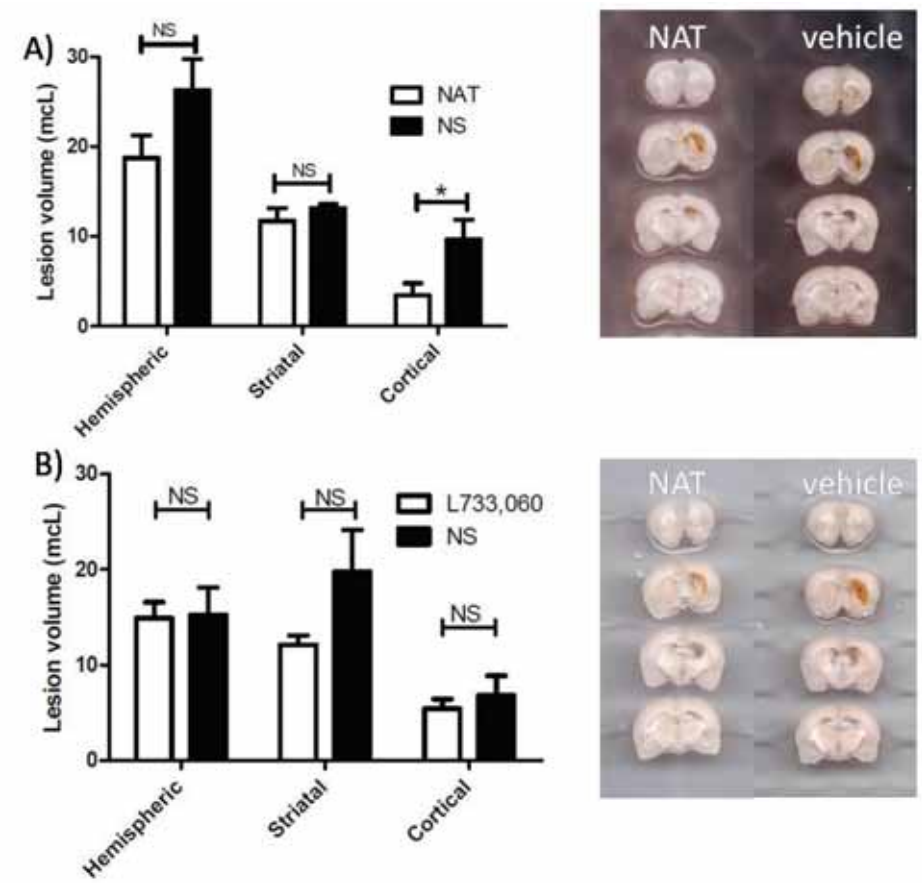


**Figure 50. Effect of NK1 receptor antagonists on lesion volumes. There was no consistent effect of NK1R antagonism on 28 day lesion volumes. NAT may have slightly reduced cortical atrophy, but this effect was not replicated following treatment with L733,060. *=p<0.05, NS=not significant.**

### 4.3.4 Histology and immunohistochemistry

The sole noticeable effect of NK1RA at 24 hours, as assessed by H&E staining, was an apparent reduction in oedema (Figure 51a-d). Red cell lysis, peri-haematomal apoptosis and neutrophil infiltration were not altered by NAT at this time point, but paracellular oedema and swelling of white matter tracts were significantly reduced . In the vehicle-treated group, haematoma-containing sections were more difficult to process (Figure 51b), being highly friable which, in hindsight, may have been due to differing water contents between the two treatment groups (see later). No differences were noted following treatment with NAT at 7 and 28 days post-ICH, or following L733,060 treatment at 28 days (not shown) except that the 7-day subventricular zone proliferative response appeared more prominent in vehicle-treated rats (Figure 51f).

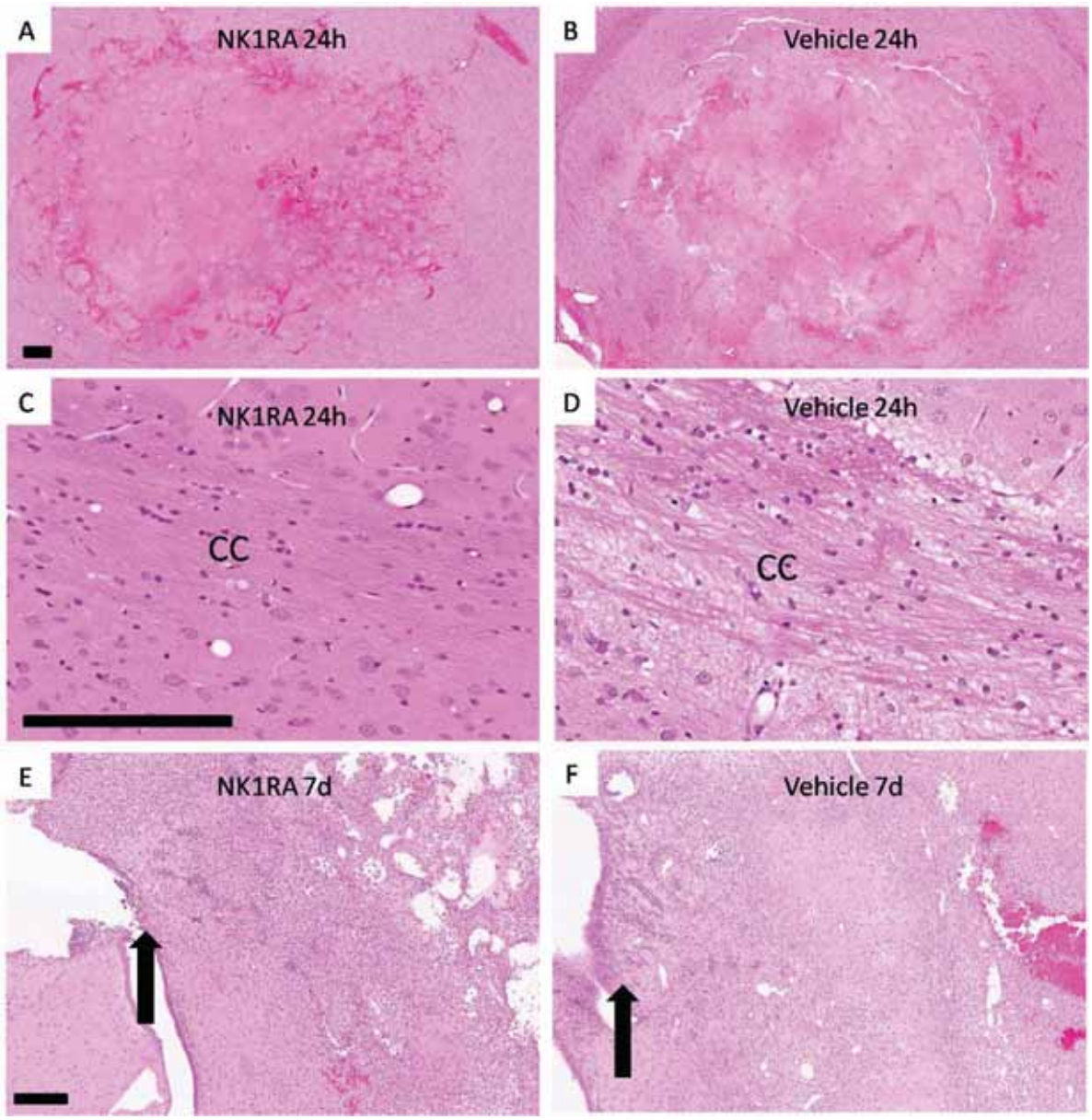


**Figure 51. The effect of NAT on H&E staining after collagenase ICH. (A, B) At 24 hours NAT- and vehicle-treated animals did not appear markedly different at 24 hours on low-power views, except that the haematoma was markedly more friable following vehicle administration. There was a subtle difference in perihaematomal pallor (A, B), which on higher-powered views was due to a reduction in oedema. (C, D) This was most obvious in white matter tracts, especially the corpus callosum, most conspicuously contralateral to injury. (E, F) At 7 days a vigorous proliferative response was seen in the subventricular zone (arrows) in vehicle, but not-NAT-treated rats. CC=corpus callosum. Scale bar=200µm.**

NK1R antagonists had no effect at any timepoint on neuronal degeneration (FJC staining (Figure 52a, b). Gliosis (GFAP immunostaining (Figure 52c, d) and leucocyte infiltration/activation (MPOX (Figure 52e, f) and ED-1 (Figure 52g, h) immunostaining) were likewise unaffected.

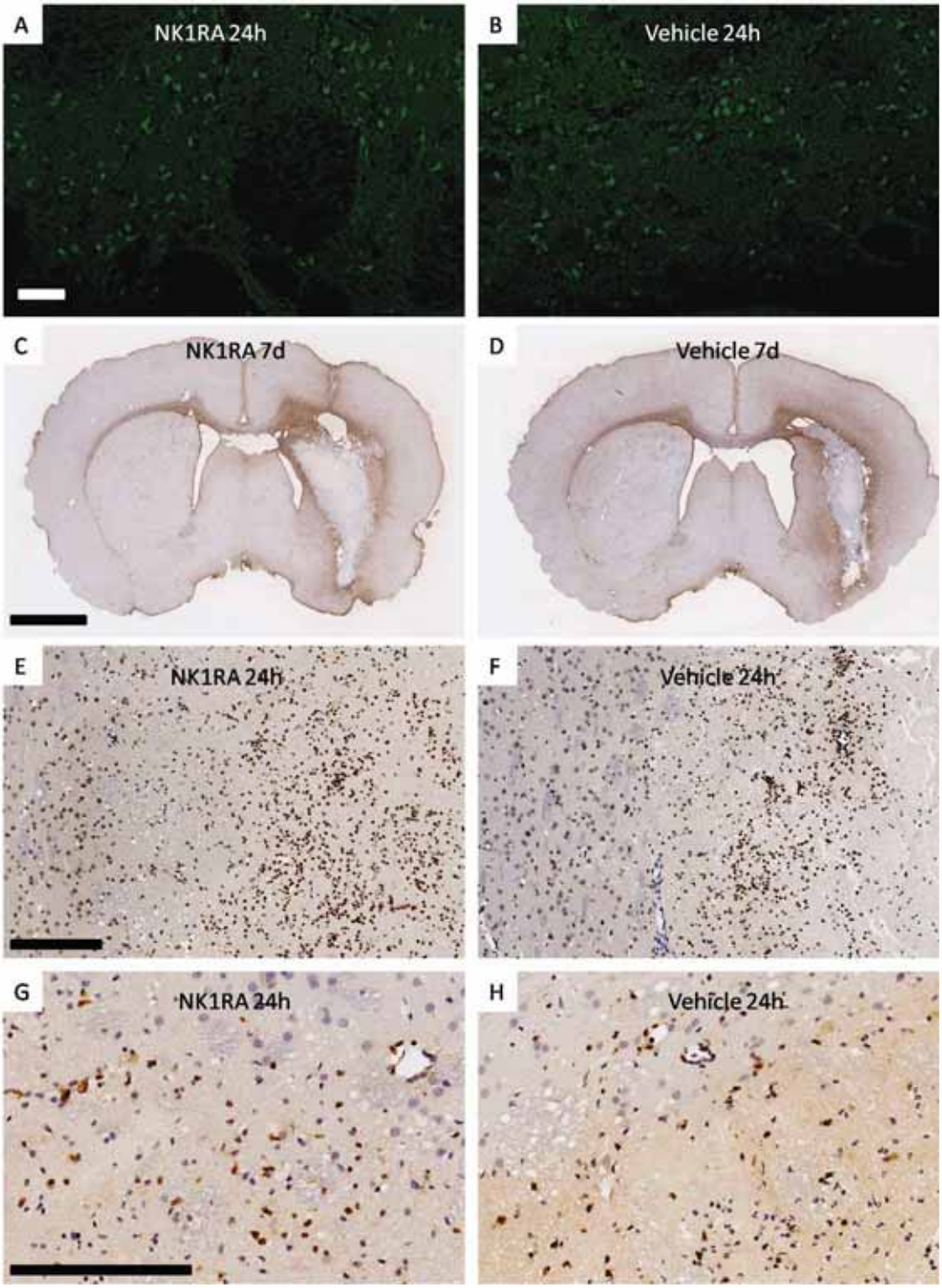


**Figure 52. Fluoro-Jade C staining, astrocyte response and leucocyte response following NK1R antagonism. There were no differences seen between NAT- and vehicle-treated groups. (A, B) Fluoro-Jade C staining at 24 hours. (C, D) Astrocyte response at 7d. (E, F) Myeloperoxidase and (G, H) ED-1 staining at 24 hours. Scale bar=200µm or 2mm (whole brain).**

There was also no effect of treatment on the intensity of SP immunostaining (Figure 53a, b). Semi-quantitation of SP immunostaining by colour deconvolution confirmed subjective impressions (Figure 53c). Although no differences were seen between treatment groups, significant differences between hemispheres were again noted, further confirming the findings of chapter 3 (that cICH leads to increased ipsilateral SP immunostaining).

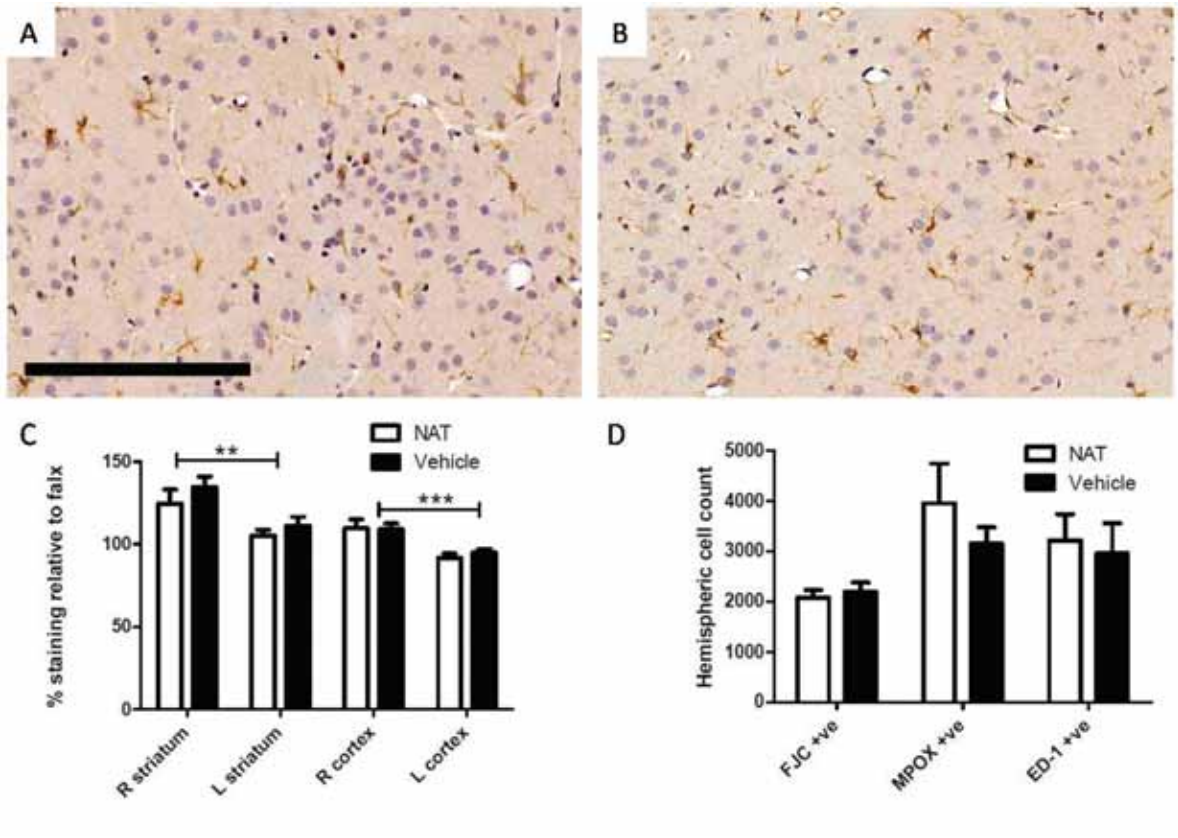


**Figure 53. Perihaematomal SP immunostaining following NAT (A) and vehicle (B) 24 hours post-collagenase ICH and quantification of SP staining intensity (C), neuronal degeneration (D) and leucocyte infiltration/activation (D). There were no significant differences between treatment groups. As outlined in chapter three, ICH led to increased perihaematomal SP immunostaining (C) predominantly (at 24 hours) in astrocytes (A,B). Scale bar=200µm. ***=p<0.001, **=p<0.01.**

FJC-, myeloperoxidase- and ED-1-positive cells were also quantified at 24 hours (Figure 53d). This confirmed the subjective impression that NK1R antagonism had no effect on neuronal degeneration or inflammatory cell infiltration/activation.

### 4.3.5 Cellular proliferation in the SVZ

Neural and glial precursor cells reside in the SVZ, where they can proliferate under various stimuli, including cerebral ischaemia[518] and intracerebral haemorrhage.[519] On light microscopy areas of progenitor cell proliferation can be visualised as subependymal 'nests' of cells,[520] which increase in area and extent following ICH.[521] Treatment with NAT appeared to reduce the area of subependymal zone cellular proliferation (Figure 51f, Figure 54).

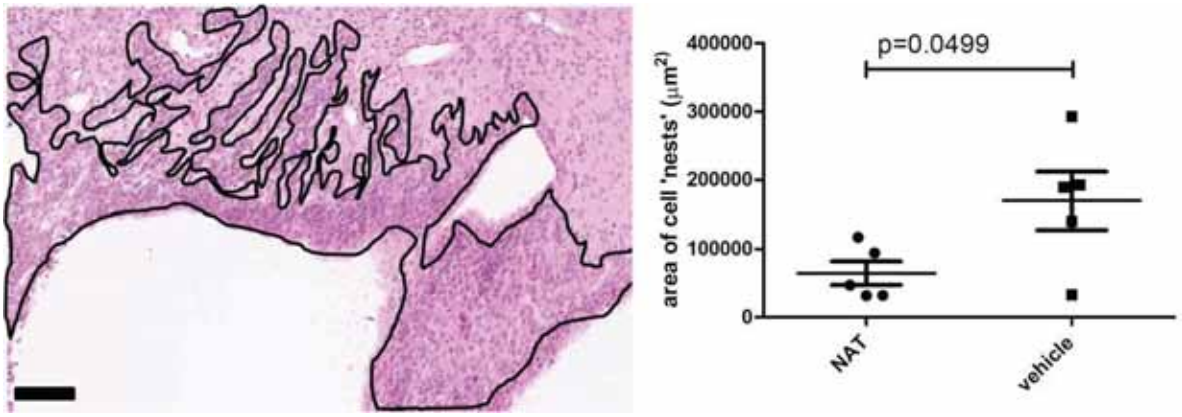


**Figure 54. The effect of NK1R antagonism on cellular proliferation in the subventricular zone. Outlined higher power view of Figure 50f. The area of apparently proliferating cells was greater in the vehicle treated group, suggesting that NAT may suppress neurogenesis and gliogenesis post-ICH. Scale bar=200μm.**

### 4.3.6 Brain oedema

H&E staining at 24 hours suggested that NAT ameliorated peri-haematomal oedema post-ICH (Figure 51). This was confirmed by the wet-weight dry-weight technique (Figure 55).

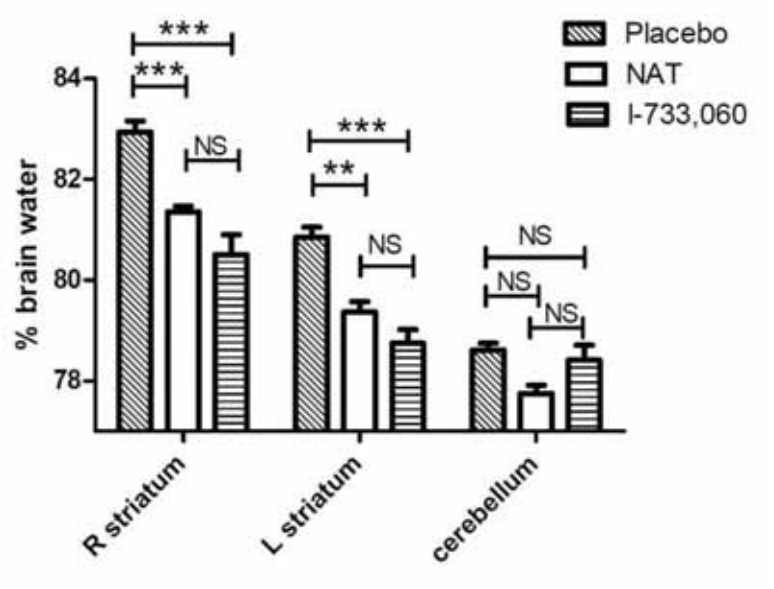


**Figure 55. Brain oedema following treatment with NK1R antagonists 24 hours post-collagenase ICH. Significant differences were seen following treatment with both NAT and L733,060. ***=p<0.001, **=p<0.01, NS=not significant.**

Both NK1R antagonists (NAT and L733,060) caused a dramatic reduction in peri-haematomal brain water content, from 82.9±0.5% to 81.4±0.2% and 80.5±0.9% respectively (P<0.001 for both comparisons). L733,060 reduced ipsilateral oedema to vehicle-ICH levels (80.4±0.4%, p=0.18 for comparison). Both NK1R antagonists even reduced brain water content in the contralateral hemisphere, to vehicle ICH levels (p<0.01 and p<0.001 for comparison with placebo). Although the beneficial effect of treatment on contralateral oedema has never been reported previously with any agent post-ICH, it is independently corroborated by H&E findings, which, as previously mentioned, in a separate group of rats, demonstrated reduced oedema in the corpus callosum contralateral to the ICH 24 hours following NAT treatment (Figure 51c, d).

No effect was seen on brain water content in the cerebellum, which served as a control, indicating that NK1R antagonists do not reduce brain water content except in the setting of a pathological elevation.

### 4.3.7 Blood-brain barrier dysfunction

It is uncertain what proportion of post-ICH oedema is of ‘vasogenic’ or ‘ionic’ origin, although both undoubtedly occur. Whether or not SP post-ICH contributes to vasogenic oedema was assessed by quantification of Evans Blue (Figure 56).

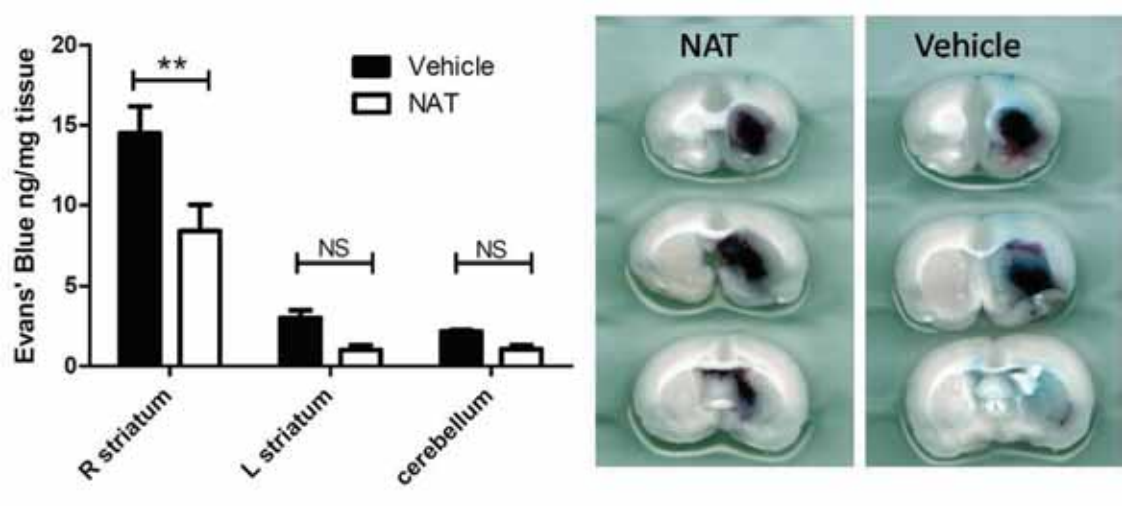


**Figure 56. The effect of NK1R antagonism on BBB disruption. Treatment with NAT caused a significant reduction in peri-haematomal Evans Blue extravasation from 12-23 hours post-collagenase ICH, compared with vehicle. **=p<0.01, NS=not significant.**

As has been found in other CNS inflammatory condition, treatment with NAT caused a significant reduction in peri-haematomal Evans Blue extravasation (from 14.5±4.8 to 9.6±3.3 ng/mg tissue, P=0.0052). Consistent with the known spread of albumin (and oedema) across the corpus callosum, treatment may also reduce contralateral Evans blue extravasation (see bottom brain slice in (Figure 56), although this difference was not statistically significant.

### 4.3.8 The effect of NK1R antagonists on functional outcome

The effect of NK1RA antagonism on behavioural outcome was assessed using both agents. The group comparing NAT with vehicle was first assessed (Figure 57). In a pre-planned interim analysis, data were unblinded after 5 animals in each group had been treated. There was no indication of benefit in the treated group, with a small trend to harm. This trend of harm was consistent across multiple behavioural tests. As the chances of finding a substantial positive effect of treatment with therapy were miniscule, and would have required resampling with a much higher sample size, the experiment was terminated early on futility grounds. This decision was also influenced by the analysis of inflammation, atrophy and leucocyte infiltrate, all of which suggested the unlikelihood of benefit.

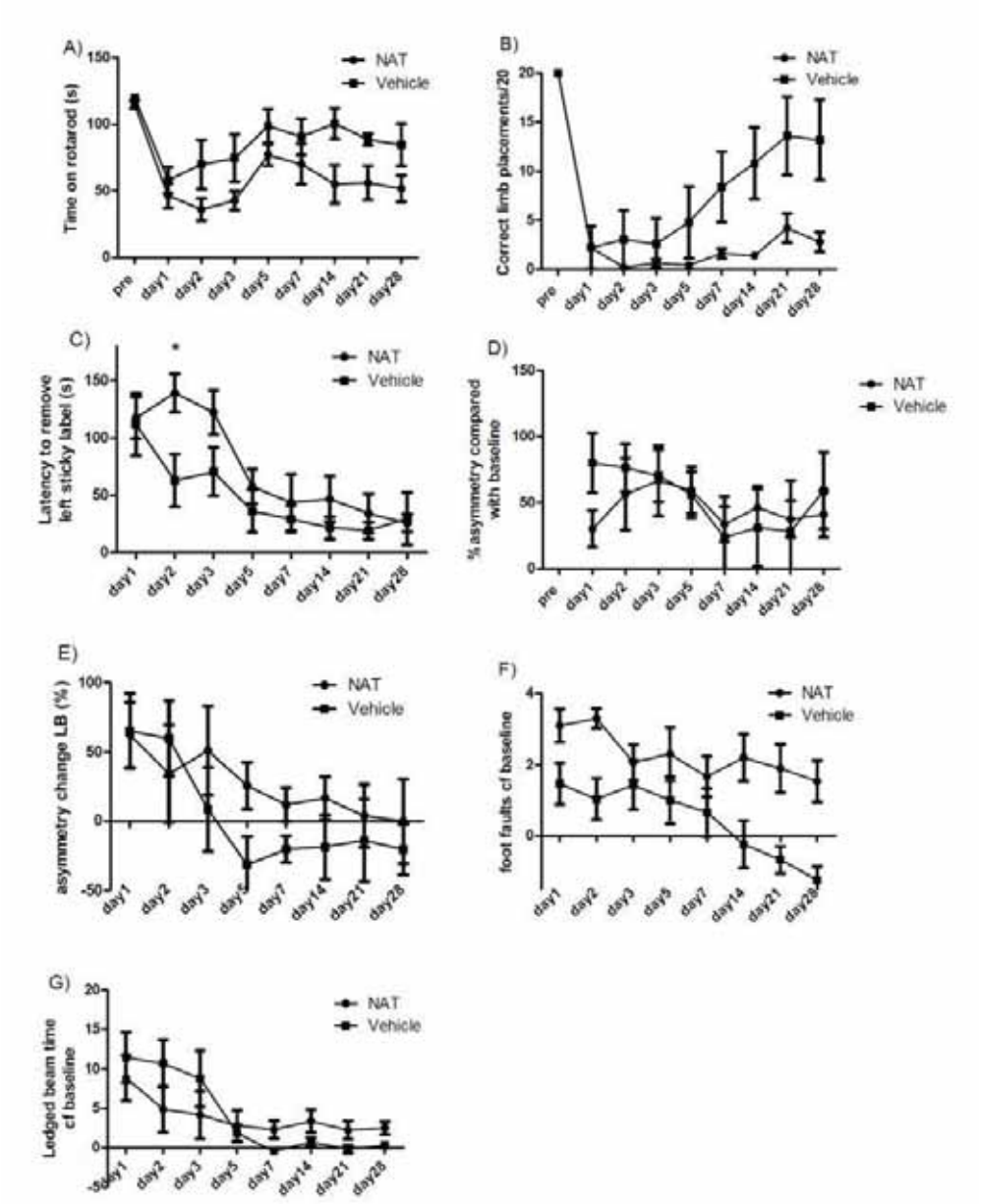


**Figure 57. Functional changes post-ICH in animals treated with NAT or vehicle. (A) Rotarod, (B) vibrissae elicited stimulation test, (C) sticky label test, (D) elevated drag test, (E) ledged beam asymmetry compared with baseline, (F) ledged beam total footfaults compared with baseline, (G) ledged beam: time to traverse compared with baseline. A trend to harm was seen with NAT, however the only significant difference was seen at day two in the sticky label test (*=p<0.05).**

Functional testing using the BBB penetrant NK1R antagonist, L733,060 again failed to show evidence of benefit (Figure 58).

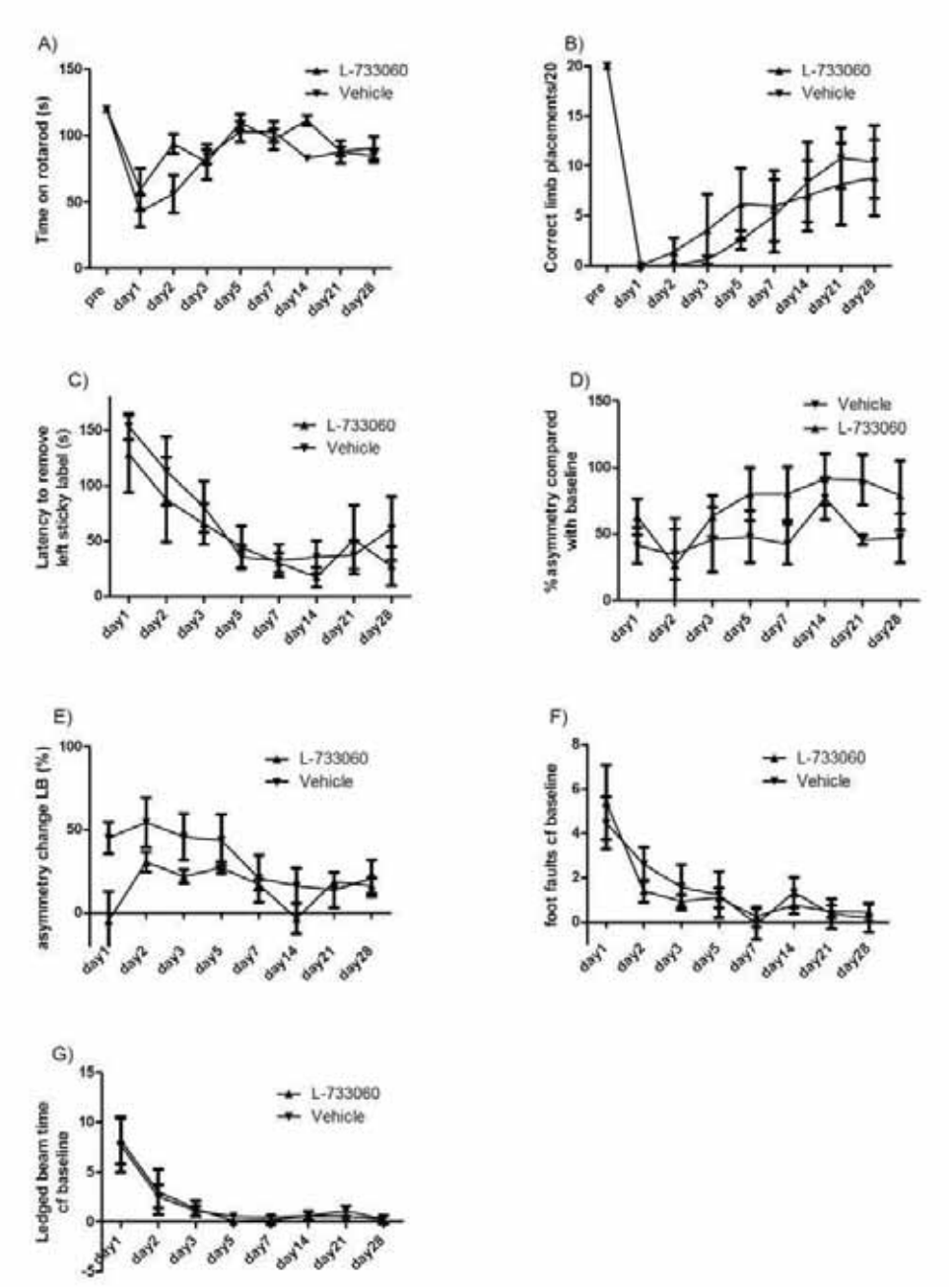


**Figure 58. Functional changes post-ICH in animals treated with L733,060 or vehicle. (A) Rotarod, (B) vibrissae elicited stimulation test, (C) sticky label test, (D) elevated drag test, (E) ledged beam asymmetry compared with baseline, (F) ledged beam total footfaults compared with baseline, (G) ledged beam: time to traverse compared with baseline. No significant differences were seen between groups.**

This experiment was, again, unblinded after 5 animals were included in each group. While there was no apparent trend to harm, as with the experiment with NAT, there was no trend of benefit seen in any behavioural test. The experiment was therefore terminated early on grounds of futility. The lack of functional benefit following L733,060 treatment was corroborated by the lack of any beneficial effect on lesion volume (Figure 50).

When the results of the two different NK1R antagonist functional outcome studies were pooled (n=10 for both NK1R antagonist and vehicle groups) no significant differences were found (not shown). The trend to harm noted in most of the NAT behavioural tests was, as would be expected, diluted. The one significantly worse result noted at day 2 in the sticky label test was not noted in the pooled analysis.

## 4.4 Discussion

The results of the current study demonstrate that NK1R antagonists diminish oedema and blood-brain barrier disruption following cICH. This is a class-effect, rather than agent specific, as the two structurally-unrelated NK1R antagonists had essentially the same effect on oedema. The results imply that sufficient BBB disruption occurs for the normally non-BBB penetrant NAT to enter the brain and exert its effects, as has been noted previously in studies of transient middle cerebral artery occlusion (tMCAO)[481] and traumatic brain injury.[461] The anti-oedema effect of NK1R antagonists was noted not only with two different antagonists, but across three conceptually related, but separate experiments: wet weight-dry weight, Evans Blue extravasation and histological analysis.

However, in contrast to the studies mentioned above, no benefit of NK1R antagonists was noted with regards to functional outcome, astrogliosis or leucocyte infiltration/ activation.[461, 481] While one criticism of the study could be that a single dose of an NK1R antagonist would be insufficient to provide protection, in the two cited studies, beneficial effects were seen with single doses acutely post-injury.

It is worth noting that there was no evidence of an elevation in intracerebral substance P following permanent middle cerebral artery occlusion (pMCAO) in the ischaemic stroke study,[481] and it is unlikely that NK1R antagonism is effective in this condition. It may be that the pathophysiology of ICH therefore more closely resembles pMCAO than tMCAO. Certainly, vascular disruption in ICH is rapid and irreversible (see chapter 1) and it is well recognised that ‘neuroprotection’ it is far more difficult to demonstrate in permanent than in transient cerebral arterial occlusion.[512]

Given the pleiotropic actions of substance P, a further possibility may be that beneficial effects of NK1R antagonism in ICH were offset by an additional deleterious effect not present in TBI and tMCAO. One possible candidate would be an increase in bleeding – the antiplatelet effect of NK1R antagonism would presumably be beneficial in IS and TBI, but detrimental in ICH. However, no difference in haematoma volumes was seen following NAT, although, admittedly, haemoglobin was not quantified spectrophotometrically.

A reduction in neurogenesis with NK1R antagonism is another and perhaps more likely candidate. It has been previously shown that administration of an NK1R antagonist following experimental ischaemic stroke reduces the proliferation of adult neural progenitor cells in both the subventricular zone (SVZ) and dentate gyrus.[518] Research in our laboratory has also demonstrated that NAT therapy decreases neuro- and gliogenesis following TBI (L Georgio, personal communication). There was a suggestion in the current study that NAT treatment may have decreased SVZ cellular proliferation at 7 days (Figure 54). However, the current experiment was not designed with this research question in mind. To provide a definitive answer, a separate experiment would be required, quantifying cells double labelled with bromodeoxyuridine,[522] and neural/glial markers. This hypothesis may seem inconsistent with the previously reported benefits of NK1R antagonism following TBI and tMCAO,[461, 481] but it is possible that functional recovery following ICH is more reliant on neuro- and gliogenesis than these two conditions.

The present study should not be seen as a contradiction of previous work showing that NK1R antagonism reduces neuroinflammation,[422, 425, 432, 433, 461, 481] nor of previous work implicating SP in oxidative stress,[387, 448] and non-apoptotic programmed neuronal death.[417] The current results merely imply that other factors predominate as causes of post-ICH inflammation and secondary injury, such as thrombin, matrix metalloproteinases and haemoglobin breakdown products.[57, 523]

The results described in the current chapter are consistent with previous studies which have demonstrated decreased oedema and/or BBB dysfunction in a variety of acute and chronic CNS inflammatory states (tMCAO,[481] TBI,[461] and HIV encephalitis[399]). These results do, however, call into question previous suggestions that post-ICH oedema and BBB dysfunction is, on the whole, deleterious.[127]

In the present study, NK1R antagonists reduced oedema at least as effectively as any previously reported therapy. A 2.4% absolute reduction (or around two thirds relative reduction) in brain water content was seen following treatment with L733,060; other studies report oedema reductions of (for instance) 1.7% with argatroban (a thrombin antagonist),[209] 1.5% with neural stem cell transplantation[271] and 1.9% following overexpression of the IL-1β receptor antagonist.[257] However, despite this dramatic reduction in acute oedema with NK1R antagonists, no improvement in functional outcome ensued. It has been previously found, in studies with thrombin antagonists, that oedema formation and reduction is correlated with worsening and then amelioration of functional deficits.[127] The present study argues that oedema is a surrogate marker of post-ICH brain injury, rather than a cause. This assertion receives support from several other studies in which treatments have reduced oedema but

not improved functional outcome – for instance therapeutic hypothermia[289] and minocycline treatment.[524, 525] The hypothesis could be directly assessed by inhibiting aquaporin-4 post-ICH. This would modulate post-ICH oedema in a relatively pure fashion – either increasing or decreasing it, depending on whether post-ICH oedema is predominantly vasogenic or ionic[138] – a question which remains unresolved.

It is likely that post-ICH oedema is only of clinical relevance following ICH in humans when it precipitates midline shift, and is neutral (or perhaps even mildly beneficial) when no mass effect ensues. This hypothesis may account for the somewhat confusing state of the human post-ICH oedema literature.[91, 123-125] In rats this fine 'tipping point' of midline shift is difficult to reliably reproduce. Oedema therapy in humans is likely to be of benefit only in patients with large haemorrhages, in the first few days post-ICH, when any additional mass effect will precipitate neurological decline (once midline shift commences, further shifts lead to dramatic neurological deterioration).[122] This cumulative mass effect is seen in 'second stage' (probably largely thrombin mediated)[57] oedema, when the haematoma is yet to be reabsorbed, and where oedema accumulation leads to a true gain in lesion volume. [125] Although oedema continues to progress for up to two weeks in humans,[72, 73, 125] after the first few days reabsorption of the haematoma has commenced (and indeed may precipitate this third oedema stage).[57] Therefore, beyond 3-4 days, gains in oedema volume are offset by losses in haematoma volume and hence oedema per se rarely causes neurological decline. [72, 125]

## 4.5 Conclusion

In summary, treatment with two structurally unrelated NK1R antagonists reduced oedema and blood-brain barrier dysfunction post cICH, without improving functional outcome or reducing lesion volume. It may be that oedema is not deleterious post-ICH in rats, or it may be that a beneficial oedema-reducing effect of NK1R antagonism was offset by a reduction in SP-mediated neuro- and gliogenesis. The current study suggests that, while NK1RAs act as effective oedema-reducing agents post-ICH when administered within a clinically relevant time-window, any clinical benefit would be limited to patients with incipient midline shift at presentation. The following chapter explores more directly the mechanisms of SP-induced oedema post-ICH. Does thrombin sit upstream of SP in the pathogenesis of post-ICH oedema?

# 5 Investigation of the effect of thrombin on substance P: is thrombin the factor which triggers SP-mediated oedema?

## 5.1 Introduction

Thrombin, a serine protease, is the final common pathway of the coagulation cascade. Damaged vascular lining activates the 'prothrombinase' complex, converting prothrombin to thrombin, which, in turn, cleaves fibrinogen to form a fibrin clot. Thrombin also feeds back to enhance the coagulation cascade, as well as activating anti-thrombotic pathways to limit clotting to the site of injury.[526] Thrombin also exerts non-clotting actions through the cleavage of so-called proteinase (or protease) activated receptors (PAR-1, -3 and -4) and, possibly, through activation of complement factors.[204]

PARs (in particular PAR-1) are widespread throughout the brain and are found on neurons, glia, microglia, pericytes and cerebrovascular endothelium.[179] Intracerebral thrombin injection in physiologically relevant quantities causes PAR-1 mediated oedema, inflammation, BBB dysfunction and neurotoxicity.[187, 188, 527] Thrombin is thought to be the predominant cause of 'second phase' oedema in experimental ICH (i.e. the next stage after clot retraction).[130, 528] Thrombin inhibition post-ICH reduces oedema, functional deficits[127] and lesion volume.[202]

Blocking thrombin post-ICH is consistently beneficial, across numerous structurally-unrelated thrombin inhibitors[200, 208, 209, 527] and in PAR-1 genetic knockout mice.[202] Thrombin antagonists are beneficial following both collagenase[529] and autologous ICH models,[130, 202, 528] and are effective in pigs,[208] rats[209] and mice.[202] There is also evidence that thrombin plays a similarly deleterious role in human ICH. ICH occurring as a complication of thrombin inhibition (whether through heparin-augmented thrombolysis or warfarin therapy) generates less perihaematomal oedema than spontaneous ICH.[70, 126]

However, post-ICH thrombin inhibition could increase the likelihood and severity of haematoma expansion; most studies showing thrombin inhibition to be beneficial have used the autologous ICH (aICH) model, which does not cause an intracerebral bleeding nidus. Haematoma expansion in humans occurs commonly and independently predicts subsequent mortality.[99] Thrombin antagonism in human ICH may increase rebleeding and thus negate any potential benefits. Even PAR inhibition may prove problematic, as platelets posses functional PAR receptors, and PAR knock-out significantly prolongs bleeding time.[530] Additionally, inhibiting thrombin may impair long-term functional recovery, as PAR-1

pathways stimulate neurogenesis, and PAR-1 knockout mice display cognitive and learning defects (PAR-1 is necessary for synaptic plasticity is some brain regions).[531]

Substance P may act downstream of thrombin in the pathophysiology of post-ICH oedema. Although inhibition of the main SP receptor (NK1) failed to reduce functional deficits and brain lesion size, acute NK1R antagonism reduced post-ICH oedema without causing haematoma expansion. Thrombin injection causes cutaneous oedema via PAR-1 mediated SP release,[178] and the results described in chapter 4 provide circumstantial evidence that this pathway may also be active intracerebrally. The experiments in this chapter were therefore designed to test directly the hypothesis that SP is a downstream mediator of thrombin-induced 'second stage' oedema post-ICH.

## 5.2 Experimental design

One hundred and three male Sprague-Dawley rats (300-340gm) were used for the experiment, as described in chapter 2.

Thirty five animals were sacrificed for histological and immunohistochemical analysis following intracerebral thrombin injection. The initial dose chosen for investigation was 10U thrombin (one mL rat plasma contains around 330U prothrombin,[532] and thus a 100µL blood clot, which contains 65µL plasma, could produce approximately 20U thrombin. However, previous studies have most frequently used either 10U[199] or 5U[533, 534] thrombin.)

However, all five rats injected with 10U thrombin required euthanasia between 6-21 hours post-injury, due to intractable seizures and distress ('barrel-rolling'). The next eleven rats were administered 5U thrombin and sacrificed at 5 or 24 hours. All bar one survived. 1U thrombin, a reportedly non-neurotoxic dose,[533] was also administered. Histological analysis demonstrated that this dose caused a similarly-sized lesion to 0.2U collagenase (see below). Hence this group was followed for the same four timepoints examined in chapter three (5 each at 5, 24, 48 hours and 7 days). Animals from chapter three, which had a nearly identical injection protocol, were used as vehicle controls.

Fifty animals were used in oedema experiments. Twenty animals were used to establish a dose-response oedema curve (two naive controls, four shams and then 2 animals per group treated with 0.125U, 0.25U, 0.5U, 1U, 2U, 3U or 5U thrombin). 10 animals were administered 5U thrombin (a highly oedematogenic dose) and administered intravenous NAT or vehicle 2 hours post-injury. The experiment was repeated following pre-treatment with L733,060, and employing lower doses of thrombin (3U and 1U).

Evans Blue studies were conducted following 1U thrombin, with pre-administration of either intravenous L733,060 or vehicle. Six animals were used for each experimental arm, as pilot studies had suggested a more homogenous level of Evans Blue extravasation than post-ICH.

As NK1R antagonism was ineffective in reducing functional deficits following collagenase ICH (cICH), behavioural studies were not performed.

### 5.2.1 24 hour lesion comparison with collagenase ICH

To determine which dose of thrombin treatment was equivalent to cICH, the area of pallor through the injection site on H&E staining was compared to the maximal cross-sectional haematomal area. Areas were manually outlined using NDPview (v1.1.27, Hamamatsu.) Areas were corrected for hemispheric swelling (corrected lesion area = lesion area x (contralateral hemisphere area/ ipsilateral area).

### 5.2.2 Histology and immunohistochemistry

At the pre-specified timepoints animals were perfuse-fixed with formalin, and their brains were extracted, sectioned, scanned and processed as described. H&E and FJC staining was performed on sections through the needle injection site (the maximal lesion area), as well as immunohistochemical staining for ED-1, GFAP, MPOX and SP, as described. Slides were scanned at high resolution and viewed with appropriate viewing software. Double labelling was also performed to determine cellular distribution of substance P.

### 5.2.3 Semi-quantitation of SP immunostaining

Semi-quantitation of peri-haematomal SP was assessed 5 and 24 hours after injection of 5U thrombin, and at all timepoints following injection of 1U thrombin, using the method outlined above. As in the previous chapter, peri-lesional regions were analysed, rather than whole hemispheres, to ensure that it was parenchymal SP which was assessed, rather than lesional SP, which can be prone to artefact.

### 5.2.4 Brain oedema

The effect of treatment with both NK1R antagonists of brain water content following thrombin injections was assessed by the wet weight dry weight method, as described in chapter 2. Animals were sacrificed at 24 hours.

### 5.2.5 Blood-brain barrier permeability

The effect of NK1R antagonism on BBB dysfunction was assessed by the Evans Blue method, as described in chapter 2. Animals were pre-treated with L733,060 or vehicle 15 minutes prior to injury with 1U thrombin. Pilot experiments demonstrated that, in the first 24 hours, Evans Blue extravasation was maximal in the 4-8 hour time-frame (Figure 59). Evans blue was therefore injected at 4hours post-injury and animals were sacrificed at 8 hours.

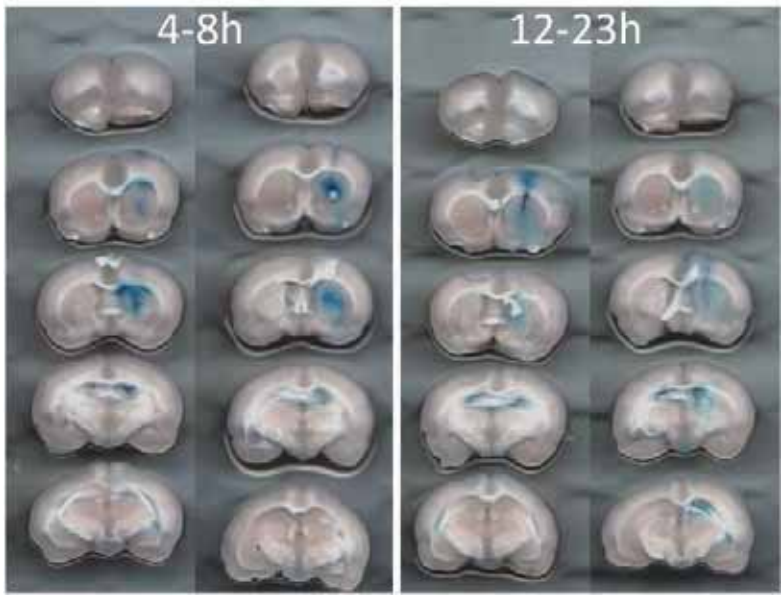


**Figure 59. Evans Blue extravasation pilot studies. The best timepoint for assessing BBB dysfunction appeared to be between 4 and 8 hours (left).**

### 5.2.6 Statistical analysis

Categorical variables were assessed with Fisher's exact test. Histological changes over time (for instance SP immunostaining) were assessed by one-way ANOVA with Bonferroni post-tests for selected inter-group comparisons. Brain water content and Evans blue quantification were also analysed by one-way ANOVA, with selected Bonferroni post-tests.

## 5.3 Results

### 5.3.1 Baseline and surgical parameters

Analysis of baseline and surgical parameters did reveal some minor differences (Table 4), although none of these are likely to have impacted on the results presented below. There were no significant weight differences. Thrombin and thrombin vehicle surgery was significantly shorter (by around 4-5 minutes), as other animals also had treatment or vehicle pre-administered by tail vein. Improvements in surgical technique over the course of this

research project also led to a reduction in anaesthetic duration when compared with collagenase controls animals (which had been operated upon 14 months prior). Temperature differences were insignificant, save for some comparisons with collagenase vehicle initial (but not final) temperature, again due to interval technique improvements. Treatment with an NK1RA did not alter temperature at 4 hours (Evans Blue group only).

Table 4. Experimental parameters

| Group | Weight | Duration | T start | T finish | T 4h post NK1R |
|---|---|---|---|---|---|
| **Thrombin** | 315±14 | 23±2 | 37.1±0.4 | 37.1±0.3 | ---- |
| **Vehicle** | 327±6 | 21±1 | 37.2±0.4 | 37.0±0.4 | ---- |
| **Thrombin (NS)** | 320±9 | 26±3 | 37.1±0.5 | 37.2±0.3 | ---- |
| **Thrombin (NK)** | 324±10 | 26±2 | 37.3±0.3 | 37.2±0.3 | ---- |
| **Throm EB (NS)** | 324±16 | 27±2 | 37.0±0.3 | 37.4±0.1 | 36.9±0.2 |
| **Throm EB (NK)** | 325±10 | 25±4 | 37.0±0.2 | 37.1±0.3 | 37.0±0.3 |
| **cICH vehicle** | 321±21 | 26±3 | 36.7±0.3 | 37.1±0.3 | ---- |

**Experimental parameters (means +/-SD) for thrombin (histology and oedema titration), oedema vehicles, thrombin-injected animals treated with normal saline (NS), thrombin-injected animals treated with NK1R antagonists (NK), post-thrombin Evans blue animals treated with normal saline or antagonist, and 'collagenase' (cICH) vehicles (given 2µL normal saline and used as vehicles for comparison with intracerebral thrombin.)**
**Units: weight=grams, duration=minutes, temperature ('T')=$^{o}$C.**

### 5.3.2 Dose titration - histology

Thrombin, as used in the present study, appeared more potent than previously reported. A separate batch of thrombin yielded identical results. In the pilot phase of experiments animals were treated with either 10U or 5U of thrombin. 10U of thrombin caused unacceptable mortality within the first 24 hours (5/5 vs 1/11 (p=0.001 for comparison)), and hence 5U of thrombin was initially used.

At 24 hours 5U of thrombin caused approximately double the cross-sectional area of injury induced by cICH (Figure 60a, c). The thrombin dose was therefore reduced to achieve a more comparable injury. A dose of 1U, previously reported to be non-injurious,[533] caused an equivalent lesion to 0.2U collagenase (Figure 60a, b). This dose was therefore used for comparisons at other timepoints (5h, 48h and 7 days).

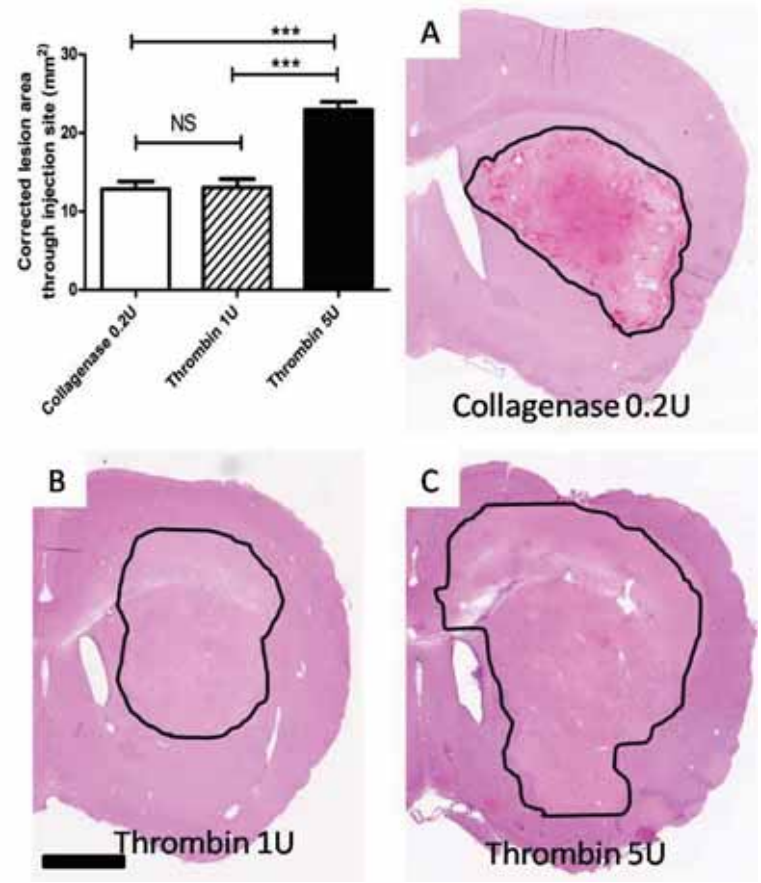


**Figure 60. Lesion size following high- and low-dose intracerebral thrombin. Cross-sectional lesion areas through injection site 24 hours post 0.2U collagenase (A), 1U thrombin (B) and 5U thrombin (C). High dose thrombin caused a larger lesion than collagenase ICH, but 1U thrombin caused a lesion of similar size. Both doses caused hemispheric swelling, the 5U dose to a greater extent. Scale bar=1mm. ***=p<0.001.**

### 5.3.3 Thrombin dose titration – oedema

As demonstrated with H&E staining, both doses of thrombin appeared to cause oedema - although perhaps the 5U dose more than the 1U dose (Figure 60a, c). Therefore dose titration studies were performed to investigate which doses of thrombin would be most suitable to test for efficacy of an NK1R antagonist.

Contrary to previous reports, but consistent with histological analysis perfomed subsequently, all doses of thrombin upwards of 0.125U produced more oedema than vehicle injection (Figure 61). Within experimental constraints (unacceptable animal mortality at higher doses) the relationship between thrombin dose and oedema was in fact found to be log linear (R squared 0.87, $p<0.001$, Dunn's test for non-linearity non-significant ($p=0.97$)).

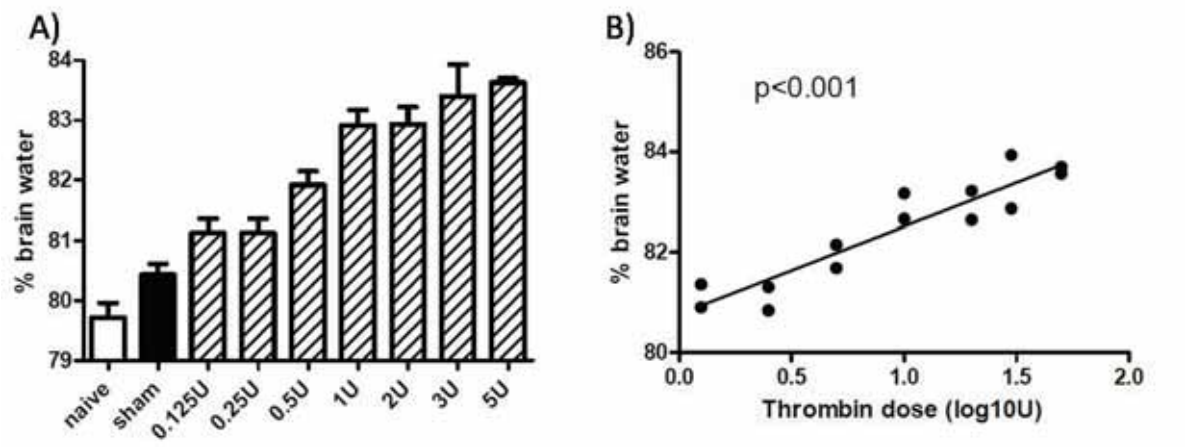


**Figure 61. A) Brain water content in the right striatum and overlying cortex 24 hours after thrombin and vehicle injection, or in sham controls. There was an incremental rise in brain water content with all doses studied. The relationship between dose and oedema was determined to be log-linear (B).**

### 5.3.4 Histology and immunohistochemistry

#### *H&E Staining*

Thrombin injection caused a large area of pan-necrosis extending radially from the injection site to the cortex (Figure 62d, e). This area could be reliably identified even at five hours by neuronal dark cell change, neuronal ballooning (Figure 62a) and by pyknotic oligodendrocytic nuclei in white matter (Figure 62b). White matter and oligodendrocytes seemed especially prone to injury, as tongues of injured white matter extended beyond the otherwise spherical border of pan-necrosis (Figure 62d, e). Similarly to ICH (Figure 54), following thrombin injection enhanced cellular proliferation in the subventricular zone was seen (Figure 62f), however, this was significantly less extensive (0.004±0.003 vs 0.17± 0.09mm$^2$; p=0.0167).

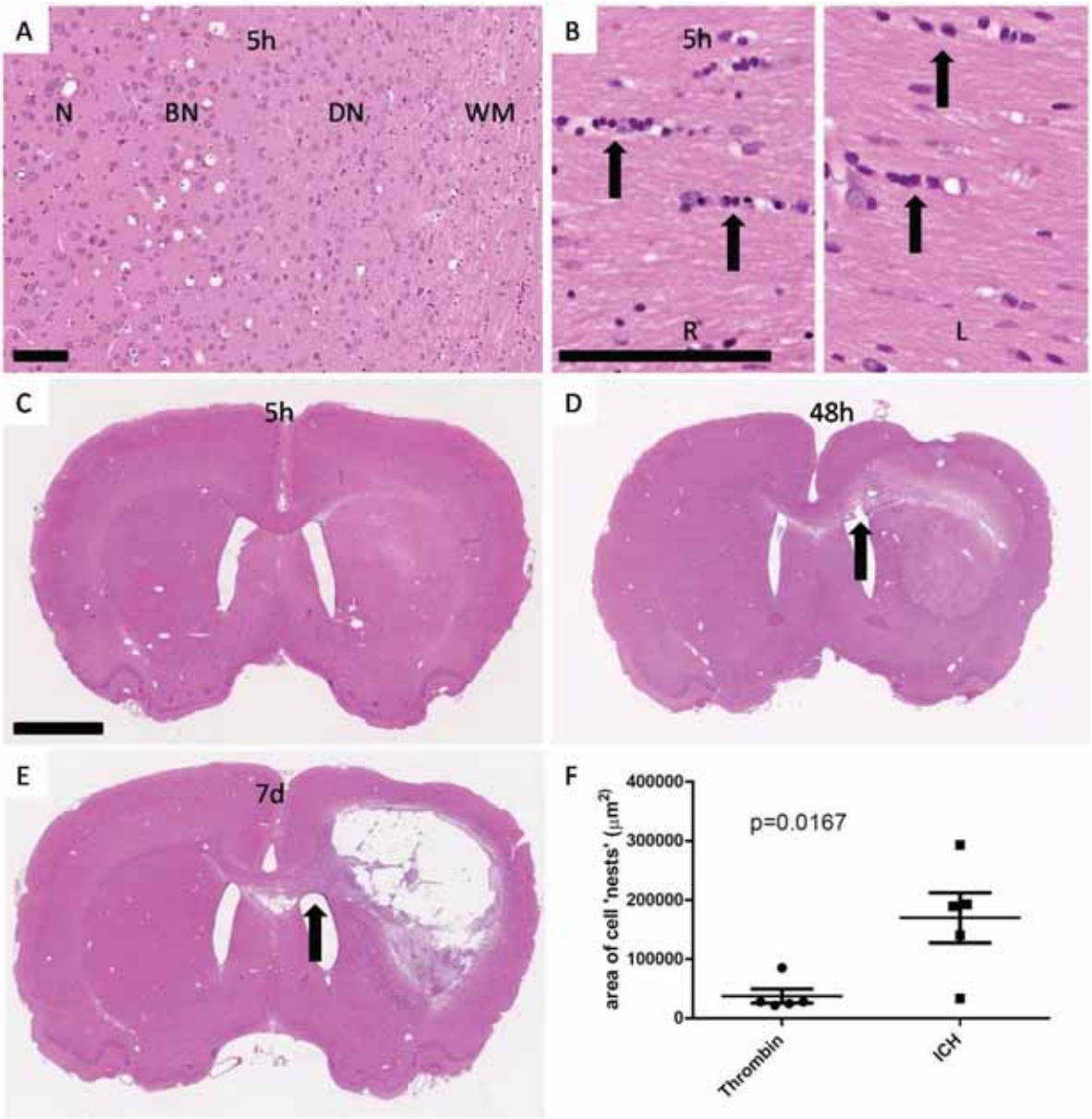


**Figure 62. H&E staining following thrombin injection. (A-C) Five hours following thrombin injection, although little change was evident on gross inspection (C), at higher power (A) regions which would later progress to pan-necrosis could be distinguished from normal areas (N) by the presence of ballooned neurons (BN), which formed a 'penumbral' rim, dark neurons (DN) or oedematous white matter (WM), which contained pyknotic oligodendrocytic nuclei (B). (D) This necrotic area was crisply demarcated at 24 not shown) and 48 hours. (E) It was phagocytosed to a glial-lined cavity at 7 days. White matter seemed particularly prone to injury, as evidenced by preferential extension into corpus callosum (arrows) and internal capsule (not shown). (F) Thrombin injections increased cellular proliferation in the subventricular zone, but far less than following collagenase ICH. Scale bar=100μm or 2mm (whole brain).**

### *SP immunostaining*

Comparison of SP immunostaining following thrombin injection and cICH revealed both similarities and differences (Figure 63).

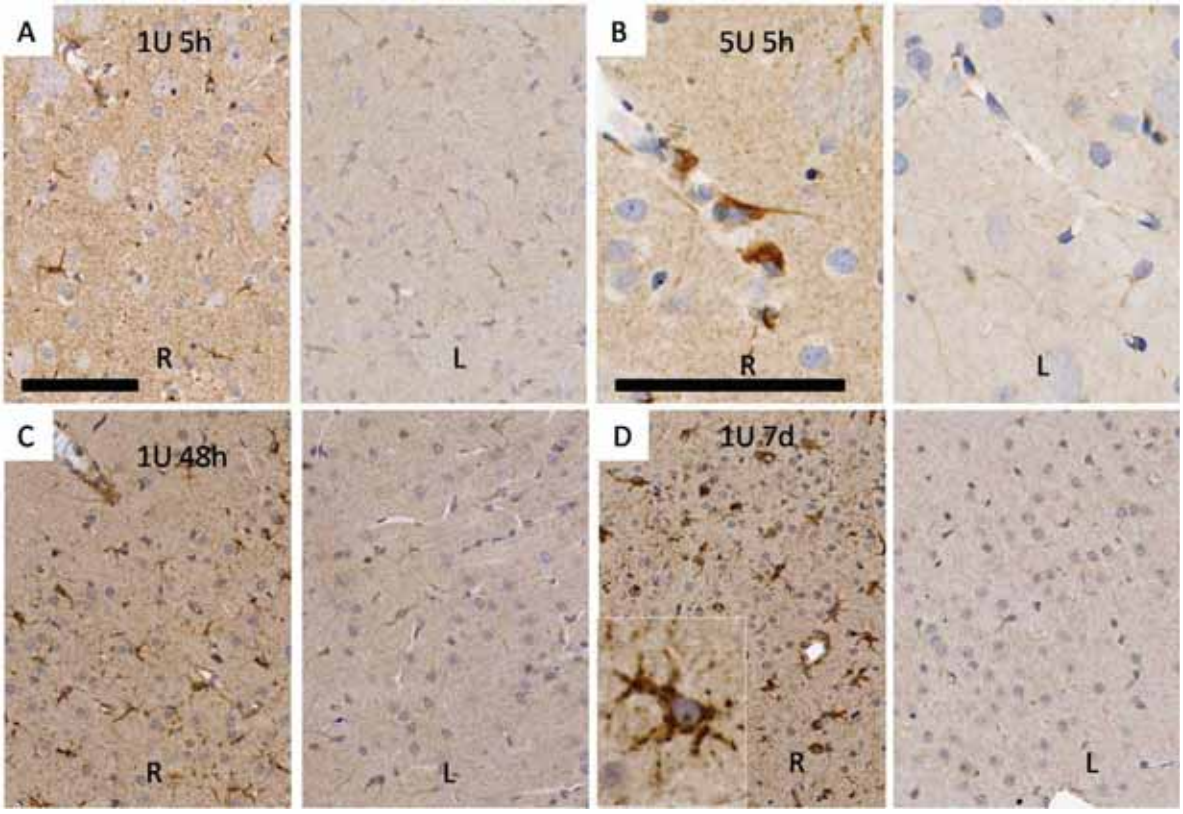


**Figure 63. SP immunostaining following intracerebral thrombin injection. There was a progressive increase in SP immunostaining of astrocytes at all timepoints studied. (A) At five hours increased background granular staining coexisted with early increased astrocytic staining. (B) This was even more marked following high-dose thrombin injections. (C) Astrocytic SP staining progressively increased from 5 to 24 (not shown) to 48 hours. (D) At seven days a rim of hypertrophied SP-containing astrocytes (insert) surrounded the glial scar. Scale bar=100µm.**

The granular SP staining seen at 5 hours following cICH (Figure 26a) was also evident following thrombin injections (Figure 63a, b). In contrast, thrombin injection caused an increase in astrocytic staining even at this early timepoint (Figure 63a, b). This increased astrocytic staining progressively increased until 48 hours (Figure 63c) and remained elevated even at 7 days (Figure 63), again in contrast with cICH (Figure 27d); hypertrophied astrocytes staining densely for SP continued to surround the injured area at this timepoint (Figure 63d inset), whereas astrocytic staining post-ICH had returned to baseline.

To objectively confirm the impression of subjective increase in SP immunostaining, the degree of SP-IR was semi-quantitated following colour deconvolution (Figure 64).

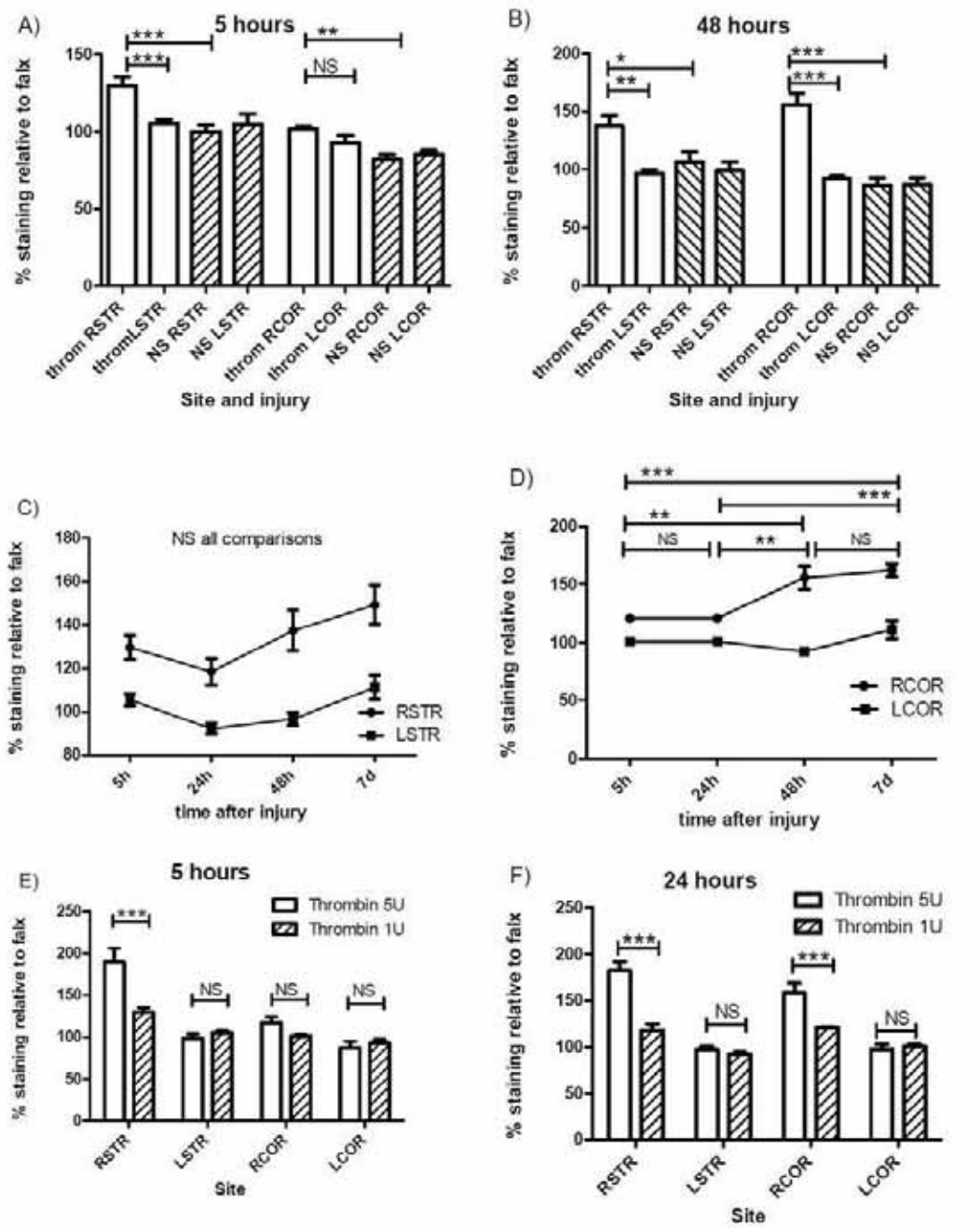


**Figure 64. Semiquantitation of SP immunostaining following thrombin injection (A-F) or vehicle controls (A,B). There was increased SP immunostaining following 1U thrombin at all timepoints (A-D). At 5 (A) and 24 hours this was predominantly evident in the striatum (A,C), but at 48 hours (B) and 7 days was evident in both striatum and cortex (B,D) at increasing levels of intensity. Thrombin 5U caused a significantly greater increase in SP immunostaining than thrombin 1U, both at 5 (E) and 24 hours (F). throm=thrombin, NS=normal saline, RCOR=right cortex, LCOR=left cortex, RSTR=right striatum, LSTR=left striatum. ***=p<0.001, **=p<0.01, *=P<0.05, NS=not significant.**

Deconvolution analysis confirmed that there was increased SP immunostaining at all timepoints surveyed (Figure 64c, d). When considered in tandem with histological

observations, the early peak in striatal SP immunoreactivity was predominantly due to diffuse granular SP immunoreactivity, whereas subsequent elevated levels of SP-IR localised to astrocytes. Both cortical and striatal SP-IR continued to increase up until at least 7 days (Figure 64c, d). Higher doses of thrombin led to a greater increase in SP-IR (Figure 64e, f).

This technique also demonstrated that thrombin injection caused substantially greater SP-IR than did cICH (Figure 65). 5U thrombin caused greater striatal SP-IR at 5 hours, and both greater cortical and striatal SP-IR at 24 hours. 1U thrombin caused greater cortical SP-IR at 24 and 48 hours and greater cortical and striatal SP-IR at 7 days. Following cICH, at this latter timepoint, astrocytic SP-IR (cortical and striatal) had decreased to baseline (Figure 28c, d), with any increased staining localised to striatal macrophages.

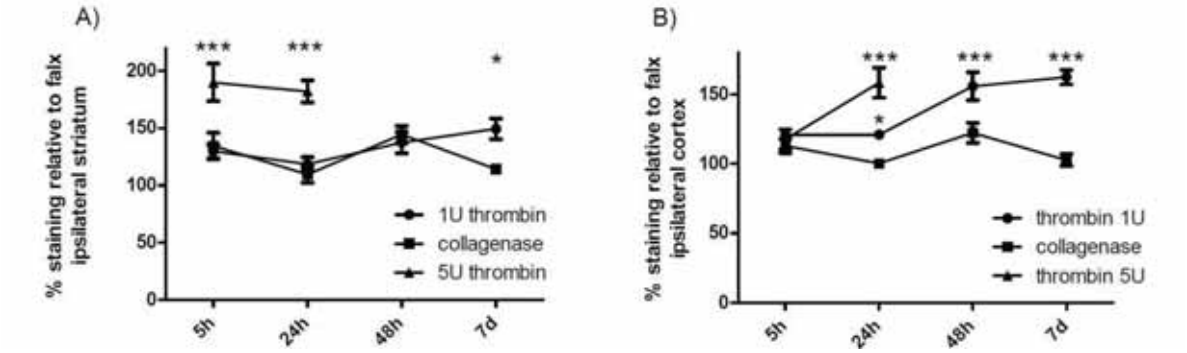


**Figure 65. Semiquantitative comparison of ipsilateral SP immunostaining following thrombin injection and collagenase ICH. (A) Greater elevation in striatal SP-IR were seen at 5 and 24 hours with high-dose thrombin, and at 7 days with thrombin 1U. (B) Cortical SP-IR was elevated to a greater extent following thrombin injection at both doses and all timepoints beyond five hours. ***=p<0.001, *=P<0.05 for comparisons with collagenase ICH.**

### *Neuronal degeneration - Fluoro-Jade C*

Similarly to following cICH, staining with Fluoro-Jade C demonstrated that intracerebral thrombin injections caused peak degeneration of neurons at 24 hours (Figure 66b).

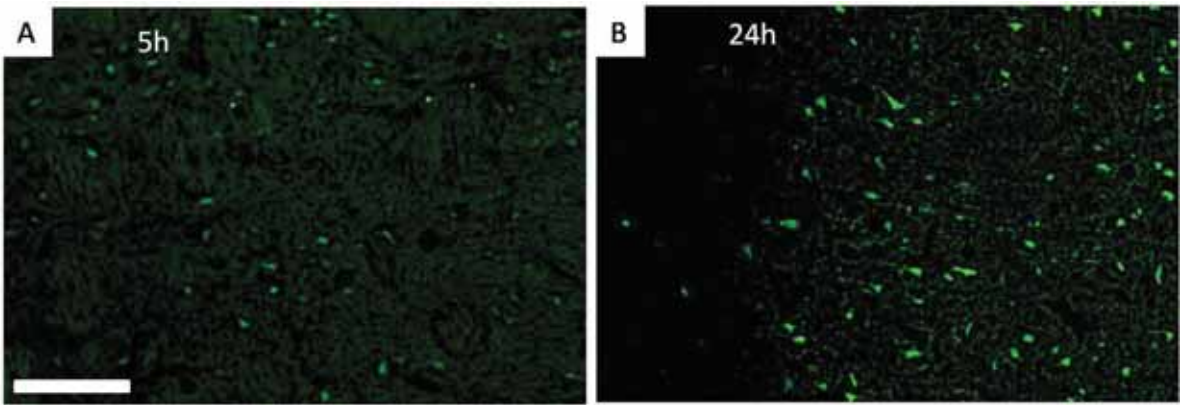


**Figure 66. Fluoro-Jade C staining following thrombin injections. (A) Sparse positively-staining neurons are visible at 5 hours. (B) At 24 hours ubiquitous strongly positive neurons are present. Scale bar=100µm.**

The process of neuronal degeneration appeared to commence slightly earlier than following cICH (as might be expected given the gradual onset of cICH). Similarly to cICH (Figure 30), FJC positive neurons peaked at 24 hours, were still visible at 48 hours (but were no more extensive) and were absent at 7 days.

### *Inflammatory reaction – myeloperoxidase and ED-1 staining*

The pattern of similar, but accelerated injury was also evident on myeloperoxidase immunostaining (Figure 67). Already at five hours neutrophils had exited into the parenchyma in significant numbers (Figure 67a), as opposed to following cICH (Figure 31a), where endothelial neutrophil adhesion only was evident. Peak neutrophil infiltration was clearly at 24 hours; it was markedly less at 48 hours and, similarly to post-ICH, absent at 7 days. The pattern of infiltration was also different; neutrophils were visible throughout the area of damage at all timepoints, as opposed to following ICH, where they formed a dense encircling rim (Figure 31b, c).

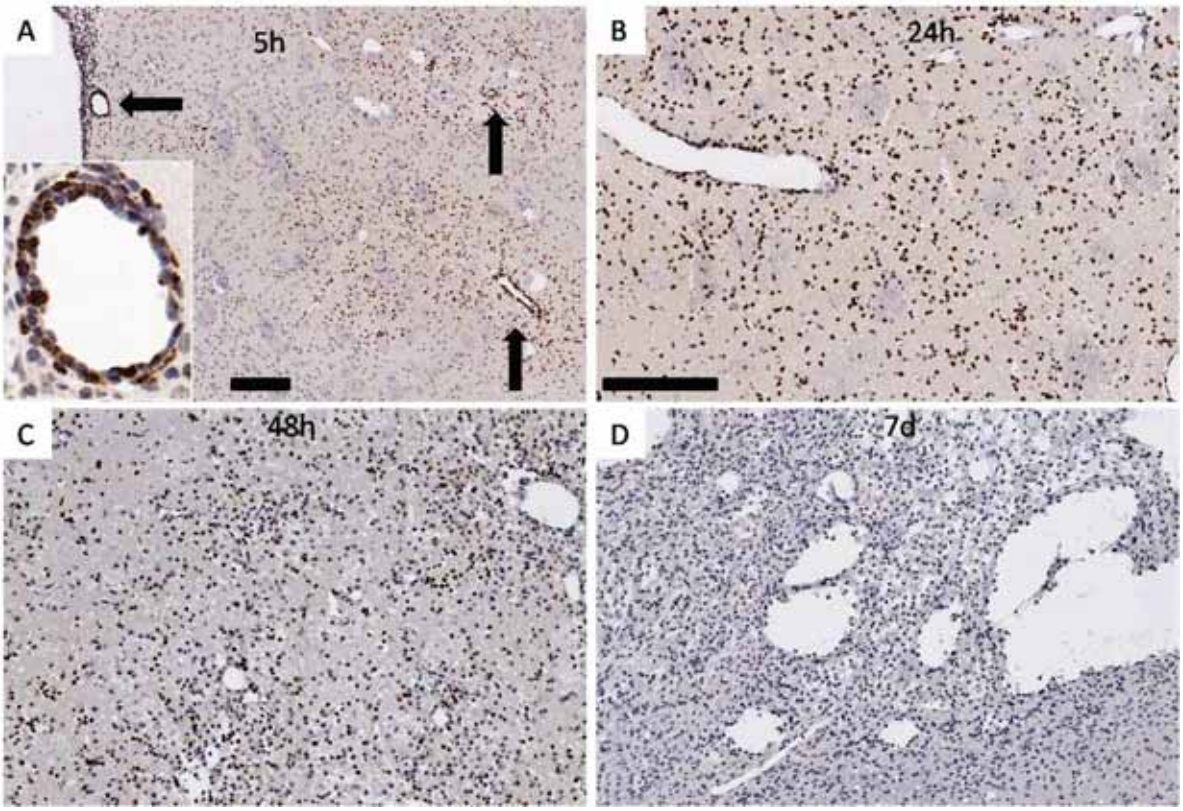


**Figure 67. Neutrophilic infiltrate (myeloperoxidase immunostaining) following thrombin injections. (A) Neutrophils are evident even at 5 hours infiltrating diffusely throughout the region of damage, centrifugally from post-capillary venules (arrows). (B) Neutrophilic infiltration is homogenous, rather than penumbral, and peaked at 24 hours, diminishing at 48 hours (C). (D) No neutrophils were evident at 7 days. Scale bar=100µm.**

Similarly, at five hours infiltrating monocytes could already be seen adhering to and exiting venules diffusely into the striatum and corpus callosum (Figure 68a). This diffuse infiltration had progressed at 24 hours (not shown) but from 48 hours more closely resembled the response following cICH (Figure 32) – i.e. a dense rim of activated microglia surrounding a central gliotic cavity lined by macrophages. Confirming the H&E impression of disproportionate white matter injury (Figure 62), macrophages were seen at 7 days extending tongue-like from the central spherical injury core into the corpus callosum (Figure 68d).

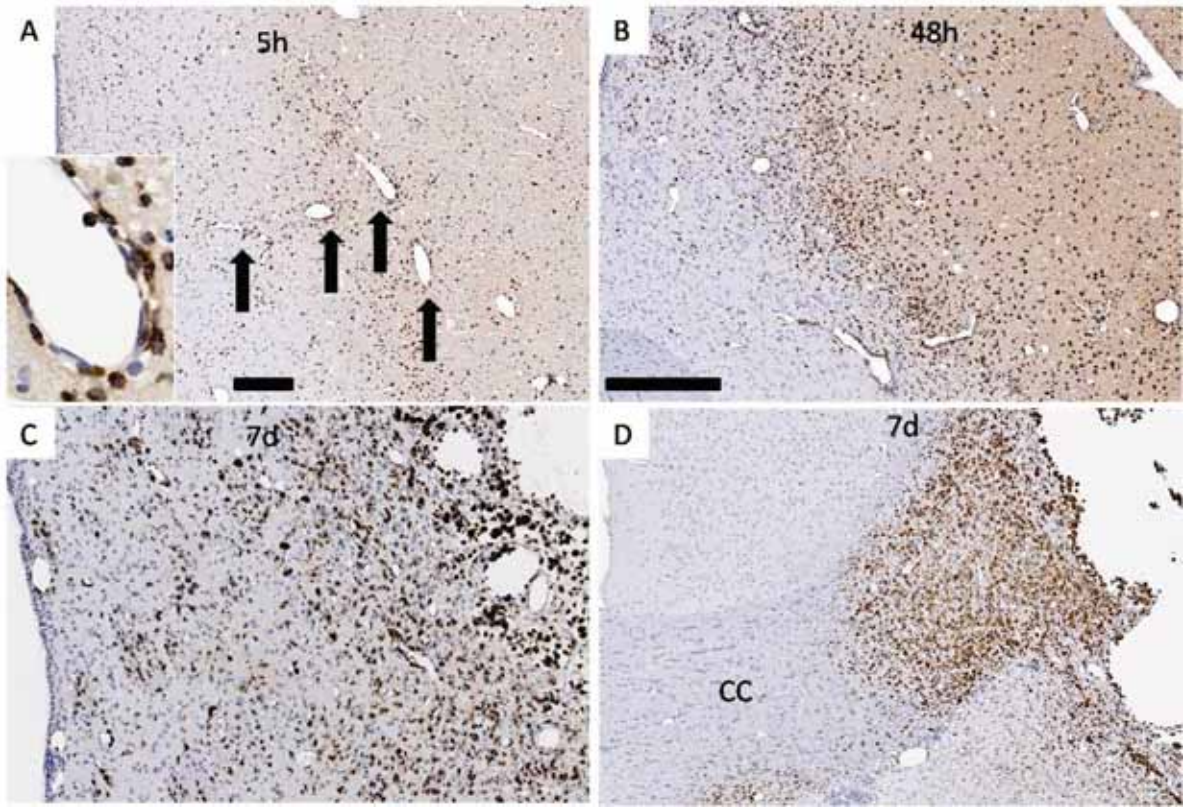


**Figure 68. Macrophage/activated microglia response (ED-1 immunostaining) following intracerebral thrombin injections. (A) Infiltrating monocytes are also seen at 5 hours diffusely, emigrating centrifugally from post-capillary venules (arrows). (B) The microglia/macrophage response progressed throughout the observation period, becoming less diffuse and more 'penumbral' by 48 hours. (C) By 7 days a dense microglial rim surrounded central macrophages. (D) The disproportionate white matter injury can be clearly identified by a 'tongue' of macrophages extending into the corpus callosum (CC). Scale bar=100µm.**

### *Astrocytic response - GFAP*

Five hours following thrombin injection there was diminished GFAP staining adjacent to the injection site with evidence of clasmatodendrosis (Figure 69a). GFAP staining then essentially

mimicked the pattern seen following cICH (Figure 33), with a progressive increase in staining, first in the lesion periphery (Figure 69b), then proceeding centripetally as the glial scar formed and contracted (Figure 69c, d). In contrast with cICH, giant plump 'gemistocytic' astrocytes were seen in the lesion's periphery at 7 days (Figure 69d insert), presumably the same large cells which stained strongly for substance P (Figure 63d).

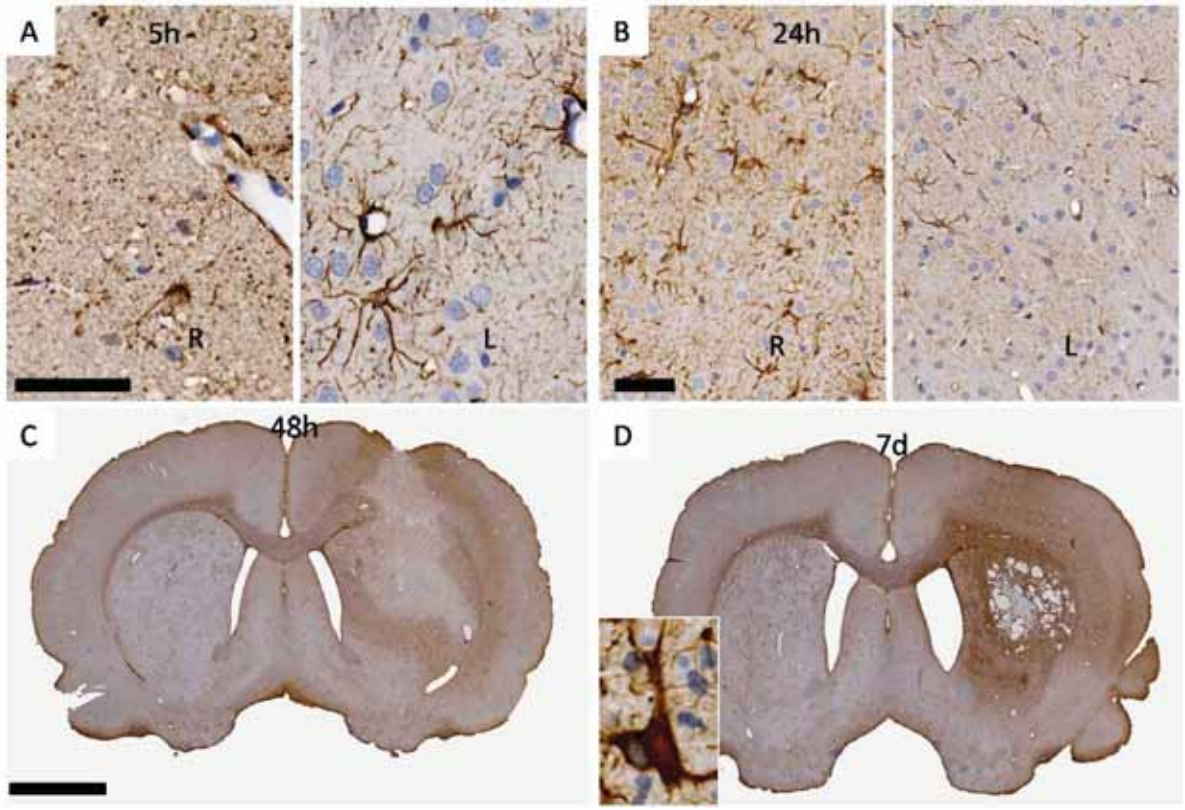


**Figure 69. Astrogliosis (GFAP immunostaining) following intracerebral thrombin injections. (A) Central disruption of GFAP immunostaining was evident at 5 hours. (B) By 24 hours increased GFAP staining could be seen in peri-lesional astrocytes. (C) This further increased at 48 hours and (D) 7 days, infiltrating and contracting centripetally. Giant astrocytes were seen around glial scar margins at 7 days (D insert), mirroring the distribution of large SP-positive cells. Scale bar=50µm, or 2mm for whole brain slices.**

### *Albumin immunostaining*

The pattern of albumin immunostaining (Figure 70) mimicked closely that seen following cICH (Figure 34), with substantial albumin-IR at 5 hours (Figure 70a), which peaked at 24 hours (Figure 70b) and then diminished thereafter (Figure 70c, d). As following cICH, there was contralesional spread of albumin, although this was most marked at 48 hours following thrombin injections (Figure 70b). There was less peri-lesional albumin-IR 7 days following thrombin injections than at the equivalent cICH timepoint (Figure 70d).

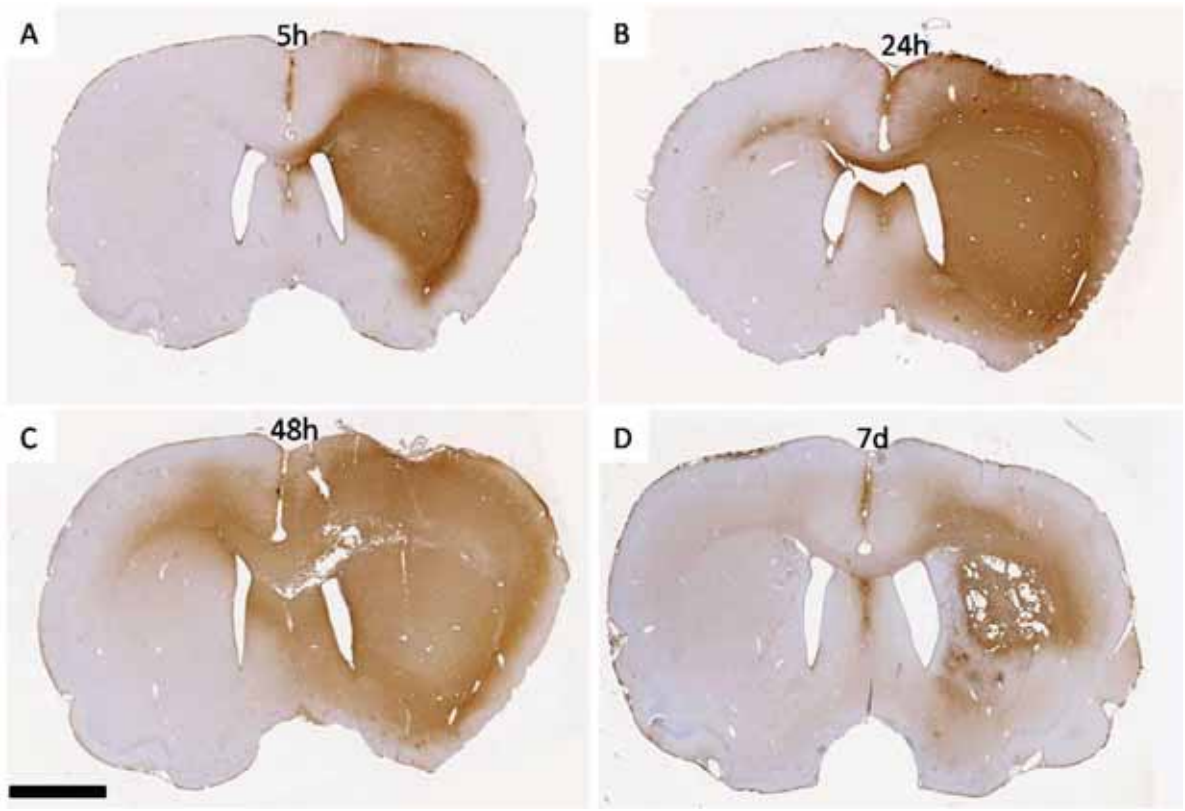


**Figure 70. Albumin staining following intracerebral thrombin injections. (A) There was already substantial albumin-IR at 5 hours, which (B) at 24 hours had increased further and begun to spread cross-callosally. (C) Contralesional spread increased further by 48 hours, although overall intensity of albumin-IR had reduced. (D) At 7 days there was residual peri-lesional albumin, staining at a markedly lower intensity. Scale bar=2mm.**

### 5.3.5 Double labelling

The full range of double labelling studies outlined following cICH were not repeated following thrombin injection, however confirmatory studies verified that the increased SP-IR seen after thrombin injection was indeed restricted to astrocytes (Figure 71).

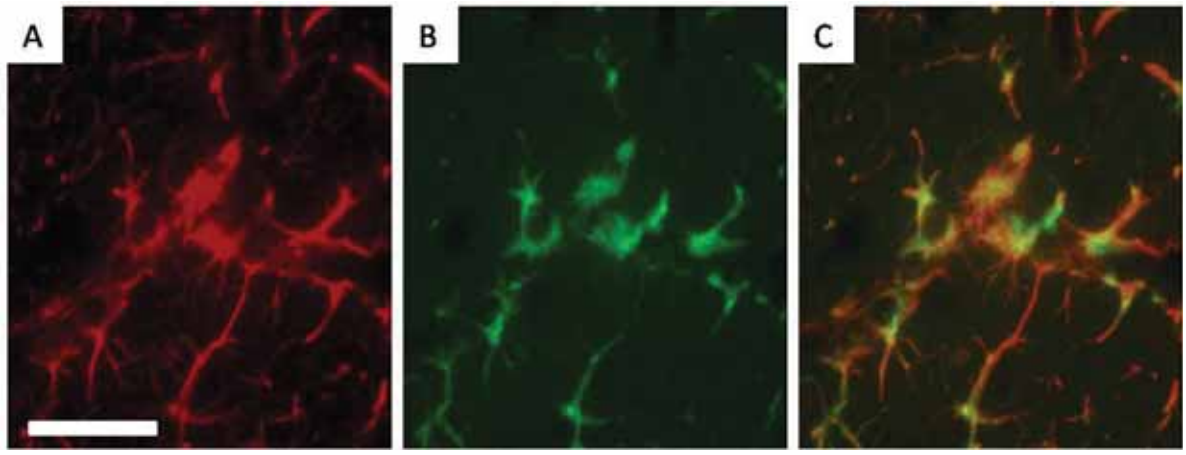


**Figure 71. Double labelling 24 hours post-thrombin injection localises increased SP immunostaining to perivascular astrocytes. (A) GFAP fluorescent immunohistochemistry, (B) SP, (C) merge. Scale bar=50µm.**

### 5.3.6 Brain oedema

The highest survivable dose of thrombin (5U) was chosen initially to test the hypothesis that NK1R antagonism (with NAT) reduces oedema (Figure 72). This dose had also produced the greatest increase in SP-IR (Figure 64) and was the most oedematogenic in dose-finding studies (Figure 61).

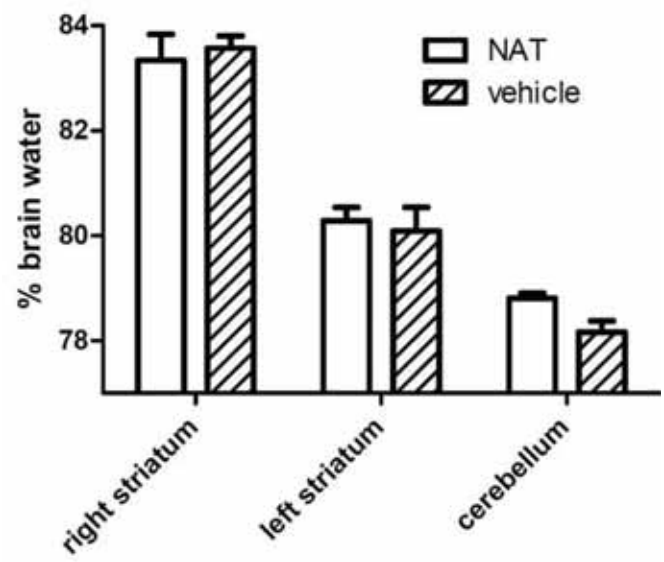


**Figure 72. Brain oedema 24 hours following 5U thrombin and intravenous NAT or vehicle. NAT failed to reduce oedema.**

No reduction in oedema was seen with the 5U thrombin dose with NAT treatment. This result was unexpected and various explanations were considered. First, that thrombin may act more quickly following direct injection than following cICH, and, thus, that the therapeutic time-window for an NK1R antagonist might be shorter than two hours. Second, that too much SP was generated by this dose, and that a more potent and blood-brain barrier penetrant agent might be required. Third, that the large area of cytotoxicity caused by 5U thrombin may overwhelm any component of vasogenic oedema. And, last, that our hypothesis may be incorrect; thrombin may not generate oedema through the release of substance P.

To determine which of these explanations was correct, the experiments were repeated using the BBB penetrant NK1RA, L733,060 (Figure 73), which was non-significantly more effective in reducing oedema post-ICH (Figure 55). L733,060 was administered 15 minutes prior to injury. Lower doses of thrombin were also used (3U and 1U – which from the dose-response curve (Figure 61) were predicted to generate slightly more (83.3%) and slightly less (82.5%) oedema than 0.2U collagenase (82.9%)).

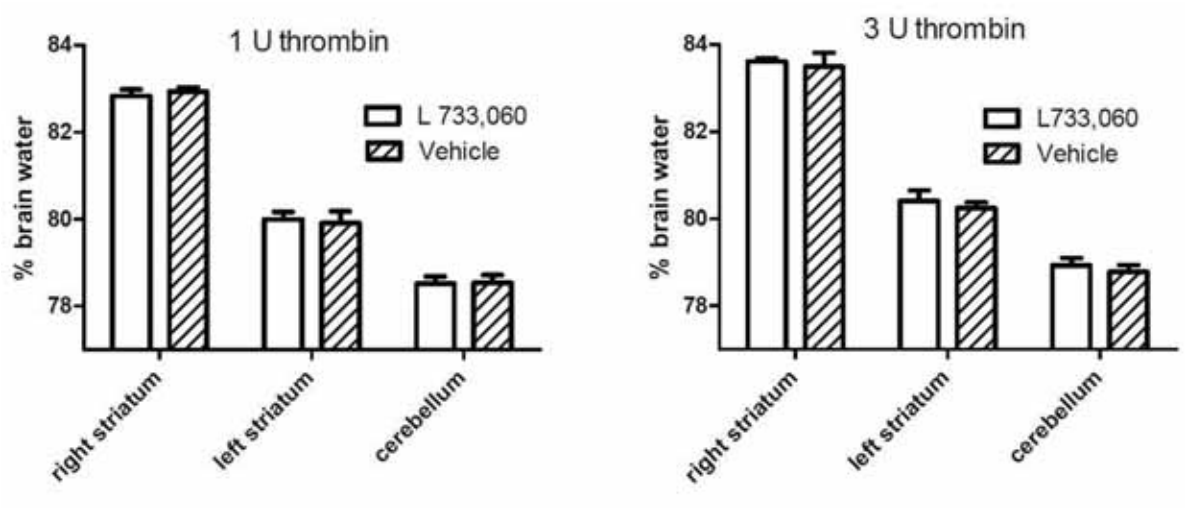


**Figure 73. Brain oedema 24 hours following 1U and 3U thrombin and intravenous L733,060 or vehicle. L733,060 failed to reduce oedema at either thrombin dose.**

Both doses of thrombin were slightly more oedematogenic than expected. Oedema in the vehicle group after 3U thrombin was 83.5±0.7%, and after 1U thrombin 82.9±0.2%. L733,060 failed to have any effect on oedema at either dose. If treatment and vehicle groups were combined, 3U produced significantly more oedema (83.6±0.5) than either 1U thrombin (82.9±0.2, p=0.0012) or 0.2U collagenase (82.9±0.4, p=0.04). This was concordant with the histology studies which suggested that 1U thrombin caused an equivalently-sized lesion to 0.2U collagenase (Figure 60a, b).

### 5.3.7 Blood-barrier dysfunction

The results of histology and oedema experiments suggested that 1U thrombin produced an essentially identically sized injury to 0.2U collagenase. Therefore BBB experiments were conducted using 1U thrombin (Figure 74), at the 4-8 timepoint suggested by pilot studies (Figure 59). Given that both NK1R antagonists had proven ineffective in reducing post-thrombin injection oedema, this experiment was performed only using L733,060, which appeared marginally more efficacious in reducing oedema post-ICH.

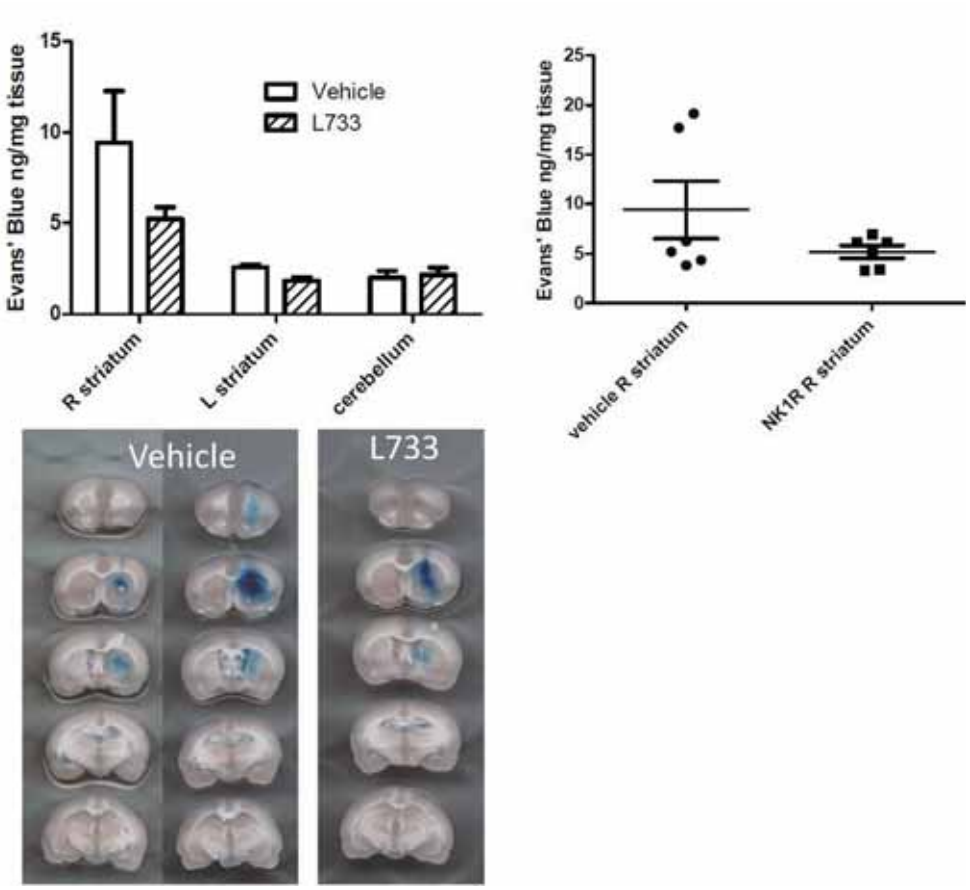


**Figure 74. Evans Blue extravasation 4-8 hours after thrombin 1U and L733,060 or vehicle. There was no significant difference with NK1R antagonism. Groups were similar save for two outliers in the vehicle group (graph right and middle bottom image).**

As with oedema studies, L733,060 had no effect on BBB disruption, although this can be said with less certainty, given the unexpectedly wide variability of data (which was not predicted from pilot studies).

## 5.4 Discussion

The results presented in this chapter confirmed previously reported consequences of intracerebral thrombin infusion,[187, 199, 527, 534] namely a rapidly developing central area of pan-necrosis (distinguishable from unaffected tissue even at 5 hours) leucocytic influx, microglial activation, oedema and blood-brain barrier disruption. This occurred in a pattern very similar to that seen following cICH, although the sequence was accelerated, in keeping with the known delay in ICH onset following injection of collagenase.[62]

As expected, SP immunoreactivity increased following thrombin injections, as occurs following ICH, although increased astrocytic SP-IR was evident earlier (at 5 hours), persisted

longer (at least 7 days) and was more extensive (Figures 63-65). However, despite a dramatic increase in SP-IR post-injury, 2 structurally unrelated NK1R antagonists did not reduce the associated cerebral oedema, whether following high-, medium-, or low-dose intracerebral thrombin (Figure 72 and 73). Likewise, BBB dysfunction was not ameliorated by NK1R antagonism (Figure 74).

These experiments essentially disprove the hypothesis that thrombin mediates post-ICH oedema by causing upregulation and release of substance P. Intracerebral thrombin injection certainly causes increased astrocytic SP-IR, but astrocytic SP in this setting did not appear related to oedema formation nor BBB dysfunction.

The results of this chapter are difficult to synthesise with both the results of preceding chapters and with the published literature. Thrombin is thought to be the main cause of early oedema post-ICH.[57] Collagenase ICH causes increased peri-haematomal SP (Chapter 3) and blocking the action of SP reduces post-ICH oedema and barrier dysfunction (Chapter 4). However, although thrombin injections increase peri-lesional SP to at least the same extent as cICH (Figure 65), blocking SP in this setting does not decrease subsequent oedema and BBB dysfunction. Several explanations can be proffered for these somewhat confusing facts.

First, it is probable that oedema mechanisms differ between collagenase and autologous ICH. Following equivalently-sized autologous and collagenase ICHs, cICH causes enhanced BBB breakdown, larger final lesion volumes and more severe functional deficits.[472] Therefore additional factors beyond the clot itself must be responsible. While thrombin has been demonstrated as the cause of early oedema post-aICH,[130, 200] the same has not, and, indeed, cannot be proven following cICH, as early thrombin inhibition will increase haematoma volumes. While thrombin undoubtedly plays a role in post collagenase-ICH oedema,[529] other factors (such as SP) may independently contribute – as opposed to 'second stage' oedema post-aICH, for which thrombin appears solely responsible.[130, 200]

Second, it is also possible that SP acts upstream, not downstream of thrombin following ICH – either increasing thrombin release (perhaps through platelet NK1 receptors)[339] or by enhancing the activity or production of thrombin co-factors – such as plasminogen, which is not neurotoxic itself at physiological levels, but which exacerbates thrombin toxicity when co-infused.[206]

Third, it may be that SP does not actually cause oedema, but, rather, prevents its clearance. Treatment of rats post-TBI with an NK1RA restores astrocytic end-feet aquaporin-4 expression otherwise lost. [535] As NK1R antagonism also reduces oedema and improves outcome, early oedema formation post-TBI is mostly likely vasogenic in nature (aquaporin-4

knockout worsens vasogenic oedema by preventing its clearance, but prevents the development of 'ionic' (or cytotoxic) oedema).[138] Therefore, oedema may be predominantly vasogenic post-cICH, but ionic/cytotoxic following thrombin injection.

A further unlikely possibility is that thrombin injection may alter the kinetics of the NK1R such that previously effective doses of the NK1R antagonist are, post-thrombin injection, insufficient. This possibility would demand that blockade of the NK1R post-thrombin injection requires up to 1000 times more NAT than following other forms of brain injury (0.025mg/kg effectively suppressed Evans Blue extravasation post-TBI in our laboratory's dose-finding studies[535]).

In either explanation, the role played by post-ICH increases in astrocytic SP-IR remains obscure. It is possible that the main role of astrocytic SP may be to promote glio- and neurogenesis; elevations in astrocytic SP are noted following traumatic brain injury,[461] intracerebral haemorrhage and ischaemic stroke,[436] and NK1R antagonism appears to block post-injury glio- and neurogenesis in all three conditions (Lauren Georgio, personal communication, Figure 54 and Park et al[518]). Thrombin injection also causes neurogenesis (Figure 62f and Yang et al[536]) and astrocytic SP may therefore also contribute to neurogenesis in this setting. Of note, however, there was substantially less neurogenesis seen following thrombin injection than following cICH (Figure 62), despite a similar level of histological injury (Figure 60a, b) and early substance P IR (Figure 65), suggesting that thrombin may be selectively neurotoxic to neural progenitor cells.

The fact that NK1R antagonists do not block post-thrombin oedema and barrier dysfunction, despite extensively upregulated astrocytic SP-IR, raises the possibility that the benefits of NK1R antagonism following cICH are not mediated by blocking astrocytic SP. This is somewhat counter-intuitive, given the perivascular localisation of both SP and the NK1R (Figure 35 and 36).

The beneficial effects of NK1R antagonists may, rather, be mediated by extra-cerebral anti-inflammatory actions (peripheral modulation of the immune response via splenectomy can reduce oedema when performed three days prior to cICH[271]). A hyperacute 'spike' in peripheral blood SP levels is seen 30 minutes following traumatic brain injury in rats[461] and it may be that this primes the peripheral immune response. It has been previously noted that BBB penetrant and non-penetrant NK1R antagonists are equally effective in the setting of ischaemic stroke and TBI; the explanation given has been that non-penetrant forms cross the BBB under injury conditions.[481, 535] An alternative may be that non-penetrant NK1R antagonists beneficially outside the central nervous system.

In our experiments thrombin appeared more potent than has been previously reported. After initially obtaining unexpectedly high levels of injury in pilot studies, experiments were repeated using a different thrombin batch, with identical results. Doses of thrombin previously reported to be toxic range from 5[533]-100U.[527] 2.5U bovine thrombin in 5µL is reportedly non-toxic.[188]

In our pilot studies 10U caused unacceptable rat mortality, 5U thrombin caused a very severe injury (Figure 60a) and 1U resulted in a lesion which approximated that that caused by a 150µL blood clot (Figure 24, Figure 60a, c). Even 0.125U thrombin probably caused more oedema than vehicle (Figure 61) (although the experiment was underpowered to prove this at lower doses.) This disparity may be partially explained by differing thrombin potencies in the rat; our experiments used rat thrombin which appears more potent[257, 533] than human and bovine thrombin.[130, 188, 527]

However, even when compared only with previous studies which have used rat thrombin, significant anomalies remain. It is possible that the concentration of thrombin may be responsible: studies reporting that 1U causes no injury have infused thrombin over 5 minutes in 50µL vehicle,[196, 533, 537] as opposed to 5µL in the present study. This may allow thrombin to diffuse more rapidly away from the injection site, or along the needle track (enhanced injury along the needle track was noted in our experiments (Figure 62d) and has been noted previously[527]). The concentrations used in our study were not unreasonable, however, as a 5µL blood clot can produce 1U thrombin.[532] It is worth noting that 5U/mL thrombin is neurotoxic *in vitro*[537] (i.e. a concentration 40x lower than used in our experiment).

Differences in injecting technique may also account for the variable results. As thrombin adsorbs to glass,[474] our experiment was designed to ensure that thrombin solutions remained within polyethylene tubing and therefore did not come into contact with the glass of the infusing syringe. This was relatively straightforward, as infusion volumes were small; it is not known whether previous studies using higher volumes have taken this precaution.

## 5.5 Conclusion

Although intracerebral thrombin injection caused significant acute elevations in peri-lesional granular and astrocytic SP-IR, NK1R antagonists did not reduce the oedema and BBB dysfunction which followed. Therefore the hypothesis that thrombin mediates early-stage post-ICH oedema via substance P was disproven. These results raise the possibility that the NK1R antagonists may reduce post-ICH oedema by acting outside the CNS. The next chapter

will preliminarily test this hypothesis by injecting various concentrations of substance P into the striatum; if the pro-inflammatory action of substance P is predominantly intracerebral, oedema and BBB dysfunction are to be expected. If not, only minimal changes will be seen.

# 6 Effects of intracerebral substance P injections.

## 6.1 Introduction

The results of the previous chapter demonstrated that NK1R antagonists do not reduce oedema and BBB dysfunction after stereotactic injection of intracerebral thrombin, even though a dramatic increase in intracerebral SP-IR was seen, which was at least as substantial as was caused by collagenase ICH (cICH) – a setting in which NK1R antagonists proved efficacious.

This surprising result raises the question: does intracerebral substance P actually cause oedema and blood-brain barrier breakdown? Does release of intracerebral substance P engage endothelial NK1 receptors to cause gap formation and plasma extravasation? Evaluation of wet-weight dry weight and Evans Blue following stereotactic injection of substance P would potentially provide an answer. A review of the literature suggests that these experiments have never previously been performed.

Subcutaneous administration of SP directly causes vasogenic oedema[538] and can either directly cause[373] or exacerbate[374, 375] cutaneous accumulation of neutrophils. Subcutaneous SP upregulates peripheral endothelial leucocyte adhesion molecules, [379] degranulates mast cells[365] (which generates further vasogenic oedema) and enhances the leucocytic production of various pro-inflammatory molecules and cytokines.[367, 382-390]

These experiments have not been replicated intracerebrally, and there is only indirect evidence that peripheral mechanisms of SP-mediated oedema and inflammation apply to the CNS. Cerebral endothelial NK1Rs have been previously demonstrated *in vivo*[445] and *in vitro*[399] and endothelial NK1R expression is also suggested by the present study (Figure 36a-c). Endothelial NK1Rs, if functionally active, must presumably be basal rather than luminal, as no cerebral Evans Blue extravasation is seen following systemic administration of either substance P,[430, 463] capsaicin (which causes neurogenic release of substance P), [430] or following stimulation of trigeminal nerves.[430] Only dural and conjunctival extravasation develops following trigeminal stimulation – that is, only in trigeminally innervated regions external to the BBB. [430]

To the best of our knowledge, only two studies have investigated the pro-inflammatory effects of intracerebral application of SP. Hu et al demonstrated that topical SP increases the permeability of isolated rat pial venules, although immature rats and quite high concentrations ($EC_{50}$ 25μM) were used.[435] McCluskey and Lampson[539] demonstrated that

substance P enhances Interferon-γ-induced class II major histocompatibility complex (MHC) upregulation in the brainstem. However, no effect was seen in the hippocampus even at high doses (50μg). Neither study investigated the effects of intracerebral SP injections on either oedema or other aspects of inflammation.

## 6.2 Experimental design

Fifty-five male Sprague-Dawley rats (300-340gm) were used for the experiment, as described in chapter 2.

Five animals were used in initial dose-finding experiments (0.1μg, 1μg, 10μg, 100μg and 200μg, dissolved in 10μL oxygen-free normal saline). These animals were sacrificed at 24 hours and examined by H&E staining and albumin immunohistochemistry for evidence of oedema and plasma extravasation. Twenty animals were then treated with 100μg SP and sacrificed at 5 hours, 24 hours, 48 hours or 7 days (5 per group). To confirm the results seen in dose-finding experiments, a group of 5 animals injected with 10μg SP was assessed at 24 hours. As there were no differences noted between this latter group and vehicle animals from chapter 3 (administered 2μL normal saline using an otherwise identical protocol) no additional vehicle animals groups were performed.

As neither circling behaviour nor deficits in the vibrissae-elicited stimulation test were observed in pilot experiments, behavioural testing was not performed.

Twelve animals were used for oedema experiments (n=6 per group). Ten animals were used in BBB experiments (n=5 per group).

### 6.2.1 Histology and immunohistochemistry

At the pre-specified timepoints animals were perfuse-fixed with formalin, and their brains were extracted, sectioned, scanned and processed as described. H&E and FJC staining was performed on sections through the needle injection site (the maximal lesion area), as well as immunohistochemical staining for ED-1, GFAP, MPOX and SP, as described. Slides were scanned at high resolution and viewed with appropriate viewing software.

### 6.2.2 Brain oedema

The effect of 100μg SP on brain oedema was assessed by the wet weight dry weight method, as described in chapter 2. Animals were administered either SP or vehicle, and sacrificed at 24 hours. As there was no statistically significant effect on brain oedema, we did not proceed with a previously-planned experiment assessing the effect of an NK1RA in this setting.

### 6.2.3 Blood-brain barrier permeability

The effect of intracerebral SP on BBB dysfunction was assessed by the Evans Blue method, as described in chapter 2. As peripheral extravasation and vasodilatation occur more or less instantaneously following neurogenic inflammatory stimuli (endothelial gap formation peaks after 1 minute[351] and vasodilatation after 5[538]) , Evans blue was administered 15 minutes prior to intracerebral injection of SP (100µg). Animals were sacrificed 5 hours after. Animals were also pre-treated with L733,060 or vehicle (simultaneous to EB injection) to determine whether the small degree of Evans Blue extravasation seen was most likely due to the small associated needle haematoma or due to vasogenic oedema.

### 6.2.4 Statistical analysis

Brain water content and Evans blue quantification were also analysed by one-way ANOVA, with selected Bonferroni post-tests.

## 6.3 Results

### 6.3.1 Baseline and experimental parameters

Table 5. Experimental parameters

| Group | Weight | Duration | T start | T finish | T 5h post NK1R |
|---|---|---|---|---|---|
| **SP 100 µg** | 318±7 | 23±2 | 37.0±0.4 | 37.1±0.3 | ---- |
| **SP 10µg** | 316±7 | 22±1 | 37.0±0.4 | 37.1±0.4 | ---- |
| **Vehicle** | 327±6 | 21±1 | 37.2±0.4 | 37.0±0.4 | ---- |
| **SP EB (NS)** | 319±9 | 42±3 | 37.1±0.4 | 37.3±0.4 | 37.1±0.2 |
| **SP EB (NK)** | 317±10 | 43±11 | 36.8±0.3 | 37.1±0.2 | 37.1±0.4 |
| **cICH vehicle** | 321±21 | 26±3 | 36.7±0.3 | 37.1±0.3 | ---- |

**Experimental parameters (means +/-SD) for animals administered SP (histology and oedema studies, 100 or 10µg ), oedema vehicles, Evans Blue SP-injected animals treated with normal saline (NS) or NK1R antagonists (NK), and 'collagenase' (cICH) vehicles (given 2µL normal saline and used as histological comparators with intracerebral SP).**
**Units: weight=grams, duration=minutes, temperature ('T')=$^{o}$C.**

### 6.3.2 Dose finding experiments

Doses of SP lower than 100µg caused no greater injury than 2µL vehicle and no greater degree of albumin extravasation (Figure 75).

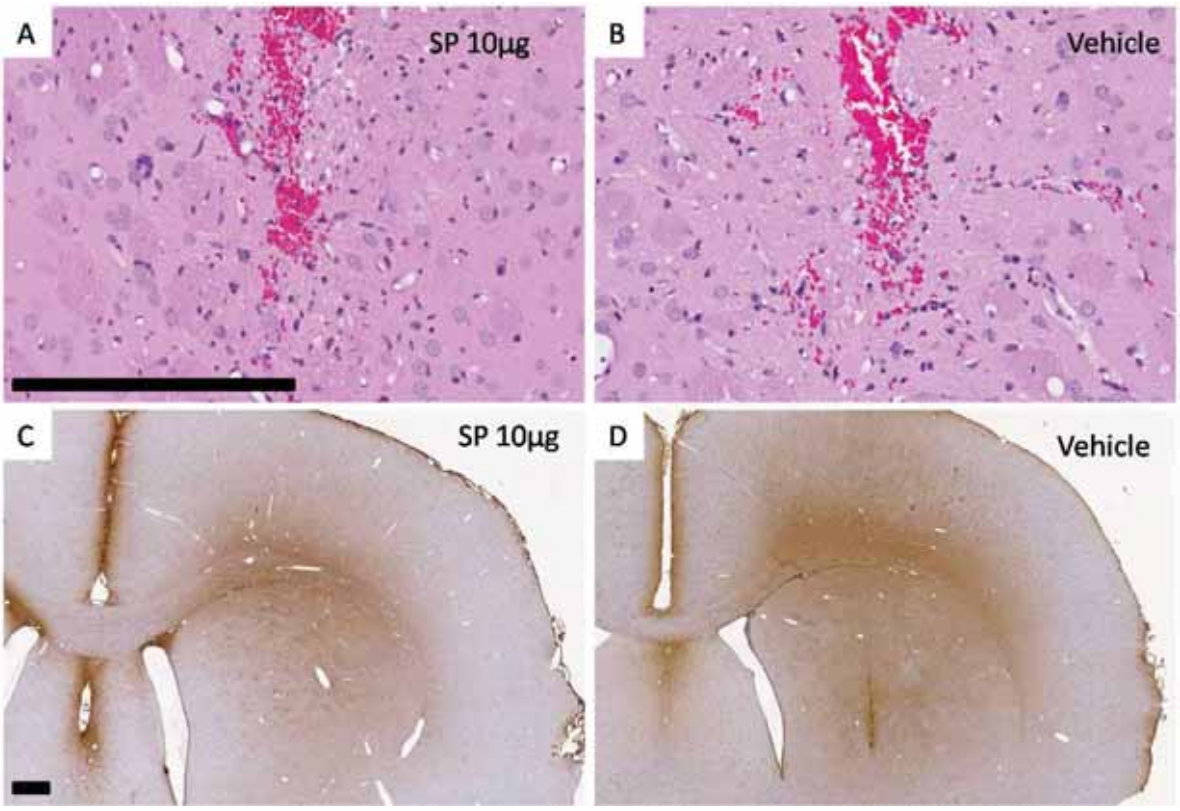


**Figure 75. Dose finding studies for intracerebral substance P injections. (A) H&E staining through striatal injection site 24 hours post-injection of SP 10µg. There was no difference between this dose of substance P and vehicle (B). (C) Albumin immunohistochemistry through striatal injection site 24 hours post-injection of SP 10µg. Albumin extravasation was similar to that seen following vehicle (D). Scale bar=500µm.**

The 100 and 200µg doses both caused a small region of striatal pallor, intra- and extracellular oedema and albumin extravasation. At the 200 µg dose SP precipitated intracerebrally to an unacceptable degree (despite appearing to dissolve without difficulty *in* vitro) and hence 100 µg was used in subsequent experiments.

### 6.3.3 Histology and immunohistochemistry

#### *HE staining*

Consistent with preliminary dose-ranging studies, the five rats administered 10µg SP had no greater injury than those administered 2µL vehicle (see above). Rats administered 100µg SP had evidence of a mild, but highly variable injury (Figure 76). At this dose, some rats at the 5, 24 and 48 hours demonstrated intracerebral precipitation of injected SP (Figure 76a-c), although less marked than was seen with the 200µg dose in dose-finding studies. The degree of resultant striatal injury (as assessed by striatal pallor at 24 hours) varied proportionally

with the area of protein precipitation (Figure 76e), suggesting protein precipitation contributed to the level of injury (which was in any case, even at worst, mild).

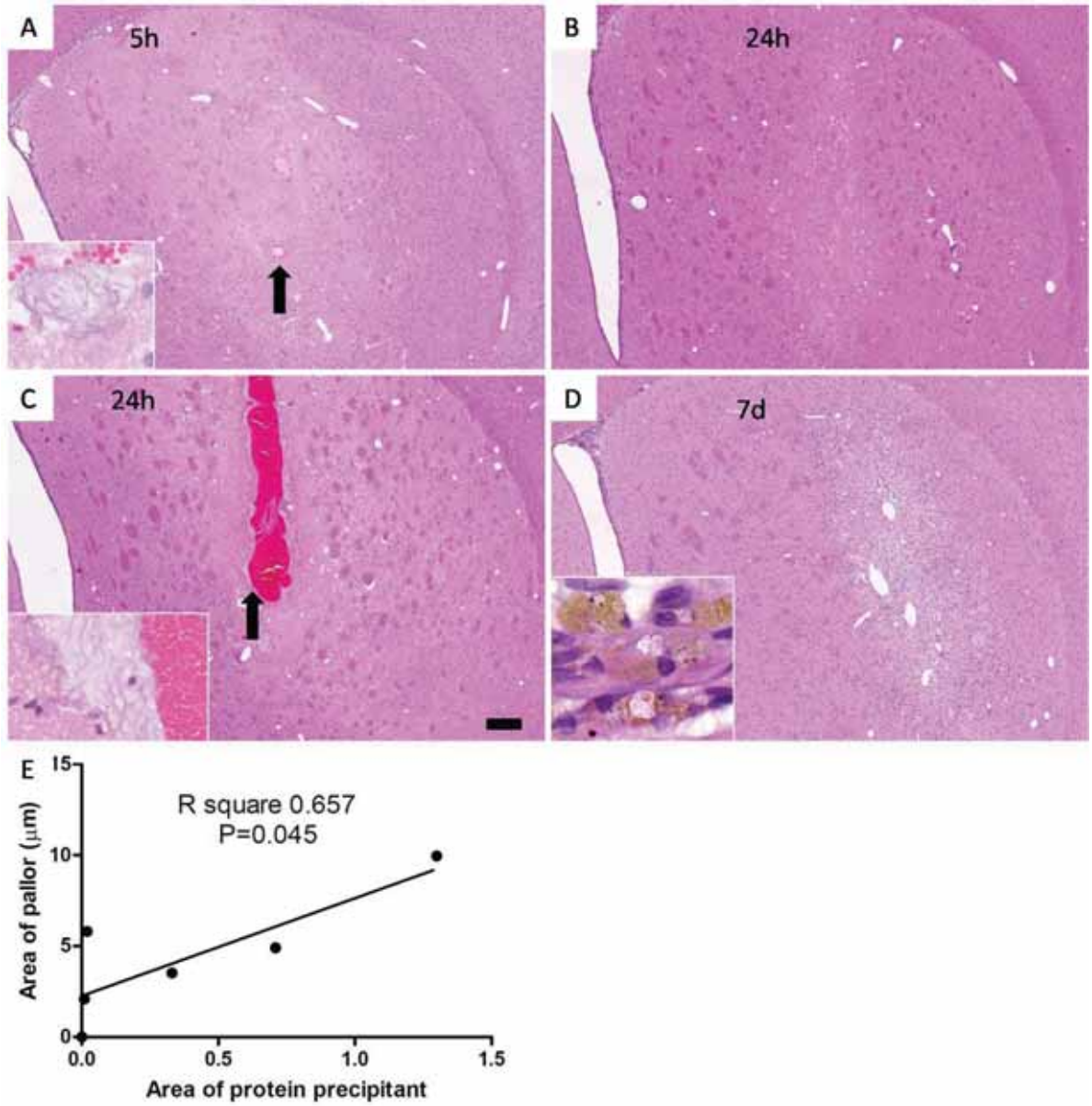


**Figure 76. H&E staining following intracerebral substance P injections (100μg). (A) At five hours there is pallor around the injection site, most marked in rats which had significant precipitation of SP (insert). (B) and (C) At 24 and 48 (not shown) hours there was a wide variation in lesion size, which varied with the degree of protein precipitation (from negligible (B) to significant (C)). In several animals a degree of haemorrhage occurred within the precipitated protein (C, arrow and insert). (D) The injured area and precipitated protein was phagocytosed to a gliotic scar by seven days. Occasional small fragments of remaining precipitated protein could be seen within macrophages (identified by their haemosiderin staining, insert). (E) There was a significant correlation between the cross-sectional area of protein precipitation and the area of striatal pallor at 24 hours. Scale bar=500μm.**

### *Neuronal degeneration - Fluoro-Jade C staining*

Consistent with findings following H&E staining, the most marked neuronal degeneration occurred in rats which also had evidence of significant protein precipitation (Figure 77). In these rats, FJC positive neurons were already easily visible at 5 hours and peaked at 24 hours. Fewer FJC positive neurons were evident at 48 hours and still fewer at 7 days. Following 10µg substance P only sparse FJC positive neurons were evident adjacent to the needle tract, similar to the number seen after vehicle injection.

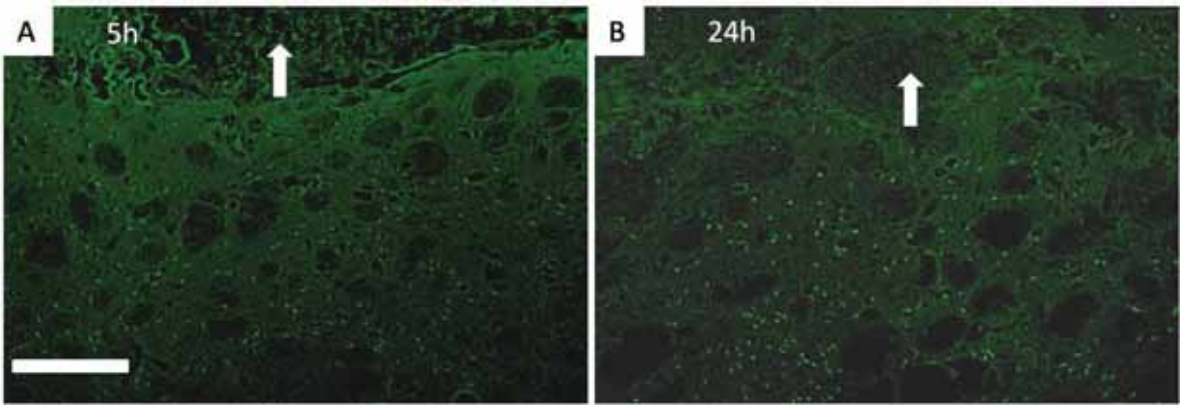


**Figure 77. Fluoro-Jade C staining following intracerebral substance P injections. (A) At five hours there was already significant neuronal degeneration adjacent to precipitated protein (arrows). (B) Neuronal degeneration peaked at 24 hours. Scale bar=100µm.**

### *Substance P immunostaining*

Substance P immunostaining revealed that most of the injected substance P had either diffused away or been metabolised by 5 hours (Figure 78).

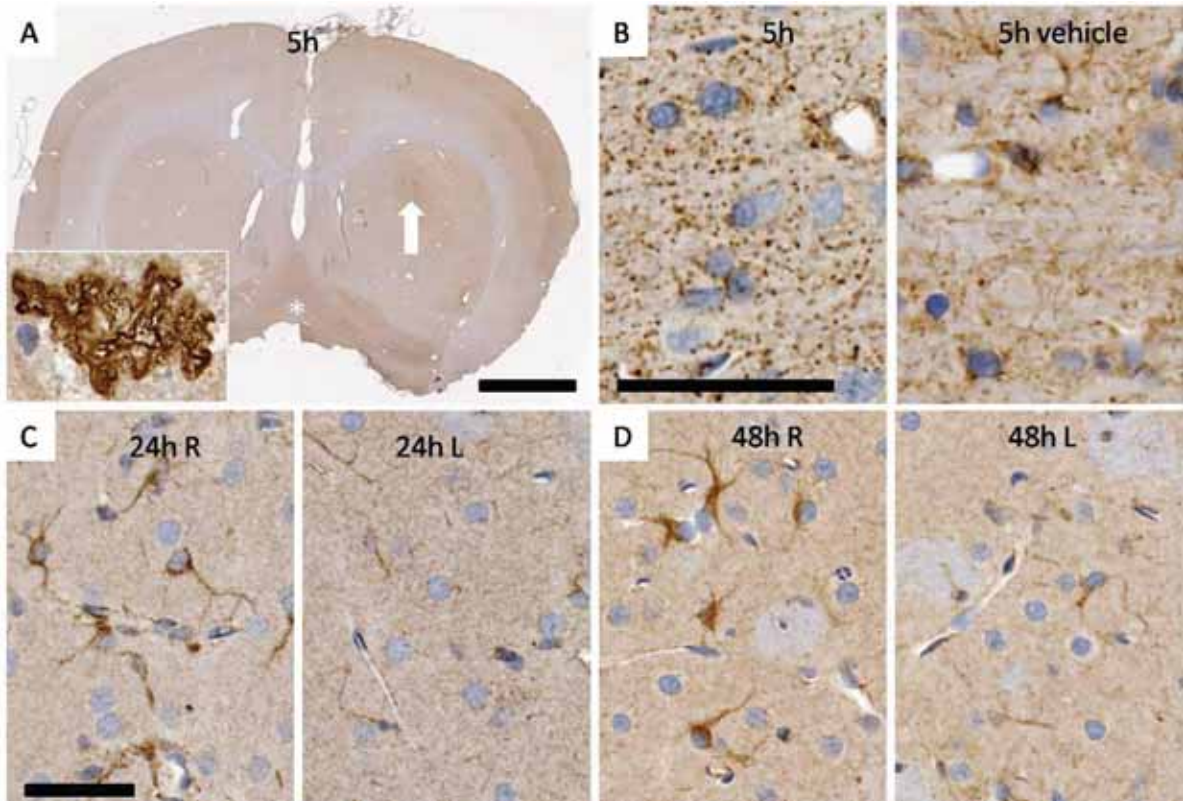


**Figure 78. SP immunostaining following intracerebral substance P injections. (A) There is a subtle increase in ipsilateral substance P at this and later timepoints. Precipitated protein stains strongly for substance P (insert). (B) At five hours granular SP staining can be seen distant to the injection site (higher power of (A)). (C) There was a mild increase in adjacent astrocytic staining at 24 hours, which increased slightly at 48 hours (D). Scale bar=50µm or 2mm for whole brain.**

Areas of precipitated protein stained strongly for SP at 5 hours (Figure 78a) and there was a generalised subtle increase in granular staining, even distant to the injection site (Figure 78b). There was no astrocytic reaction at this time-point, but at 24 and 48 hours a mild increase in astrocytic SP-IR was seen (Figure 78c, d). Phagocytosis of precipitated SP was evident at 48 hours; by 7 days only residual intracellular fragments were seen (not shown).

### *Inflammatory cell response – myeloperoxidase and ED-1 immunostaining*

There was surprisingly little evidence of neutrophil and monocyte infiltration at early timepoints, the degree of which differed little from vehicle injection (Figure 79a, c), even in rats with a moderate-sized striatal injury. At five hours there was a marked contrast with cICH (Figure 31 and 32) and, especially, intracerebral thrombin injections (Figure 67 and 68). Even at 24 hours the neutrophil and monocytic infiltrate was notably sparser (Figure 79b). There were few remaining neutrophils at 48 hours and none at seven days. The macrophage/microglial response at these latter timepoints (Figure 79d) resembled more

closely that which was demonstrated in previous chapters, although it was still far less extensive and intense.

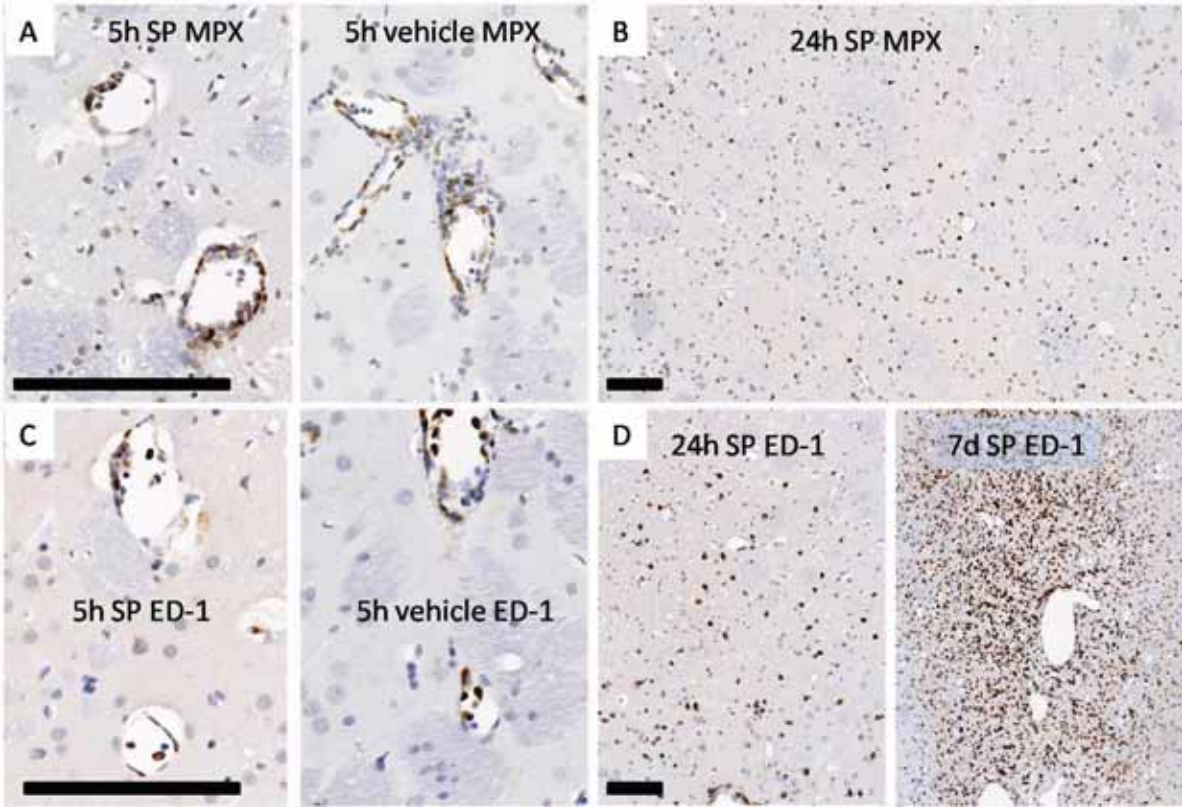


**Figure 79. Leucocyte infiltration/activation following intracerebral substance P injections (myeloperoxidase and ED-1 immunostaining). (A) At five hours neutrophil infiltration does not differ between SP injections and vehicle. (B) Neutrophil infiltration peaked at 24 hours, but was sparse at worst. (C) Monocyte infiltration did not differ from vehicle at five hours. (D) Sparse monocyte infiltration/microglial activation was seen at 24 hours. By 7 days a more typical phagocytic response was evident. Scale bar=100µm.**

### *Astrocytic response - GFAP immunostaining*

Unsurprisingly, GFAP immunoreactivity was most significantly increased in those animals with H&E evidence of histological injury (i.e. those with precipitation of SP protein). More interestingly, however, was the diffuse elevation in GFAP-IR seen in those animals which appeared otherwise uninjured (Figure 80). This was evident at 24 hours and progressed over time, to a similar extent as seen following thrombin and collagenase injections (Figure 33, Figure 69). The increase in GFAP-IR at 24 hours following 10µg SP was less marked, but still appeared greater than that seen with vehicle (not shown). No timepoints apart from 24 hours was assessed in rats administered 10µg.

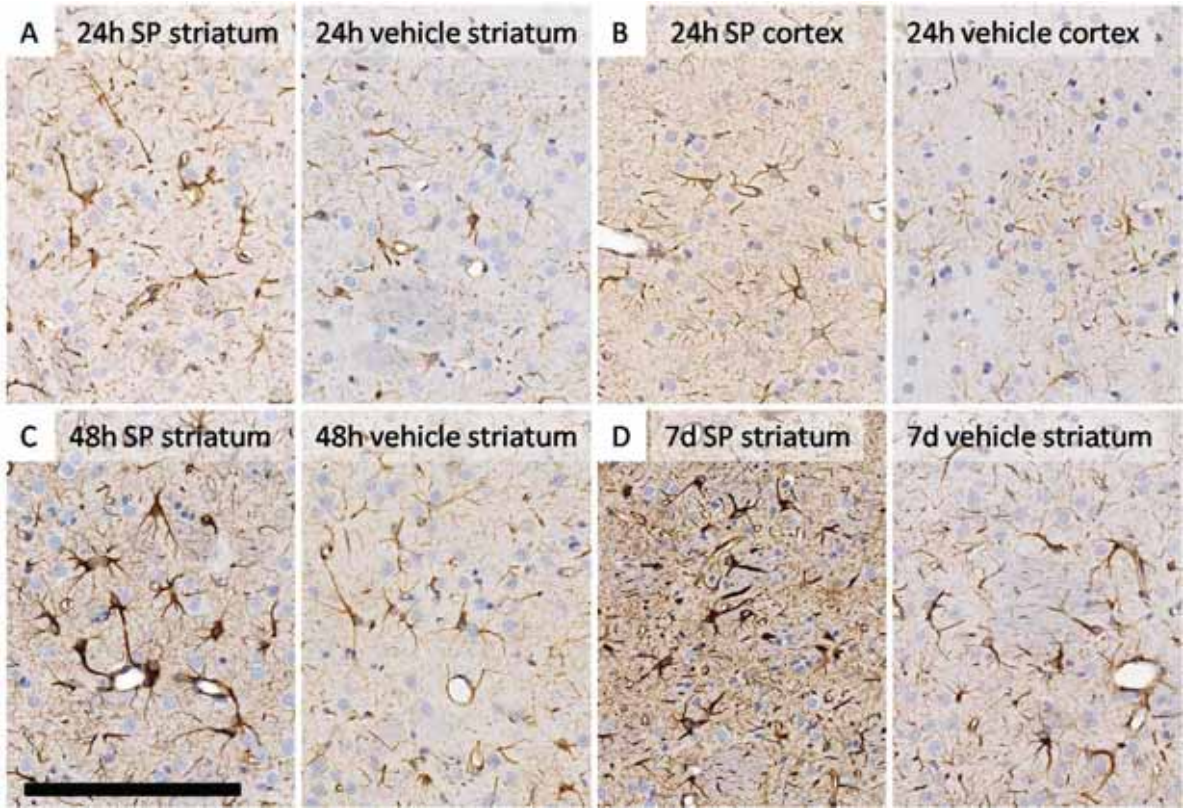


**Figure 80. Astrocyte response following intracerebral substance P injections. (A), (B) Compared with vehicle controls, there was increased GFAP staining in the striatum and cortex of brains which appeared otherwise histologically normal, even quite distant from the injection site. (C), (D) In similarly otherwise unaffected brains the increase in striatal and cortical (not shown) GFAP staining had progressed at 48hours and 7days. Scale bar=100µm.**

### *Albumin immunostaining*

Similarly to the responses seen following thrombin injection (Figure 70), albumin-IR was noted at 5 hours, increased at 24 hours, became more diffuse but less intense at 48 hours, and was markedly reduced at 7 days (Figure 81). There was, however, little contralateral spread of albumin-IR, and the overall intensity of staining was markedly less intense than seen with thrombin injection.

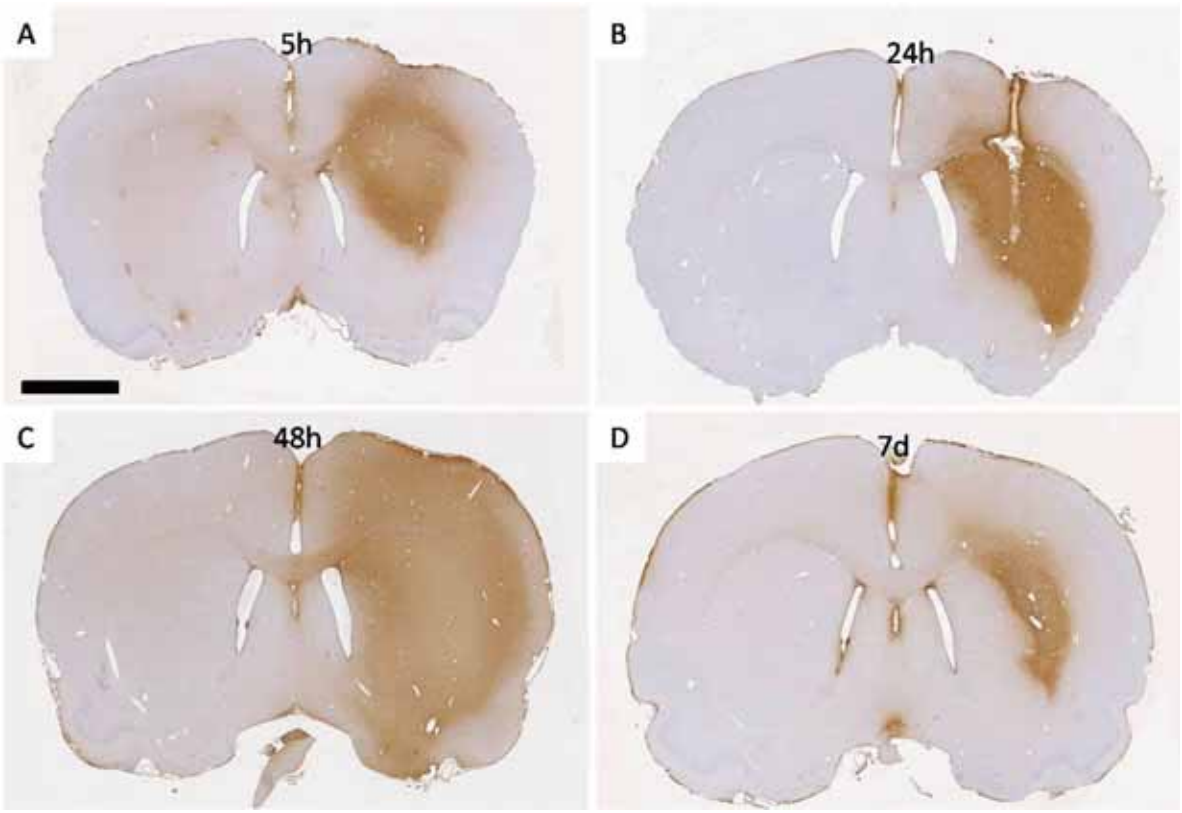


**Figure 81. Albumin immunostaining following intracerebral substance P injections. (A) Albumin-IR was elevated already at five hours. (B) It increased further by 24 hours (C) By 48 hours it had become more diffuse, but less intense. (D) By seven days a marked reduction was seen. Scale bar=2mm.**

### 6.3.4 Brain oedema

There was minimal histological evidence of oedema seen at 24 hours in H&E sections (Figure 76b), suggesting that a single dose of substance P did not cause substantial oedema. This was confirmed by the wet-weight/ dry-weight method (Figure 82).

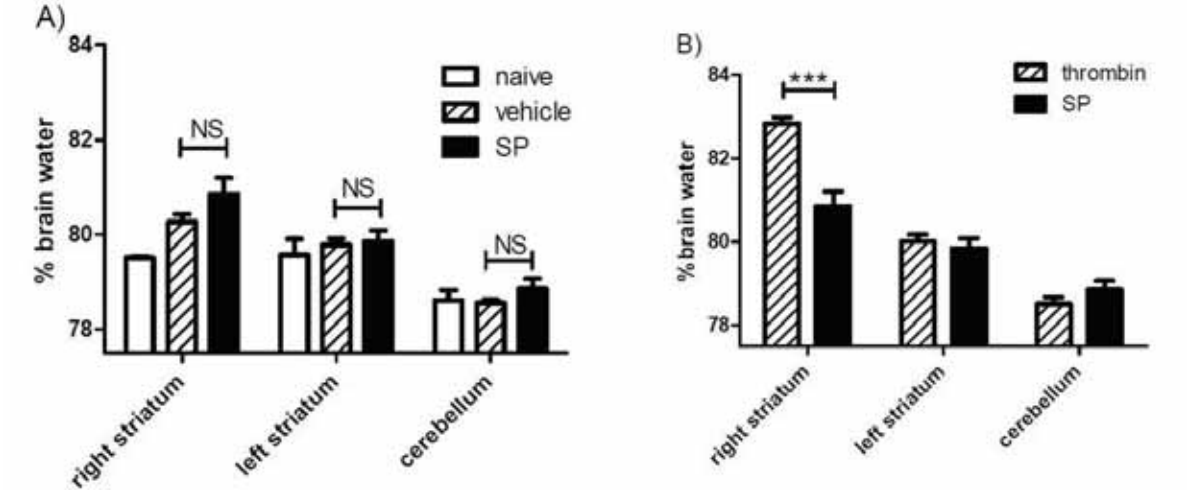


**Figure 82. Brain oedema 24 hours following intracerebral substance P injections. (A) SP injection did not increase oedema beyond vehicle levels. (B) There was significantly less oedema that was seen following thrombin injections (and collagenase ICH (not shown)). ***=p<0.001, NS=not significant.**

Oedema did not differ significantly from that seen following vehicle injection (80.9±0.9 vs 80.3±0.4%; p=0.16: Figure 82a). SP injection caused less than a quarter of the oedema seen following 'low-dose' thrombin injection (82.8 ±0.3 vs 80.9±0.9%; p=0.0009: Figure 82b). Given that SP injections did not increase oedema beyond vehicle levels, a planned experiment testing the effect of NK1R antagonism on oedema did not proceed.

### 6.3.5 Blood-brain barrier dysfunction

Pilot experiments did suggest that SP injection caused a measurable increase in ipsilateral Evans Blue extravasation (Figure 83a), although to a much lesser degree than was seen following cICH. It was unclear whether this was purely due to the small amount of haemorrhage induced by SP injections (EB was administered prior to injury). Therefore the effects of an NK1R antagonist on EB were assessed (Figure 83b). No reduction in EB extravasation was seen, suggesting that the EB elevation was not due to canonical SP-NK1R interactions, but was rather caused by the small degree of haemorrhage from needle trauma or by the striatal injury caused by the precipitation of SP protein.

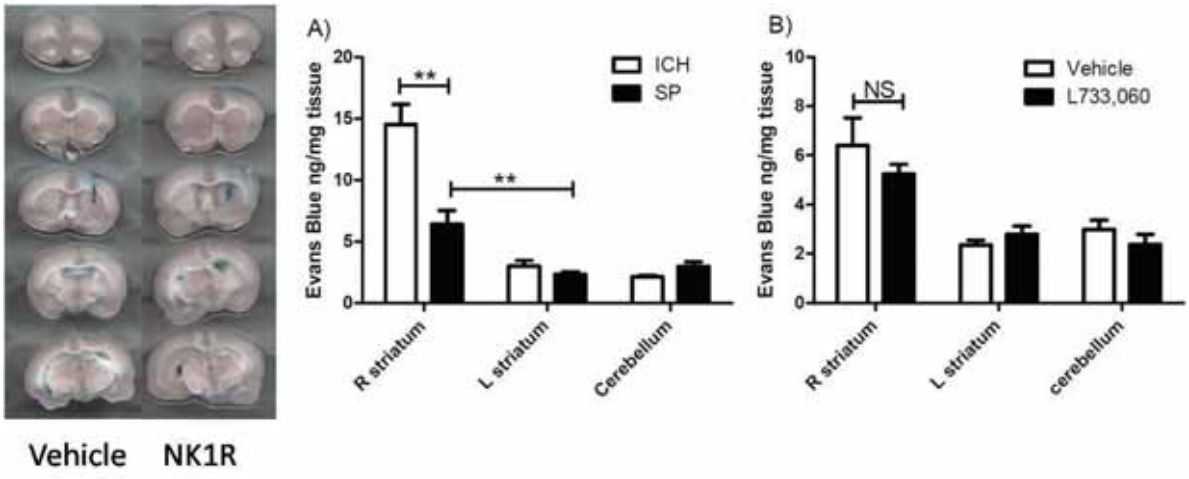


**Figure 83. Evans blue extravasation 0-5 hours following intracerebral substance P injections. Most EB leakage was around the needle tract following both vehicle and NK1R treatment. (A) Although a measureable EB extravasation occurred when compared contralaterally, this was minor compared to that seen following collagenase ICH. (B) NK1R treatment had no effect on the degree of EB extravasation. **=p<0.01, NS=not significant.**

## 6.4 Discussion

The results of this chapter demonstrate that stereotactic injection of large amounts of intracerebral substance P is only mildly deleterious, with most of the ill-effects associated with precipitation of the injected protein, which occurred to a variable extent. Amounts of SP

less than 100µg (which did not precipitate) had minimal effects. Supraphysiological boluses of intracerebral SP appear insufficient, in themselves, to cause oedema, BBB dysfunction or leucocytic infiltration.

The lack of effect demonstrated was unlikely because of inadequate dosing; subcutaneous injection of substance P causes oedema when injected at doses as low as 40 nanograms[540] – that is, 2500-fold less than used in the present study (100 µg). We estimate that our dose represents the amount that would be found in 800gm of homogenised rat caudate.[541] Our findings, while surprising, are supported by some previous research; inhibitors of neutral endopeptidase and angiotensin converting enzyme (the main enzymes responsible for SP metabolism) do not cause cerebral Evans Blue leakage, despite producing substantial leakage extracerebrally.[463] Capsaicin, which produces extravasation peripherally through secondary release of substance P, causes no oedema when injected intracerebrally.[430]

It is possible that intracerebral SP may only enhance, but not in itself produce inflammatory responses in the CNS. When added to *in vitro* microglial/ astrocytic cultures SP can significantly enhance cytokine production induced by bacterial pathogens but has no effect when applied in isolation.[432] Similarly, substance P enhances IFN-γ mediated MHC-II upregulation in the brainstem at doses as small as 1ng, but has no effect when injected by itself (no potentiating effect whatsoever was seen in the hippocampus, even with doses as high as 50µg.)[539]

Likewise intracerebral SP may enhance, but not cause cerebral oedema. SP can cause permeability of cultured cerebrovascular endothelium following cytokine stimulation[399] but central (Figure 81 and 83) and systemic[430, 463] administration of SP in isolation does not. One possible explanation is that SP induces gap formation of cerebrovascular endothelium, but that no vasogenic oedema can ensue unless other constituents of the BBB are also disrupted (the basement membrane and astrocytes).

A further possibility is that the anti-inflammatory actions of NK1R antagonists following cICH may be peripherally, not centrally mediated. This was also suggested by the results described in chapter 5, in which NK1R antagonism was not able to reduce any aspect of inflammation post-thrombin injection, despite thrombin injection causing significantly elevated SP-IR. Intriguingly, this hypothesis has support from studies into EAE, a multiple sclerosis model. Although slightly different models of the disease were used in the two experiments, systemic administration of an NK1R antagonist potently reduced neuroinflammation,[421] whereas intracerebroventricular administration was without benefit.[542] Notably, in this latter study, substance P injected intracerebrally did not exacerbate disease (27µg injected daily for two weeks). Previously it has been surmised that non-BBB penetrant NK1R antagonists can be

effective post-acute brain injury due to a temporary BBB breakdown allowing drugs access to the CNS.[461, 481] The results of this chapter suggests, rather, that they may act peripherally.

Other less likely mechanisms of NK1RA benefit include a reduction in brain oedema through an anti-diuretic effect,[543] or a reduction in brain oedema through decreasing post-ICH hypertensive responses (although NK1R antagonists do not appear to effect blood pressure in otherwise untreated rats, they may decrease central sympathomimetic responses to organ hypoperfusion).[544] The effects on NK1R antagonists on urinary flow and post-ICH blood pressure were not measured in our experiments.

In the current study, despite the amount of substance P injected (100µg), the amount of SP-IR was not increased at the 5 hour time-point. While this may seem surprising, SP is metabolised extremely efficiently. Microdialysis studies have previously demonstrated that striatal SP is metabolised at around 0.3mcg/min[545] – which would completely metabolise 100mcg substance P in around 5 hours. Additionally, the small molecular weight of SP may also allow diffusion into CSF as a means of clearance. Consistent with these observations, functional effects of cerebral SP microinjection are also of brief duration; 10µg injected into the substantia nigra causes contraversive circling for 10 minutes only.[546] The minimal astrocytic SP seen at 5 hours argues strongly that elevated astrocytic SP seen at 24 and 48 hours in brain injury of various kinds is due to *de novo* synthesis. It is not due to astrocytic uptake of SP (such as occurs, for instance, with glutamate[547]).

The obvious major limitation of this chapter was the extent to which SP precipitated in the brain. At lower doses of SP (10µg and below), where no precipitation occurred, no effects were evident other than a mild increase in GFAP-IR. It is important to emphasise that even 10µg is an extremely large dose in physiological terms.[541] Precipitation of SP could have been reduced by infusion in a higher volume of vehicle, but effects of the infused substance P would have been more difficult to disentangle from the greater injury seen with higher vehicle volumes (Chapter 3). However, as little or no precipitation occurred in several rats receiving the 100µg dose at each timepoint, valid conclusions about the effects of SP microinjections can still be drawn.

If intracerebral substance P causes neither oedema nor BBB dysfunction, then what is the function of elevated astrocytic SP, which is seen not only following ICH (Figure 27) and thrombin injection (Figure 63), but also following TBI,[535] rMCAO[481] and intracerebral injection of vehicle (Figure 39a)? The only consistent intracerebral effect of SP injections demonstrated (also evident at the 10µg dose) was elevation in GFAP-IR (Figure 80), raising the possibility that one of the roles of SP intracerebrally may be to promote astrogliosis. As astrocytes appear to upregulate both SP (Figure 35) and the NK1R (Figure 36) post-injury, a

feed-forward loop could eventuate. This is somewhat inconsistent with the lack of reduction in astrogliosis following NK1R treatment of cICH rats, however, an NK1R-mediated reduction in astrogliosis has previous been demonstrated following both ischaemic stroke[481] and various CNS infections.[422, 432]

Other putative roles for elevated astrocytic SP include the promotion of angiogenesis,[548] and the upregulation of glio- and neurogenesis.[518] Although the results of this chapter did not demonstrate an effect of stereotactic SP injections on subventricular zone cellular proliferation, it is likely that a sustained exposure to SP would be needed to induce a proliferative response (rather than a one-off bolus). The effect of SP on cerebral angiogenesis was not examined in this thesis and has never, to our knowledge, been previously reported; however, as SP induces peripheral angiogenesis both *in vitro*[548] and *in vivo* [549] such an experiment would certainly be worthwhile.

Given the rapid metabolism of SP[545] and the known tachyphylaxis of the NK1R,[334] a constant infusion of a lower concentration of SP (for instance 1µg/µL/hour) infused over a period of hours to days may produce different results. It would be of great interest whether such an infusion causes astrogliosis, angiogenesis and/or subventricular zone cellular proliferation. Infusions could be combined with a small cICH to investigate the hypothesis that SP may act intracerebrally to exacerbate, but not cause oedema after ICH. Conversely, a peripheral infusion of SP combined with a small cICH could strengthen the hypothesis that the oedematogenic effects of SP are mediated peripherally.

## 6.5 Conclusion

The results of the present chapter demonstrate that a single intracerebral injection of a large amount of substance P is insufficient to cause oedema, BBB dysfunction or leucocytic infiltration. Results are consistent with one of two hypotheses, either: that SP can only enhance the action of other intracerebral pro-inflammatory factors following cICH, or; that the pro-inflammatory action of SP following ICH is peripherally mediated.

# 7 Exploration of the potential mechanisms of NK1RA-mediated oedema reduction following collagenase ICH.

## 7.1 Introduction

Elevated levels of SP are found following ICH, and inhibition of SP via its main receptor (NK1) reduced subsequent oedema and BBB dysfunction. This effect was consistent with previous studies in ischaemic stroke and traumatic brain injury.[461, 481] Thrombin is thought to be the main trigger of early post-ICH oedema and BBB dysfunction (at least in the autologous ICH model).[57] However, following thrombin injection, even though dramatic acute elevations in SP-IR were observed, NK1R inhibition was ineffective at reducing the subsequent acute oedema and BBB dysfunction (Chapter 5).

These results are difficult to synthesise conceptually, and two mutually non-exclusive explanations were raised. First, that oedema mechanisms may differ significantly between collagenase and autologous ICH models. SP may act synergistically with factors which are active following collagenase ICH (cICH), but inactive following autologous ICH (aICH) or thrombin injection. Second, that SP's main locus of action following cICH may be outside the CNS. This latter hypothesis was partly supported by the results of the previous chapter, where intracerebral SP microinjection failed to cause significant intracerebral inflammation.

To provide further evidence for or against these hypotheses, two experiments were performed. First, the effect of NK1R antagonists on oedema post-aICH were examined. It was hypothesised that NK1RA would be ineffective in this setting, thus providing evidence for heterogenous oedema mechanisms post autologous- and collagenase-ICH. As it is generally accepted that thrombin is the main cause of post-aICH oedema,[57] if NK1R antagonism did not reduce oedema in this setting, a separate pathway (involving substance P) must contribute to oedema following collagenase ICH.

The second experiment examined the effects of NK1RA post-cICH in previously splenectomised rats. If SP modulates the peripheral, rather than central immune response post-ICH, it was hypothesised that NK1R antagonism would fail to reduce oedema in this setting. Recent reports suggest that the peripheral immune response (orchestrated by the spleen) can influence inflammation following acute brain injury.[271, 550] In a recent study of post-ICH neural stem cell (NSC) transplantation,[271] benefits of transplantation appeared to be mediated by lodgement of NSCs in the spleen, and were largely negated by splenectomy.[271]

## 7.2 Experimental design

Twenty-one male Sprague-Dawley rats (300-340gm) were used for the experiment, as described in chapter 2.

Ten animals underwent aICH as per chapter three. Two hours following ICH animals were briefly reanaesthetised and administered either L733,060 or vehicle via the tail vein (n=5 per group).

Eleven animals underwent splenectomy. One animal died of intraabdominal sepsis 72 hours post-procedure and was replaced. Animals were allowed to recover for two weeks prior to cICH, which was performed in an identical fashion to chapters 3 & 4. Animals were administered L733,060 or vehicle via the tail vein, two hours following ICH, identically to chapter 4 (n=5 per group).

Animals in both experiments were sacrificed at 24 hours post-ICH for quantification of brain oedema via the wet weight-dry weight method.

## 7.3 Results

### 7.3.1 Baseline and experimental parameters

Table 6. Experimental parameters

| Group | Weight | $Dur^n$ | T start | T finish | T 24 h | pH | $pO_2$ | $pCO_2$ |
|---|---|---|---|---|---|---|---|---|
| **aICH (NS)** | 320±7 | 64±4 | 37.0±0.3 | 37.2±0.3 | 37.5±0.3 | 7.47±0.02 | 114±14 | 37±2 |
| **aICH (NK)** | 327±11 | 64±3 | 37.3±0.4 | 37.2±0.3 | 37.1±0.1 | 7.46±0.02 | 132±22 | 40±3 |
| **cICH (~~S~~, NS)** | 324±6 | 24±1 | 36.8±0.6 | 37.1±0.5 | ---- | ---- | ---- | ---- |
| **cICH (S, NS)** | 318±4 | 21±2 | 37.0±0.4 | 37.0±0.2 | ---- | ---- | ---- | ---- |
| **cICH (S, NK)** | 323±4 | 20±2 | 37.1±0.5 | 37.3±0.5 | ---- | ---- | ---- | ---- |

**Experimental parameters (means +/-SD) for autologous ICH (aICH) and collagenase ICH animals (cICH) (the latter with (S) or without (~~S~~) previous splenectomy) treated with normal saline (NS) or NK1R antagonist (NK). Units: weight=grams, $dur^n$=minutes of anaesthesia, temperature ('T')=$^oC$, partial pressures=mmHg.**

There were no significant differences between groups, save for the expected significantly longer duration of anaesthesia in the autologous ICH animals. NK1R antagonism did not affect temperature at 24 hours post-injury in the autologous group (or, as previously determined (Table 3), 24 hours after cICH).

### 7.3.2 Brain oedema following autologous ICH

Autologous ICH caused significant ipsilateral oedema at 24 hours (81.7±0.5 ipsilaterally vs 80.6±0.2% contralaterally; p=0.0027, Figure 84a). Less oedema occurred than following cICH (82.9±0.5 vs 81.7±0.5; p<0.001), in keeping with the nearly 30% smaller haematoma volume (Figure 24). Although comparisons with thrombin vehicles are less valid (as only 5µL normal saline was infused and a smaller needle used), aICH led to significantly greater oedema, both ipsi- and contralaterally (81.7±0.5 vs 80.4±0.4%; p=0.0056 and 80.6±0.2 vs 79.8±0.4%; p=0.0048). Despite aICH producing significant oedema, no effect of NK1R antagonism was seen (Figure 84b), either ipsilaterally (81.7±0.5 vs 81.4±0.2; p=0.29) or contralaterally (80.5±0.4 vs 80.6±0.2; p=0.55).

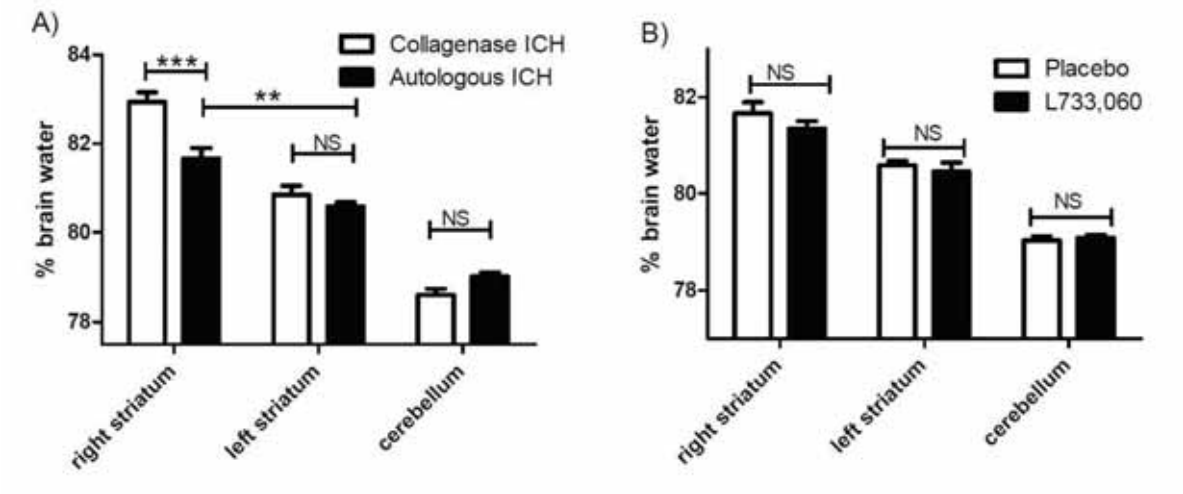


**Figure 84. Brain oedema after autologous ICH and the effect of an NK1R antagonist. (A) Autologous ICH caused significant ipsilateral oedema at 24 hours, but less than was seen after collagenase ICH. (B) NK1R antagonism did not reduce oedema following autologous ICH. ***=p<0.001, **=p<0.01, NS=not significant.**

### 7.3.3 Brain oedema in splenectomised rats

Contrary to expectations and previous reports,[271] splenectomy (performed two week prior to ICH) did not lead to a subsequent reduction in peri-haematomal oedema measured 24 hours post-cICH (Figure 85a).

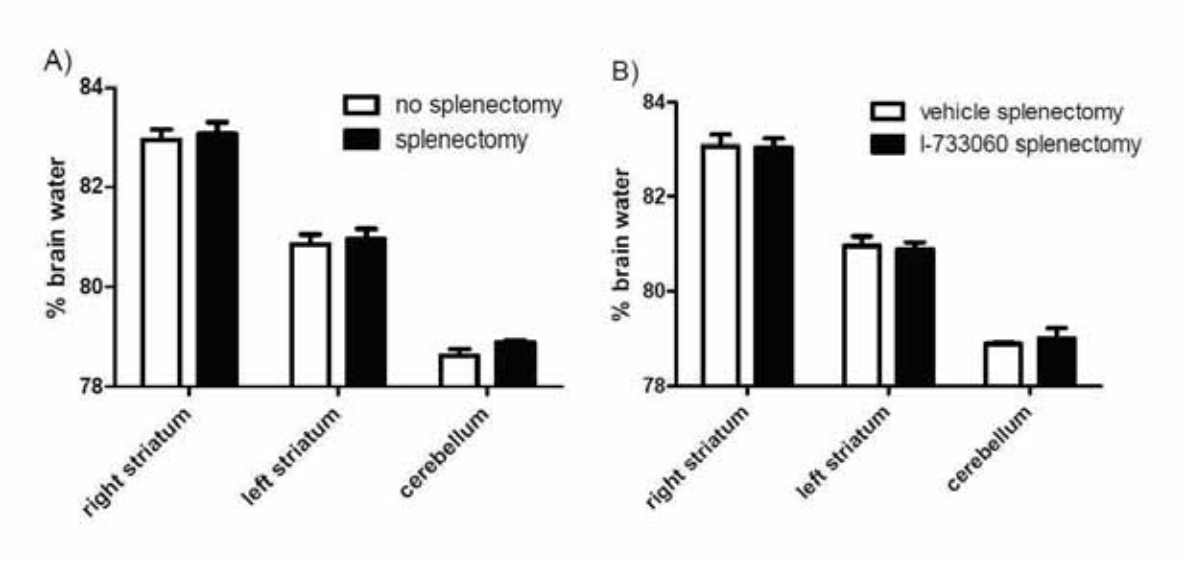


**Figure 85. Brain oedema in splenectomised collagenase ICH rats and the effect of an NK1R antagonist. (A) Splenectomy did not reduce post-ICH oedema. (B) Splenectomy negated the anti-oedema effect of NK1R antagonism. All comparisons non-significant.**

Also contrary to expectations, NK1R antagonists were rendered ineffective by splenectomy, in contrast to their efficacy in non-splenectomised cICH rats (Figure 55).

## 7.4 Discussion

The results of this chapter suggest that oedema mechanisms do indeed differ between collagenase and autologous ICH; NK1R antagonism was dramatically effective in the former (Figure 55) and without effect in the latter (Figure 84). Thrombin, therefore, may not play the same dominant role in early oedema formation following cICH that it plays in the autologous model.[57]

Collagenase causes ICH by dissolving the basement membrane,[62] of which collagen type IV is a major constituent. Substance P is unlikely to exacerbate this primary damage, as haematoma volumes were not increased by NK1R antagonism (Figure 49). Previous experiments have demonstrated that substance P can cause gap formation in cultured cerebrovascular endothelium.[399] Perhaps SP, although insufficient when injected by itself (Figure 82), can cause intracerebral oedema when other components of the BBB are damaged (i.e. astrocytes and basement membrane). This would be expected to occur more prominently following collagenase than aICH.

However, this hypothesis is inconsistent with the results of the second experiment (Figure 85), which demonstrated that splenectomy abrogates the anti-oedema effect of NK1R

antagonists. If SP's oedematogenic mechanism of action post-ICH is via endothelial NK1Rs, it is difficult to explain how this interaction can be prevented by NK1R antagonism in naive rats, but not in rats previously splenectomised.

One possible explanation for these results is that splenectomy, by causing a circulating monocytosis and thrombocytosis,[551] promotes oedema and inflammation which overwhelm the anti-oedema effects of NK1R antagonist. However, if this were the case then splenectomised vehicle-treated rats would be expected to develop more oedema than rats treated with vehicle only. A more probable explanation is that following cICH, substance P is released into the vasculature, which then acts via NK1 receptors in the spleen to promote inflammation – although, in this explanation, less oedema would be expected in splenectomised rats.

This latter hypothesis does receive some support from previous research. The beneficial effects of post-ICH neural stem cell transplantation have been shown to be spleen-mediated.[271] Following cICH splenic TNF-α, IL-1β, IL-4 and IL-6 are upregulated. These effects are blocked by NSCs, which lodge predominantly in the spleen at early timepoints. NSC transplant reduces post-ICH oedema, neutrophil infiltration and microglial activation.[271] Any benefits were completely blocked by splenectomy 3 days prior to ICH. Splenectomy alone was anti-inflammatory, although to a much smaller extent than NSC transplantation. This latter observation suggests that the anti-inflammatory effect of modulating splenic responses is potentially greater than completely eliminating splenic immune responses. SP is known to down-regulate macrophage secretion of TGF-β (an anti-inflammatory cytokine),[390] and therefore a possible benefit on NK1R antagonism may be to enhance splenic TGF-β production.

As no anti-oedema effect was seen in our study when rats were splenectomised two weeks prior to ICH, it is possible that preconditioning was responsible for the previously reported anti-inflammatory effect of splenectomy 3 days prior to ICH.[271] Preconditioning refers to the ability of a non-injurious stimulus (for instance hypoxia) to increase an organism's ability to withstand a subsequent lethal injury.[198] Activation of the innate immune system, as occurs following major abdominal surgery,[552] is an effective preconditioning stimulus.[553] In our experiment, rats were splenectomised 2 weeks prior, a timepoint at which inflammatory preconditioning has dissipated.[554] Considering the results of Lee *et al*[271] and our study in tandem, the benefits of NSC transplantation post-ICH may be mediated more by enhancement of splenic anti-inflammatory mechanisms, than by prevention of spleen-mediated inflammation.

The hypothesis that NK1R reduces post-cICH oedema by splenic immunomodulation could be supported by analysis of splenic cytokine production following cICH, with and without an NK1R antagonist. Enhanced production of anti-inflammatory cytokines following NK1R antagonism would be expected. A comparison of SP plasma levels following collagenase and aICH would also be of interest as would the effect of capsaicin C-fibre ablation on SP plasma levels and splenic cytokine production post-ICH.

As NK1R antagonists may act peripherally, rather than centrally, it is also possible that blockade of peripheral tachykinins other than SP (haemo- and endokinins) may be responsible for oedema reduction post –ICH.[391] Haemokinin in particular is expressed by inflammatory cells,[555] although its functional significance remains to be determined. Knockdown studies of the TAC-1 and TAC-4 genes, which encode SP and haemokinin respectively, with small interfering RNA (siRNA) may help determine which peptide has the dominant effect.

The unequivocal lack of NK1R antagonist benefit in this chapter may raise the possibility that the previous post-ICH oedema experiments were spurious (Figure 55). However, these experiments were blinded, highly significant (p=0.0005), and consistent across two NK1R antagonists, making a spurious result unlikely.

## 7.5 Conclusion

The results of this chapter supported the hypotheses that oedema mechanisms differ between autologous and collagenase ICH, with an additional non-thrombin pathway (involving substance P) likely to be operational in the latter. Further, evidence was obtained supporting the hypothesis that, following cICH, the benefits of NK1R antagonism may be mediated peripherally, rather than centrally, perhaps through enhancing splenic anti-inflammatory factors.

# 8 Summary and future directions

The experiments detailed in this thesis have shown that levels of intracerebral substance P are substantially elevated following experimental ICH, especially following collagenase ICH (cICH). Elevated SP-IR was diffuse and granular at 5 hours, but found within astrocytes at 24 and 48 hours. Elevated astrocytic SP-IR was accompanied by an increase in astrocytic NK1R expression, suggestive of a feed-forward loop.

Post-cICH administration of two structurally unrelated NK1R antagonists reduced subsequent oedema and BBB dysfunction, without reducing lesion volume, functional deficits or leucocytic infiltration. A reduction in cellular proliferation in the subventricular zone was also seen following NK1R treatment. The lack of functional benefit seen following treatment with NK1R antagonists suggested either that oedema and BBB dysfunction are not determinants of functional outcome, or that these potentially beneficial effects were offset by the potentially deleterious effect of a reduction in glio- and neurogenesis.

Given that thrombin causes subcutaneous oedema by stimulating peripheral nerves to release SP,[178] which acts via NK1R on endothelia[556] to promote intercellular gap formation,[351] and also that thrombin is thought to be the main mediator of early post-ICH oedema,[57] it was hypothesised that thrombin generates oedema by causing release of intracerebral substance P. However, although thrombin injections caused both significant oedema and elevations in intracerebral SP-IR at several doses, oedema was not decreased by either pre- or post-administration of two separate NK1R antagonists. NK1R antagonism also did not reduce BBB dysfunction post-thrombin injection. The anti-oedema efficacy of NK1R antagonism following cICH, but not thrombin injection, suggested that post-cICH oedema is not solely thrombin-mediated. This was corroborated by assessment of post-autologous ICH (aICH) oedema, which an NK1R antagonist failed to reduce.

These results suggested elevated levels of intracerebral substance P do not necessarily cause oedema and BBB dysfunction. This was confirmed by examining the effects of intracerebral substance P injection. Therefore two alternative hypotheses were formed: either, that intracerebral substance P may act as an oedema co-factor in cICH, but not be sufficient itself to cause oedema, or, that the anti-oedema effects of NK1R antagonists are peripherally mediated. This latter hypothesis was supported by studies of cICH in previously splenectomised rats; splenectomy negated the anti-oedema effect of NK1R antagonism. As substance P antagonists have been reported to both decrease inflammatory cytokines and increase anti-inflammatory cytokines,[432] a possible explanation is that the protective effects of NK1R antagonism following ICH are mediated by splenic secretion of anti-inflammatory

cytokines, an effect which is lost following splenectomy. This hypothesis, however, sits somewhat uncomfortably with the fact that splenectomy itself has no effect on post-ICH oedema.

The results of the current thesis certainly call into question the notion that the means by which SP causes oedema post-brain injury is as simple as peripheral 'neurogenic inflammation'.[461] Clearly more work needs to be performed in this area: the intracerebral response to a continuous intracerebral SP infusion is perhaps the most vital (measuring astrogliosis, neuro- and gliogenesis,[518] angiogenesis,[548] brain water content and barrier dysfunction). Such an infusion could be combined with a small ICH to help either refute or support the evidence for a peripheral action of NK1R antagonists (although this could be compromised by leakage of SP across a damaged BBB). If a central action of SP is suggested, it would be worth exploring where the main source of substance P post-injury (i.e. perivascular C-fibres or astrocytes) This could be answered by selectively ablating the trigeminal sensory ganglion pre-brain injury, and looking for an effect or intracerebral substance P levels and an effect on brain oedema.

If intracerebral infusions of SP did not appear to worsen post-ICH oedema, then doubt would remain as to whether it is SP (and not haemokinin) which is activating the NK1R. This could be resolved by pre-ICH treatment with anti-TAC-1 (or TAC-4 for haemokinin[322]) siRNA (small interfering RNA). Of interest also would be the effects of splenectomy pre-TBI[461] and ischaemic stroke[481] on the efficacy of NK1R antagonists.

Less helpful would be studies in TAC-1 knockout mice, as a reduction in neurogenesis may be seen,[518] blunting the assessment of any short-term beneficial effects. In an analogous fashion, knock-out studies of PAR-1 and MMP-9 in acute brain injury are compromised by their dual roles – initially deleterious,[202] but, in the subacute phase, necessary for recovery.[263, 531]

As mentioned in the introduction, SP has a number of putatively deleterious roles intracerebrally beyond effects on oedema formation, including enhancement of glutamatergic transmission,[445] priming and chemotactic effects on leucocytes[388, 557] and upregulation of NF-κB signalling,[389, 558] all of which are deleterious following ICH.[57] The results of this thesis would suggest, however, that the role played by substance P in promoting these post-ICH secondary injury pathways is relatively minor compared to that played by thrombin, iron and matrix metalloproteinases.[57]

The inconsistent effects of NK1R antagonists on post-ICH oedema, and lack of effect of functional outcome and lesion volumes suggests that pursuing NK1R antagonists as a

treatment option following ICH is unlikely to prove successful, except perhaps in the setting of patients with large haemorrhages and incipient herniation. Further testing on NK1RA is underway in other large animal species to determine whether its anti-oedema effect can be replicated.

Whether or not intracerebral infusion of SP is subsequently proven to influence BBB function, the role of astrocytic SP warrants further exploration. Elevation in astrocytic SP was consistently seen, whether following vehicle injection, collagenase or autologous ICH, or injection of substance P. Apart from the seemingly disproportionate and prolonged elevation in SP seen after thrombin injection, the response appeared stereotyped, regardless of injury mechanism. It was evident at 24 hours, progressed by 48 hours and diminished by 7 days. Similar findings have been reported following reversible MCAO[481] and traumatic brain injury,[535] suggesting that this astrocytic response is a non-specific reaction to brain injury. The function of this elevated astrocytic SP is, however, uncertain. It is unlikely to mediate oedema formation as blockade of NK1Rs following thrombin injection did not reduce oedema, despite the presence of substantially elevated astrocytic SP-IR. The results described in chapter 6 hinted that SP may cause astrogliosis; although NK1R antagonists did not decrease gliosis following ICH, they appear to do so following cerebral ischaemia[481] and in the setting of CNS infections.[422, 432] Other possible roles for astrocytic SP include the promotion of astrocytic and neural precursor proliferation[518] and the enhancement of cerebral angiogenesis.[548, 549]

As well as illuminating the central question of the role of SP post-ICH, the results contained in this thesis also have suggested several other possible avenues of future investigation.

First, our results would suggest that thrombin is even more potently deleterious than has previously been reported. 1U of rat thrombin (the amount produced by a 5µL blood clot) caused as great an injury as a cICH of approximately 150µL. Our results warrant confirmation, as they run contrary to much previous literature (as outlined in chapter 5). However, if confirmed, they suggest that 'anti-thrombin' factors are pivotal in limiting the deleterious action of thrombin (factors such as serum-derived anti-thrombin III, protease nexin-1, plasminogen activator inhibitor-1 and thrombomodulin).[559] Variability in the action of various anti-thrombins may be a cause of variability in recovery following ICH. Enhancement of these factors may prove beneficial.

Additionally, our results suggested that thrombin injection, despite causing similarly-sized brain lesions to cICH, caused substantially less subventricular zone (SVZ) cellular proliferation, indicating, perhaps, that thrombin is directly toxic to neural progenitor cells (NPCs) (this would not be surprising, as thrombin is toxic to mature neurons in vitro). [214, 215]

One of the most powerful determinants of outcome following ICH is the presence of intraventricular haemorrhage;[114] the reasons for this are unclear and probably multiple, but one hypothesis worthy of investigation is that intraventricular thrombin kills hippocampal and SVZ NPCs, impairing neuroplasticity (and hence recovery) post-ICH. This could be explored by a comparison of NPC proliferation following a small striatal ICH, with or without intraventricular administration of thrombin.

Numerous other facets of intracerebral thrombin-induced injury require elucidation. It is not known what proportion of thrombin's deleterious effects are mediated by PAR-1 (or -3, or -4) receptors. This could be determined by the coadministration of intracerebral thrombin with selective or broad-spectrum PAR inhibitors. Notwithstanding concern about the possible anti-platelet effects of PAR antagonism,[530] thrombin inhibition through PAR inhibition would be attractive clinically, as direct anticoagulant effects of direct thrombin inhibitors would be largely avoided. If, however, it appears that the bulk of thrombin-induced damage is through less-specific protease activity, direct thrombin inhibition would be required. If direct thrombin inhibitors were required, concerns about rebleeding could potentially be obviated by commencing treatment only in patients without a 'spot sign' on CTA angiography acutely,[102] or by delaying initiation of antithrombin therapy beyond the first 24 hours[560] (although our experiments would suggest that thrombin toxicity (at least in rats) is well advanced even by 5 hours).

The failure of numerous neuroprotection trials in humans[561] suggest that a multi-modal approach to ICH may be necessary – for instance combining a thrombin inhibitor with an iron chelator.[562] If rebleeding rates with either direct thrombin antagonists or PAR inhibitors are prohibitive, it may be worthwhile combining an iron chelator with antagonism of known factors downstream of thrombin – for instance IL-1β[257] and MMPs.[202]

The ability of NK1R antagonists to reduce oedema following cICH, but not aICH, points to differing injury mechanisms. The main 'species' of cerebral oedema following both these forms of ICH remains unclear (i.e. vasogenic or ionic ('cytotoxic')).[57] Studies on cerebral oedema using aquaporin-4 inhibitors would be worthwhile to clarify what the main form of oedema is in each model,[138] and whether it varies over time (i.e. cytotoxic initially but perhaps vasogenic subsequently). As aquaporin inhibitors would be expected to cause a relatively 'pure' reduction or increase in brain water content,[138] these experiments would determine whether oedema *per se* is deleterious following experimental ICH.

## Conclusion

Elevated levels of substance P and its NK1 receptor were found perihaematomally following cICH. NK1R antagonism reduced subsequent oedema formation and BBB disruption. Further experiments suggested that, contrary to expectations, thrombin does not appear to be the cause of post-cICH NK1R mediated oedema. Additional work pointed to the complexity of SP/NK1R involvement following acute brain injury. Further work is required to resolve outstanding uncertainties surrounding the mechanism and site of NK1R-mediated pathophysiological processes post-ICH (and *pari passu,* other forms of acute brain injury.)